Universidade Estadual de Campinas

Faculdade de Engenharia Elétrica e de Computação

Diana Cristina González González

Distributed Multiantenna-Selection Schemes for Amplify-and-Forward Relay Networks

Esquemas Distribuídos para Seleção de Múltiplas Antenas em Redes com Retransmissores do Tipo Amplifica-e-Encaminha

Campinas

2015

Diana Cristina González González

Distributed Multiantenna-Selection Schemes for Amplify-and-Forward Relay Networks

Esquemas Distribuídos para Seleção de Múltiplas Antenas em Redes com Retransmissores do Tipo Amplifica-e-Encaminha

Tese apresentada à Faculdade de Engenharia Elétrica e de Computação como parte dos requisitos exigidos para a obtenção do título de Doutora em Engenharia Elétrica, na Área de concentração: Telecomunicações e Telemática.

Orientador: José Cândido Silveira Santos Filho

Este exemplar corresponde à versão final da tese defendida pela aluna Diana Cristina González González, e orientada pelo Prof. Dr. José Cândido Silveira Santos Filho.

_____

Campinas
2015

COMISSÃO JULGADORA - TESE DE DOUTORADO

Candidata: Diana Cristina González González RA: 098424
Data da Defesa: 26 de novembro de 2015

Título da Tese: "Distributed Multiantenna-Selection Schemes for Amplify-and-Forward Relay Networks"
(Esquemas distribuídos para seleção de múltiplas antenas em redes com retransmissores do tipo amplifica-e-encaminha).

Prof. Dr. José Cândido Silveira Santos Filho (Presidente, FEEC/UNICAMP)
Prof. Dr. Marcelo Eduardo Pellenz (PUCPR)
Prof. Dr. Ugo Silva Dias (UnB)
Prof. Dr. Paulo Cardieri (FEEC/UNICAMP)
Prof. Dr. Gustavo Fraidenraich (FEEC/UNICAMP)

A ata de defesa, com as respectivas assinaturas dos membros da Comissão Julgadora, encontra-se no processo de vida acadêmica do aluno.

Aos meus pais, irmãos e sobrinhos,
e ao meu companheiro de vida.

Agradecimentos

Os meus mais profundos agradecimentos ao Prof. José Cândido Silveira Santos Filho, meu orientador, que, com seu constante apoio e paciência, e com sua forma metódica, crítica e brilhante de conduzir as discussões, guiou o meu trabalho.

Aos meus pais, pelo imenso carinho, encorajamento e disponibilidade irrestrita. Ensinaram-me que a distância aos sonhos é proporcional ao esforço e ao inverso do temor. Aos meus irmãos e suas lindas famílias, meus sinceros agradecimentos.

Aos Profs. Gustavo Fraidenraich, Marcelo Pellenz, Paulo Cardieri e Ugo Dias, pela gentileza de terem aceitado fazer parte da banca desta tese. Suas orientações, além de enriquecerem meu trabalho, me proporcionaram uma nova visão na área.

Aos professores e colegas do laboratório WissTek e da FEEC. Em especial, ao Prof. Michel Yacoub, por seu constante apoio.

Aos meus amigos desta aventura singular, Luisa, Xiomara, César, Sofia, Mônica, Juan, Éverton, Miguel, Carlos, Cícero, Geisa, Sofi, Gustavo, Eli, Joel, Michelle, Cassio, Matheus, Sergio, seu Cândido e dona Sônia, graças aos quais posso chamar de lar este lindo país.

Aos Profs. Germán Acero, Ricardo Quintana, Marcela Rodríguez, Sandra Cancino, Enrique Estupiñan, Henry Moreno e Javier Chaparro, e à Escuela Colombiana de Ingeniería Julio Garavito, pelo apoio.

Aos integrantes da CPG da FEEC, Prof. Pedro Peres, Noêmia, Camila e Jerusa, pela colaboração.

À CAPES, pela concessão da bolsa.

Por último, mas não menos importante, a Deus, por cada novo minuto de vida. Eles chegam carregados de uma energia mágica que me fortalece para nunca desistir de meus sonhos.

"Cada sonho que você deixa para trás
é um pedaço do seu futuro
que deixa de existir."
(Steve Jobs)

Resumo

A seleção de antena na transmissão tem sido apresentada como uma estratégia promissora para explorar os benefícios do uso de múltiplas antenas em sistemas de comunicações com retransmissores. No entanto, essa abordagem pode exigir um montante considerável de estimações de canal, transmissões de realimentação e atraso, dado que a sua implementação ótima e centralizada requer o monitoramento do estado do canal de todos os enlaces. Para aliviar essas deficiências, este trabalho propõe e analisa um conjunto de esquemas subótimos de seleção de antena na transmissão para sistemas com retransmissores do tipo amplifica-e-encaminha, os quais podem ser implementados de uma forma distribuída. Nos esquemas propostos, a antena é selecionada com base na informação local do estado de canal que está disponível na fonte, requerendo, portanto, um atraso e uma carga de realimentação pequenos e constantes. Tal abordagem é considerada em uso conjunto com diferentes técnicas, incluindo métodos de combinação de diversidade (combinação por máxima razão e combinação por seleção) no destino, protocolos de ganho fixo ou variável no relay, e transceptores com múltiplas antenas no relay. Além disso, para o caso particular em que o retransmissor tem ganho fixo e uma única antena, considera-se também o uso de um mecanismo de seleção de enlace na fonte. Para cada caso, o desempenho do sistema é avaliado em termos de probabilidade de outage, eficiência espectral e/ou vazão. O foco principal é direcionado à probabilidade de outage, para a qual são deduzidas expressões exatas e limitantes de desempenho. Uma análise assintótica é também efetuada para enriquecer a compreensão do comportamento do sistema quando operando sob alta relação sinal-ruído. Finalmente, como contribuição isolada, uma estratégia subótima e simples de alocação de potência é elaborada para um sistema com múltiplos retransmissores do tipo decodifica-e-encaminha, considerando-se enlaces com erros e codificação de fonte distribuída.

Palavras-chave: Diversidade cooperativa, canal com retransmissão, seleção de antena na transmissão, probabilidade de outage, combinação por máxima razão, combinação por seleção, seleção de enlace, eficiência espectral, alocação de potência.

Abstract

Transmit-antenna selection has been presented as a promising strategy for exploiting the benefits of multiple antennas in relaying communication systems. However, this approach may demand a considerable amount of channel estimations, feedback transmissions, and delay, since its optimal centralized implementation requires monitoring the channel state of all links. To alleviate those impairments, this work proposes and analyzes a set of suboptimal transmit-antenna selection schemes for amplify-and-forward relaying systems, which can be implemented in a distributed manner. In the proposed schemes, the antenna is selected based on the local channel-state information that is available at the source, thus requiring a low and constant delay/feedback overhead. Such an approach is considered along with different techniques, including diversity combining methods (maximal-ratio combining and selection combining) at the destination, fixed- and variable-gain protocols at the relay, and multi-antenna transceivers at the relay. A link-selection mechanism at the source is also considered for the special case of a single-antenna fixed-gain relay. For each case, the system performance is assessed in terms of outage probability, spectral efficiency, and/or throughput. The main focus is placed on the outage probability, for which exact or bound expressions are derived. An asymptotic analysis is also performed to provide further insights into the system behavior at high signal-to-noise ratio. Finally, as an isolated contribution, a simple suboptimal power allocation strategy is designed for a decode-and-forward multi-relay system with lossy intra-links and distributed source coding.

Key-words: Cooperative diversity, outage probability, relay channel, transmit antenna selection, selection combining, maximal-ratio combining, link selection, spectral efficiency, power allocation.

List of Figures

List of Tables

List of Acronyms

Acronym	Connotation
AF	amplify-and-forward
a.k.a.	also known as
AS	antenna selection
AOPA	asymptotically optimal power allocation
AWGN	additive white Gaussian noise
BER	bit error rate
BSC	binary symmetric channel
CDF	cumulative distribution function
CEO	chief executive office
CSI	channel state information
DAS	distributed transmit-antenna selection
dB	decibel
DF	decode-and-forward
DSC	distributed source coding
EPA	equal power allocation
IEEE	Institute of Electrical and Electronics Engineers
JD	joint decoding
LS	link selection
MIMO	multiple-input multiple-output
MRC	maximal-ratio combining
PDF	probability density function
PMF	probability mass function
SC	selection combining
SER	symbol error rate
SNR	signal-to-noise ratio
TAS	transmit-antenna selection

List of Symbols

Symbol	Connotation
$\Gamma(\cdot)$	gamma function
$\delta(\cdot)$	discrete delta function
$E[\cdot]$	expectation
$\mathrm{Ei}(\cdot)$	exponential integral function
$\max$	maximum of either a function or a list of values
$\min$	minimum of either a function or a list of values
$\arg\max$	argument of the maximum
$\Pr(\cdot)$	probability of an event
$f_Z(\cdot)$	probability density function of a generic random variable Z
$K_n(\cdot)$	nth-order modified Bessel function of the second kind
$B(\cdot, \cdot)$	beta function
$\psi(\cdot)$	digamma function
P_{out}	outage probability
$h_b(\cdot)$	binary entropy function
$H(\cdot)$	entropy of a random variable
$I(\cdot; \cdot)$	mutual information between random variables

List of Publications

Journal papers

- D. C. González, D. B. da Costa, and J. C. S. Santos Filho, " Distributed suboptimal schemes for TAS/SC and TAS/LS in fixed-gain AF relaying systems," *IEEE Trans. Wireless Commun.*, vol. 13, no. 11, pp. 604–6053, Nov. 2014.

- D. C. González, D. B. da Costa, and J. C. S. Santos Filho, "Distributed TAS/MRC and TAS/SC schemes for fixed-gain AF systems with multi-antenna relay," *IEEE Trans. Wireless Commun.*, under review.

- D. C. González, D. B. da Costa, and J. C. S. Santos Filho, "An efficient distributed approach for TAS/SC and TAS/MRC in variable-gain AF relaying systems," *IEEE Trans. Commun.*, under review.

- D. C. González, A. Wolf, J. C. S. Santos Filho, and G. Fettweis, "Decode-and-forward multirelay systems with lossy intra-links and distributed source coding: outage probability and power allocation," *IEEE Trans. Commun.*, under review.

Conference papers

- D. C. González, D. B. da Costa, and J. C. S. Santos Filho, "Distributed transmit-antenna selection scheme for relaying systems with selection combining," in *Proc. XXXI Brazilian Telecommunications Symposium (SBrT)*, Fortaleza, Brazil, 1–4 Sep. 2013.

- D. C. González, D. B. da Costa, and J. C. S. Santos Filho, "A distributed transmit antenna selection scheme for fixed-gain multi-antenna AF relaying systems," in *Proc. 9th International Conference Cognitive Radio Oriented Wireless Networks and Communications (CROWNCOM)*, Oulu, Finland, 2–4 Jun. 2014, pp. 254–259.

Contents

Chapter 1

Introduction

Multiantenna cooperative relaying schemes have emerged as a promising strategy to boost the reliability, capacity, and coverage of wireless communication systems [1–5]. In order to alleviate the deleterious impact of spectrum scarcity, multipath fading, shadowing, and path loss on communications, such schemes benefit from the well-known advantages offered by multiple-input multiple-output (MIMO) techniques [6–10], namely, spatial diversity and spatial multiplexing, while creating an extended virtual antenna array based on a collection of distributed antennas from multiple collaborating terminals [8,11]. However, implementing those schemes may be rather intricate, due to common restrictions in power, complexity, cost, and antenna size. As a result, practical realistic implementations of multiantenna relaying schemes usually limit the use of multiantenna devices to a few particular nodes, or restrict the total number of antennas in the various nodes [12], or both.

These practical limitations can be addressed by opting for simplified multiantenna techniques. At the transmitter side, a technique that proves attractive is transmit-antenna selection (TAS), which retains the essential benefits of more sophisticated MIMO schemes [13,14] at a reduced cost and complexity. In this technique, the best antenna is selected for transmission, based on the channel state information (CSI) of the multiple links from source to destination. This CSI must be first estimated at various nodes and then sent to the transmitter, thus requiring some feedback notifications. The required number of bits of feedback information varies depending on the number of source, relay, and destination antennas [13]. In optimal centralized TAS schemes, it is usually the destination that chooses the best antenna that the source should transmit with, based on the full CSI of all available links. Afterwards, the destination feeds the index of the selected antenna back to the source. This process may incur a considerable delay and feedback overhead. Indeed, as the number of antennas increases, such scheme may rapidly become infeasible in practice. Therefore, suboptimal distributed antenna-selection schemes (DAS) based on partial CSI of a subset of links are of great practical interest.

At the receiver side, in the destination, the signal replicas coming from the direct and relaying links must be properly combined to yield a considerable diversity gain. Although there are several diversity techniques available, only the two most popular ones, namely, maximal-ratio combining (MRC) and selection combining (SC), shall be discussed in this

work. On the one hand, MRC is the optimal linear combining scheme, which is attained by co-phasing, weighting, and adding the received signals from all diversity paths [15]. However, its implementation is relatively intricate, since it requires multiple channel estimations to adequately weight each path with a factor proportional to the corresponding signal level, as well as a complex hardware design with a dedicated receiver chain for each antenna [16]. On the other hand, SC is a simpler suboptimal scheme, where the diversity path with the highest signal-to-noise ratio (SNR) is selected. In this scheme, no channel estimation is required and a single receiver chain suffices to process the selected path. Choosing one of these combining techniques represents a trade-off between performance and complexity, and a suitable decision shall depend on the system requirements and available resources.

Another important aspect of cooperative systems is how each relay processes the received signal before forwarding it to another relay or to the final destination. This processing can follow different protocols, which can be divided into two main groups: transparent relaying and regenerative relaying [7, 11, 17–19]. In the transparent relaying protocols, the relay does not access the information contents of the received message, i.e., the latter is not detected by the former. Instead, the relay only performs some linear (analog) operations (e.g., amplification and phase shifting) in order to prepare the signal for retransmission [7]. In this group, the amplify-and-forward (AF) relaying protocol is by far the most widely used. The AF protocol has a reduced hardware complexity, since the relay does not perform any kind of detection. In contrast, AF relays may exhibit noise accumulation, since the relay amplifies and retransmits a noisy version of the transmitted source signal, without decoding it [20, 21]. In addition, two types of amplification are usually employed for the AF protocol, namely, variable gain and fixed gain. In the former, the relay requires the instantaneous CSI of the source-relay link in order to achieve a fixed transmit power all the time. In the latter, the relay employs the average CSI of the source-relay link in order to achieve a fixed average transmit power [22, 23]. Contrarily to these transparent protocols, in regenerative relaying, the relay extracts the information sent by the source, by applying some procedure to recover the original source message prior to retransmission. In this group, the most prominent protocol is decode-and-forward (DF). In this protocol, the relay decodes, re-encodes, and retransmits the source message to the destination. The DF protocol achieves a better performance than the AF protocol, but it requires a much more complex implementation [7].

1.1   Related Work and Motivation

Several studies have proposed and tested various relaying schemes with the integrated use of TAS techniques, at the transmitter side, and diversity-combining methods, at the receiver side, including those in [4, 12, 24–33] and the references therein. A timeline is presented in Fig. 1.1. In a pioneering work [24], the authors derived an optimal selection criteria for the TAS/MRC scheme operating over a multi-antenna, half-duplex, dual-hop AF relaying network. Based on a bit-error rate (BER) analysis, they concluded that the optimal TAS strategy achieves the same diversity order of a more sophisticated communication scheme that fully and simultaneously exploits all transmit antennas. The
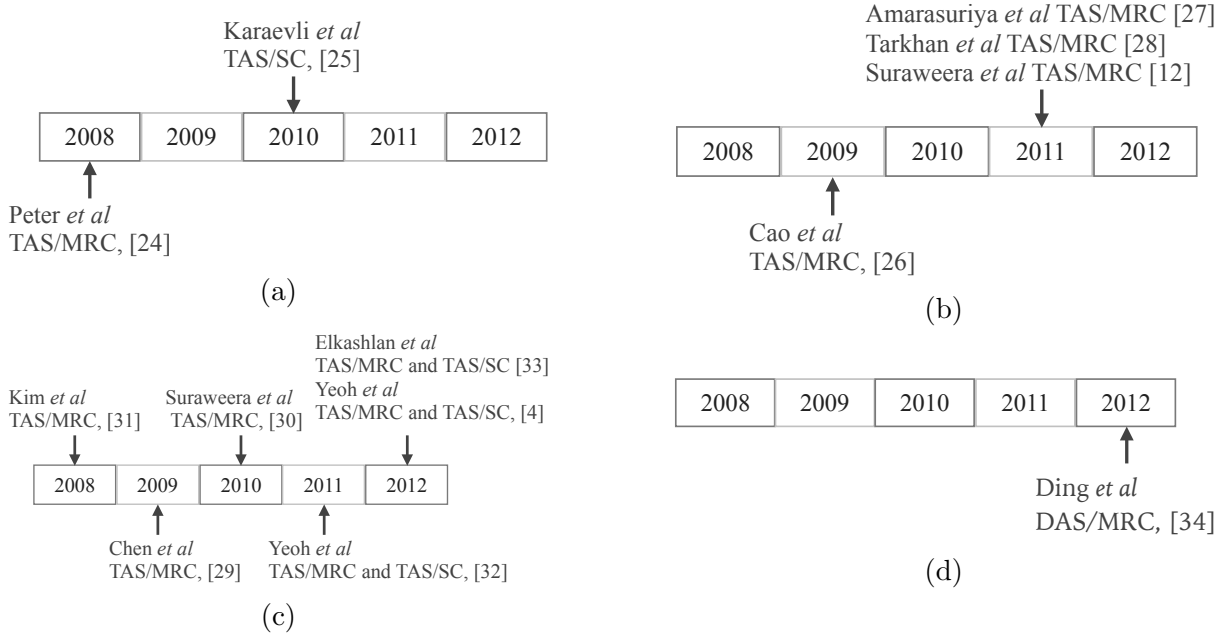
Figure 1.1: Timeline of TAS relaying techniques: (a) optimal centralized schemes; (b) suboptimal schemes disregarding the channel state of some transmission links; (c) optimal schemes under no direct link; (d) distributed suboptimal schemes.

main drawback of this scheme is its high complexity when performing an exhaustive search for the best transmit antenna. A similar study for TAS/SC was presented in [25], leading to similar conclusions as well. In this case, the diversity order was investigated based on an asymptotic analysis of the symbol-error rate (SER). The results showed that DAS/SC achieves the same diversity order of TAS/MRC, as indeed expected. These two works on optimal centralized TAS schemes are illustrated in Fig. 1.1a.

Afterwards, aiming to reduce complexity, some suboptimal TAS strategies have been explored by the research community. In most of these explorations, suboptimal selection criteria have been considered that disregard the channel state of some transmission links between source and destination [12, 26–28] (see Fig. 1.1b). The authors in [26] proposed two suboptimal, low-complexity TAS strategies for the same network configuration originally employed in [24]. These strategies were based on the local CSI at the source, that is, on the channel state of the source-destination link (a.k.a. direct link) and source-relay link (a.k.a. first hop). More specifically, the SNR of either the direct link or the first hop was maximized in the proposed strategies. The performance of these strategies was investigated via simulation, and the results revealed that the maximization of the direct-link SNR can achieve the same diversity order as the optimal centralized strategy. Later on, the authors in [27] unfolded a mathematical analysis of the two strategies introduced in [26]. For both strategies, lower bound expressions of the outage probability and SER were derived under Nakagami-m fading. Another suboptimal strategy was introduced in [28], once again for the network configuration used in [24]. Therein, an adaptive TAS rule was designed, dynamically based on the CSI of either the direct link or the direct link and first hop, depending on the state of these links. The performance of this strat-

egy was investigated via simulation. Finally, the authors in [12] assessed analytically and compared the performance of two TAS/MRC schemes (optimal and suboptimal) in a dual-hop, variable-gain AF relaying network with a multi-antenna source, a single-antenna relay, and a single-antenna destination. The TAS rule for the proposed suboptimal strategy was based solely on the CSI of direct link. A tight upper bound was used to derive CDF expressions for the SNR of the two schemes, based on which some performance measures were then investigated, such as outage probability, average BER, and mean channel capacity.

TAS techniques have been also widely addressed for dual-hop AF relaying networks under the absence of a usable direct link, as in [4, 29–33] (see Fig. 1.1c). This assumption reduces the complexity of the TAS scheme, since it becomes then sufficient to maximize the first- and second-hop SNRs separately. In [29], the authors derived the SER and outage probability for a TAS/MRC relaying network with a multi-antenna source, a multi-antenna destination, and a single-antenna AF variable-gain relay. This scheme was generalized in [31] and [30], by assuming a multi-antenna relay. More specifically, the authors in [31] derived the PDF of the end-to-end SNR, and provided a BER expression when using M-PSK over Rayleigh fading channels. This work was complemented in [30], by considering the performance analysis of other metrics, such as outage probability, moments of the end-to-end SNR, and error rates for some modulation schemes, including M-QAM. Based on the same relaying network, the authors in [32] investigated a distributed TAS/MRC strategy, which selects the best transmit antennas at the source and relay by maximizing the corresponding local CSIs. For this scheme, exact closed-form expressions were derived for the outage probability and SER, based on the CDF of the end-to-end SNR. In addition, asymptotic high-SNR expressions were also derived for each of these metrics. Afterwards, the authors in [33] further explored the scheme proposed in [32], but now considering SC at the destination. In [32] and [33], Nakagami-m fading was assumed. The results therein showed that the two schemes (TAS/MRC and TAS/SC) achieve the same diversity order. Finally, the authors in [4] investigated the operation of such schemes when operating with multiple relays under Weibull fading.

An efficient distributed approach was introduced in [34] for a DAS/MRC scheme operating over a single-antenna fixed-gain AF relay (see Fig. 1.1d). Unlike all the aforementioned TAS strategies, this approach avoids the full CSI of optimal centralized schemes while considering all the links in the antenna-selection mechanism. Importantly, it achieves a satisfactory performance under a constant and low delay/feedback overhead. Such characteristics render the new approach highly attractive from a practical perspective. Therefore, further investigations into the potentials of this approach become timely and important.

1.2   Contributions and Outline

In light of the above discussion, the main scope of this dissertation is to conceive and test a myriad of generalizations, extensions, and derivatives inspired by the distributed approach introduced in [34]. More specifically, we design and analyze a set of low-cost, low-complexity, suboptimal distributed transmit-antenna selection schemes for amplify-

and-forward relaying networks, by considering many different network configurations. In addition, an independent "unplanned" contribution is presented at the end, somewhat disconnected from the other contributions, but still into the context of relaying networks. The following chapters are replicas of manuscripts that we have published in or submitted to journals and conferences along the research activities. Next we present an annotated outline of the rest of this dissertation.

Chapter 2. This Chapter investigates the performance of a DAS/SC scheme for dual-hop fixed-gain AF relaying systems, containing a source equipped with N_t antennas, as well as a single-antenna relay and destination. It is assumed that all channels undergo flat independent Rayleigh fading — this is also assumed in all subsequent chapters. As already mentioned, the proposed antenna-selection strategy is inspired by the distributed TAS strategy proposed in [34]. However, in contrast to that work, which uses MRC at the destination, our work proposes and analyzes the use of SC instead, in order to reduce the system complexity. On the other hand, like in [34], the proposed strategy has a reduced delay and feedback overhead, requiring only a 2-bit pilot signaling to inform the source with relevant information for the antenna selection. The performance of the proposed DAS/SC scheme is assessed in terms of outage probability, for which analytical lower and upper bounds are derived, since an exact closed-form solution to the inherently intricate mathematical framework seems infeasible. Moreover, the analytical results are verified via Monte Carlo simulation. In addition, a high-SNR analysis of these bounds is performed to provide insights into the asymptotic behavior and system diversity order. The results reveal that the proposed scheme achieves a diversity order of $N_t + 1$, being the same achieved by its optimal centralized TAS counterpart as well as by the DAS/MRC scheme originally proposed in [34]. Importantly, the proposed scheme performs closely to the optimal one. Therefore, for practical purposes, it represents an interesting alternative, giving an excellent trade-off between complexity and performance.

Chapter 3. This Chapter extends the work in Chapter 2, by further detailing the derivation process and enhancing the discussions related to the DAS/SC scheme, in addition to introducing and investigating a new distributed mechanism for transmit-antenna selection and link selection (DAS/LS) — either the direct link or the relaying link is selected for communication. The primary motivation behind the proposed DAS/LS scheme is to reduce the loss in spectral efficiency due to the multi-hop transmission, as follows. In this scheme, a TAS rule identical to that of the DAS/SC scheme is used. However, unlike DAS/SC, the selection between the direct link or relaying link is no longer performed at the destination, after the transmission process, but at the source instead, before the transmission process. This way, the average spectral efficiency is improved, once a time slot is saved whenever the direct link happens to be selected for communication. Exact closed-form expressions are derived for the outage probability, mean spectral efficiency, and high-SNR asymptotic behavior of the DAS/LS scheme. Our analytical results for DAS/SC and DAS/LS are verified using Monte Carlo simulation, and compared against those of centralized (TAS/MRC and TAS/SC) and distributed (DAS/MRC) schemes previ-

ously investigated in the literature. While both centralized and distributed DAS/SC and DAS/MRC schemes achieve full diversity order, equal to $N_t + 1$, the proposed DAS/LS scheme achieves a nearly-full diversity order, equal to N_t. However, in terms of spectral efficiency, the DAS/LS scheme outperforms all the others.

Chapter 4. This Chapter generalizes the DAS/MRC scheme proposed in [34] to the multi-antenna relay scenario, by considering one half-duplex fixed-gain AF relay with N_{rr} receive antennas and N_{rt} transmit antennas. Similarly to [34], the investigated network is composed of one source with N_t antennas and one single-antenna destination. In order to assess the performance of the generalized DAS/MRC scheme, lower and upper bounds for the outage probability are derived. Moreover, an asymptotic expression for each of these bounds at high SNR is obtained in closed form. From these results, it is observed that the proposed DAS scheme achieves a full diversity order, equal to $N_t + \min(N_{rt}, N_{rr})$. Some representative scenarios, using different number of antennas at the source and relay, are presented and analyzed. Additionally, Monte Carlo simulations are run to support the derived analytical bounds. Importantly, the underlying distributed strategy is shown to perform closely to the costly optimal centralized TAS/MRC scheme, especially when the relay approaches the destination.

Chapter 5. This Chapter complements the contribution introduced in Chapter 4, by describing in more detail the mathematical analysis of the generalized DAS/MRC scheme and extending the amount of investigated scenarios and related discussions. In addition, a corresponding generalized (multi-antenna relay) version of the DAS/SC scheme presented in Chapter 3 is also designed and analyzed. Similarly to the DAS/MRC scheme, the central metric used to assess the performance of the generalized DAS/SC scheme is the outage probability. Analytical lower bounds for the outage probability of the proposed schemes are derived and compared. Importantly, the derived bounds prove to be very tight approximations to the exact outage performance. Moreover, capitalizing on a strikingly interesting property of Stirling numbers of the second kind, closed-form asymptotic expressions for these bounds were obtained. The proposed distributed schemes achieve the same diversity order, equal to $N_t + \min(N_{rt}, N_{rr})$, which is identical to that of their optimal centralized counterparts. In order to verify the accuracy of the analytical framework, Monte Carlo simulation results are also provided. The impact on the outage probability is discussed for different system parameters, such as average SNR, relay location, and number of antennas.

Chapter 6. This Chapter introduces and analyzes new DAS/MRC and DAS/SC schemes for dual-hop AF relaying systems. However, differently from all previous Chapters, in which fixed-gain relaying is used, herein we extend the distributed approach to the variable-gain scenario, leading to a distinct design framework. Once again, we consider a source with N_t antennas, as well as a single-antenna relay and a single-antenna destination. Analytical lower bounds for the outage probability of the proposed schemes are derived, since an exact analysis looks intractable. Impor-

tantly, the obtained bounds prove to be extremely tight approximations to the exact outage performance. In addition, a closed-form asymptotic analysis at high SNR is performed for these bounds, revealing that both proposed schemes achieve a full order diversity of $N_t + 1$, the same achieved by its optimal centralized counterpart. Monte Carlo simulation is used to validate our analytical results. Furthermore, the proposed distributed schemes are shown to perform closely to the costly centralized counterparts, especially when the relay approaches the source or destination.

Chapter 7. This Chapter brings an isolated contribution, which leaves the TAS topic addressed in the previous Chapters. This contribution resulted from a three-months research visit to the Technische Universität Dresden, Germany, as part of the project RESCUE, funded by the European Commission, and aimed at the development of efficient communication technologies for highly challenging environments (e.g., during catastrophes or disasters). In this Chapter, the outage performance of a distributed source coding scheme is investigated for a decode-and-forward multirelay system inspired by the so-called Chief Executive Officer problem. The CEO problem suggests that the source message can be recovered at the destination by combining a set of corrupted replicas forwarded by multiple relays, as long as these replicas are sufficiently correlated with the original message. We consider a binary source that transmits a message through multiple lossy intra-links, modeled as independent binary symmetric channels (BSC). As a result, each relay detects a possibly erroneous replica of the source message, re-encoding and forwarding it to the destination via a block Rayleigh fading channel. The destination, in turn, must reconstruct the source message by jointly decoding all received replicas. In order to derive an analytical expression for the outage probability of such scheme, the Slepian-Wolf Theorem is revisited and adapted to comply with the engineering requirements of the problem at hand. Furthermore, based on an asymptotic analysis, a simple and highly effective power allocation strategy is designed for the investigated system. Our results and discussions find important applications in emerging technologies for robust and efficient communications in unpredictable environments.

Bibliography

[1] A. Sendonaris, E. Erkip, and B. Aazhang, "Increasing uplink capacity via user co-operation diversity," in *Proc. IEEE Symposium on Information Theory*, Cambridge, MA, 16–21 Aug. 1998, p. 156.

[2] E. Li, S. Yang, and H. Wu, "A source-relay selection scheme in two-way amplify-and-forward relaying networks," *IEEE Commun. Lett.*, vol. 16, no. 10, pp. 1564–1567, Oct. 2012.

[3] V. N. Q. Bao, B. P. L. Phuong, and T. T. Thanh, "Performance analysis of TAS/SC-based MIMO decode-and-forward relaying for multi-hop transmission over Rayleigh fading channels," in *Proc. International Conference on Communications and Electronics (ICCE)*, Santander, Spain, 1–6 Jul. 2012, pp. 150–155.

[4] P. Yeoh, M. Elkashlan, N. Yang, D. Benevides da Costa, and T. Duong, "MIMO multi-relay networks with TAS/MRC and TAS/SC in Weibull fading channels," in *Proc. IEEE 23rd International Symposium on Personal Indoor and Mobile Radio Communications (PIMRC)*, Sydney, NSW, 9–12 Sep. 2012, pp. 2314–2318.

[5] E. C. V. D. Meulen, "Three-terminal communication channels," *Advances in Applied Probability*, vol. 3, no. 1, pp. 120–154, 1971.

[6] D. Tse and P. Viswanath, *Fundamentals of Wireless Communication*, 1st ed. New York, NY: Cambridge University Press, 2005.

[7] M. Dohler and Y. Li, *Cooperative Communications: Hardware, Channel and PHY*, 1st ed. Chichester, UK: John Wiley and Sons Ltd, 2010.

[8] A. Molisch and M. Win, "MIMO systems with antenna selection," *IEEE Microwave Magazine*, vol. 5, no. 1, pp. 46–56, Mar 2004.

[9] L. Zheng and D. N. C. Tse, "Diversity and freedom: A fundamental tradeoff in multiple antenna channels," in *Proc. IEEE Int. Symp. Information Theory (ISIT)*, Lausanne, Switzerland, 2002, p. 476.

[10] Z. L. and D. N. C. Tse, "Diversity and multiplexing: A fundamental tradeoff in multipleantenna channels," *IEEE Trans. Inform. Theory*, vol. 49, pp. 1073–1096, May 2003.

[11] J. Laneman, D. Tse, and G. W. Wornell, "Cooperative diversity in wireless networks: Efficient protocols and outage behavior," *IEEE Trans. Information Theory*, vol. 50, pp. 3062–3080, 2004.

[12] H. A. Suraweera, P. J. Smith, A. Nallanathan, and J. S. Thompson, "Amplify-and-forward relaying with optimal and suboptimal transmit antenna selection," *IEEE Trans. Wireless Commun.*, vol. 10, no. 6, pp. 1874–1885, Jun. 2011.

[13] S. Sanayei and A. Nosratinia, "Antenna selection in MIMO systems," *IEEE Commun. Mag.*, vol. 42, no. 10, pp. 68–73, Oct. 2004.

[14] N. T. B. Tam, T. Tran-Thien, T. Do-Hong, and V. N. Q. Bao, "Performance analysis of decode-and-forward relaying for multi-hop Alamouti transmission over Rayleigh fading channels," in *Proc. IEEE Conference International Advanced Technologies for Communications (ATC)*, Ho Chi Minh City, Vietnam, 20–22 Oct. 2010, pp. 195–200.

[15] Y.-W. P. Hong, C.-C. Kuo, and W.-J. Huang, *Cooperative Communications and Networking*, 1st ed. New York, NY: Springe, 2010.

[16] M. K. Simon and M. Alouini, *Digital Communication over Fading Channels: A Unified Approach to Performance Analysis.* John Wiley & Sons, 2000.

[17] T. M. Cover and A. A. El Gamal, "Capacity theorems for the relay channel," *IEEE Trans. on Inform. Theory*, vol. 25, no. 5, pp. 572–584, 1979.

[18] M. Souryal and B. Vojcic, "Performance of amplify-and-forward and decode-and-forward relaying in Rayleigh fading with turbo codes," in *Proc. IEEE Acoustics, Speech and Signal Processing (ICASSP)*, Toulouse, Fr, 14–19 May 2006, pp. IV–IV.

[19] E. Hossain, D. I. Kim, and V. K. Bhargava, *Cooperative Cellular Wireless Networks*, 1st ed. Cambridge, UK: Cambridge University Press, 2011.

[20] K. J. R. Liu, W. Su, and A. K. Wasinki, *Cooperative Communications and Networking*, 1st ed. Cambridge, UK: Cambridge University Press, 2009.

[21] J. Zhao and A. Wittneben, "Cellular relaying networks: State of the art and open issues," in *Proc. IEEE Acoustics, Speech and Signal Processing (ICASSP)*, Toulouse, Fr, 14–19 May 2005, pp. IV–IV.

[22] M. Hasna and M. S. Alouini, "A performance study of dual-hop transmissions with fixed gain relays," *IEEE Trans. Wireless Commun.*, vol. 3, pp. 1963–1968, Nov. 2012.

[23] R. Nabar, H. Bolcskei, and F. Kneubuhler, "Fading relay channels: Perfor- mance limits and space-time signal design," *IEEE J. Select. Areas in Commun*, vol. 22, no. 6, pp. 1099–1109, Aug 2003.

[24] S. W. Peters and R. W. Heath, "Nonregenerative MIMO relaying with optimal trans-mit antenna selection," *IEEE Signal Process. Lett*, vol. 15, pp. 421–424, 2008.

[25] I. L. Karaevli, I. Altunbas, and G. Karabulut, "Performance analysis of cooperative relaying scheme applying TAS/SC," in *Proc. IEEE Symposium on Computers and Communications (ISCC)*, Riccione, Italy, 22–25 Jun. 2010, pp. 127–132.

[26] L. Cao, X. Zhang, Y. Wang, and D. Yang, "Transmit antenna selection strategy in amplify-and-forward MIMO relaying," in *Proc. IEEE Conference Wireless Communications and Networking (WCN)*, Budapest, Hungary, 5–8 Apr. 2009, pp. 1–4.

[27] G. Amarasuriya, C. Tellambura, and M. Ardakani, "Performance analysis framework for transmit antenna selection strategies of cooperative MIMO AF relay networks," *IEEE Trans. Veh. Technol.*, vol. 60, no. 7, pp. 3030–3044, Sep. 2011.

[28] A. A. Tarkhan, F. Farzaneh, and B. H. Khalaj, "Efficient suboptimal transmit antenna selection for MIMO relay channels," in *Proc. IEEE International Symposium on Computer Networks and Distributed Systems (CNDS)*, Tehran, Iran, 23–24 Feb. 2011, pp. 45–48.

[29] S. Chen, W. Wang, X. Zhang, and D. Zhao, "Performance of amplify-and-forward MIMO relay channels with transmit antenna selection and maximal-ratio combining," in *Proc. IEEE Conference Wireless Communications and Networking (WCN)*, Budapest, Hungary, 5–8 Apr. 2009, pp. 1–6.

[30] H. A. Suraweera, P. J. Smith, A. Nallanathan, and J. S. Thompson, "Amplify-and-forward relay transmission with end-to-end antenna selection," *IEEE Trans. Wireless Commun.*, vol. 10, no. 6, pp. 1–6, Jun. 2010.

[31] J. B. Kim and D. Kim, "BER analysis of dual-hop amplify-and-forward MIMO relaying with best antenna selection in Rayleigh fading channels," *IEICE Trans. Commun*, vol. E91-B, no. 8, pp. 2772–2775, Aug. 2008.

[32] P. L. Yeoh, M. Elkashlan, and I. Collings, "Exact and asymptotic SER of distributed TAS/MRC in MIMO relay networks," *IEEE Trans. Wireless Commun.*, vol. 10, no. 3, pp. 751–756, Mar. 2011.

[33] M. Elkashlan, P. L. Yeoh, N. Yang, T. Duong, and C. Leung, "A comparison of two MIMO relaying protocols in Nakagami-m fading," *IEEE Trans. Veh. Technol.*, vol. 61, no. 3, pp. 1416–1442, Mar. 2012.

[34] H. Ding, J. Ge, D. B. da Costa, and T. Tsiftsis, "A novel distributed antenna selection scheme for fixed-gain amplify-and-forward relaying systems," *IEEE Trans. Veh. Technol.*, vol. 61, no. 6, pp. 2836–2842, Jul. 2012.

Chapter 2

Distributed Transmit-Antenna Selection Scheme for Relaying Systems with Selection Combining

Diana C. González, Daniel B. da Costa, and José Cândido S. Santos Filho[1]

Abstract

The use of multiple antennas at the node terminals of relay networks potentially improves cooperative diversity in terms of both reliability and spectral efficiency. A simple practical approach to exploit such potentials at the transmitter side is to appropriately select one out of the many transmit antennas available. In this work, we propose and analyze a dual-hop fixed-gain amplify-and-forward relaying system based on a distributed transmit antenna selection scheme, along with a selection-combining treatment of the direct and relaying signals at the destination. We derive analytical lower and upper bounds for the outage probability of the proposed scheme in single-fold integral form. In addition, asymptotic expressions for these bounds at high signal-to-noise ratio are obtained in closed form. Our results reveal that the proposed scheme achieves full diversity order. More importantly, the underlying distributed strategy of transmit antenna selection is shown to perform closely to the costly optimal centralized solution.

2.1 Introduction

Several studies have suggested the combined use of multiple-input–multiple-output (MIMO) techniques and cooperative communications in order to improve the reliability of wireless systems, by fully exploiting multipath signal diversity [1], [2], [3]. However, in practice, the implementation of such multiantenna systems is constrained by restrictions in power, complexity, and antenna size. Realistic schemes usually limit the use of multiple antennas to specific relay network nodes, or strongly restrict the total number of antennas [4].

As well known, the impairments of multipath fading on communications can be alleviated by using both transmit as well as receive diversity techniques. At the transmitter side, these techniques include, for example, space-time coding and transmit antenna selection (TAS); at the receiver side, they include many diversit-combining schemes such as maximum-ratio combining (MRC) and selection combining (SC) [2]. Many dual-hop networks with TAS at the source and MRC at the destination have been recently proposed and analyzed in the literature (see, for example, [4], [5], and the references therein). In particular, the TAS/MRC combination is widely used, because TAS reduces the complexity and power requirements at the transmitter—although it is not an optimal beamforming technique [6]—and because MRC is the optimal linear combining technique [7]. On the other hand, the MRC implementation requires many channel estimations and complex hardware resources, since each antenna needs a separate receiver chain [8]. In contrast, SC needs no channel estimation and only requires a single receiver chain. Thus, knowing that both combining techniques achieve the same diversity order, SC represents an excellent trade-off between complexity and performance.

Very few studies have considered the TAS/SC combination in relay networks, including the following. In [2], the end-to-end performance is analyzed for a regenerative (multihop, decode-and-forward) MIMO relaying system. This system assumes that the receivers have perfect channel state information (CSI) in order to apply TAS at the transmission, and then the best-antenna information is fed back to the transmitter using partial CSI. Karaevli *et al.* [9] determined the performance of a cooperative system with a single relay and multiple antennas at the source and destination. In this system, TAS is employed to choose the transmit antenna with the largest end-to-end SNR at the source and relay, by using feedbacks from destination. Finally, in [3], a performance comparison between TAS/MRC and TAS/SC schemes in MIMO relay networks is performed. It was found that the SNR advantage of TAS/MRC over TAS/SC in balanced hops does not depend on the number of relays.

In systems with TAS, a feedback usually exists that informs the transmitter the best antenna to select. This feedback contains CSI of various links of the system. That is, the channel knowledge improves the overall system performance. The required bits of feedback information varies depending on the number of source and destination antennas [10].

In this work, we capitalize on the distributed antenna selection (DAS) scheme proposed in [5] for a relaying network under a dual-hop, fixed-gain, amplify-and-forward (AF) scenario with a multiple-antenna source and single-antenna relay and destination. On the

other hand, differently from [5], which uses MRC, we propose and analyze the use of SC at the destination, in order to reduce the system complexity. A remarkable feature of the TAS scheme used here is the requirement of CSI with low and constant delay/feedback overhead, regardless of the number of transmit antennas [5]. We derive analytical lower and upper bounds for the outage probability of the proposed scheme in single-fold integral form. In addition, asymptotic expressions for these bounds at high signal-to-noise ratio are obtained in closed form. Our results reveal that the proposed scheme achieves full diversity order. More importantly, the underlying distributed strategy of transmit antenna selection is shown to perform closely to the costly optimal centralized solution.

Throughout this paper, $f_Z(\cdot)$ denotes the probability density function (PDF) of a generic random variable Z, $E[\cdot]$ denotes expectation, and $\Pr(\cdot)$ denotes probability.

2.2 System Model and Antenna Selection Scheme

2.2.1 System Model

We consider a half-duplex dual-hop communication system containing a source S with N_t antennas, a single-antenna fixed-gain AF relay R, and a single-antenna destination D. Furthermore, we consider that the noise term in all of the nodes is an additive white Gaussian noise (AWGN) with mean power N_0, and that all of the links undergo independent flat Rayleigh fading. The terminals are assumed to operate on a time-division multiple access basis.

Before data transmission, TAS is employed at S, in order to find the best transmit antenna that maximizes the end-to-end SNR. After that, a conventional two-slots cooperative transmission takes place. As mentioned before, this system is similar to that presented in [5], but differs from that in the sense that the direct- and relaying-link signals are now combined at D by means of SC, instead of MRC. Accordingly, the end-to-end SNR from the ith antenna at S to D can be written as

$$\gamma_i = \max\left(\gamma_{SD,i}, \frac{\gamma_{SR,i}\gamma_{RD}}{\gamma_{RD} + C}\right), \tag{2.1}$$

where $\gamma_{SD,i} \triangleq \frac{P_S}{N_0}|h_{SD,i}|^2$, $\gamma_{SR,i} \triangleq \frac{P_S}{N_0}|h_{SR,i}|^2$, $\gamma_{RD} \triangleq \frac{P_R}{N_0}|h_{RD}|^2$, and $C = 1 + \bar{\gamma}_{SR}$, with $\bar{\gamma}_{SR} = E[\gamma_{SR,i}]$. In these expressions, $|h_{SD_i}|^2$, $|h_{SR_i}|^2$, and $|h_{RD}|^2$ denote the channel power coefficients of the links from the ith antenna at S to D, from the ith antenna at S to R, and from R to D, respectively; and P_S and P_R denote the transmit powers at S and R, respectively. As commonly adopted in the literature [5], we assume an homogeneous network, in which $E[\gamma_{SR,i}] = \bar{\gamma}_{SR}$ and $E[\gamma_{SD,i}] = \bar{\gamma}_{SD}$, for any $i = 0, \ldots, N_t$, that is, all links from each antenna at S to D (or to R) undergo identically distributed fading conditions. Finally, the fixed-gain relaying factor G at R is adjusted according to [11]

$$G^2 = \mathrm{E}\left[\frac{P_R}{P_S|h_{SR_i}|^2 + N_0}\right]. \tag{2.2}$$
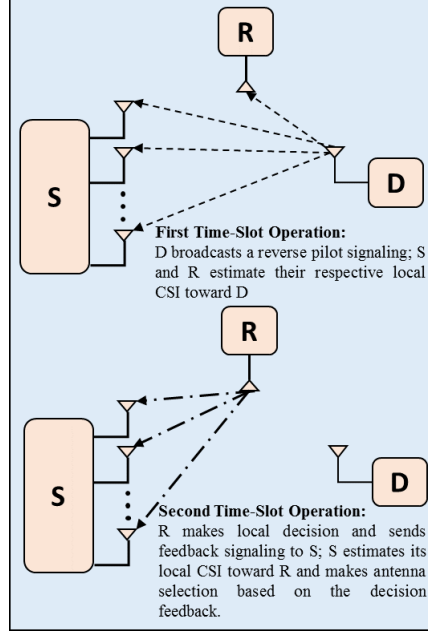
Figure 2.1: Operation of the DAS scheme (reproduced from [5, Fig. 1]).

2.2.2 Antenna Selection Scheme

The optimal selection criterion for TAS/SC chooses the i^*th transmit antenna that maximizes the end-to-end SNR, i.e.,

$$i^* = \arg \max_i [\gamma_i]. \tag{2.3}$$

Although optimal, such a scheme entails a large amount of delay and feedback overhead, due to the full system CSI required for decision. Alternatively, a much simpler suboptimal and distributed solution is provided in [5] In this DAS scheme, the local CSI available at S is exploited to its furthest extent in order to assist the decision, incurring a negligible delay and feedback overhead. In that work, the DAS concept is motivated and supported by an important inequality involving the end-to-end SNR of the MRC reception and the SNRs of the various links [5, Eq. (4)]. Here, since we use SC, the corresponding motivation and support is given by the following inequality [12], [13]

$$\gamma_i < \max \left[\gamma_{SD,i}, \gamma_{SR,i} \min \left[\frac{\gamma_{RD}}{C}, 1 \right] \right] \triangleq \widetilde{\gamma}_i. \tag{2.4}$$

The DAS scheme is performed in two time slots [5], as shown in Fig. 2.1. In the first time slot, D sends to R and S a 1-bit reverse pilot signaling. Then, R and S use this bit to estimate their respective local CSIs γ_{RD} and $\gamma_{SD,i}$. In the second time slot, R compares its local CSI with C, which may produce two outputs: $\gamma_{RD} \geq C$ or $\gamma_{RD} < C$. In the first case, R sends to S a 1-bit message "1" to indicate that $\gamma_{RD} \geq C$ and, in this case, $\gamma_{SD,i}$ and $\gamma_{SR,i}$, which are available at S ($\gamma_{SR,i}$ can be readily estimated from the 1-bit message), are sufficient to apply the selection rule $\max \widetilde{\gamma}_i$. In the second case, R sends to S a 1-bit message "0" to indicate that $\gamma_{RD} < C$. In this case, from (2.4), the application of $\max \widetilde{\gamma}_i$ would depend on the additional knowledge of γ_{RD}, which is unavailable at S.

Then, a suboptimal decision can be attained from the available CSI as proposed by [4], by performing the solely maximization of $\gamma_{SD,i}$. In summary, the transmit-antenna selection rule of the proposed DAS/SC scheme is given as follows:

$$i^* = \begin{cases} \bar{i} = \arg\max\limits_{i} \left[\max\left[\gamma_{SD,i}, \gamma_{SR,i}\right]\right] & \gamma_{RD} \geq C \\ \underline{i} = \arg\max\limits_{i} \left[\gamma_{SD,i}\right] & \gamma_{RD} < C. \end{cases} \tag{2.5}$$

The great advantage of DAS over other AS schemes is its greatly reduced delay/feedback overhead. In conventional AS schemes, $O(\log N_t)$ bits of feedback information are required, as shown in [10], [4], and [7]. In contrast, in the DAS scheme, only a 2-bit pilot/feedback signaling is required, at the cost of some additional hardware complexity at the source.

2.3 Outage Analysis

The outage probability is the probability that the maximum mutual information between source and destination drops below a predefined spectral efficiency R_0 (bits/s/Hz). In our system, it can be formulated as

$$P_{out}^{\text{DAS}} =$$

$$\underbrace{\Pr\left(\gamma_{RD} \geq C, \max\left[\gamma_{SD,\bar{i}}, \frac{\gamma_{SR,\bar{i}}\gamma_{RD}}{\gamma_{RD} + C}\right] < z \triangleq 2^{2R_0} - 1\right)}_{P_1}$$

$$+ \underbrace{\Pr\left(\gamma_{RD} < C, \max\left[\gamma_{SD,\underline{i}}, \frac{\gamma_{SR,\underline{i}}\gamma_{RD}}{\gamma_{RD} + C}\right] < z\right)}_{P_2}. \tag{2.6}$$

Considering the extreme complexity of obtaining an exact closed-form expression for the above outage probability, we derive instead lower and upper bounds of it, based on the inequality in (2.4). The analysis is performed separately for each term P_1 and P_2. We begin by deriving a lower bound for P_1, which can be expressed as

$$\begin{aligned} P_1 &> \Pr\left(\gamma_{RD} \geq C, \max\left[\gamma_{SD,\bar{i}}, \gamma_{SR,\bar{i}} \min\left[\frac{\gamma_{RD}}{C}, 1\right]\right] < z\right) \\ &\overset{(a)}{=} \Pr\left(\gamma_{RD} \geq C, \max\limits_{i}\left[\max\left[\gamma_{SD,i}, \gamma_{SR,i}\right]\right] < z\right) \triangleq P_1^{\text{LB}} \\ &= \Pr\left(\gamma_{RD} \geq C\right)\Pr\left(\gamma_{SD,i} < z\right)^{N_t}\Pr\left(\gamma_{SR,i} < z\right)^{N_t} \\ &= e^{-\frac{C}{\bar{\gamma}_{RD}}}\left(1 - e^{-\frac{z}{\bar{\gamma}_{SD}}}\right)^{N_t}\left(1 - e^{-\frac{z}{\bar{\gamma}_{SR}}}\right)^{N_t}, \end{aligned} \tag{2.7}$$

where, in step (a), we apply the DAS rule given in (2.5) for $\gamma_{RD} \geq C$. Focusing on the high-SNR behavior, an asymptotic analysis of P_1^{LB} is performed. As a result, at high SNR, (2.7) can be expressed, after some algebraic manipulations, as

$$P_1^{\text{LB}} \simeq e^{-\frac{C}{\bar{\gamma}_{RD}}}\left(\frac{z^2}{\bar{\gamma}_{SD}\bar{\gamma}_{SR}}\right)^{N_t}. \tag{2.8}$$

In a similar way, an upper bound for P_1 can be obtained as [12][2]

$$
\begin{aligned}
P_1 &< \Pr\left(\gamma_{RD} \geq C, \max\left[\gamma_{SD,\bar{i}}, \frac{\gamma_{SR,\bar{i}}}{2}\min\left[\frac{\gamma_{RD}}{C}, 1\right]\right] < z\right) \\
&< \Pr\left(\gamma_{RD} \geq C, \max\left[\frac{\gamma_{SD,\bar{i}}}{2}, \frac{\gamma_{SR,\bar{i}}}{2}\min\left[\frac{\gamma_{RD}}{C}, 1\right]\right] < z\right) \\
&= \Pr\left(\gamma_{RD} \geq C, \max_i\left[\max\left[\gamma_{SD,i}, \gamma_{SR,i}\right]\right] < 2z\right) \triangleq P_1^{\mathrm{UB}} \\
&\simeq e^{-\frac{C}{\bar{\gamma}_{RD}}}\left(\frac{(2z)^2}{\bar{\gamma}_{SD}\bar{\gamma}_{SR}}\right)^{N_t}.
\end{aligned}
\tag{2.9}
$$

We now focus on the analysis of the term P_2. Using again the inequality in (2.4) and the DAS rule in (2.5) for $\gamma_{RD} < C$, a lower bound for P_2 is obtained as

$$
\begin{aligned}
P_2 &> \Pr\left(\gamma_{RD} < C, \max\left[\gamma_{SD,\underline{i}}, \gamma_{SR,\underline{i}}\min\left[\frac{\gamma_{RD}}{C}, 1\right]\right] < z\right) \\
&= \Pr\left(\gamma_{RD} < C, \max\left[\gamma_{SD,\underline{i}}, \frac{\gamma_{SR,\underline{i}}\gamma_{RD}}{C}\right] < z\right) = P_2^{\mathrm{LB}} \\
&= \Pr\left(\gamma_{RD} < C, \max\left[\max_j\left[\gamma_{SD,j}\right], \frac{\gamma_{SR,i}\gamma_{RD}}{C}\right] < z\right).
\end{aligned}
\tag{2.10}
$$

Using the concepts of probability theory presented in [4], P_2^{LB} can be further obtained in a single-fold integral form as

$$
\begin{aligned}
P_2^{\mathrm{LB}} &\\
&= \int_0^C f_{\gamma_{RD}}(x)\Pr\left(\max\left[\max_j\left[\gamma_{SD,j}\right], \frac{x}{C}\gamma_{SR,i}\right] < z\right) dx \\
&= \int_0^1 \frac{C}{\bar{\gamma}_{RD}}e^{-\frac{Cy}{\bar{\gamma}_{RD}}}\Pr\left(\max\left[\max_j\left[\gamma_{SD,j}\right], y\gamma_{SR,i}\right] < z\right) dy \\
&= \int_0^1 \frac{C}{\bar{\gamma}_{RD}}e^{-\frac{Cy}{\bar{\gamma}_{RD}}}\Pr\left(\max_j\left[\gamma_{SD,j}\right] < z\right)\Pr\left(y\gamma_{SR,i} < z\right) dy \\
&= \left(1 - e^{-\frac{z}{\bar{\gamma}_{SD}}}\right)^{N_t}\underbrace{\int_0^1 \frac{C}{\bar{\gamma}_{RD}}e^{-\frac{Cy}{\bar{\gamma}_{RD}}}\left(1 - e^{-\frac{z}{y\bar{\gamma}_{SR}}}\right) dy}_{\varphi}.
\end{aligned}
\tag{2.11}
$$

In the Appendix B.1, we have derived a simple high-SNR asymptotic expression for φ. Accordingly, after some algebraic manipulations, P_2^{LB} can be asymptotically expressed as

$$
\begin{aligned}
P_2^{\mathrm{LB}} &\simeq \left(\frac{z}{\bar{\gamma}_{SD}}\right)^{N_t}\left(\frac{z}{\bar{\gamma}_{SR}\mu_2}\left(\ln z - \ln\bar{\gamma}_{RD} - \psi(1) - \psi(2)\right)\right) \\
&= \frac{z^{N_t+1}}{(\bar{\gamma}_{SD})^{N_t}\bar{\gamma}_{RD}\mu_2}\left(\ln\frac{z}{\bar{\gamma}_{RD}} - \psi(1) - \psi(2)\right),
\end{aligned}
\tag{2.12}
$$

where $\mu_2 \triangleq \frac{\bar{\gamma}_{RD}}{\bar{\gamma}_{SR}}$. By following a similar procedure, an upper bound for P_2 can be written as [13]

$$
\begin{aligned}
P_2 &< \Pr\left(\gamma_{RD} < C, \max\left[\gamma_{SD,\underline{i}}, \gamma_{SR,\underline{i}}\min\left[\frac{\gamma_{RD}}{C}, 1\right]\right] < 2z\right) \\
&= P_2^{\mathrm{UB}},
\end{aligned}
\tag{2.13}
$$

---

[2]Note that the exact expression of P_1^{UB} has been omitted. Similarly to P_1^{LB}, this is given by (2.7), but with z replaced by $2z$.

which is seen to have an identical form to P_2^{LB} in (2.10), with z replaced by $2z$. Accordingly, an asymptotic expression for P_2^{UB} can be readily obtained from (2.12) as

$$P_2^{\text{UB}} \simeq \frac{(2z)^{N_t+1}}{(\bar{\gamma}_{SD})^{N_t}\bar{\gamma}_{RD}\mu_2}\left(\ln\frac{2z}{\bar{\gamma}_{RD}} - \psi(1) - \psi(2)\right). \tag{2.14}$$

The derived exact and asymptotic bounds for P_1 and P_2 can be now added as in (2.6) to yield corresponding bounds for P_{out}. In particular, asymptotic lower and upper bounds at high SNR are obtained respectively as

$$P_{out}^{\text{DAS,LB}} \simeq \begin{cases} e^{-\frac{1}{\mu_2}}\left(\frac{z^2}{\bar{\gamma}_{SD}\bar{\gamma}_{SR}}\right)^{N_t} + \frac{z^{N_t+1}}{(\bar{\gamma}_{SD})^{N_t}\bar{\gamma}_{RD}\mu_2} \\ \quad \times \left(\ln\frac{z}{\bar{\gamma}_{RD}} - \psi(1) - \psi(2)\right) & \text{if } N_t = 1 \\[2em] \frac{z^{N_t+1}}{(\bar{\gamma}_{SD})^{N_t}\bar{\gamma}_{RD}\mu_2} \\ \quad \times \left(\ln\frac{z}{\bar{\gamma}_{RD}} - \psi(1) - \psi(2)\right) & \text{if } N_t \geq 2 \end{cases} \tag{2.15}$$

$$P_{out}^{\text{DAS,UB}} \simeq \begin{cases} e^{-\frac{1}{\mu_2}}\left(\frac{(2z)^2}{\bar{\gamma}_{SD}\bar{\gamma}_{SR}}\right)^{N_t} + \frac{(2z)^{N_t+1}}{(\bar{\gamma}_{SD})^{N_t}\bar{\gamma}_{RD}\mu_2} \\ \quad \times \left(\ln\frac{2z}{\bar{\gamma}_{RD}} - \psi(1) - \psi(2)\right) & \text{if } N_t = 1 \\[2em] \frac{(2z)^{N_t+1}}{(\bar{\gamma}_{SD})^{N_t}\bar{\gamma}_{RD}\mu_2} \\ \quad \times \left(\ln\frac{2z}{\bar{\gamma}_{RD}} - \psi(1) - \psi(2)\right) & \text{if } N_t \geq 2. \end{cases} \tag{2.16}$$

Finally, from (2.15) and (2.16), it can be seen that DAS/SC exhibits a full diversity order of $N_t + 1$, the same achieved by DAS/MRC [5]. This, allied to the simplicity of SC, renders the proposed DAS/SC scheme highly attractive in practice.

2.4 Numerical Results and Discussions

In this section, we assess the outage performance of the proposed DAS/SC scheme by investigating some representative examples and scenarios. Monte Carlo simulation is performed to provide the exact performance as well as to support our analytical bounds. Without loss of generality, we assume that the end-to-end spectral efficiency is $R_0 = 1$ bit/s/Hz and that the path loss exponent is $\beta = 4$. We also assume that the channel mean power is proportional to $d^{-\beta}$, with d being the distance between the transceivers. The distance between S and D is normalized to unity, as in [5].[3]

Fig. 2.2 presents the outage performance versus d_{SR} for both DAS and optimal AS schemes using two and three antennas at the source. From this figure, we observe that the outage performance of DAS/SC improves when the relay is closer to destination, approaching the performance of optimal AS. This behavior is due to the probability of $\gamma_{RD} \geq C$ being higher when d_{SR} is close to unity, thus causing the DAS selection rule being

---

[3]Again, as in [5], we assume a linear network topology, in which S and R transmit with the same SNR P, and $d_{SD} = d_{SR} + d_{RD}$, where d_{SD}, d_{SR}, and d_{RD} represent the distance of the links $S \to D$, $S \to R$, and $R \to D$, respectively. The corresponding average link SNRs can be formulated as $\bar{\gamma}_{SD} = Pd_{SD}^{-\beta}$, $\bar{\gamma}_{SR} = Pd_{SR}^{-\beta}$, and $\bar{\gamma}_{RD} = Pd_{RD}^{-\beta}$.
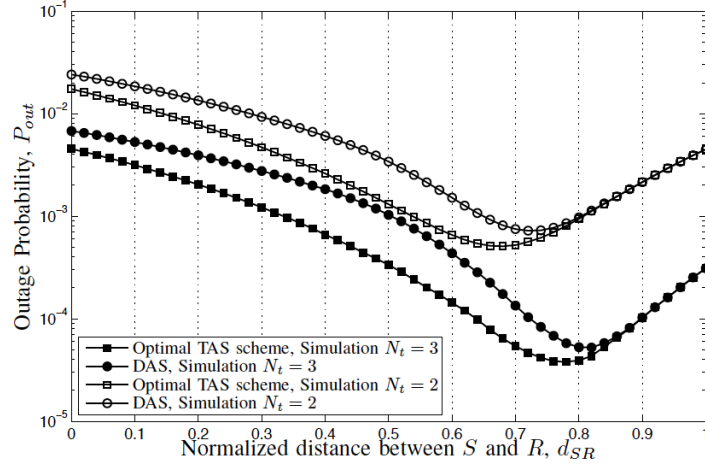
Figure 2.2: Comparison of different AS schemes in terms of outage probability ($P = 10$ dB).
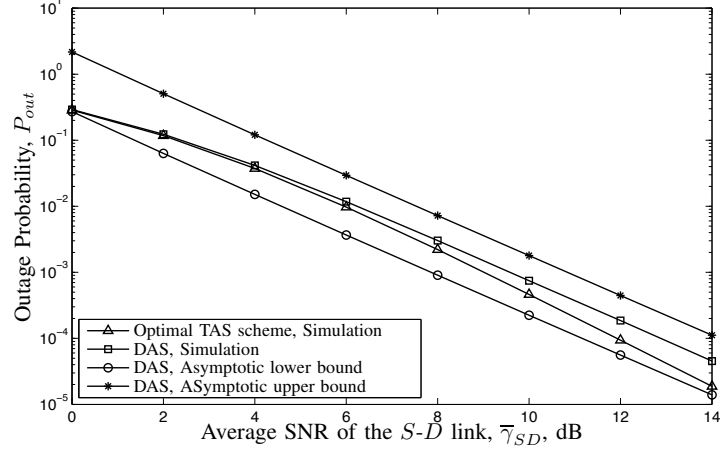
Figure 2.3: Outage probability versus average SNR of the $S \to D$ link for different AS schemes ($d_{SR} = 0.7$, $N_t = 2$).

indeed optimal during most of the time. A similar behavior is reported for DAS/MRC in [5]. In particular, when $N_t = 2$, the DAS/SC is observed to achieve its best performance with $d_{SR} \simeq 0.7$; when $N_t = 3$, the best performance is observed with $d_{SR} \simeq 0.75$. In both cases, the outage probability of DAS/SC is seen to be very close to that of the optimal AS scheme. We now address two representative scenarios in order to assess the outage performance of DAS while varying the average SNR. The distance values used were established based on the results of several Monte Carlo simulations, which confirmed the observation from Fig. 2.2 that, for relays placed at $0.6 - 0.8$, the outage performance of DAS/SC is improved and close to the optimal AS scheme. In other words, the relay has been positioned to comply with these best-performance cases. Fig. 2.3 depicts the outage probability of the first proposed scenario, configured with $d_{SR} = 0.7$ and $N_t = 2$, and Fig. 2.4 depicts a second scenario with $d_{SR} = 0.8$ and $N_t = 3$. In both scenarios, we see that the performance of the proposed DAS/SC is comparable to that of the optimal AS scheme, while widely outperforming this in terms of feedback overhead. Additionally, we
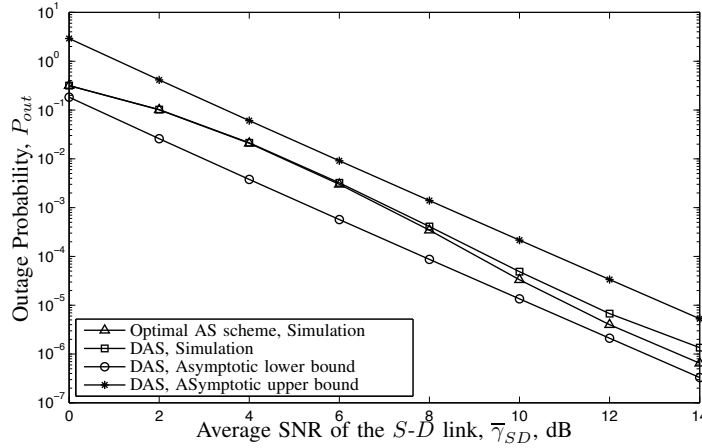
Figure 2.4: Outage probability versus average SNR of the $S \to D$ link for different AS schemes ($d_{SR} = 0.75$, $N_t = 3$).

note from the curves that our analytical bounds for the outage probability approach the exact (simulated) values in the medium-to-high SNR regime.

2.5 Conclusions

In this paper, we presented an analysis of the outage performance for a dual-hop fixed-gain AF relaying system that combines DAS and SC techniques for distributed transmit antenna selection and diversity exploitation. We derived closed-form expressions for lower and upper high-SNR asymptotic bounds of the outage probability. Monte Carlo simulations have been performed to support the derived analytical expressions. Our results reveal that the proposed scheme achieves full diversity order. More importantly, the underlying distributed strategy of transmit antenna selection is shown to perform closely to the costly optimal centralized solution.

Bibliography

[1] E. Li, S. Yang, and H. Wu, "A source-relay selection scheme in two-way amplify-and-forward relaying networks," *IEEE Commun. Lett.*, vol. 16, no. 10, pp. 1564–1567, Oct. 2012.

[2] V. N. Q. Bao, B. P. L. Phuong, and T. T. Thanh, "Performance analysis of TAS/SC-based MIMO decode-and-forward relaying for multi-hop transmission over Rayleigh fading channels," in *Proc. International Conference on Communications and Electronics (ICCE)*, Santander, Spain, 1–6 Jul. 2012, pp. 150–155.

[3] P. Yeoh, M. Elkashlan, N. Yang, D. Benevides da Costa, and T. Duong, "MIMO multi-relay networks with TAS/MRC and TAS/SC in Weibull fading channels," in *Proc. IEEE 23rd International Symposium on Personal Indoor and Mobile Radio Communications (PIMRC)*, Sydney, NSW, 9–12 Sep. 2012, pp. 2314–2318.

[4] H. A. Suraweera, P. J. Smith, A. Nallanathan, and J. S. Thompson, "Amplify-and-forward relaying with optimal and suboptimal transmit antenna selection," *IEEE Trans. Wireless Commun.*, vol. 10, no. 6, pp. 1874–1885, Jun. 2011.

[5] H. Ding, J. Ge, D. B. da Costa, and T. Tsiftsis, "A novel distributed antenna selection scheme for fixed-gain amplify-and-forward relaying systems," *IEEE Trans. Veh. Technol.*, vol. 61, no. 6, pp. 2836–2842, Jul. 2012.

[6] G. Amarasuriya, C. Tellambura, and M. Ardakani, "Performance analysis framework for transmit antenna selection strategies of cooperative MIMO AF relay networks," *IEEE Trans. Veh. Technol.*, vol. 60, no. 7, pp. 3030–3044, Sep. 2011.

[7] Z. Chen, J. Yuan, and B. Vucetic, "Analysis of transmit antenna selection/maximal-ratio combining in Rayleigh fading channels," *IEEE Trans. Veh. Technol.*, vol. 54, no. 4, pp. 1312–1321, Jul. 2005.

[8] M. K. Simon and M. Alouini, *Digital Communication over Fading Channels: A Unified Approach to Performance Analysis.* John Wiley & Sons, 2000.

[9] I. L. Karaevli, I. Altunbas, and G. Karabulut, "Performance analysis of cooperative relaying scheme applying TAS/SC," in *Proc. IEEE Symposium on Computers and Communications (ISCC)*, Riccione, Italy, 22–25 Jun. 2010, pp. 127–132.

[10] S. Sanayei and A. Nosratinia, "Antenna selection in MIMO systems," *IEEE Commun. Mag.*, vol. 42, no. 10, pp. 68–73, Oct. 2004.

[11] G. K. Karagiannidis, "Performance bounds of multihop wireless communications with blind relays over generalized fading channels," *IEEE Trans. Wireless Commun.*, vol. 5, no. 3, pp. 498–503, Mar. 2006.

[12] H. Ding, J. Ge, D. B. da Costa, and Z. Jiang, "Diversity and coding gains of fixed-gain amplify-and-forward with partial relay selection in Nakagami-m fading," *IEEE Commun. Lett.*, vol. 14, no. 8, pp. 734–736, Aug. 2010.

[13] F. Xu, F. C. M. Lau, and D. W. Yue, "Diversity order for amplify-and-forward dual-hop systems with fixed-gain relay under Nakagami fading channels," *IEEE Trans. Wireless Commun.*, vol. 9, no. 1, pp. 92–98, Jan. 2010.

[14] I. S. Gradshteyn and I. M. Ryzhik, *Table of Integrals, Series, and Products*, 7th ed. San Diego, CA: Academic Press, 2007.

Chapter 3

Distributed Suboptimal Schemes for TAS/SC and TAS/LS in Fixed-Gain AF Relaying Systems

Diana C. González, Daniel B. da Costa, and José Cândido S. Santos Filho[1]

Abstract

We design and analyze two distributed suboptimal schemes for transmit-antenna selection and link selection in a dual-hop, fixed-gain, amplify-and-forward relaying system, composed by one multi-antenna source, one single-antenna destination, and one single-antenna relay. The proposed schemes share the same antenna-selection policy, but differ from each other in the way the direct or relaying link is selected for communication. In a first scheme, the link is selected after transmission, at the destination; in a second scheme, it is selected before transmission, at the source. A great advantage of the proposed schemes over the optimal centralized solution is their low and constant delay/feedback overhead, regardless of the number of transmit antennas. In addition, the second scheme brings an improved spectral efficiency, once it saves one time slot when selecting the direct link. We derive analytical lower and upper bounds for the outage probability of the first scheme, in single-fold integral form, and exact closed-form expressions for the outage probability and mean spectral efficiency of the second scheme. We also perform an asymptotic analysis, showing that the first scheme achieves full diversity order, whereas the second scheme achieves full diversity order minus one, as a penalty for its improved spectral efficiency.

3.1 Introduction

The combined use of multiple-input–multiple-output (MIMO) techniques and cooperative communications has been suggested by many studies as a promising strategy to enhance the reliability and capacity of wireless systems [1]-[3]. Such multiantenna and multiterminal systems can fully benefit from spatial diversity and spatial multiplexing, thereby alleviating the adverse impact of spectrum scarcity and multipath fading on communications. In practice, however, implementing those systems may be rather intricate, due to restrictions in power, complexity and antenna size. For this reason, realistic implementations commonly end up by limiting the use of multiantenna devices to few particular nodes of the network, and by severely restricting the total amount of multiple antennas in these devices [4].

The deleterious effects of multipath fading on communications can be mitigated by means of transmit as well as receive diversity techniques. At the transmitter side, these techniques include the appropriate selection of one (desirably the best) out of many transmit antennas available for transmission. This is known as transmit antenna selection (TAS). At the receiver side, they include the use of several diversity-combining methods such as maximal-ratio combining (MRC) and selection combining (SC) [2].

Many recent studies have proposed and analyzed the combined use of TAS at the source and MRC at the destination (also known as TAS/MRC) in dual-hop networks (see, for example, [4], [5], and the references therein). The TAS/MRC combination has become popular because TAS reduces the complexity and power requirements at the transmitter—although it is not an optimal beamforming technique [6]—and because MRC is the optimal linear combining technique [7]. However, performance has its cost. The MRC scheme requires many channel estimations and a complex hardware setup, for each antenna needs a dedicated receiver chain [8]. In contrast, the SC implementation is much simpler, avoiding the channel estimations and allowing for a single receiver chain that is shared among the multiple antennas. Therefore, since both combining techniques achieve the same diversity order, SC represents an attractive balance between complexity and performance.

Notwithstanding its attractiveness, the TAS/SC combination in relaying networks has been considered in very few studies, including the following. In [2], a regenerative, multi-hop, decode-and-forward (DF) MIMO relaying system was analyzed. In this system, it was assumed that the receivers have perfect channel state information (CSI) and feed back the best-antenna selection to the transmitter, using partial CSI. In [3], a performance comparison between the TAS/MRC and TAS/SC schemes in MIMO relaying networks was performed. It was found that, in balanced hops, the advantage of TAS/MRC over TAS/SC in terms of reliability does not depend on the number of relays. In [8], the performance of a cooperative system with a single-antenna relay, a multiantenna source, and a multiantenna destination was evaluated. In this system, by using feedback CSI from the destination, a TAS scheme was employed at the source in order to choose the transmit antenna with the largest end-to-end signal-to-noise ratio (SNR). In [10], the performance of a MIMO amplify-and-forward (AF) cooperative system based on TAS/SC was analyzed in terms of outage probability and symbol error rate, under the Rayleigh

fading condition. An antenna selection technique that achieves full diversity order while reducing complexity and power consumption was applied in [11], where the performance of a MIMO cooperative network was analyzed by using joint transmit and receive antenna selection (TRAS) over a flat and asymmetric Nakagami-m fading channel. Finally, in [12], the performance of a dual hop AF system based on TAS and generalized selection combining (GSC) was analyzed, considering a network composed by a single-antenna relay, a multiantenna source, and a multiantenna destination, under the presence of error in the feedback relay-source channel.

In TAS schemes, some feedback from the network nodes is usually needed to provide the transmitter with enough information for the appropriate selection of the transmit antenna that gives the best overall performance. This feedback contains CSI from the various direct and relaying links of the network. In centralized optimal schemes, a full feedback is necessary, containing CSI of all the links. Such a feedback requires a number of bits that varies according to the number of source and destination antennas [13]. As the number of antennas increase, the delay and complexity involved in a full feedback may rapidly become prohibitive in practice. Therefore, suboptimal distributed transmit-antenna selection (DAS) schemes, which alleviate the need for CSI feedback, are of great practical interest.

Both centralized (TAS) and distributed (DAS) antenna-selection schemes, when used along with diversity-combining techniques at the destination, do improve the system reliability, but at the expense of spectral efficiency. This is because in these schemes the relaying link is always employed for transmission, which requires an additional time slot. As a result, the spectral efficiency of schemes such as TAS/MRC, TAS/SC, DAS/MRC, and DAS/SC is only half of that one attained by direct transmission. A way for reducing the loss in spectral efficiency while maintaining part of the gain in reliability is to move the diversity-combining method from destination to source. Indeed, in our scenario, this is only applicable to the SC case. In this case, instead of choosing (the best) between direct or relaying link at the destination after the transmission has taken place, the system can make this choice at the source, before transmission. This is generally known as link selection (LS). Of course, LS may require some CSI at the source and may be somewhat less reliable than SC in practice, due to partial or imperfect CSI. But LS improves the spectral efficiency when compared to SC, once it saves one time slot when the direct link happens to be selected for transmission. Because of this, the average spectral efficiency of the combinations TAS/LS and DAS/LS lies somewhere between that one attained by direct transmission and half of this. In [14], the performance of optimal centralized LS schemes was analyzed for variable-gain as well as fixed-gain relaying with transmit beamforming, achieving a full diversity order. The same scenario was considered in [15], but under a distributed LS mechanism, which was shown to provide a nearly-optimal outage performance while reducing the CSI feedback overhead.

In this work, we design and analyze a DAS/SC scheme and a DAS/LS scheme for a dual-hop, fixed-gain, amplify-and-forward relaying network with one multiantenna source, one single-antenna relay, and one single-antenna destination. Both schemes employ the same DAS policy, based on a policy introduced for a DAS/MRC scheme in [5]. However, differently from [5], which uses MRC, we propose to use either (i) SC, in order to reduce

the system complexity, or (ii) LS, in order to increase the spectral efficiency at the expense of some reliability. A great advantage of our proposals is the requirement of CSI with constant and low delay/feedback overhead, despite the number of transmit antennas. The main contributions of this work include the following:

- Two new distributed low-cost schemes—DAS/SC and DAS/LS—are designed for cooperative relaying systems;

- Analytical lower and upper bounds are derived in single-fold integral form for the outage probability of the DAS/SC scheme;

- Exact closed-form expressions are derived for the outage probability and mean spectral efficiency of the DAS/LS scheme;

- Closed-form asymptotic analysis at high SNR is performed for these bounds and exact expressions, revealing that (i) the DAS/SC scheme achieves full diversity order, equal to the number of transmit antennas plus one, and that (ii) the DAS/LS scheme achieves a nearly-full diversity order, equal to the number of transmit antennas;

- The outage probability and spectral efficiency of the proposed schemes are compared against those of centralized (TAS/MRC and TAS/SC) and distributed (DAS/MRC) schemes previously investigated in the literature. In terms of outage probability, the proposed distributed schemes are shown to perform closely to the costly centralized solutions. In terms of spectral efficiency, the proposed DAS/LS scheme is shown to outperform the other schemes.

The remainder of this paper is organized as follows. In Section 3.2, we present the system model and the proposed DAS/SC and DAS/LS schemes. In Section 3.3, we analyze the outage probability of the proposed schemes, by deriving either analytical bounds or exact closed-form expressions. An asymptotic analysis is also performed, allowing for the evaluation of the diversity order of the two schemes. In Section 3.4, we derive the spectral efficiency of the DAS/LS scheme[2]. In Section 3.5, we present some numerical results and discussions. Finally, in Section 3.6, we summarize the main conclusions of this work.

Throughout this paper, $f_W(\cdot)$ and $F_W(\cdot)$ denote the probability density function (PDF) and the cumulative distribution function (CDF) of a generic random variable W, respectively, $E[\cdot]$ denotes expectation, and $\Pr(\cdot)$ denotes probability.

3.2   System Model and Proposed Schemes

We consider a half-duplex dual-hop wireless communication system containing a source S with N_t antennas, a single-antenna fixed-gain AF relay R, and a single-antenna destination D. Furthermore, we consider that all the links are subject to independent flat Rayleigh fading and additive white Gaussian noise (AWGN) with mean power N_0. The terminals are assumed to operate on a time-division multiple access basis.

---

[2]As aforementioned, the spectral efficiency of the DAS/SC is trivial, being half of that one attained by direct transmission.

3.2.1 DAS/SC Scheme

Before the data transmission, a DAS operation is performed at S, in order to find the desirably-best transmit antenna that maximizes the end-to-end SNR. After that, a conventional two-slots cooperative transmission takes place. As previously indicated, this system is similar to the one presented in [5], but differs from that in the sense that the direct-link and relaying-link signals are now combined at D by means of SC, instead of MRC. Accordingly, the end-to-end received SNR from the ith antenna at S to D can be expressed as

$$\gamma_i = \max\left(Y_i, \frac{X_i Z}{Z + C}\right), \tag{3.1}$$

where $Y_i \triangleq \frac{P_S}{N_0}|h_{Y,i}|^2$ is the direct-link received SNR from the ith antenna at S to D, $X_i \triangleq \frac{P_S}{N_0}|h_{X,i}|^2$ is the first-hop received SNR from the ith antenna at S to R, $Z \triangleq \frac{P_R}{N_0}|h_Z|^2$ is the second-hop received SNR from R to D, and $C = 1 + \overline{X}$, with $\overline{X} = E[X_i]$. In these expressions, P_S denotes the transmit power at S; P_R denotes the transmit power at R; and $|h_{Y_i}|^2$, $|h_{X_i}|^2$, and $|h_Z|^2$ denote the channel power coefficients of the links from the ith antenna at S to D, from the ith antenna at S to R, and from R to D, respectively. As commonly adopted in the literature [5], we assume an homogeneous network topology, in which $E[X_i] = \overline{X}$ and $E[Y_i] = \overline{Y}$, for any $i = 0, \ldots, N_t$, that is, all links from each antenna at S to D (or to R) undergo identically distributed fading conditions, and $E[Z] = \overline{Z}$. Because of the Rayleigh-fading assumption, Y_i, X_i, and Z are exponentially distributed variates.

Although optimal, such a scheme requires the full-system CSI for decision, demanding a large amount of delay and feedback overhead. Alternatively, we capitalize on a much simpler suboptimal and distributed decision policy introduced in [5] for a DAS/MRC scheme. In this scheme, the decision is almost exclusively assisted by the local CSI available at S, incurring a negligible delay and feedback overhead. In that work, the DAS policy is motivated and supported by an important inequality involving the end-to-end SNR of the MRC output and the SNRs of the various network links [5, Eq. (4)]. Here, instead of MRC, we use SC, so that the corresponding motivation and support is given by the following inequality [16], [17]:

$$\gamma_i < \max\left[Y_i, X_i \min\left[\frac{Z}{C}, 1\right]\right] \triangleq \widetilde{\gamma}_i. \tag{3.2}$$

In an optimal centralized TAS/SC scheme, the i^*th transmit antenna is selected that maximizes the end-to-end SNR, i.e.,

$$i^* = \arg\max_i \left[\gamma_i\right]. \tag{3.3}$$

The DAS operation is accomplished in two time slots [5], as shown in Fig. 3.1. In the first time slot, D sends to R and S a 1-bit reverse pilot signaling. Then, based on this message, R and S estimate their respective local CSIs Z and Y_i. In the second time slot, R compares its local CSI with C, yielding two possible outputs: $Z \geq C$ or $Z < C$. In
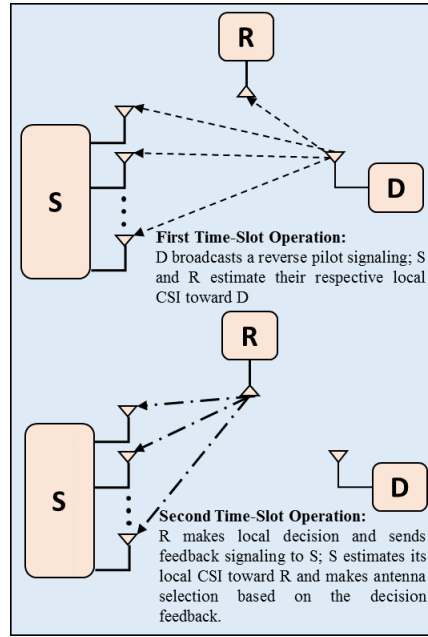
Figure 3.1: The DAS operation (reproduced from [5, Fig. 1]).

the first case, R reports to S a 1-bit message "1" indicating that $Z \geq C$, and thus the local CSIs[3] Y_i and X_i at S suffice to support the selection rule $\max \tilde{\gamma}_i = \max\left[\max\left[Y_i, X_i\right]\right]$, since $\min\left[Z/C, 1\right] = 1$. In the second case, R transmits to S a 1-bit message "0" indicating that $Z < C$. In this case, $\min\left[Z/C, 1\right] = Z/C$, so that the application of the selection rule $\max \tilde{\gamma}_i = \max\left[\max\left[Y_i, X_i Z/C\right]\right]$ would depend on the additional knowledge of the second-hop CSI Z, which is unavailable at S. Instead, if $Z < C$, a relaxed suboptimal decision can be attained from the available local CSI at S, by performing the solely maximization of the direct-link SNRs Y_i, as proposed in [4]. In summary, the transmit-antenna selection rule of the proposed DAS/SC scheme is given as follows:

$$i^* = \begin{cases} \bar{i} = \arg\max_i \left[\max\left[Y_i, X_i\right]\right], & \text{if } Z \geq C \\ \underline{i} = \arg\max_i \left[Y_i\right], & \text{if } Z < C. \end{cases} \tag{3.4}$$

In conventional TAS schemes, $O(\log N_t)$ bits of feedback information are required, as shown in [13], [4], and [7]. The great advantage of DAS over centralized TAS schemes is its reduced delay/feedback overhead. In the proposed DAS/SC scheme, only a 2-bit pilot/feedback signaling is required, at the cost of some additional hardware complexity.

After the i^*th transmit antenna has been selected, the transmission process is carried out in two time slots. Subsequently, SC is employed at D to choose either the direct-link signal or the relaying-link signal, so as to maximize the end-to-end received SNR γ of the proposed DAS/SC scheme, which is then written as

$$\gamma = \max\left(Y_{i^*}, \frac{X_{i^*} Z}{Z + C}\right). \tag{3.5}$$

---

[3] X_i can be readily estimated at S from the 1-bit message sent by R.

Table 3.1: Link-Selection Rule

CSI	Decision
$Z \geq C,\, Y_{i^*} \geq X_{i^*}$	Direct Link
$Z \geq C,\, X_{i^*} \geq Y_{i^*}$	Relaying Link
$Z < C$	Direct Link

3.2.2 DAS/LS Scheme

The transmit-antenna selection rule of the proposed DAS/LS scheme is identical to that of the previous DAS/SC scheme, as described in (3.4). But now, in order to improve the spectral efficiency, the selection between direct or relaying link shall be moved from D to S and performed before transmission. From (3.5), it can be seen that such a LS operation would in principle require the knowledge of Y_{i^*}, X_{i^*}, and Z at S. However, since Z is no local CSI at S, this task would demand a centralized implementation with considerable feedback overhead. Alternatively, as in the DAS operation, we shall employ a suboptimal distributed approach to perform the LS decision.

The central idea is to support the link selection not based on the exact maximum SNR value γ_{i^*} between the preselected direct and relaying links, but on the upper bound $\widetilde{\gamma}_{i^*}$ of this value, as defined by the inequality in (3.2). In other words, the link selection is performed by comparing Y_{i^*} with $X_{i^*} \min[Z/C, 1]$, as follows. Recall that S knows whether $Z \geq C$ or $Z < C$, from the previous DAS operation. When $Z \geq C$, then $X_{i^*} \min[Z/C, 1] = X_{i^*}$, and thus S compares Y_{i^*} with X_{i^*}. If $Y_{i^*} \geq X_{i^*}$, the direct link is selected; if $Y_{i^*} < X_{i^*}$, the relaying link is selected. On the other hand, when $Z < C$, then $X_{i^*} \min[Z/C, 1] = X_{i^*} Z/C$, but since Z is not available as a local CSI at S to support the decision, then the direct link is selected (somewhat arbitrarily). Table 3.1 summarizes the link-selection rule. Accordingly, the end-to-end received SNR γ of the proposed DAS/LS scheme can be written as

$$\gamma = \begin{cases} Y_{i^*}, & \text{if } Z \geq C \text{ and } Y_{i^*} \geq X_{i^*} \\ \frac{X_{i^*} Z}{Z + C}, & \text{if } Z \geq C \text{ and } Y_{i^*} < X_{i^*} \\ Y_{i^*}, & \text{if } Z < C. \end{cases} \tag{3.6}$$

After the i^*th transmit antenna and the communication link have been selected, the transmission process is carried out in one or two time slots, depending on whether the direct link or the relaying link was selected, respectively. As a result, the mean spectral efficiency of this scheme outperforms that of the DAS/SC scheme, as shall be detailed in Section 3.4.

3.3 Outage Analysis

In this section, we investigate the outage probability of the proposed schemes, by deriving single-fold integral-form analytical bounds for DAS/SC and exact closed-form expressions for DAS/LS. An asymptotic analysis is also performed in each case, revealing the diversity order of the proposed schemes.

3.3.1 DAS/SC Scheme

The outage probability is defined as the probability that the maximum mutual information between source and destination drops below a predefined target spectral efficiency $\Re_s$ (bits/s/Hz). In the proposed DAS/SC scheme, using (3.4) and (3.5), the outage probability can be formulated as

$$
P_{out}^{\text{DAS/SC}} =
$$

$$
\underbrace{\Pr\left(Z \geq C, \max\left[Y_{\bar{i}}, \frac{X_{\bar{i}}Z}{Z+C} \right] < \tau \triangleq 2^{2\Re_s} - 1 \right)}_{I_1} + \underbrace{\Pr\left(Z < C, \max\left[Y_{\underline{i}}, \frac{X_{\underline{i}}Z}{Z+C} \right] < \tau \right)}_{I_2}.
$$

$$(3.7)$$

Considering the mathematical intricacy of an exact analysis for the above outage probability, we shall instead obtain lower and upper bounds of it. In this task, we exploit the following known relationships:

$$
\frac{X_i}{2} \min\left[\frac{Z}{C}, 1 \right] \leq \frac{X_i Z}{Z+C} \leq X_i \min\left[\frac{Z}{C}, 1 \right].
$$

$$(3.8)$$

Next, we analyze the terms I_1 and I_2 separately. We begin by deriving a lower bound for I_1, which can be expressed as

$$
\begin{aligned}
I_1 &\overset{(a)}{\geq} \Pr\left(Z \geq C, \max\left[Y_{\bar{i}}, X_{\bar{i}} \min\left[\frac{Z}{C}, 1 \right] \right] < \tau \right) \\
&\overset{(b)}{=} \Pr\left(Z \geq C, \max_i \left[\max\left[Y_i, X_i \right] \right] < \tau \right) \triangleq I_1^{\text{LB}} \\
&= \Pr\left(Z \geq C \right) \Pr\left(Y_i < \tau \right)^{N_t} \Pr\left(X_i < \tau \right)^{N_t} \\
&\overset{(c)}{=} e^{-\frac{C}{\bar{Z}}} \left(1 - e^{-\frac{\tau}{\bar{Y}}} \right)^{N_t} \left(1 - e^{-\frac{\tau}{\bar{X}}} \right)^{N_t},
\end{aligned}
$$

$$(3.9)$$

where, in step (a), we used (3.8); in step (b), we applied the DAS rule given in (3.4) for $Z \geq C$; and, in step (c), we used the well-known expression for the CDF of exponentially distributed variates. Focusing on the high-SNR behavior, an asymptotic analysis of I_1^{LB} is performed. As a result, at high SNR, (3.9) can be expressed, after some algebraic manipulations, as

$$
I_1^{\text{LB}} \simeq e^{-\frac{C}{\bar{Z}}} \left(\frac{\tau^2}{\bar{Y}\bar{X}} \right)^{N_t}.
$$

$$(3.10)$$

In a similar way, an upper bound for I_1 and its asymptote can be obtained as[4]

$$I_1 \leq \Pr\left(Z \geq C, \max\left[Y_{\bar{i}}, \frac{X_{\bar{i}}}{2}\min\left[\frac{Z}{C}, 1\right]\right] < \tau\right)$$

$$\leq \Pr\left(Z \geq C, \max\left[\frac{Y_{\bar{i}}}{2}, \frac{X_{\bar{i}}}{2}\min\left[\frac{Z}{C}, 1\right]\right] < \tau\right)$$

$$= \Pr\left(Z \geq C, \max_i\left[\max\left[Y_i, X_i\right]\right] < 2\tau\right) \triangleq I_1^{\mathrm{UB}}$$

$$= e^{-\frac{C}{\overline{Z}}}\left(1 - e^{-\frac{2\tau}{\overline{Y}}}\right)^{N_t}\left(1 - e^{-\frac{2\tau}{\overline{X}}}\right)^{N_t} \tag{3.11}$$

$$\simeq e^{-\frac{C}{\overline{Z}}}\left(\frac{(2\tau)^2}{\overline{Y}\,\overline{X}}\right)^{N_t}. \tag{3.12}$$

We proceed by analyzing the term I_2. Using again the relationships in (3.2) and the DAS rule in (3.4) for $Z < C$, a lower bound for I_2 can be formulated as

$$I_2 \geq \Pr\left(Z < C, \max\left[Y_{\underline{i}}, X_{\underline{i}}\min\left[\frac{Z}{C}, 1\right]\right] < \tau\right)$$

$$= \Pr\left(Z < C, \max\left[Y_{\underline{i}}, \frac{X_i Z}{C}\right] < \tau\right) \triangleq I_2^{\mathrm{LB}}$$

$$= \Pr\left(Z < C, \max\left[\max_j\left[Y_j\right], \frac{X_i Z}{C}\right] < \tau\right). \tag{3.13}$$

Using a similar approach to that presented in [4], I_2^{LB} can be further developed into a single-fold integral form as

$$I_2^{\mathrm{LB}} = \int_0^C f_Z(u)\Pr\left(\max\left[\max_j\left[Y_j\right], \frac{u}{C}X_i\right] < \tau\right) du$$

$$= \int_0^1 \frac{C}{\overline{Z}}e^{-\frac{Cv}{\overline{Z}}}\Pr\left(\max\left[\max_j\left[Y_j\right], vX_i\right] < \tau\right) dv$$

$$= \int_0^1 \frac{C}{\overline{Z}}e^{-\frac{Cv}{\overline{Z}}}\Pr\left(\max_j\left[Y_j\right] < \tau\right)\Pr\left(vX_i < \tau\right) dv$$

$$= \left(1 - e^{-\frac{\tau}{\overline{Y}}}\right)^{N_t}\underbrace{\int_0^1 \frac{C}{\overline{Z}}e^{-\frac{Cv}{\overline{Z}}}\left(1 - e^{-\frac{\tau}{v\overline{X}}}\right) dv}_{\varphi}. \tag{3.14}$$

A simple closed-form asymptotic expression for φ at high SNR is derived in Appendix C.1. Accordingly, after some algebraic manipulations, I_2^{LB} can be asymptotically expressed as

$$I_2^{\mathrm{LB}} \simeq \left(\frac{\tau}{\overline{Y}}\right)^{N_t}\left(\frac{\tau}{\overline{X}\mu_2}\left(\ln\overline{Z} - \ln\tau + \psi(1) + \psi(2) - \Gamma\left(0, \frac{C}{\overline{Z}}\right)\right)\right)$$

$$= \frac{\tau^{N_t+1}}{(\overline{Y})^{N_t}\overline{X}\mu_2}\left(\ln\frac{\overline{Z}}{\tau} + \psi(1) + \psi(2) - \Gamma\left(0, \frac{C}{\overline{Z}}\right)\right), \tag{3.15}$$

where $\mu_2 \triangleq \frac{\overline{Z}}{\overline{X}}$. By following a similar procedure, an upper bound for I_2 can be written as

$$I_2 \leq \Pr\left(Z < C, \max\left[Y_{\underline{i}}, X_{\underline{i}}\min\left[\frac{Z}{C}, 1\right]\right] < 2\tau\right) = I_2^{\mathrm{UB}}, \tag{3.16}$$

---

[4]Note that the expressions for I_1^{UB} are identical to those for I_1^{LB}, but with τ replaced by 2τ.

which is seen to have an identical form to I_2^{LB} in (3.13), with τ replaced by 2τ. Accordingly, an asymptotic expression for I_2^{UB} can be readily obtained from (3.15) as

$$I_2^{\text{UB}} \simeq \frac{(2\tau)^{N_t+1}}{(\overline{Y})^{N_t}\overline{X}\mu_2} \left(\ln \frac{\overline{Z}}{2\tau} + \psi(1) + \psi(2) - \Gamma\left(0, \frac{C}{\overline{Z}}\right) \right). \tag{3.17}$$

The derived exact and asymptotic lower (or upper) bounds for I_1 and I_2 can be now added as in (3.7) to yield a corresponding lower (or upper) bound for $P_{out}^{\text{DAS/SC}}$. In particular, asymptotic lower and upper bounds at high SNR are obtained respectively as

$$P_{out}^{\text{DAS/SC,LB}} \simeq \begin{cases} e^{-\frac{1}{\mu_2}} \left(\frac{\tau^2}{\overline{YX}}\right)^{N_t} + \frac{\tau^{N_t+1}}{(\overline{Y})^{N_t}\overline{X}\mu_2} \\ \times \left(\ln \frac{\overline{Z}}{\tau} + \psi(1) + \psi(2) - \Gamma\left(0, \frac{C}{\overline{Z}}\right) \right) & \text{if } N_t = 1 \\[2ex] \frac{\tau^{N_t+1}}{(\overline{Y})^{N_t}\overline{X}\mu_2} \\ \times \left(\ln \frac{\overline{Z}}{\tau} + \psi(1) + \psi(2) - \Gamma\left(0, \frac{C}{\overline{Z}}\right) \right) & \text{if } N_t \geq 2 \end{cases} \tag{3.18}$$

$$P_{out}^{\text{DAS/SC,UB}} \simeq \begin{cases} e^{-\frac{1}{\mu_2}} \left(\frac{(2\tau)^2}{\overline{YX}}\right)^{N_t} + \frac{(2\tau)^{N_t+1}}{(\overline{Y})^{N_t}\overline{X}\mu_2} \\ \left(\ln \frac{\overline{Z}}{2\tau} + \psi(1) + \psi(2) - \Gamma\left(0, \frac{C}{\overline{Z}}\right) \right) & \text{if } N_t = 1 \\[2ex] \frac{(2\tau)^{N_t+1}}{(\overline{Y})^{N_t}\overline{X}\mu_2} \\ \times \left(\ln \frac{\overline{Z}}{2\tau} + \psi(1) + \psi(2) - \Gamma\left(0, \frac{C}{\overline{Z}}\right) \right) & \text{if } N_t \geq 2. \end{cases} \tag{3.19}$$

Finally, from (3.18) and (3.19), it can be seen that the proposed DAS/SC scheme exhibits a full diversity order of $N_t + 1$, the same achieved by DAS/MRC [5]. This, allied to the simplicity of SC, renders the proposed DAS/SC scheme highly attractive in practice.

3.3.2 DAS/LS Scheme

Using (3.4) and (3.6), the outage probability of the proposed DAS/LS scheme can be formulated as

$$P_{out}^{DAS/LS} = \underbrace{\Pr\left(Z \geq C, Y_{\bar{i}} \geq X_{\bar{i}}, Y_{\bar{i}} < \upsilon \triangleq 2^{\Re_s} - 1 \right)}_{J_1}$$

$$+ \underbrace{\Pr\left(Z \geq C, X_{\bar{i}} \geq Y_{\bar{i}}, \frac{X_{\bar{i}}Z}{Z+C} < \tau \triangleq 2^{2\Re_s} - 1 \right)}_{J_2}$$

$$+ \underbrace{\Pr\left(Z < C, Y_{\underline{i}} < \upsilon \right)}_{J_3}. \tag{3.20}$$

Note that, for a given target espectral efficiency $\Re_s$, two different SNR outage levels must now be defined, namely $\upsilon \triangleq 2^{\Re_s} - 1$ and $\tau \triangleq 2^{2\Re_s} - 1$, in order to comply with the use of one or two time slots for transmission, respectively. Next we derive exact closed-form expressions and high-SNR asymptotes for J_1, J_2 and J_3.

Exact Analysis

We begin with the term J_1, which can be developed as

$$J_1 = \Pr\left(Z \geq C, Y_{\bar{i}} \geq X_{\bar{i}}, Y_{\bar{i}} < \upsilon\right)$$
$$= \Pr\left(Z \geq C\right) \int_0^{\upsilon} f_{X_{\bar{i}}}(x) \Pr\left(x \leq Y_{\bar{i}} < \upsilon\right) dx$$
$$= \Pr\left(Z \geq C\right) \left(F_{X_{\bar{i}}}(z) F_{Y_{\bar{i}}}(\upsilon) - \int_0^{\upsilon} f_{X_{\bar{i}}}(x) F_{Y_{\bar{i}}}(x)\, dx\right). \tag{3.21}$$

Using the DAS rule in (3.4) and knowing that the channel power coefficients are exponentially distributed, J_1 can be further developed as

$$J_1 = e^{-\frac{C}{\overline{Z}}}\left(\left(1 - e^{-\frac{\upsilon}{\overline{X}}}\right)^{N_t}\left(1 - e^{-\frac{\upsilon}{\overline{Y}}}\right)^{N_t} - \underbrace{\int_0^{\upsilon} N_t\left(1 - e^{-\frac{x}{\overline{X}}}\right)^{N_t-1}\frac{1}{\overline{X}}e^{-\frac{x}{\overline{X}}}\left(1 - e^{-\frac{x}{\overline{Y}}}\right)^{N_t} dx}_{\alpha}\right), \tag{3.22}$$

where the term α can be rewritten using the binomial theorem [18, Eq. (3.1.1)] as

$$\alpha = \int_0^{\upsilon} N_t \sum_{j=0}^{N_t}\binom{N_t-1}{j}(-1)^j e^{-\frac{jx}{\overline{X}}}\frac{1}{\overline{X}}e^{-\frac{x}{\overline{X}}}\sum_{m=0}^{N_t}\binom{N_t}{m}(-1)^m e^{-\frac{mx}{\overline{Y}}}\, dx$$
$$= \frac{N_t}{\overline{X}}\sum_{j=0}^{N_t}\sum_{m=0}^{N_t}\binom{N_t-1}{j}(-1)^j\binom{N_t}{m}(-1)^m \int_0^{\upsilon} e^{-\frac{jx}{\overline{X}}}e^{-\frac{mx}{\overline{Y}}}e^{-\frac{x}{\overline{X}}}\, dx. \tag{3.23}$$

Replacing (3.23) into (3.22), and after some algebraic simplifications, an exact closed-form expression for J_1 is then obtained as

$$J_1 = e^{-\frac{C}{\overline{Z}}}\left(\left(1 - e^{-\frac{\upsilon}{\overline{X}}}\right)^{N_t}\left(1 - e^{-\frac{\upsilon}{\overline{Y}}}\right)^{N_t}\right.$$
$$\left. - N_t\sum_{j=0}^{N_t}\sum_{m=0}^{N_t}\binom{N_t-1}{j}(-1)^j\binom{N_t}{m}(-1)^m\frac{\left(1 - e^{-\upsilon\left(\frac{(1+j)}{\overline{X}}+\frac{m}{\overline{Y}}\right)}\right)\overline{Y}}{m\overline{X}+(1+j)\overline{Y}}\right). \tag{3.24}$$

We now proceed with the evaluation of the term J_2. Using a similar approach to that used for J_1, the term J_2 can be developed as

$$J_2 = \Pr\left(Z \geq C, X_{\bar{i}} > Y_{\bar{i}}, \frac{X_{\bar{i}}Z}{Z+C} < \tau\right)$$
$$= \int_C^{\infty} f_Z(z) \Pr\left(Y_{\bar{i}} < X_{\bar{i}} < \frac{(C+z)\tau}{z}\right) dz$$
$$= \int_C^{\infty} f_Z(z) \int_0^{\tau+\frac{C\tau}{z}} f_{Y_{\bar{i}}}(y) \Pr\left(y < X_{\bar{i}} < \tau + \frac{C\tau}{z}\right) dy dz$$
$$= \int_C^{\infty} f_Z(z) F_{Y_{\bar{i}}}(\tau + \frac{C\tau}{z}) F_{X_{\bar{i}}}(\tau + \frac{C\tau}{z}) dz - \int_C^{\infty} f_Z(z) \int_0^{\tau+\frac{C\tau}{z}} f_{Y_{\bar{i}}}(y) F_{X_{\bar{i}}}(y)\, dy dz. \tag{3.25}$$

Using the DAS rule in (3.4) and knowing that the channel power coefficients are exponentially distributed, J_2 can be further developed as

$$J_2 = \underbrace{\int_C^\infty \frac{1}{\overline{Z}} e^{-\frac{z}{\overline{Z}}} \left(1 - e^{-\frac{\tau + \frac{C\tau}{z}}{\overline{Y}}}\right)^{N_t} \left(1 - e^{-\frac{\tau + \frac{C\tau}{z}}{\overline{X}}}\right)^{N_t} dz}_{\Phi}$$

$$- \underbrace{\int_C^\infty \frac{1}{\overline{Z}} e^{-\frac{z}{\overline{Z}}} \int_0^{\tau + \frac{C\tau}{z}} N_t \left(1 - e^{-\frac{y}{\overline{Y}}}\right)^{N_t - 1} \frac{1}{\overline{Y}} e^{-\frac{y}{\overline{Y}}} \left(1 - e^{-\frac{y}{\overline{X}}}\right)^{N_t} dy\, dz.}_{\Psi} \qquad (3.26)$$

Infinite-series representations for the terms Φ and Ψ are derived in Appendices C.2 and C.3, respectively. Using these representations into (3.26), an exact infinite-series representation for J_2 is then obtained as

$$J_2 = e^{-\frac{C}{\overline{Z}}} + \sum_{k=0}^\infty \sum_{j=1}^{N_t} \binom{N_t}{j} (-1)^j \frac{(-\tau C)^k}{k!} \frac{\Gamma(1 - k, \frac{c}{z})}{\overline{Z}^k}$$

$$\left(e^{-j\tau} j^k \left(\frac{e^{-\frac{1}{\overline{X}}}}{(\overline{X})^k} + \frac{e^{\frac{-1}{\overline{Y}}}}{(\overline{Y})^k} \right) + \sum_{m=1}^{N_t} \binom{N_t}{m} (-1)^m e^{-\tau\left(\frac{m}{\overline{Y}} + \frac{j}{\overline{X}}\right)} \left(\frac{m}{\overline{Y}} + \frac{j}{\overline{X}} \right)^k \right)$$

$$+ \sum_{j=0}^{N_t} \sum_{m=0}^{N_t} \binom{N_t}{j} (-1)^j \binom{N_t}{m} (-1)^m \frac{\overline{X}}{m\overline{Y} + (1+j)\overline{X}}$$

$$\left(e^{-\frac{C}{\overline{Z}}} - e^{-\tau\left(\frac{(1+j)}{\overline{Y}} + \frac{m}{\overline{X}}\right)} \sum_{k=0}^\infty \frac{\left(-\tau C\left(\frac{(1+j)}{\overline{Y}} + \frac{m}{\overline{X}}\right)\right)^k}{k!} \frac{\Gamma(1 - k, \frac{C}{\overline{Z}})}{\overline{Z}^k} \right). \qquad (3.27)$$

Finally, we address the analysis of the term J_3, which is indeed simple. Using the DAS rule in (3.4) and knowing that the channel power coefficients are exponentially distributed, an exact closed-form expression for J_3 is obtained as

$$\begin{aligned} J_3 &= \Pr\left(Z < C, Y_{\underline{i}} < \upsilon\right) \\ &= \Pr\left(Z < C\right) \Pr\left(Y_{\underline{i}} < \upsilon\right) \\ &= \Pr\left(Z < C\right) \Pr\left(\max_i \left[Y_i < \upsilon\right]\right) \\ &= \left(1 - e^{-\frac{C}{\overline{Z}}}\right) \left(1 - e^{-\frac{\upsilon}{\overline{Y}}}\right)^{N_t}. \end{aligned} \qquad (3.28)$$

Asymptotic Analysis

In order to assess the diversity order of the proposed DAS/LS scheme, we derive a high-SNR asymptote for its outage probability. We address the terms J_1, J_2 and J_3 separately. Using the Maclaurin series for the exponential function into (3.24) while preserving only the lowest-order terms in $1/\overline{X}$ and $1/\overline{Y}$, a high-SNR asymptote for J_1 is obtained as

$$\begin{aligned} J_1 &\simeq e^{-\frac{C}{\overline{Z}}} \left(\left(\frac{\upsilon}{\overline{X}}\right)^{N_t} \left(\frac{\upsilon}{\overline{Y}}\right)^{N_t} - N_t \sum_{j=0}^{N_t} \sum_{m=0}^{N_t} \binom{N_t - 1}{j} (-1)^j \binom{N_t}{m} (-1)^m \frac{\upsilon}{\overline{X}} \right) \\ &\simeq e^{-\frac{1}{\mu_2}} \left(\frac{\upsilon^2}{\overline{X}\,\overline{Y}}\right)^{N_t}. \end{aligned} \qquad (3.29)$$

Similarly, preserving in (3.27) only the lowest-order terms in $1/\overline{Y}$ and $1/\overline{X}$, J_2 can be expressed as

$$J_2 \simeq e^{-\frac{C}{Z}}$$

$$+ \sum_{j=1}^{N_t} \binom{N_t}{j}(-1)^j \left(e^{-\frac{\tau j}{X}}e^{-\frac{C}{Z}} + e^{-\frac{\tau j}{Y}}e^{-\frac{C}{Z}}\right) + \sum_{j=1}^{N_t}\sum_{m=1}^{N_t} \binom{N_t}{j}(-1)^j \binom{N_t}{m}(-1)^m e^{-\tau\left(\frac{m}{Y}+\frac{j}{X}\right)}e^{-\frac{C}{Z}}$$

$$+ \sum_{j=0}^{N_t}\sum_{m=0}^{N_t} \frac{\binom{N_t}{j}(-1)^j \binom{N_t}{m}(-1)^m N_t\overline{X}}{m\overline{Y}+(1+j)\overline{X}} \left(e^{-\frac{C}{Z}} - e^{-\tau\left(\frac{(1+j)}{Y}+\frac{m}{X}\right)}e^{-\frac{C}{Z}}\right). \tag{3.30}$$

After the combined use of the Maclaurin series for the exponential function and the binomial theorem into (3.30), a high-SNR asymptote for J_2 is obtained as

$$J_2 \simeq e^{-\frac{C}{Z}}\left(1 + \sum_{j=1}^{N_t} \binom{N_t}{j}(-1)^j \left(e^{-j\frac{\tau}{X}} + e^{-j\frac{\tau}{Y}}\right) + \sum_{j=1}^{N_t}\sum_{m=1}^{N_t} \binom{N_t}{j}(-1)^j \binom{N_t}{m}(-1)^m e^{-\tau\left(\frac{m}{Y}+\frac{j}{X}\right)}\right.$$

$$\left. + \sum_{j=0}^{N_t}\sum_{m=0}^{N_t} \binom{N_t}{j}(-1)^j \binom{N_t}{m}(-1)^m \frac{N_t\overline{X}}{m\overline{Y}+(1+j)\overline{X}} \left(\tau\left(\frac{(1+j)}{\overline{Y}}+\frac{m}{\overline{X}}\right)\right)\right)$$

$$\simeq e^{-\frac{C}{Z}}\left(-1 + \left(1-e^{-\frac{\tau}{X}}\right)^{N_t} + \left(1-e^{-\frac{\tau}{Y}}\right)^{N_t} + \left(-1+\left(1-e^{-\frac{\tau}{X}}\right)^{N_t}\right)\left(-1+\left(1-e^{-\frac{\tau}{Y}}\right)^{N_t}\right)\right.$$

$$\left. + \sum_{j=0}^{N_t}\sum_{m=0}^{N_t} \binom{N_t}{j}(-1)^j \binom{N_t}{m}(-1)^m \frac{N_t\tau}{\overline{Y}}\right)$$

$$\simeq e^{-\frac{C}{Z}}\left(-1 + \left(\frac{\tau}{\overline{X}}\right)^{N_t} + \left(\frac{\tau}{\overline{Y}}\right)^{N_t} + \left(-1+\left(\frac{\tau}{\overline{X}}\right)^{N_t}\right)\left(-1+\left(\frac{\tau}{\overline{Y}}\right)^{N_t}\right)\right)$$

$$\simeq e^{-\frac{1}{\mu_2}}\left(\frac{\tau^2}{\overline{XY}}\right)^{N_t}. \tag{3.31}$$

Finally, a high-SNR asymptote for J_3 is obtained as

$$J_3 = \left(1-e^{-\frac{1}{\mu_2}}\right)\left(1-e^{-\frac{\upsilon}{\overline{Y}}}\right)^{N_t}$$

$$\simeq \left(1-e^{-\frac{1}{\mu_2}}\right)\left(\frac{\upsilon}{\overline{Y}}\right)^{N_t}. \tag{3.32}$$

Note from (3.29), (3.31), and (3.32) that both J_1 and J_2 provide a diversity order of $2N_t$, whereas J_3 provides a diversity order of N_t. The high-SNR performance is governed by the lowest-order term, so that the asymptote for the outage probability of the proposed DAS/LS scheme equals the asymptote for J_3, that is,

$$P_{out}^{DAS/LS} \simeq \left(1-e^{-\frac{1}{\mu_2}}\right)\left(\frac{\upsilon}{\overline{Y}}\right)^{N_t}, \tag{3.33}$$

which gives a diversity order of N_t. This is less than the full diversity order of $N_t + 1$ achieved by the proposed DAS/SC scheme, but it is compensated by an improved spectral efficiency, as shown next.

3.4 Mean Spectral Efficiency

In this section, we address the mean spectral efficiency $\overline{\Re}_s$ of the proposed schemes. For comparison, consider a certain spectral efficiency $\Re_s$ attained by direct transmission. In the DAS/SC scheme, the transmission process is accomplished in two time slots, because the relaying link is always used for transmission. Therefore, the mean spectral efficiency of the DAS/SC scheme is half of that one attained by direct transmission, that is,[5]

$$\overline{\Re}_s^{\text{DAS/SC}} = \frac{\Re_s}{2}. \tag{3.34}$$

In contrast, in the DAS/LS scheme, the transmission process is accomplished in one or two time slots, depending on whether the direct link or the relaying link is selected for transmission, respectively. If the direct link is selected, then the spectral efficiency equals $\Re_s$; otherwise, if the relaying link is selected, then the spectral efficiency equals $\Re_s/2$. Therefore, the mean spectral efficiency of the DAS/LS scheme lies somewhere between $\Re_s/2$ and $\Re_s$, and can be obtained from the LS rule in Table 3.1 as

$$
\begin{aligned}
\overline{\Re}_s^{\text{DAS/LS}} =& \Re_s \Pr\left(Z \geq C, Y_{\bar{i}} \geq X_{\bar{i}}\right) + \frac{\Re_s}{2} \Pr\left(Z \geq C, X_{\bar{i}} > Y_{\bar{i}}\right) + \Re_s \Pr\left(Z < C\right) \\
=& \Re_s \Pr\left(Z \geq C\right) \Pr\left(Y_{\bar{i}} \geq X_{\bar{i}}\right) + \frac{\Re_s}{2} \Pr\left(Z \geq C\right) \Pr\left(X_{\bar{i}} > Y_{\bar{i}}\right) + \Re_s \Pr\left(Z < C\right) \\
\overset{(a)}{=}& \Re_s \left(1 - \frac{1}{2} e^{-\frac{C}{\overline{Z}}} \Pr\left(X_{\bar{i}} > Y_{\bar{i}}\right)\right) \\
\overset{(b)}{=}& \Re_s \left(1 - \frac{1}{2} e^{-\frac{C}{\overline{Z}}} \sum_{j=1}^{N_t} \sum_{m=1}^{N_t} \binom{N_t - 1}{j - 1} (-1)^j \binom{N_t}{m} (-1)^m \frac{N_t \overline{X}}{m\overline{Y} + j\overline{X}}\right),
\end{aligned} \tag{3.35}
$$

where in step (a) we used the fact that Z is an exponentially distributed variate, and in step (b) we used the exact closed-form expression derived for $\Pr\left(X_{\bar{i}} > Y_{\bar{i}}\right)$ in Appendix C.4.

3.5 Numerical Results and Discussions

In this section, we assess the outage probability and spectral efficiency of the proposed schemes by applying our analytical expressions to representative sample cases. Monte Carlo simulations are also performed, either as a check for the analytical expressions or as a way to address other schemes in the literature. Besides the DAS/SC and DAS/SC schemes proposed here, we also include the DAS/MRC scheme proposed in [5] and the centralized optimal schemes TAS/SC and TAS/MRC in our comparisons. Without loss of generality, we assume that the target spectral efficiency is $\Re_s = 1$ bit/s/Hz and that the path loss exponent is $\beta = 4$. We also assume that the channel mean power is proportional to $d^{-\beta}$, with d being the distance between the transceivers. As in [5], the distance d_{SD} of the S-D link is normalized to unity, and a linear network topology is considered, in which S and R transmit with the same power $P_S = P_R = P$, and $d_{SD} = d_{SR} + d_{RD}$, where d_{SR} and d_{RD} represent the distance of the links S-R and R-D, respectively. The corresponding average

---

[5]From a practical viewpoint, we assume here that the direct and relaying-link transmissions employ modulation schemes with identical alphabet sizes.
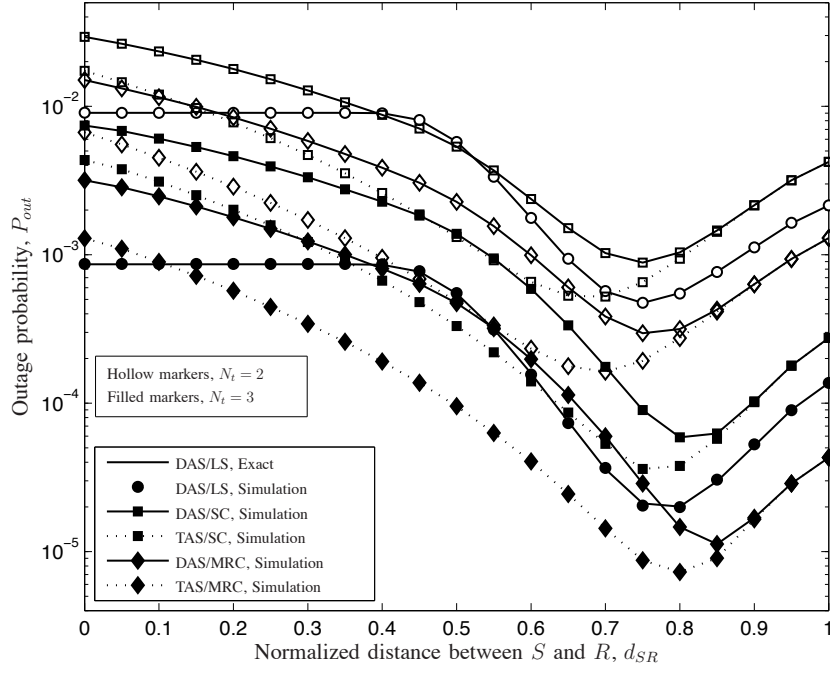
Figure 3.2: Comparison of proposed and existing antenna-selection schemes in terms of outage probability ($P_S/N_0 = P_R/N_0 = 10$ dB).

link SNRs can be formulated as $\overline{Y} = Pd_{SD}^{-\beta}/N_0$, $\overline{X} = Pd_{SR}^{-\beta}/N_0$, and $\overline{Z} = Pd_{RD}^{-\beta}/N_0$. Fig. 3.2 presents the simulated outage performance versus d_{SR} for the proposed (DAS/SC and DAS/LS) and existing (DAS/MRC, TAS/SC, and TAS/MRC) schemes, using two and three antennas at the source. Our exact analytical expression for DAS/LS is also included in the figure. As expected, TAS/MRC is better than DAS/MRC, followed by TAS/SC and DAS/SC. However, when DAS/LS is included in the comparison, an interesting and subtle behavior is observed. In principle, one may expect the performance of DAS/LS to fall below that of DAS/SC, because the former preselects the direct or relaying link at the source before transmission, based on *partial* CSI, while the latter postselects one of the two links at the destination after transmission, based on *full* CSI. On the other hand, as mentioned before, DAS/LS has an improved spectral efficiency when compared to DAS/SC and to the other schemes (TAS/MRC, DAS/MRC, and TAS/SC), since it saves one time slot when the direct link is selected for transmission. Incidentally, in this work, the outage event is defined in terms of a target spectral efficiency, so that the corresponding SNR threshold decreases when a single time slot is used for transmission ($2^{\Re_s} - 1$ for single time slot, $2^{2\Re_s} - 1$ for two time slots). Taking all this into consideration, DAS/LS may outperform the other schemes (even the TAS/MRC!), depending on the relay position and on the number of source antennas, as observed in Fig. 3.2. From the figure, we observe that the outage performance of DAS/SC improves when the relay is placed closer to the destination, approaching the performance of the optimal centralized TAS/SC scheme. This behavior is due to the probability of $Z \geq C$ being higher when d_{RD} is smaller, thus causing the DAS selection rule being indeed optimal during most of the time. A similar behavior is observed for DAS/MRC, in accordance with the reports in [5].
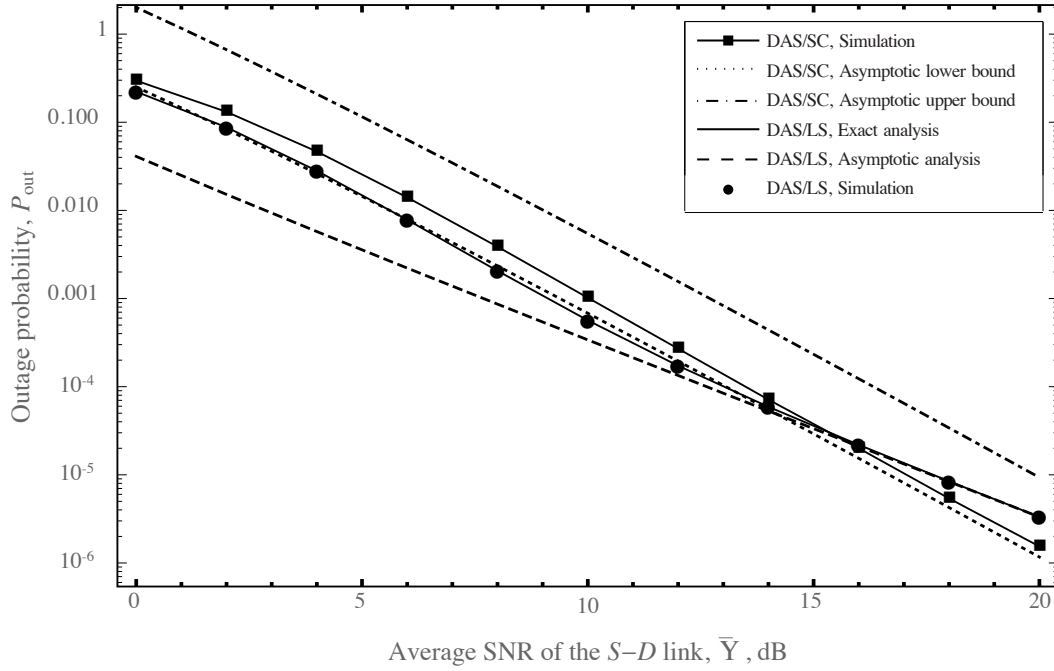
Figure 3.3: Outage probability versus average SNR of the S-D link for the proposed schemes ($d_{SR} = 0.7$, $N_t = 2$).

In particular, the best performance achieved by DAS/SC is observed around the relay positions $d_{SR} \simeq 0.7$ for $N_t = 2$ and $d_{SR} \simeq 0.75$ for $N_t = 3$. These values are also close to those for DAS/MRC. The best-performance relay positions for DAS/LS are slightly closer to the destination, around $d_{SR} \simeq 0.75$ for $N_t = 2$ and $d_{SR} \simeq 0.80$ for $N_t = 3$. Interestingly, we also notice from the figure that the relay position has little impact on the performance of DAS/LS when the relay is closer to the source. This is because in that scenario there is a high probability of $Z < C$, causing the relaying link to be ignored by the LS rule.

Based on the best-performance relay positions established from Fig. 3.2 and confirmed by several other simulations, we now address two representative scenarios in order to assess the outage probability of the proposed schemes DAS/SC and DAS/LS while varying the average SNR. In the first scenario, depicted in Fig. 3.3, we set $d_{SR} = 0.7$ and $N_t = 2$; in the second scenario, depicted in Fig. 3.4, we set $d_{SR} = 0.8$ and $N_t = 3$. In all of the cases, we observe a perfect match between the simulation and the exact analytical results for DAS/LS. As for DAS/SC, note that the derived lower bound turns out to be a very tight approximation to the exact (simulated) outage performance at medium to high SNR. On the other hand, regardless of the tightness of these bounds, they are of great practical importance to assess the system performance, because no other analytical solution (exact or approximate) exists to this problem. In addition, the presented bounds allow for the exact derivation of the system diversity order, which is a key performance parameter. From the figures, note the difference between the diversity orders of the two schemes, which are equal to $N_t + 1$ and N_t, for DAS/SC and DAS/LS, respectively. At high SNR, this one-unit-lower diversity order has a strong deleterious impact on the performance of DAS/LS scheme.

Fig. 3.5 shows a comparison of the proposed and existing schemes, in terms of outage
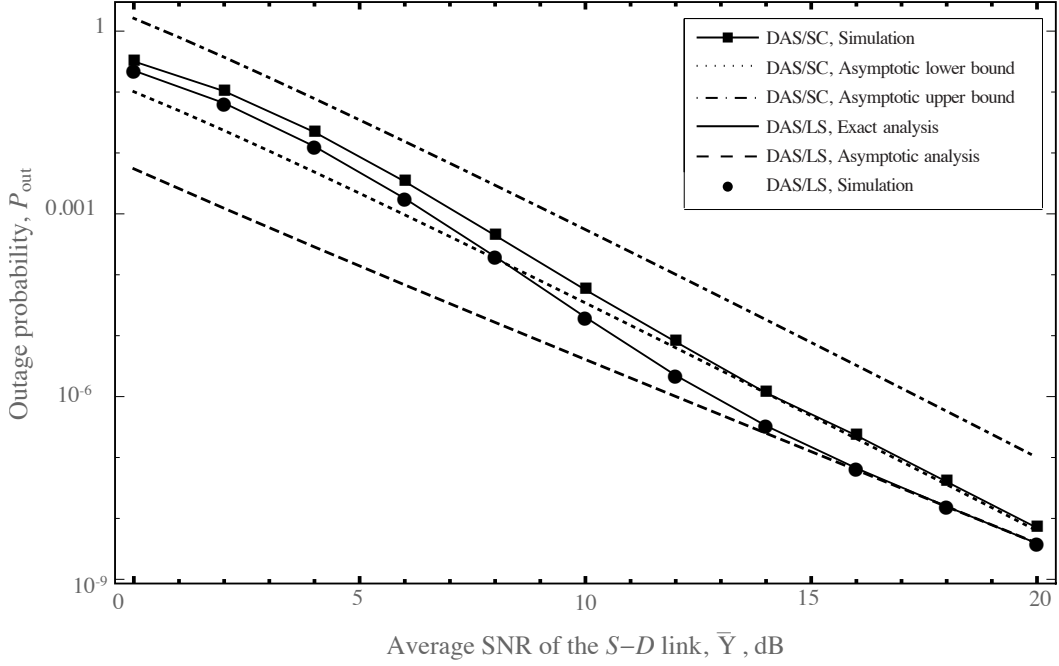
Figure 3.4: Outage probability versus average SNR of the *S-D* link for the proposed schemes ($d_{SR} = 0.75$, $N_t = 3$).

probability, for the two scenarios of Figs. 3.3 and 3.4. In both cases, we see that the performance of the proposed DAS/SC is comparable to that of the optimal TAS/SC scheme, while widely outperforming this in terms of feedback overhead. Moreover, we observe that the DAS/SC scheme proposed here represents an SNR loss of approx. 1.8 dB and 1.3 dB, for $N_t = 2$ and $N_t = 3$, respectively, when compared with the DAS/MRC. As for the DAS/LS scheme, as explained before, it may outperform the other schemes at low to medium SNR, depending on the relay position and on the number of source antennas. On the other hand, DAS/LS gives the worst performance among all the schemes at the high-SNR regime, due to its reduced diversity order. In Fig. 3.6, we compare the impact of relay position on the mean spectral efficiency of the proposed schemes, for $N_t = 2$ and $N_t = 3$. When R is placed close to S, we observe that $\overline{\Re}_s$ rapidly increases towards $\Re_s$. The reason for this is that the probability of $Z < C$ is high in this case, causing the direct link to be most frequently selected for transmission. In contrast, when R is moved toward D, the referred probability increases, causing the relaying link to be more frequently selected, so that $\overline{\Re}_s$ tends to decrease. Indeed, after reaching a minimum, $\overline{\Re}_s$ increases back to $\Re_s/2$ as R approaches D. By comparing these curves against the corresponding outage curves given in Fig. 2, we notice that the minimum values of $\overline{\Re}_s$ and P_{out} are not achieved for the same relay position. From the figures, the best-outage relay position seems to represent a good compromise between outage probability and spectral efficiency for the proposed DAS/LS scheme. It is noteworthy that the spectral efficiency of all of the remaining schemes is only $\Re/2$.
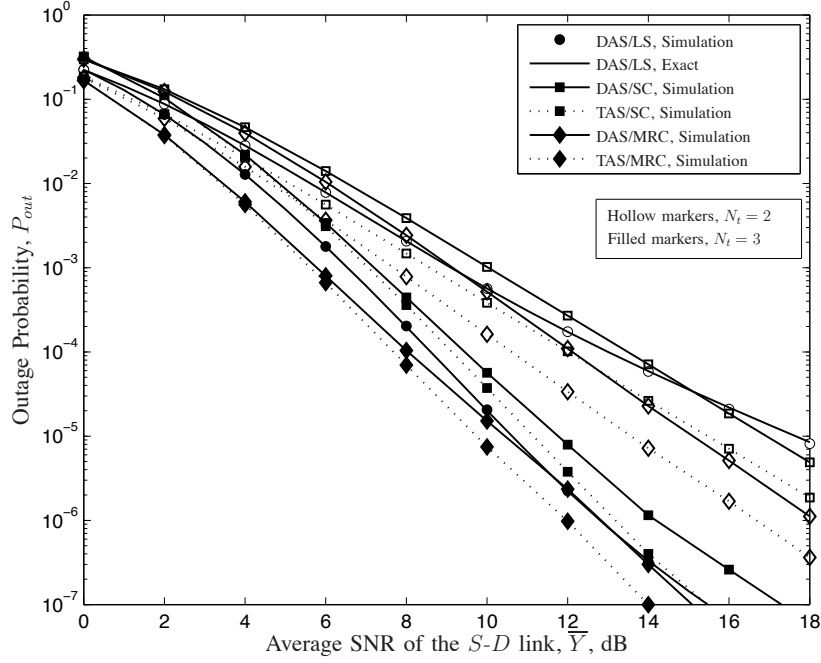
Figure 3.5: Outage probability versus average SNR of the S-D link for proposed and existing schemes ($d_{SR} = 0.7$, $N_t = 2$ and $d_{SR} = 0.8$, $N_t = 3$).
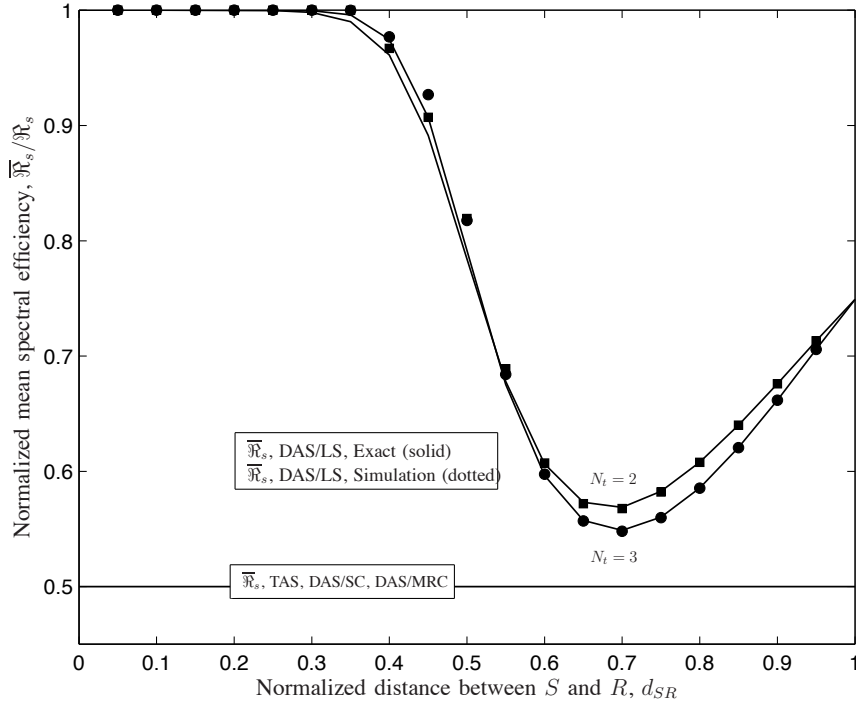
Figure 3.6: Comparison of proposed schemes in terms of spectral efficiency ($P_S/N_0 = P_R/N_0 = 10$ dB).

3.6 Conclusions

This paper proposed and analyzed two distributed suboptimal schemes for the joint selection of transmit antenna and communication link in dual-hop, fixed-gain, amplify-

and-forward relaying networks with a N_t-antenna source, a single-antenna relay, and a single-antenna destination. Both schemes follow the same antenna-selection policy, but distinct link-selection policies. In the first scheme, DAS/SC, in order to select either the direct link or the relaying link, selection combining is employed at the destination after transmission. In the second scheme, DAS/LS, link-selection is used instead at the source, before transmission. We derived single-fold, integral-form lower and upper bounds for the outage probability of the DAS/SC scheme, and exact analytical expressions for the outage probability of the DAS/LS scheme. Besides, we derived closed-form high-SNR asymptotic expressions for outage probability of both schemes. The derived analytical expressions have been checked via Monte Carlo simulations. Our asymptotic results revealed that the DAS/SC scheme achieves a full diversity order of $N_t + 1$, and that the DAS/LS scheme achieves a lower diversity order of N_t. In addition, we derived an exact closed-form expression for the mean spectral efficiency of the DAS/LS scheme, which is higher than those of the proposed DAS/SC and of other existing schemes. Importantly, the underlying distributed strategies of transmit-antenna selection were shown to perform closely to the costly optimal centralized solutions.

Bibliography

[1] E. Li, S. Yang, and H. Wu, "A source-relay selection scheme in two-way amplify-and-forward relaying networks," *IEEE Commun. Lett.*, vol. 16, no. 10, pp. 1564–1567, Oct. 2012.

[2] V. N. Q. Bao, B. P. L. Phuong, and T. T. Thanh, "Performance analysis of TAS/SC-based MIMO decode-and-forward relaying for multi-hop transmission over Rayleigh fading channels," in *Proc. International Conference on Communications and Electronics (ICCE)*, Santander, Spain, 1–6 Jul. 2012, pp. 150–155.

[3] P. Yeoh, M. Elkashlan, N. Yang, D. Benevides da Costa, and T. Duong, "MIMO multi-relay networks with TAS/MRC and TAS/SC in Weibull fading channels," in *Proc. IEEE 23rd International Symposium on Personal Indoor and Mobile Radio Communications (PIMRC)*, Sydney, NSW, 9–12 Sep. 2012, pp. 2314–2318.

[4] H. A. Suraweera, P. J. Smith, A. Nallanathan, and J. S. Thompson, "Amplify-and-forward relaying with optimal and suboptimal transmit antenna selection," *IEEE Trans. Wireless Commun.*, vol. 10, no. 6, pp. 1874–1885, Jun. 2011.

[5] H. Ding, J. Ge, D. B. da Costa, and T. Tsiftsis, "A novel distributed antenna selection scheme for fixed-gain amplify-and-forward relaying systems," *IEEE Trans. Veh. Technol.*, vol. 61, no. 6, pp. 2836–2842, Jul. 2012.

[6] G. Amarasuriya, C. Tellambura, and M. Ardakani, "Performance analysis framework for transmit antenna selection strategies of cooperative MIMO AF relay networks," *IEEE Trans. Veh. Technol.*, vol. 60, no. 7, pp. 3030–3044, Sep. 2011.

[7] Z. Chen, J. Yuan, and B. Vucetic, "Analysis of transmit antenna selection/maximal-ratio combining in Rayleigh fading channels," *IEEE Trans. Veh. Technol.*, vol. 54, no. 4, pp. 1312–1321, Jul. 2005.

[8] M. K. Simon and M. Alouini, *Digital communication over fading channels: A unified approach to performance analysis.* John Wiley & Sons, 2000.

[9] I. L. Karaevli, I. Altunbas, and G. Karabulut, "Performance analysis of cooperative relaying scheme applying TAS/SC," in *Proc. IEEE Symposium on Computers and Communications (ISCC)*, Riccione, Italy, 22–25 Jun. 2010, pp. 127–132.

[10] I. L. Karaevli, G. Karabulut Kurt, and I. Altunbas, "Analysis of cooperative MIMO transmission system with transmit antenna selection and selection combining," *Wirel. Commun. Mob. Comput.*, vol. 12, no. 14, pp. 1266–1275, Oct. 2010.

[11] A. Yilmaz and O. Kucur, "Performance of joint transmit and receive antenna selection in dual hop amplify-and-forward relay network over Nakagami-m fading channels," *Wirel. Commun. Mob. Comput.*, vol. 14, no. 1, pp. 103–114, Jan. 2014.

[12] ——, "End-to-end performance of transmit antenna selection and generalized selection combining in dual-hop amplify-and-forward relay network in the presence of feedback errors," *Wirel. Commun. Mob. Comput.*, Mar. 2012.

[13] S. Sanayei and A. Nosratinia, "Antenna selection in MIMO systems," *IEEE Commun. Mag.*, vol. 42, no. 10, pp. 68–73, Oct. 2004.

[14] P. L. Yeoh, M. Elkashlan, and I. Collings, "Selection relaying with transmit beamforming: A comparison of fixed and variable gain relaying," *IEEE Trans. Commun.*, vol. 59, no. 6, pp. 1720–1730, Jun. 2011.

[15] H. Ding, J. Ge, D. B. da Costa, and Z. Jiang, "Link selection schemes for selection relaying systems with transmit beamforming: new and efficient proposals from a distributed concept," *IEEE Trans. Veh. Technol.*, vol. 61, no. 2, pp. 533–552, Feb. 2012.

[16] ——, "Diversity and coding gains of fixed-gain amplify-and-forward with partial relay selection in Nakagami-m fading," *IEEE Commun. Lett.*, vol. 14, no. 8, pp. 734–736, Aug. 2010.

[17] F. Xu, F. C. M. Lau, and D. W. Yue, "Diversity order for amplify-and-forward dual-hop systems with fixed-gain relay under Nakagami fading channels," *IEEE Trans. Wireless Commun.*, vol. 9, no. 1, pp. 92–98, Jan. 2010.

[18] I. S. Gradshteyn and I. M. Ryzhik, *Table of Integrals, Series, and Products*, 7th ed. San Diego, CA: Academic Press, 2007.

Chapter 4

A Distributed Transmit Antenna Selection Scheme for Fixed-Gain Multi-Antenna AF Relaying Systems

Diana C. González, Daniel B. da Costa, and José Cândido S. Santos Filho[1]

Abstract

Antenna selection has arisen as an attractive strategy in multi-antenna systems due to its reduced complexity and cost. In this paper, the outage performance of a distributed transmit antenna selection scheme for dual-hop fixed-gain amplify-and-forward relaying systems is investigated. Our analysis considers a multi-antenna source, a multi-antenna relay, and a single-antenna destination, in which selection combining and maximal-ratio combining are employed at the relay and destination receptions, respectively. Lower and upper bounds for the outage probability of the proposed scheme are derived as the sum of two terms, one term given in closed form and the other term given in single integral form. Moreover, asymptotic expressions for these bounds at high signal-to-noise ratio are obtained in closed form. The results show that our scheme presents full diversity order. More importantly, the underlying distributed strategy is shown to perform closely to the costly optimal centralized antenna selection.

---

[1]This Chapter is a replica of the following manuscript: D. C. González, D. B. da Costa, and J. C. S. Santos Filho, "A distributed transmit antenna selection scheme for fixed-gain multi-antenna AF relaying systems," in *Proc. 9th International Conference Cognitive Radio Oriented Wireless Networks and Communications (CROWNCOM)*, Oulu, Finland, 2–4 Jun. 2014, pp. 254–259.

4.1   Introduction

Multi-antenna relaying systems are expected to be widely utilized in future wireless communication networks, since the advantages offered by multiple-input multiple-output (MIMO) and relaying techniques can be fully exploited. However, a potential drawback of the use of multiple antennas is their complex hardware and increased cost [1]. To alleviate this, transmit antenna selection (TAS) has arisen as an alternative low-cost low-complexity strategy to capture the advantages of MIMO systems. Nevertheless, in order to provide the knowledge necessary for the transmitter to select the best antenna, the implementation of TAS schemes usually requires feedback channels for acquiring the channel state information (CSI) of all links. The required bits of feedback information vary depending on the number of antennas at the nodes [1]. In this case, when the number of antennas increases, the delay and complexity involved in the selection mechanism may rapidly become prohibitive in practice.

Several works have shown and explored the advantages of TAS schemes, but a substantial amount of CSI feedback has been observed in most of them. For instance, the optimal TAS strategy was studied in [2] for a dual-hop MIMO amplify-and-forward (AF) relaying system, in which an exhaustive search for the best antenna at the source and relay was required. A different optimal TAS strategy was examined in [3] assuming a variable-gain AF relay and Nakagami-m fading. Two suboptimal TAS strategies were also analyzed in [3], in which the feedback overhead was reduced at the expense of system performance. More recently, a distributed TAS scheme was proposed in [4] assuming a single-antenna fixed-gain AF relay.

In this work, we generalize the scheme proposed in [4] by considering a fixed-gain AF relay with multiple antennas in both transmission and reception. Our scheme provides a low and constant delay/feedback overhead, despite of the number of transmit antennas. We derive lower and upper bounds for the outage probability of the proposed scheme as the sum of two terms, one term given in closed form and the other term given in single integral form. Moreover, an asymptotic expression for each of these bounds at high signal-to-noise ratio (SNR) is obtained in closed form. It is noteworthy that such analysis is considerably more intricate than that of the scheme in [4]. Our results show that the proposed scheme presents full diversity order. More importantly, its underlying distributed strategy is shown to perform closely to the costly optimal centralized TAS.

Throughout this paper, $f_Z(\cdot)$ denotes the probability density function (PDF) of a generic random variable Z, $E[\cdot]$ denotes expectation, and $\Pr(\cdot)$ denotes probability.

4.2   System Model and Antenna Selection Scheme

4.2.1   System Model

Consider a dual-hop relaying system composed of one source S with N_t antennas, one single-antenna destination D, and one half-duplex fixed-gain AF relay R with N_{rr} receive antennas and N_{rt} transmit antennas. A time-division multiple access scheme is assumed and all the channels undergo flat Rayleigh fading.

Before data transmission, the transmit antenna at S that maximizes the end-to-end instantaneous SNR is chosen according to the procedure to be described in the next subsection. Afterwards, a conventional cooperative transmission takes place in two time slots. In the first time slot, the signals received by the multiple antennas at R are combined using a selection combining (SC) scheme, and, in the second time slot, the signals coming from the direct and relaying links[2] are combined at D using a maximal-ratio combining (MRC) scheme. The end-to-end SNR from the ith antenna at S to D (through the kth receive antenna and jth transmit antenna at R) can be written as

$$\gamma_{i,k,j} = \gamma_{S_iD} + \frac{\gamma_{S_iR_k}\gamma_{R_jD}}{\gamma_{R_jD} + C},\tag{4.1}$$

where $\gamma_{S_iD} \triangleq \frac{P_S}{N_0}|h_{S_iD}|^2$, $\gamma_{S_iR_k} \triangleq \frac{P_S}{N_0}|h_{S_iR_k}|^2$, $\gamma_{R_jD} \triangleq \frac{P_R}{N_0}|h_{R_jD}|^2$, and $C = 1 + \bar{\gamma}_{S_iR_k}$, with $\bar{\gamma}_{S_iR_k} = E[\gamma_{S_iR_k}]$. In these expressions, $|h_{S_iD}|^2$, $|h_{S_iR_k}|^2$, and $|h_{R_jD}|^2$ denote the channel power gains of the links from the ith antenna at S to D, from the ith antenna at S to the kth antenna at R, and from the jth antenna at R to D, respectively; P_S and P_R stand for the transmit powers at S and R, respectively; and N_0 denotes the additive white Gaussian noise (AWGN) at each receiving terminal. We assume a homogeneous network, in which $E[\gamma_{S_iR_k}] = \bar{\gamma}_{SR}$, $E[\gamma_{S_iD}] = \bar{\gamma}_{SD}$, and $E[\gamma_{R_jD}] = \bar{\gamma}_{RD}$, for any $i = 1,\ldots,N_t$, any $k = 1,\ldots,N_{rr}$, and any $j = 1,\ldots,N_{rt}$. The fixed-gain relaying factor is adjusted according to [5] as $G^2 = E\left[\frac{P_R}{P_S|h_{S_iR_k}|^2+N_0}\right]$.

4.2.2 Antenna Selection Strategy

The optimal selection criterion chooses the best transmit antennas at S and R that maximize the end-to-end SNR, i.e.,

$$(i^*, k^*, j^*) = \arg\max_{i,k,j}\left[\gamma_{i,k,j}\right].\tag{4.2}$$

Note that the optimal scheme entails a large amount of delay and feedback overhead due to the full system CSI required for decision. To alleviate this, relying on the idea pioneeringly proposed in [4], a suboptimal (yet efficient) distributed antenna selection (DAS) scheme is presented next. In this scheme, the local CSI available at S is exploited to its furthest extent in order to assist the decision, incurring a negligible delay and feedback overhead.

The DAS concept is motivated and supported by the following inequality involving the end-to-end SNR:

$$\gamma_{i,k,j} < \gamma_{S_iD} + \gamma_{S_iR_k}\min\left[\frac{\gamma_{R_jD}}{C}, 1\right] \triangleq \tilde{\gamma}_i.\tag{4.3}$$

The DAS scheme is performed in two time slots [4]. In the first time slot, D sends to R and S a 1-bit reverse pilot signaling. Then, R and S use this bit to estimate their respective local CSIs γ_{R_jD} and γ_{S_iD}. At this time, based on γ_{R_jD}, the relay selects its optimal antenna to transmit data, by applying the selection rule $j^* = \arg\max_{j}\left[\gamma_{R_jD}\right]$. In the second time slot, R compares its local CSI $\gamma_{R_{j^*}D}$ with C, yielding two cases:

---

[2]The relay employs a TAS scheme to forward to the destination the signal received from the source. This will be described next.

- Case I: If $\gamma_{R_{j*}D} \geq C$, R sends to S a 1-bit message "1". In this case, by using (4.3), γ_{S_iD} and $\gamma_{S_iR_k}$, which are available at S, are sufficient to apply the selection rule $\max\{\widetilde{\gamma}_{i,k,j*}\}$.

- Case II: If $\gamma_{R_{j*}D} < C$, R sends to S a 1-bit message "0". In this case, by using (4.3), the application of $\max\{\widetilde{\gamma}_{i,k,j*}\}$ would require the additional knowledge of $\gamma_{R_{j*}D}$, which is unavailable at S. Therefore, somewhat arbitrarily, a suboptimal decision will be employed that depends solely on the maximization of γ_{S_iD}, which is available at S. All in all, the TAS rule of the proposed DAS scheme is summarized as follows:

$$i^* = \begin{cases} \bar{i} = \arg\max_i \left[\gamma_{S_iD} + \max_k \left[\gamma_{S_iR_k} \right] \right], & \text{if } \gamma_{R_{j*}D} \geq C \\ \underline{i} = \arg\max_i \left[\gamma_{S_iD} \right], & \text{if } \gamma_{R_{j*}D} < C. \end{cases} \qquad (4.4)$$

It is noteworthy that the major advantage of DAS over other antenna selection schemes is its reduced delay/feedback overhead, requiring only a 2-bit pilot/feedback signaling, at the expense of some additional hardware complexity at the source.

4.3   Performance Analysis

In this section, the outage probability for the proposed scheme will be analyzed. Such a metric can be defined as the probability that the end-to-end SNR falls below a given threshold, commonly written in terms of a target spectral efficiency $\Re_0$, being mathematically formulated as

$$P_{out}^{\text{DAS}} = \underbrace{\Pr\left(\gamma_{R_{j*}D} \geq C, \left(\gamma_{S_{\bar{i}}D} + \frac{\gamma_{S_{\bar{i}}R_{k*}}\gamma_{R_{j*}D}}{\gamma_{R_{j*}D} + C} \right) < z \triangleq 2^{2\Re_0} - 1 \right)}_{P_1}$$
$$+ \underbrace{\Pr\left(\gamma_{R_{j*}D} < C, \left(\gamma_{S_{\underline{i}}D} + \frac{\gamma_{S_{\underline{i}}R_{k*}}\gamma_{R_{j*}D}}{\gamma_{R_{j*}D} + C} \right) < z \right)}_{P_2}. \qquad (4.5)$$

Since an exact closed-form expression for the above expression is mathematically intractable, lower and upper bounds for the outage probability will be derived instead, based on the following paramount relationships:

$$\frac{\gamma_{S_iR_k}}{2} \min\left[\frac{\gamma_{R_jD}}{C}, 1 \right] \leq \frac{\gamma_{S_iR_k}\gamma_{R_jD}}{\gamma_{R_jD} + C} \leq \gamma_{S_iR_k} \min\left[\frac{\gamma_{R_jD}}{C}, 1 \right]. \qquad (4.6)$$

In order to evaluate the terms P_1 and P_2, we first derive a lower bound P_1^{LB} for P_1, using (4.6), as follows:

$$
\begin{aligned}
P_1 &> \Pr\left(\gamma_{R_{j^*}D} \geq C, \left(\gamma_{S_{\bar{i}}D} + \gamma_{S_{\bar{i}}R_{k^*}} \min\left[\frac{\gamma_{R_{j^*}D}}{C}, 1\right]\right) < z\right) \\
&\stackrel{(a)}{=} \Pr\left(\gamma_{R_{j^*}D} \geq C, \max_i\left(\gamma_{S_iD} + \max_k\left(\gamma_{S_iR_k}\right)\right) < z\right) \triangleq P_1^{\text{LB}} \\
&= \Pr\left(\gamma_{R_{j^*}D} \geq C\right) \Pr\left(\left(\gamma_{S_iD} + \max_k\left(\gamma_{S_iR_k}\right)\right) < z\right)^{N_t} \\
&= \Pr\left(\gamma_{R_{j^*}D} \geq C\right) \left(\int_0^z f_{\gamma_{SD}}(x) \Pr\left(\left(x + \max_k\left(\gamma_{S_iR_k}\right)\right) < z\right) dx\right)^{N_t} \\
&= \Pr\left(\gamma_{R_{j^*}D} \geq C\right) \left(\underbrace{\int_0^z \frac{1}{\bar{\gamma}_{SD}} e^{-\frac{x}{\bar{\gamma}_{SD}}} \left(1 - e^{-\frac{z-x}{\bar{\gamma}_{SR}}}\right)^{N_{rr}} dx}_{\alpha}\right)^{N_t},
\end{aligned}
\tag{4.7}
$$

where in step (a) we applied the DAS rule given in (4) for $\gamma_{R_{j^*}D} \geq C$. The term α can be rewritten using the binomial theorem [6, Eq. (1.111)] as

$$
\begin{aligned}
\alpha &= \int_0^z \frac{1}{\bar{\gamma}_{SD}} e^{-\frac{x}{\bar{\gamma}_{SD}}} \sum_{j=0}^{N_{rr}} \binom{N_{rr}}{j} (-1)^j e^{-j\frac{z-x}{\bar{\gamma}_{SR}}} dx \\
&= \sum_{j=0}^{N_{rr}} \binom{N_{rr}}{j} (-1)^j e^{-j\frac{z}{\bar{\gamma}_{SR}}} \frac{1}{\bar{\gamma}_{SD}} \int_0^z e^{j\frac{x}{\bar{\gamma}_{SR}} - \frac{x}{\bar{\gamma}_{SD}}} dx \\
&= \sum_{j=0}^{N_{rr}} \binom{N_{rr}}{j} (-1)^j e^{-j\frac{z}{\bar{\gamma}_{SR}}} \left(\frac{\left(1 - e^{-\frac{z}{\bar{\gamma}_{SD}} + \frac{jz}{\bar{\gamma}_{SR}}}\right) \bar{\gamma}_{SR}}{j\bar{\gamma}_{SD} - \bar{\gamma}_{SR}}\right).
\end{aligned}
\tag{4.8}
$$

Then, by substituting (4.8) in (4.7), a lower bound for P_1 can be derived in closed form as

$$
P_1^{\text{LB}} = \left(1 - \left(1 - e^{-\frac{C}{\bar{\gamma}_{RD}}}\right)^{N_{rt}}\right) \left(\sum_{j=0}^{N_{rr}} \binom{N_{rr}}{j} (-1)^j \left(\frac{\left(e^{-j\frac{z}{\bar{\gamma}_{SR}}} - e^{-\frac{z}{\bar{\gamma}_{SD}}}\right) \bar{\gamma}_{SR}}{j\bar{\gamma}_{SD} - \bar{\gamma}_{SR}}\right)\right)^{N_t}.
\tag{4.9}
$$

In order to assess the asymptotic behavior of P_1^{LB}, a high-SNR expression for the term α can be derived from its definition as

$$
\begin{aligned}
\alpha &= \int_0^z \frac{1}{\bar{\gamma}_{SD}} e^{-\frac{z-y}{\bar{\gamma}_{SD}}} \left(1 - e^{-\frac{y}{\bar{\gamma}_{SR}}}\right)^{N_{rr}} dy \\
&\simeq \left(\frac{1}{\bar{\gamma}_{SR}}\right)^{N_{rr}} \frac{1}{\bar{\gamma}_{SD}} \frac{z^{N_{rr}+1}}{(N_{rr}+1)},
\end{aligned}
\tag{4.10}
$$

which, when replaced in (4.7), yields a corresponding high-SNR asymptotic lower bound for P_1 as

$$
P_1^{\text{LB}} \simeq \left(1 - \left(1 - e^{-\frac{C}{\bar{\gamma}_{RD}}}\right)^{N_{rt}}\right) \left(\left(\frac{1}{\bar{\gamma}_{SR}}\right)^{N_{rr}} \frac{1}{\bar{\gamma}_{SD}} \frac{z^{N_{rr}+1}}{(N_{rr}+1)}\right)^{N_t}.
\tag{4.11}
$$

Using (4.6), it can be shown that an upper bound P_1^{UB} for P_1 and its asymptote can be directly attained by replacing z with $2z$ into (4.9) and (4.11), respectively.

Similarly, a lower bound P_2^{LB} for P_2 can be formulated as

$$P_2 > \Pr\left(\gamma_{R_{j^*}D} < C, \left(\gamma_{S_{\underline{i}}D} + \gamma_{S_{\underline{i}}R_{k^*}} \min\left[\frac{\gamma_{R_{j^*}D}}{C}, 1\right]\right) < z\right) \tag{4.12}$$

$$= \Pr\left(\gamma_{R_{j^*}D} < C, \left(\gamma_{S_{\underline{i}}D} + \frac{\gamma_{S_{\underline{i}}R_{k^*}}\gamma_{R_{j^*}D}}{C}\right) < z\right) = P_2^{\text{LB}} \tag{4.13}$$

$$= \Pr\left(\gamma_{R_{j^*}D} < C, \left(\max_m\left[\gamma_{S_mD}\right] + \max_k\left[\gamma_{S_iR_k}\right]\frac{\gamma_{R_{j^*}D}}{C}\right) < z\right). \tag{4.14}$$

By using the principles of probability theory, P_2^{LB} can be elaborated as

$$P_2^{\text{LB}} = \int_0^C f_{\gamma_{RD}}(x)\Pr\left(\left(\max_m\left[\gamma_{S_mD}\right] + \max_k\left[\gamma_{S_iR_k}\right]\frac{x}{C}\right) < z\right)dx \tag{4.15}$$

$$= \int_0^1 Cf_{\gamma_{RD}}(Cu)\Pr\left(\left(\max_m[\gamma_{S_mD}] + \max_k[\gamma_{S_iR_k}]u\right) < z\right)du \tag{4.16}$$

$$= \int_0^1 Cf_{\gamma_{RD}}(Cu)\int_0^z f_{\gamma_{SR}}(y)\Pr\left(\left(\max_m\left[\gamma_{S_mD}\right] + yu\right) < z\right)dydu \tag{4.17}$$

$$= \int_0^1 Cf_{\gamma_{RD}}(Cu)\int_0^z \frac{1}{u}f_{\gamma_{SR}}\left(\frac{v}{u}\right)\Pr\left(\max_m[\gamma_{S_mD}] < z-v\right)dvdu \tag{4.18}$$

$$= \int_0^1 \frac{CN_{rt}}{\bar{\gamma}_{RD}}e^{-\frac{Cu}{\bar{\gamma}_{RD}}}\left(1 - e^{-\frac{Cu}{\bar{\gamma}_{RD}}}\right)^{N_{rt}-1}\frac{N_{rr}}{u\bar{\gamma}_{SR}}$$

$$\times \underbrace{\int_0^z e^{-\frac{v}{u\bar{\gamma}_{SR}}}\left(1 - e^{-\frac{v}{u\bar{\gamma}_{SR}}}\right)^{N_{rr}-1}\left(1 - e^{-\frac{z-v}{\bar{\gamma}_{SD}}}\right)^{N_t}dv}_{\varphi}\,du, \tag{4.19}$$

where the term φ can be calculated using the binomial theorem [6, Eq. (1.111)] as

$$\varphi = \sum_{m=0}^{N_t}\sum_{j=0}^{N_{rr}}\binom{N_t}{m}\binom{N_{rr}-1}{j}(-1)^m(-1)^j\frac{\left(e^{-\frac{(1+j)z}{u\bar{\gamma}_{SR}}} - e^{-\frac{mz}{\bar{\gamma}_{SD}}}\right)u\bar{\gamma}_{SR}\bar{\gamma}_{SD}}{mu\bar{\gamma}_{SR} - (1+j)\bar{\gamma}_{SD}}. \tag{4.20}$$

Then, by substituting (4.20) into (4.15), a lower bound for P_2 can be derived in single integral form as

$$P_2^{\text{LB}} = \int_0^1 \frac{CN_{rt}}{\bar{\gamma}_{RD}}e^{-\frac{Cu}{\bar{\gamma}_{RD}}}\left(1 - e^{-\frac{Cu}{\bar{\gamma}_{RD}}}\right)^{N_{rt}-1}\frac{N_{rr}}{u}\sum_{m=0}^{N_t}\sum_{j=0}^{N_{rr}}\binom{N_t}{m}\binom{N_{rr}-1}{j}(-1)^m(-1)^j$$

$$\times \frac{\left(e^{-\frac{(1+j)z}{u\bar{\gamma}_{SR}}} - e^{-\frac{mz}{\bar{\gamma}_{SD}}}\right)u\bar{\gamma}_{SD}}{mu\bar{\gamma}_{SR} - (1+j)\bar{\gamma}_{SD}}du. \tag{4.21}$$

In order to assess the asymptotic behavior of P_2^{LB}, we simplify the term φ defined in (4.15) by using the binomial theorem [6, Eq. (1.111)] and the MacLaurin series of exponential functions [6, Eq. (1.211.1)], obtaining

$$\varphi = \sum_{i=1}^{N_{rr}}\binom{N_{rr}-1}{i-1}(-1)^{i-1}\int_0^z e^{-\frac{iv}{u\bar{\gamma}_{SR}}}\left(\frac{z-v}{\bar{\gamma}_{SD}}\right)^{N_t}dv$$

$$= \sum_{i=1}^{N_{rr}}\binom{N_{rr}-1}{i-1}(-1)^{i-1}e^{-\frac{iz}{u\bar{\gamma}_{SR}}}\left(\frac{1}{\bar{\gamma}_{SD}}\right)^{N_t}\sum_{n=0}^{\infty}\left(\frac{i}{u\bar{\gamma}_{SR}}\right)^n\frac{z^{N_t+n+1}}{n!(N_t+n+1)}. \tag{4.22}$$

By substituting (4.22) into (4.15) and using again the binomial theorem, P_2^{LB} can be rewritten as

$$
\begin{aligned}
P_2^{\text{LB}} =& N_{rt} \frac{N_{rr}}{\bar{\gamma}_{SR}} \left(\frac{1}{\bar{\gamma}_{SD}} \right)^{N_t} \sum_{i=1}^{N_{rr}} \binom{N_{rr}-1}{i-1} (-1)^{i-1} \sum_{j=0}^{N_{rt}} \binom{N_{rt}-1}{j-1} (-1)^{j-1} \\
& \times \sum_{n=0}^{\infty} \underbrace{\frac{z^{N_t+n+1} i^n \bar{\gamma}_{SR}^{-n}}{n!\,(N_t+n+1)} \int_0^1 \frac{C}{\bar{\gamma}_{RD}} u^{-n-1} e^{-\frac{iz}{u\bar{\gamma}_{SR}}} e^{-\frac{jCu}{\bar{\gamma}_{RD}}}\,du}_{\Phi_n} .
\end{aligned}
\tag{4.23}
$$

The behavior of Φ_n in the high-SNR regime is characterized in Appendices D.1 and D.2. In Appendix D.1, Φ_n is determined for $n=0$, yielding

$$
\Phi_0 \simeq
\begin{cases}
\frac{z^{N_t+1}}{(N_t+1)} \frac{\left(\frac{jCiz}{\bar{\gamma}_{SR}\bar{\gamma}_{RD}} \right)^{n_1}}{n_1!^2 \mu_2} \left(-\ln\left(\frac{jiz}{\bar{\gamma}_{RD}} \right) + \psi(n_1+1) - (-1)^{n_1} \Gamma\left(-n_1, \frac{jC}{\bar{\gamma}_{RD}} \right) \right), & \text{if } N_{rr} = N_{rt} \\[2ex]
\frac{z^{N_t+1}}{(N_t+1)} \frac{\left(\frac{jCiz}{\bar{\gamma}_{SR}\bar{\gamma}_{RD}} \right)^{n_1}}{n_1!^2 \mu_2} \left(-\ln\left(\frac{jiz}{\bar{\gamma}_{RD}} \right) - (-1)^{n_1} \Gamma\left(-n_1, \frac{jC}{\bar{\gamma}_{RD}} \right) \right), & \text{if } N_{rr} < N_{rt} \\[2ex]
\frac{z^{N_t+1}}{(N_t+1)} \frac{\left(\frac{jCiz}{\bar{\gamma}_{SR}\bar{\gamma}_{RD}} \right)^{n_1}}{n_1!^2 \mu_2} \left(-\ln\left(\frac{jiz}{\bar{\gamma}_{RD}} \right) \right), & \text{if } N_{rr} > N_{rt},
\end{cases}
\tag{4.24}
$$

where $\mu_2 \triangleq \bar{\gamma}_{RD}/\bar{\gamma}_{SR}$ and $n_1 \triangleq \min(N_{rr}, N_{rt}) - 1$. In Appendix D.2, Φ_n is determined for $n > 0$, in which two intervals for n are established ($1 \leq n \leq n_1$ and $n > n_1$), yielding

$$
\Phi_{n|_1^{n_1}} \simeq
\begin{cases}
\frac{z^{N_t+n_1+1}}{n!(N_t+n+1)\mu_2} \left(\frac{jCi}{\bar{\gamma}_{SR}\bar{\gamma}_{RD}} \right)^{n_1} \left((-1)^{n+1} \frac{1}{(n1-n)!n_1!} \ln\left(\frac{jiz}{\bar{\gamma}_{RD}} \right) \right. \\
\qquad \left. - \frac{(-1)^{n_1-n}}{(n1-n)!} \Gamma\left(-n_1, \frac{jC}{\bar{\gamma}_{RD}} \right) \right), & \text{if } N_{rr} \leq N_{rt} \\[2ex]
\frac{z^{N_t+n_1+1}}{n!(N_t+n+1)\mu_2} \left(\frac{jCi}{\bar{\gamma}_{SR}\bar{\gamma}_{RD}} \right)^{n_1} \left((-1)^{n+1} \frac{1}{(n1-n)!n_1!} \ln\left(\frac{jiz}{\bar{\gamma}_{RD}} \right) \right), & \text{if } N_{rr} > N_{rt}
\end{cases}
\tag{4.25}
$$

$$
\Phi_{n|_{n_1+1}^{\infty}} \simeq
\begin{cases}
\frac{z^{N_t+n_1+1}}{n!(N_t+n+1)\mu_2} \left(\frac{jCi}{\bar{\gamma}_{SR}\bar{\gamma}_{RD}} \right)^{n_1} \frac{(n-n_1-1)!}{n_1!} (-1)^{n_1}, & \text{if } N_{rr} = N_{rt} \\[2ex]
0, & \text{otherwise.}
\end{cases}
\tag{4.26}
$$

As done before for the term P_1, using (4.6), it can be shown that an upper bound P_2^{UB} for P_2 and its asymptote can be directly attained by replacing z with $2z$ into (4.21) and (4.23).

Finally, by adding as in (4.5) the asymptotic bounds derived for P_1 and P_2, corresponding asymptotic lower and upper bounds for P_{out} are obtained, respectively, as

$$
P_{out}^{\text{DAS,LB}} \simeq
\begin{cases}
P_1^{\text{LB}} + P_2^{\text{LB}}, & \text{if } N_t = 1 \text{ and } N_{rr} \leq N_{rt} \\[2ex]
P_2^{\text{LB}}, & \text{otherwise}
\end{cases}
\tag{4.27}
$$

$$
P_{out}^{\text{DAS,UB}} \simeq
\begin{cases}
P_1^{\text{UB}} + P_2^{\text{UB}}, & \text{if } N_t = 1 \text{ and } N_{rr} \leq N_{rt} \\[2ex]
P_2^{\text{UB}}, & \text{otherwise.}
\end{cases}
\tag{4.28}
$$

Remarks:

1. Using (4.27), (4.28), and the asymptotic bounds for P_1 and P_2, it can be shown that the proposed DAS scheme achieves full diversity order, being equal to $N_t + \min(N_{rr}, N_{rt})$.

2. As shown in (4.23), both lower and upper asymptotic bounds for P_2 are given in terms of an infinite series. In order to observe the convergence of this series, two cases are analyzed: (i) when $N_{rr} \neq N_{rt}$, only the first $n_1 + 1$ terms are taken into consideration, since the series is zero for terms greater than n_1; (ii) when $N_{rr} = N_{rt}$, similarly to [4], the convergence is proved using the convergence test of [6, Eq. (0.223)].

4.4 Numerical Results and Discussions

In this section, representative numerical results are presented and Monte Carlo simulations are run to support the derived analytical bounds. In our plots, as a sample case, we assume that the target spectral efficiency is $\Re_0 = 1$ bit/s/Hz and that the path loss exponent is $\beta = 4$. We also assume that the channel mean power is proportional to $d^{-\beta}$, with d being the distance between the transceivers. The distance between S and D is normalized to unity, as in [4][3]. Figs. 4.1 and 4.2 show the outage probability for two major system configurations, namely $\{N_t = 2,\ d_{SR} = 0.7\}$ and $\{N_t = 3,\ d_{SR} = 0.8\}$, respectively. It is noteworthy that, in each case, the relay has been placed at the position d_{SR} that provides the best outage performance, and such a position was previously established through simulations. These prior simulation results have not been presented here due to space limitations. From the figures, note that the performed analysis for the exact and asymptotic bounds is validated, and that the diversity order, determined as $N_t + \min(N_{rr}, N_{rt})$, is verified. For instance, using the system configuration $\{N_t = 2,\ N_{rr} = 2,\ N_{rt} = 2\}$ the diversity order equals 4, which agrees with the asymptotes's slope in Fig. 2. In addition, both figures compares the performance of the proposed DAS and optimal TAS schemes, which can be seen to be very similar.

---

[3]Again, as in [4], we assume a linear network topology, in which S and R transmit with the same SNR P, and $d_{SD} = d_{SR} + d_{RD}$, where d_{SD}, d_{SR}, and d_{RD} represent the distance of the links $S \to D$, $S \to R$, and $R \to D$, respectively. The corresponding average link SNRs can be formulated as $\bar{\gamma}_{SD} = Pd_{SD}^{-\beta}$, $\bar{\gamma}_{SR} = Pd_{SR}^{-\beta}$, and $\bar{\gamma}_{RD} = Pd_{RD}^{-\beta}$.
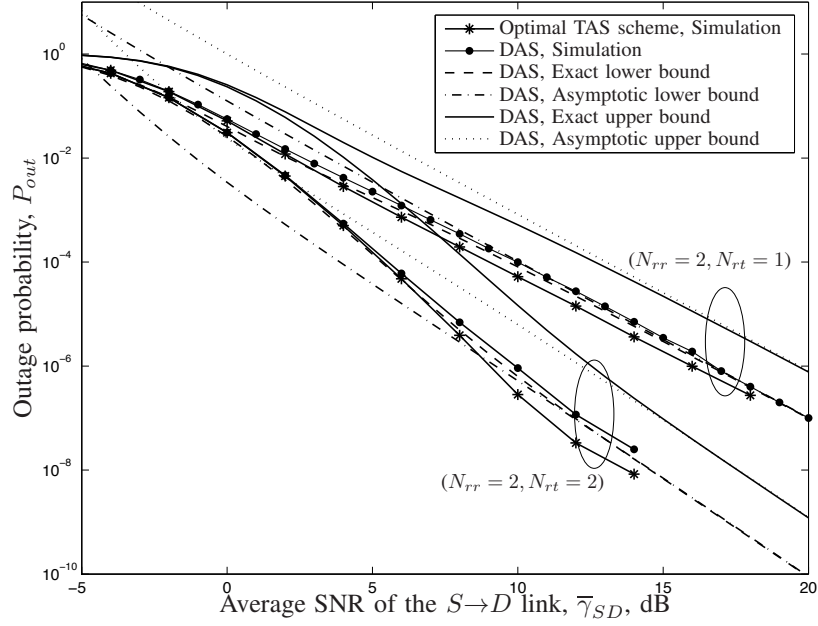
Figure 4.1: Outage probability versus average SNR of the $S \to D$ link for different AS schemes ($d_{SR} = 0.7$, $N_t = 2$).
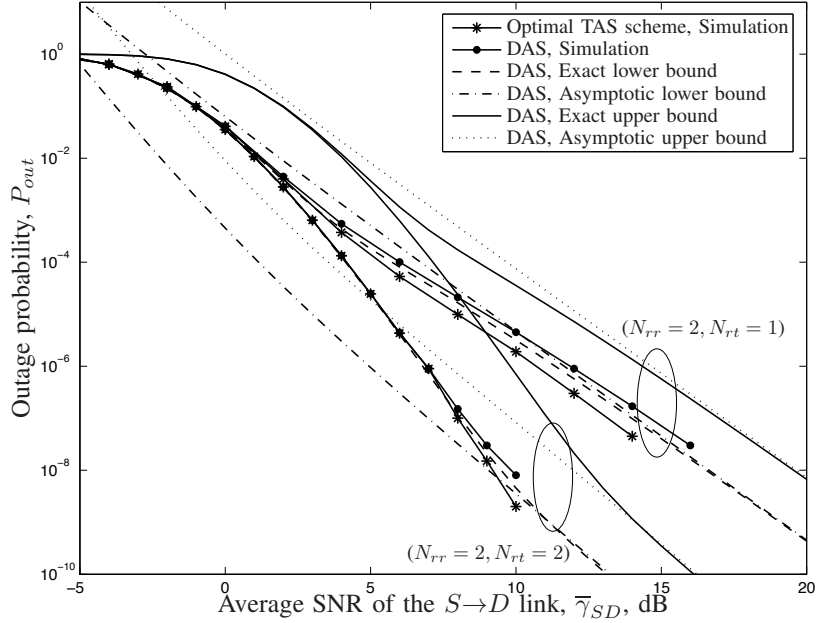
Figure 4.2: Outage probability versus average SNR of the $S \to D$ link for different AS schemes ($d_{SR} = 0.8$, $N_t = 3$).

Bibliography

[1] S. Sanayei and A. Nosratinia, "Antenna selection in MIMO systems," *IEEE Commun. Mag.*, vol. 42, no. 10, pp. 68–73, Oct. 2004.

[2] S. W. Peters and R. W. Heath, "Nonregenerative MIMO relaying with optimal transmit antenna selection," *IEEE Signal Process. Lett*, vol. 15, pp. 421–424, 2008.

[3] G. Amarasuriya, C. Tellambura, and M. Ardakani, "Performance analysis framework for transmit antenna selection strategies of cooperative MIMO AF relay networks," *IEEE Trans. Veh. Technol.*, vol. 60, no. 7, pp. 3030–3044, Sep. 2011.

[4] H. Ding, J. Ge, D. B. da Costa, and T. Tsiftsis, "A novel distributed antenna selection scheme for fixed-gain amplify-and-forward relaying systems," *IEEE Trans. Veh. Technol.*, vol. 61, no. 6, pp. 2836–2842, Jul. 2012.

[5] G. K. Karagiannidis, "Performance bounds of multihop wireless communications with blind relays over generalized fading channels," *IEEE Trans. Wireless Commun.*, vol. 5, no. 3, pp. 498–503, Mar. 2006.

[6] I. S. Gradshteyn and I. M. Ryzhik, *Table of Integrals, Series, and Products*, 7th ed. San Diego, CA: Academic Press, 2007.

Chapter 5

Distributed TAS/MRC and TAS/SC Schemes for Fixed-Gain AF Systems with Multi-Antenna Relay

Diana C. González, Daniel B. da Costa, and José Cândido S. Santos Filho[1]

Abstract

Although transmit-antenna selection (TAS) is an alternative low-cost strategy to capture the advantages of multi-antenna systems, its application may require a large amount of feedback transmissions. Owing to this fact and in order to reduce such requirement, herein we analyze the performance of two *distributed* TAS (DAS) schemes. One scheme employs maximal-ratio combining (DAS/MRC) at the destination, whereas the other employs selection combining (DAS/SC). We consider a dual-hop fixed-gain amplify-and-forward relaying network, equipped with multi-antenna source/relay nodes and a single-antenna destination. A lower bound expression is derived for the outage probability of each investigated scheme. Importantly, the derived bounds prove to be very tight approximations to the exact outage performance. Also, capitalizing on a strikingly interesting property of Stirling numbers of the second kind, we provide closed-form asymptotic expressions for the obtained bounds. Our results show that the diversity order of the proposed distributed schemes is identical to that of their optimal centralized counterparts, namely $N_t + \min(N_{rr}, N_{rt})$, with N_t, N_{rr}, and N_{rt} denoting the number of transmit antennas at the source, the number of receive antennas at the relay, and the number of transmit antennas at the relay, respectively. In addition, as the relay approaches the destination, the outage performance of the proposed schemes approaches the optimal one.

5.1   Introduction

Multiple transmit and receive antenna systems have attracted much attention in the context of wireless relaying communications, because they offer a significant improvement in data rate and link reliability. However, this improvement comes along with an increase in complexity, size, and cost in hardware design. To alleviate such impairments, transmit-antenna selection (TAS) strategies have emerged as a promising simplified solution, while retaining many of the benefits of more sophisticated multiple-input multiple-output (MIMO) relaying systems [1], [2]. With the aim to mitigate the adverse effects of fading, TAS schemes are usually accompanied by some diversity-combining techniques at the receiver side, such as maximal-ratio combining (MRC) and selection combining (SC) [1]. As well known, these two techniques represent a trade-off between performance and complexity. On the one hand, MRC is the optimal linear combining technique [3], but its implementation is more difficult, since it requires multiple channel estimations and a complex hardware, with a dedicated receiver chain for each antenna [4]. On the other hand, SC is a suboptimal technique, but with a simpler implementation, since it requires a single receiver chain which is shared among multiple antennas.

In order to select the best transmit antenna, optimal TAS schemes require the channel state information (CSI) of all links, which can be in principle obtained by means of feedback. However, the required bits of feedback information vary depending on the number of antennas at the nodes [1]. As the number of antennas increases, the delay, full channel estimation, feedback overhead, and exhaustive antenna search involved into optimal centralized TAS mechanisms may rapidly become infeasible in practice. To alleviate this, suboptimal and/or *distributed* TAS (DAS) strategies with reduced feedback overhead have been proposed along the last years. Recent works on dual-hop network configurations with TAS or DAS at the source and MRC or SC at the destination (also known as TAS/MRC, TAS/SC, DAS/MRC, and DAS/SC) include those in [5]-[15] and the references therein. The authors in [5] derived an optimal TAS strategy at the source and relay for a nonregenerative half-duplex MIMO relaying system, in which it was verified that the proposed strategy can achieve full diversity order. However, as mentioned before, such an optimal antenna selection may be too complex. To overcome this, the authors in [6] and [7] studied some suboptimal low-complexity TAS strategies and proved that they can achieve the same diversity order as the optimal strategy. In [8], it was presented an amplify-and-forward (AF) relaying scheme for a MIMO multi-relay network operating over Rician, Nakagami-m, Weibull, and generalized-K fading channels, in which the performances of TAS/MRC and TAS/SC were compared. In [9] and [10], TAS/MRC MIMO relaying schemes operating in the absence of the direct link were investigated. In [9], the source and destination nodes were equipped with multiple antennas, while a single-antenna relay was considered. In such scheme, the antenna selection process at the source required a feedback path from all links, which becomes prohibitive when the number of antennas increases. Differently, in [10], all the nodes (source, destination, and relay) were assumed to be equipped with multiple antennas. A DAS strategy was then employed, so that the selection criteria at the source was based solely on the source-relay link information, while the selection criteria at the relay was based on the relay-destination link

information. The authors in [11] analytically investigated and compared the performance of two TAS/MRC schemes in a dual-hop AF relaying network. A tight upper bound was used in order to derive expressions for the cumulative distribution function (CDF) of the end-to-end signal-to-noise ratio (SNR). In [12], optimal and suboptimal TAS strategies were presented assuming a variable-gain AF relaying network subject to Nakagami-m fading, where the feedback overhead was reduced at the expense of system performance. In [13], adopting a TAS/SC scheme, the authors examined the performance of a cooperative system with a single relay and multiple antennas at all nodes. Such method was applied at both source and relay nodes, requiring full feedback from the destination. The authors in [16] have modeled AF relay schemes as a keyhoke channel. In [17], [18], it was studied clustering structure of wireless multiantennas channels, from which closed-form expressions for the ergodic capacity considering equal and unequal number of scatterers in each cluster were derived.

The selection mechanism of many DAS schemes in the literature fully ignore the CSI of certain network links. On the other hand, a DAS/MRC suboptimal scheme was proposed in [14] assuming a single-antenna fixed-gain AF relay, in which the CSI of all links was considered to select the transmit antenna. More recently, capitalizing on [14], a similar distributed mechanism was designed and analyzed for a DAS/SC scheme [15]. In that work, it was shown that the DAS/SC scheme achieves the same diversity order as the DAS/MRC scheme, but with a simpler implementation.

In this paper, we design and analyze generalized versions of the DAS/MRC and DAS/SC schemes introduced in [14] and [15], respectively. In contrast to these previous works, where a single-antenna fixed-gain AF relay was studied, herein we consider a fixed-gain AF relay with multiple antennas at both transmission and reception. Analytical lower bounds for the outage probability of the proposed schemes are derived, since an exact analysis looks very intractable. Importantly, the derived bounds prove to be very tight approximations to the exact outage performance. Also, capitalizing on a strikingly interesting property of Stirling numbers of the second kind, we provide closed-form asymptotic expressions for the obtained bounds. It is worth noting that the analytical treatment of such generalized schemes requires more sophisticated mathematical procedures than those for the particular schemes in [14] and [15]. In order to evaluate the system performance and verify the accuracy of our analytical framework, Monte Carlo simulation results are also provided. Both DAS/MRC and DAS/SC schemes reveal to achieve full diversity order, and a comparative analysis of their complexity and performance is presented. It is shown that, as the relay approaches the destination, the underlying distributed strategy into those schemes performs closely to the costly optimal centralized TAS mechanism, while requiring a low and constant delay/feedback overhead, despite the number of transmit antennas.

Throughout this paper, $f_Z(\cdot)$ denotes the probability density function (PDF) of a generic random variable Z, $E[\cdot]$ denotes expectation, and $\Pr(\cdot)$ denotes probability.

5.2   System Model and Antenna Selection Scheme

5.2.1   System Model

We consider a dual-hop relaying system composed by one source S with N_t antennas, one single-antenna destination D, and one half-duplex fixed-gain AF relay R with N_{rr} receive antennas and N_{rt} transmit antennas. Additionally, we assume that the system employs time-division multiple access and that all the channels undergo independent flat Rayleigh fading and additive white Gaussian noise with mean power N_0.

Before data transmission, the transmit antenna at S that maximizes the end-to-end instantaneous SNR is chosen, according to the procedure to be described in the next subsection. Afterwards, a conventional cooperative transmission takes place in two time slots. In the first time slot, the signal replicas from S (first hop) are combined at R using SC, and in the second time slot the signals from S (direct link) and R (second hop[2]) are combined at D, by using one of two different methods: SC or MRC. Therefore, the end-to-end SNR from the ith antenna at S to D (through the kth receive antenna and jth transmit antenna at R) can be written as

$$\text{MRC:} \quad \gamma_{i,k,j} = \gamma_{S_iD} + \frac{\gamma_{S_iR_k}\gamma_{R_jD}}{\gamma_{R_jD} + C} \tag{5.1}$$

$$\text{SC:} \quad \gamma_{i,k,j} = \max\left[\gamma_{S_iD}, \frac{\gamma_{S_iR_k}\gamma_{R_jD}}{\gamma_{R_jD} + C}\right], \tag{5.2}$$

where $\gamma_{S_iD} \triangleq \frac{P_S}{N_0}|h_{S_iD}|^2$ is the direct-link received SNR from the ith antenna at S to D, $\gamma_{S_iR_k} \triangleq \frac{P_S}{N_0}|h_{S_iR_k}|^2$ is the first-hop received SNR from the ith antenna at S to the kth receive antenna at R, $\gamma_{R_jD} \triangleq \frac{P_R}{N_0}|h_{R_jD}|^2$ is the second-hop received SNR from the jth transmit antenna at R to D, and $C \triangleq 1 + \bar{\gamma}_{S_iR_k}$, with $\bar{\gamma}_{S_iR_k} = E[\gamma_{S_iR_k}]$. In these expressions, $|h_{S_iD}|^2$, $|h_{S_iR_k}|^2$, and $|h_{R_jD}|^2$ denote the channel power gains of the corresponding links, and P_S and P_R stand for the transmit powers at S and R, respectively. We assume an homogeneous network, in which $E[\gamma_{S_iR_k}] = \bar{\gamma}_{SR}$, $E[\gamma_{S_iD}] = \bar{\gamma}_{SD}$, and $E[\gamma_{R_jD}] = \bar{\gamma}_{RD}$, $\forall i = 1, \ldots, N_t$, $\forall k = 1, \ldots, N_{rr}$, and $\forall j = 1, \ldots, N_{rt}$. The fixed-gain relaying factor is adjusted according to [19] as $G^2 = E\left[P_R/(P_S|h_{S_iR_k}|^2 + N_0)\right]$.

5.2.2   Antenna Selection Scheme

The optimal selection criterion chooses the best transmit antennas at S and R that maximize the end-to-end SNR in the system, i.e.,

$$(i^*, k^*, j^*) = \arg\max_{i,k,j}\{\gamma_{i,k,j}\}. \tag{5.3}$$

Note that the optimal scheme entails a large amount of delay and feedback overhead due to the full system CSI required for decision. To alleviate this, relying on the idea pioneeringly proposed in [14], a suboptimal (yet efficient) DAS scheme is presented next.

---

[2]The relay employs a TAS scheme to forward to the destination the signal received from the source. This will be described in the next subsection.

In this scheme, the local CSI available at S is exploited to its furthest extent in order to assist the decision, incurring a negligible delay and feedback overhead.

The concepts of DAS/MRC and DAS/SC are motivated and supported by the following inequalities, respectively, involving the end-to-end SNR:

$$\text{MRC:} \quad \gamma_{i,k,j} < \gamma_{S_iD} + \gamma_{S_iR_k} \min\left[\frac{\gamma_{R_jD}}{C}, 1\right] \triangleq \widetilde{\gamma}_{i,k,j} \tag{5.4}$$

$$\text{SC:} \quad \gamma_{i,k,j} < \max\left[\gamma_{S_iD}, \gamma_{S_iR_k} \min\left[\frac{\gamma_{R_jD}}{C}, 1\right]\right] \triangleq \widetilde{\gamma}_{i,k,j}. \tag{5.5}$$

The DAS operation is performed in two time slots [14], as shown in Fig. 5.1. In the first
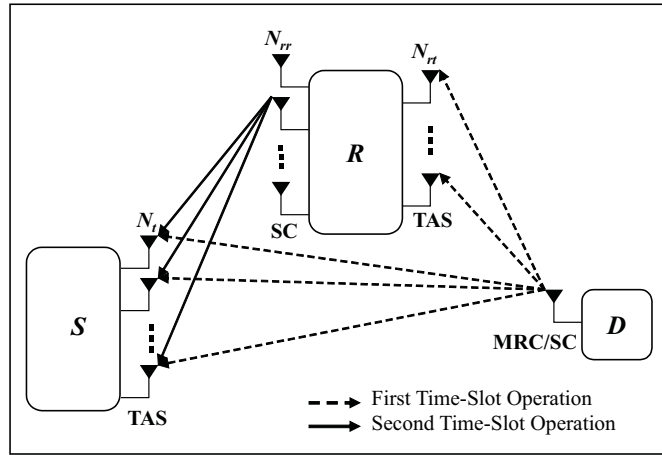
Figure 5.1: Operation of the DAS scheme.

time slot, D sends to R and S a 1-bit reverse pilot signaling. Then, R and S use this message to estimate their respective local CSIs γ_{R_jD} and γ_{S_iD}. At this time, based on γ_{R_jD}, the relay selects its optimal antenna to transmit data, by applying the following selection rule:

$$\text{DAS/MRC and DAS/SC:} \quad j^* = \arg\max_j \left\{\gamma_{R_jD}\right\}. \tag{5.6}$$

In the second time slot, R compares its local CSI $\gamma_{R_{j^*}D}$ with C, yielding two cases:

- If $\gamma_{R_{j^*}D} \geq C$, R sends to S a 1-bit message "1". In this case, by using (5.4) and (5.5), γ_{S_iD} and $\gamma_{S_iR_k}$, which are available at S, are sufficient to apply the selection rule $\max\{\widetilde{\gamma}_{i,k,j^*}\}$.

- If $\gamma_{R_{j^*}D} < C$, R sends to S a 1-bit message "0". In this case, by using (5.4) and (5.5), the application of $\max\{\widetilde{\gamma}_{i,k,j^*}\}$ would require the additional knowledge of $\gamma_{R_{j^*}D}$, which is unavailable at S. Therefore, somewhat arbitrarily, a suboptimal decision will be employed that depends solely on the maximization of γ_{S_iD}, which is available at S.

From the above, the TAS rule at the source of the proposed DAS schemes is summarized as follows:

$$\text{DAS/MRC:} \quad i^* = \begin{cases} \bar{\bar{i}} = \arg\max_i \left\{ \gamma_{S_i D} + \max_k \{\gamma_{S_i R_k}\} \right\}, & \text{if } \gamma_{R_{j^*} D} \geq C \\ \underline{i} = \arg\max_i \{\gamma_{S_i D}\}, & \text{if } \gamma_{R_{j^*} D} < C \end{cases} \tag{5.7}$$

$$\text{DAS/SC:} \quad i^* = \begin{cases} \bar{i} = \arg\max_i \left\{ \max\left[\gamma_{S_i D}, \max_k\{\gamma_{S_i R_k}\} \right] \right\}, & \text{if } \gamma_{R_{j^*} D} \geq C \\ \underline{i} = \arg\max_i \{\gamma_{S_i D}\}, & \text{if } \gamma_{R_{j^*} D} < C. \end{cases} \tag{5.8}$$

Finally, since SC is employed at the relay reception of both schemes, we have that

$$\text{DAS/MRC and DAS/SC:} \quad k^* = \arg\max_k \left\{ \gamma_{S_{i^*} R_k} \right\}. \tag{5.9}$$

It is noteworthy that the major advantage of DAS over other antenna selection schemes is its reduced delay/feedback overhead, requiring only a 2-bit pilot/feedback signaling, at the expense of some additional hardware complexity at the source.

5.3 Outage Analysis

In this section, we analyze the outage probability of the proposed schemes, DAS/MRC and DAS/SC. This metric is defined as the probability that the end-to-end SNR falls below a given threshold z, commonly written in terms of a target spectral efficiency $\Re_0$. Because the proposed schemes operate on a half-duplex basis, it follows that $z = 2^{2\Re_0} - 1$. For clarity and structure, our analytical results shall be organized as a set of theorems and corollaries.

5.3.1 DAS/MRC

Proposition 1. The outage probability of the DAS/MRC scheme can be mathematically formulated as

$$P_{\text{out}}^{\text{DAS/MRC}} = I_1 + I_2, \tag{5.10}$$

where

$$I_1 = \Pr\left(\gamma_{R_{j^*} D} \geq C, \gamma_{S_{\bar{\bar{i}}} D} + \frac{\gamma_{S_{\bar{\bar{i}}} R_{k^*}} \gamma_{R_{j^*} D}}{\gamma_{R_{j^*} D} + C} < z \right) \tag{5.11}$$

$$I_2 = \Pr\left(\gamma_{R_{j^*} D} < C, \gamma_{S_{\underline{i}} D} + \frac{\gamma_{S_{\underline{i}} R_{k^*}} \gamma_{R_{j^*} D}}{\gamma_{R_{j^*} D} + C} < z \right). \tag{5.12}$$

Proof. Based on the CSI of the relay-destination link, the algorithm used for the transmit antenna selection at the source has two possible choices, as expressed by (5.7):

- If $\gamma_{R_{j^*} D} \geq C$, the transmit antenna selection at the source is made according to the rule $\bar{\bar{i}}$. In this case, an outage occurs when the end-to-end SNR from the $\bar{\bar{i}}$th antenna at S to D (through the k^*th receive antenna and j^*th transmit antenna at R) falls below the threshold z. This end-to-end SNR is written as in (5.1). Therefore, the joint probability I_1 of $\gamma_{R_{j^*} D} \geq C$ and an outage event can be formulated as in (5.11).

- If $\gamma_{R_{j^*}D} < C$, the transmit antenna selection at the source is made according to the rule $\underline{i}$. Except for the antenna index, the outage definition and the end-to-end SNR are written exactly as in the previous case. Therefore, the joint probability I_2 of $\gamma_{R_{j^*}D} < C$ and an outage event can be formulated as in (5.12).

Finally, since $\gamma_{R_{j^*}D} \geq C$ and $\gamma_{R_{j^*}D} < C$ are complementary events, the outage probability can be obtained by adding I_1 and I_2, as in (5.10). □

1. Bound Analysis

Unfortunately, an exact closed-form solution to the general mathematical framework provided in Proposition 1 seems infeasible. Instead, we derive a lower bound for the outage probability. This bound is based on the following paramount relationships:

$$\frac{\gamma_{S_i R_k}\gamma_{R_j D}}{\gamma_{R_j D} + C} \leq \gamma_{S_i R_k} \min\left[\frac{\gamma_{R_j D}}{C}, 1\right]. \tag{5.13}$$

The ultimate aim is to obtain a closed-form asymptotic expression for the bound derived, which shall be presented in Section 5.3.1-2. Hereafter, I_1^{LB} and I_2^{LB} denote the lower bounds of I_1 and I_2, respectively.

Corollary 1. From Proposition 1, I_1^{LB} can be expressed as

$$I_1^{\mathrm{LB}} = \Pr\left(\max_j\{\gamma_{R_j D}\} \geq C\right) \Pr\left(\gamma_{S_i D} + \max_k\{\gamma_{S_i R_k}\} < z\right)^{N_t}. \tag{5.14}$$

Proof. See Appendix E.1. □

Corollary 2. From Proposition 1, I_2^{LB} can be expressed as

$$I_2^{\mathrm{LB}} = \Pr\left(\max_j\{\gamma_{R_j D}\} < C, \max_m\{\gamma_{S_m D}\} + \max_k\{\gamma_{S_i R_k}\}\frac{\gamma_{R_{j^*}D}}{C} < z\right). \tag{5.15}$$

Proof. See Appendix E.2. □

Theorem 1. For the propagation scenario considered in this work (independent flat Rayleigh fading), I_1^{LB} specializes to the following closed-form expression:

$$I_1^{\mathrm{LB}} = \left(1 - \left(1 - e^{-\frac{C}{\bar{\gamma}_{RD}}}\right)^{N_{rt}}\right)\left(\sum_{j=0}^{N_{rr}}\binom{N_{rr}}{j}(-1)^j\left(\frac{\left(e^{-j\frac{z}{\bar{\gamma}_{SR}}} - e^{-\frac{z}{\bar{\gamma}_{SD}}}\right)\bar{\gamma}_{SR}}{j\bar{\gamma}_{SD} - \bar{\gamma}_{SR}}\right)\right)^{N_t}. \tag{5.16}$$

Proof. See Appendix E.3. □

Theorem 2. For the propagation scenario considered in this work (independent flat Rayleigh fading), I_2^{LB} specializes to the following single-fold integral form expression:

$$I_2^{\mathrm{LB}} = \int_0^1 \frac{C N_{rt} N_{rr}}{\bar{\gamma}_{RD}} e^{-\frac{Cu}{\bar{\gamma}_{RD}}}\left(1 - e^{-\frac{Cu}{\bar{\gamma}_{RD}}}\right)^{N_{rt}-1}$$

$$\times \sum_{m=0}^{N_t}\sum_{j=0}^{N_{rr}}\binom{N_t}{m}\binom{N_{rr}-1}{j}(-1)^m(-1)^j\frac{\left(e^{-\frac{(1+j)z}{u\bar{\gamma}_{SR}}} - e^{-\frac{mz}{\bar{\gamma}_{SD}}}\right)\bar{\gamma}_{SD}}{mu\bar{\gamma}_{SR} - (1+j)\bar{\gamma}_{SD}}du. \tag{5.17}$$

Proof. See Appendix E.4. □

Combining the above results into (5.10), a lower bound for the outage probability of the DAS/MRC scheme can be written as $P_{\text{out}}^{\text{DAS/MRC}} \geq I_1^{\text{LB}} + I_2^{\text{LB}}$.

2. Asymptotic Bound Analysis

In order to assess the asymptotic behavior of $P_{\text{out}}^{\text{DAS/MRC}}$, which provides further insight into the achievable system diversity order, a high-SNR analysis of I_1^{LB} and I_2^{LB} is now formulated. Hereafter, $\tilde{I}_1^{\text{LB}}$, $\tilde{I}_2^{\text{LB}}$, and $\tilde{P}_{\text{out}}^{\text{DAS/MRC,LB}}$ denote the asymptotic lower bounds of I_1, I_2, and $P_{\text{out}}^{\text{DAS/MRC}}$, respectively.

Corollary 3. From Theorem 1, $\tilde{I}_1^{\text{LB}}$ can be obtained as

$$\tilde{I}_1^{\text{LB}} = \left(1 - \left(1 - e^{-\frac{1}{\mu_2}}\right)^{N_{rt}}\right) \left(\left(\frac{1}{\bar{\gamma}_{SR}}\right)^{N_{rr}} \frac{1}{\bar{\gamma}_{SD}} \frac{z^{N_{rr}+1}}{(N_{rr}+1)}\right)^{N_t}, \qquad (5.18)$$

where $\mu_2 \triangleq \bar{\gamma}_{RD}/\bar{\gamma}_{SR}$.

Proof. See Appendix E.5. □

Corollary 4. From Theorem 2, $\tilde{I}_2^{\text{LB}}$ can be obtained as

$$\tilde{I}_2^{\text{LB}} = N_{rt} \frac{N_{rr}}{\bar{\gamma}_{SR}} \left(\frac{1}{\bar{\gamma}_{SD}}\right)^{N_t} \sum_{i=1}^{N_{rr}} \binom{N_{rr}-1}{i-1} (-1)^{i-1} \sum_{j=0}^{N_{rt}} \binom{N_{rt}-1}{j-1} (-1)^{j-1} \sum_{n=0}^{\infty} \tilde{\Phi}_n, \quad (5.19)$$

where $\tilde{\Phi}_n$ is defined as

$$\tilde{\Phi}_0 = \begin{cases} \left(\frac{1}{\bar{\gamma}_{SR}}\right)^{n_1} \left(\frac{ji}{\mu_2}\right)^{n_1} \frac{z^{N_t+1+n_1}}{n_1!^2(N_t+1)\mu_2} \left(-\ln\left(\frac{jiz}{\bar{\gamma}_{RD}}\right)\right. \\ \left. +2\psi(n_1+1) - (-1)^{n_1}\Gamma\left(-n_1, \frac{j}{\mu_2}\right)\right), & \text{if } N_{rr} = N_{rt} \\[3mm] \left(\frac{1}{\bar{\gamma}_{SR}}\right)^{n_1} \left(\frac{ji}{\mu_2}\right)^{n_1} \frac{z^{N_t+1+n_1}}{n_1!^2(N_t+1)\mu_2} \\ \left(-\ln\left(\frac{jiz}{\bar{\gamma}_{RD}}\right) - (-1)^{n_1}\Gamma\left(-n_1, \frac{j}{\mu_2}\right)\right), & \text{if } N_{rr} < N_{rt} \\[3mm] \left(\frac{1}{\bar{\gamma}_{SR}}\right)^{n_1} \left(\frac{ji}{\mu_2}\right)^{n_1} \frac{z^{N_t+1+n_1}}{n_1!^2(N_t+1)\mu_2} \left(-\ln\left(\frac{jiz}{\bar{\gamma}_{RD}}\right)\right), & \text{if } N_{rr} > N_{rt} \end{cases} \qquad (5.20)$$

$$\tilde{\Phi}_{n|_1^{n_1}} = \begin{cases} \left(\frac{1}{\bar{\gamma}_{SR}}\right)^{n_1} \frac{z^{N_t+n_1+1}}{n!(N_t+n+1)\mu_2} \left(\frac{ji}{\mu_2}\right)^{n_1} \\ \left((-1)^{n+1} \frac{1}{(n_1-n)!n_1!} \ln\left(\frac{jiz}{\bar{\gamma}_{RD}}\right)\right. \\ \left. -\frac{(-1)^{n_1-n}}{(n_1-n)!}\Gamma\left(-n_1, \frac{j}{\mu_2}\right)\right), & \text{if } N_{rr} \leq N_{rt} \\[3mm] \left(\frac{1}{\bar{\gamma}_{SR}}\right)^{n_1} \frac{z^{N_t+n_1+1}}{n!(N_t+n+1)\mu_2} \left(\frac{ji}{\mu_2}\right)^{n_1} \\ \left((-1)^{n+1} \frac{1}{(n_1-n)!n_1!} \ln\left(\frac{jiz}{\bar{\gamma}_{RD}}\right)\right), & \text{if } N_{rr} > N_{rt} \end{cases} \qquad (5.21)$$

$$\tilde{\Phi}_{n|_{n_1+1}^{\infty}} = \begin{cases} \left(\frac{1}{\bar{\gamma}_{SR}}\right)^{n_1} \frac{z^{N_t+n_1+1}}{n!(N_t+n+1)\mu_2} \left(\frac{ji}{\mu_2}\right)^{n_1} \\ \frac{(n-n_1-1)!}{n_1!} (-1)^{n_1}, & \text{if } N_{rr} = N_{rt} \\[3mm] 0, & \text{otherwise,} \end{cases} \qquad (5.22)$$

with $n_1 \triangleq \min(N_{rr}, N_{rt}) - 1$, $\Gamma(\cdot)$ being the gamma function, and $\psi(\cdot) = \frac{d}{dx} \ln \Gamma(x) = \frac{\Gamma'(x)}{\Gamma(x)}$ being the digamma function.

Proof. See Appendix E.6. □

Finally, these asymptotic lower bounds for I_1 and I_2 can be added as in (5.10), yielding corresponding bounds for the outage probability. This is detailed in the following theorem.

Theorem 3. An asymptotic lower bound for $P_{\text{out}}^{\text{DAS/MRC}}$ is obtained as

$$\tilde{P}_{\text{out}}^{\text{DAS/MRC,LB}} = \begin{cases} \tilde{I}_1^{\text{LB}} + \tilde{I}_2^{\text{LB}}, & \text{if } N_t = 1 \text{ and } N_{rr} \leq N_{rt} \\ \tilde{I}_2^{\text{LB}}, & \text{otherwise.} \end{cases} \tag{5.23}$$

Proof. First, let us consider the asymptotic lower bound. From (5.18) and (5.19)–(5.22), the diversity orders of the terms $\tilde{I}_1^{\text{LB}}$ and $\tilde{I}_2^{\text{LB}}$ are given by $N_t N_{rr} + N_t$ and $N_t + \min(N_{rr}, N_{rt})$, respectively. These values coincide for the special case $N_t = 1$ and $N_{rr} \leq N_{rt}$, yielding $1 + N_{rr}$. Otherwise, the diversity order of $\tilde{I}_1^{\text{LB}}$ exceeds that of $\tilde{I}_2^{\text{LB}}$. In each case, the asymptotic expression $\tilde{P}_{\text{out}}^{\text{DAS/MRC,LB}}$ is obtained by preserving only the lowest-order terms of the sum $\tilde{I}_1^{\text{LB}} + \tilde{I}_2^{\text{LB}}$, thus leading to (5.23). □

Remarks:

- A similar procedure can be applied to derive an upper bound for $P_{\text{out}}^{\text{DAS/MRC}}$. The resulting upper bound is somewhat loose, but it has the same diversity order as the lower bound. Therefore, based on the Pinching Theorem [20] and on the above discussion in the proof of Theorem 3, if follows that the proposed DAS/MRC scheme achieves full diversity order, that is, $N_t + \min(N_{rr}, N_{rt})$.

- In (5.19), $\tilde{I}_2^{\text{LB}}$ is written in terms of an infinite series, namely $\sum_{n=0}^{\infty} \tilde{\Phi}_n$. On the other hand, note in (5.22) that the terms for $n > n1$ are nil if $N_{rr} \neq N_{rt}$. In addition, if $N_{rr} = N_{rt}$, it can be shown that the sum of those terms reduces to $\sum_{n=n_1+1}^{\infty} \Phi_n = \frac{{}_2F_3[\{1,1,2+n_1+N_t\},\{2+n_1,3+n_1+N_t\},1]}{(2+n_1+N_t)(1+n_1)!}$. Therefore, our analytical expression for $\tilde{I}_2^{\text{LB}}$ is actually written in closed form.

5.3.2 DAS/SC

Some of the following theorems and corollaries for the DAS/SC scheme can be proved based on a mathematical framework similar to that of corresponding theorems and corollaries already proved here for the DAS/MRC scheme. In such cases, for the lack of space, the proofs shall be omitted. Of course, in those proofs, all DAS/MRC equations involved give place to their DAS/SC counterparts.

Proposition 2. The outage probability of the proposed DAS/SC scheme can be mathematically formulated as

$$P_{\text{out}}^{\text{DAS/SC}} = J_1 + J_2, \tag{5.24}$$

where

$$J_1 = \Pr\left(\gamma_{R_{j*}D} \geq C, \max\left[\gamma_{S_{\bar{i}}D}, \frac{\gamma_{S_{\bar{i}}R_{k*}}\gamma_{R_{j*}D}}{\gamma_{R_{j*}D}+C}\right] < z\right). \tag{5.25}$$

$$J_2 = \Pr\left(\gamma_{R_{j*}D} < C, \max\left[\gamma_{S_{\underline{i}}D}, \frac{\gamma_{S_{\underline{i}}R_{k*}}\gamma_{R_{j*}D}}{\gamma_{R_{j*}D}+C}\right] < z\right). \tag{5.26}$$

Proof. As in the DAS/MRC scheme, the antenna selection algorithm of the DAS/SC scheme has also two possible choices, depending on the CSI of the relay-destination link. This is expressed in (5.8). Therefore, the proof of Proposition 2 follows the same rationale presented for Proposition 1, by using (5.2) and (5.8) instead of (5.1) and (5.7), respectively. □

1. Bound Analysis

As in the DAS/MRC scheme, there seems to be no exact closed-form solution to the general mathematical framework provided in Proposition 2. Alternatively, we derive again a lower bound for the outage probability, based on the inequalities in (5.13). As before, our ultimate aim is to obtain a closed-form asymptotic expression for the bound derived, which shall be presented in Section 5.3.2-2. Hereafter, J_1^{LB} and J_2^{LB} denote the lower bounds of J_1 and J_2, respectively.

Corollary 5. From Proposition 2, J_1^{LB} can be expressed as

$$J_1^{\mathrm{LB}} = \Pr\left(\max_j\{\gamma_{R_jD}\} \geq C\right)\Pr\left(\gamma_{S_iD} < z\right)^{N_t}\Pr\left(\max_k\{\gamma_{S_iR_k}\} < z\right)^{N_t}. \tag{5.27}$$

Proof. This proof[3] is similar to that of Corollary 1. □

Corollary 6. From Proposition 2, J_2^{LB} can be expressed as

$$J_2^{\mathrm{LB}} = \Pr\left(\max_j\{\gamma_{R_jD}\} < C, \max\left[\max_m\{\gamma_{S_mD}\}, \max_k\{\gamma_{S_iR_k}\}\frac{\gamma_{R_{j*}D}}{C}\right] < z\right). \tag{5.28}$$

Proof. This proof[4] is similar to that of Corollary 2. □

Theorem 4. For the propagation scenario considered in this work (independent flat Rayleigh fading), J_1^{LB} specializes to the following closed-form expression:

$$J_1^{\mathrm{LB}} = \left(1 - \left(1 - e^{-\frac{C}{\bar{\gamma}_{RD}}}\right)^{N_{rt}}\right)\left(1 - e^{-\frac{z}{\bar{\gamma}_{SD}}}\right)^{N_t}\left(1 - e^{-\frac{z}{\bar{\gamma}_{SR}}}\right)^{N_{rr}N_t}. \tag{5.29}$$

Proof. This result follows directly from (5.27), by specializing the involved probabilities to the Rayleigh case and using the well-known result that the cumulative distribution of the maximum is the product of the marginal distributions. □

---

[3]Although in the original manuscript this proof has been omitted for the lack of space, it is presented here for completeness, in Appendix E.7.

[4]Although in the original manuscript this proof has been omitted for the lack of space, it is presented here for completeness, in Appendix E.8.

Theorem 5. For the propagation scenario considered in this work (independent flat Rayleigh fading), J_2^{LB} specializes to the following single-fold integral form expression:

$$J_2^{\text{LB}} = \int_0^1 \frac{CN_{rt}}{\bar{\gamma}_{RD}} e^{-\frac{Cu}{\bar{\gamma}_{RD}}} \left(1 - e^{-\frac{Cu}{\bar{\gamma}_{RD}}}\right)^{N_{rt}-1} \left(1 - e^{-\frac{z}{u\bar{\gamma}_{SR}}}\right)^{N_{rr}} \left(1 - e^{-\frac{z}{\bar{\gamma}_{SD}}}\right)^{N_t} du. \quad (5.30)$$

Proof. This proof[5] is similar to that of Theorem 2. □

As in the DAS/MRC scheme, by combining the above results into (5.24), outage probability bound of the DAS/SC scheme can be written as $P_{\text{out}}^{\text{DAS/SC}} \geq J_1^{\text{LB}} + J_2^{\text{LB}}$.

2. Asymptotic Bound Analysis

In order to assess the asymptotic behavior and the diversity order of the DAS/SC scheme, we now perform a high-SNR analysis of J_1^{LB} and J_2^{LB}. Hereafter, $\tilde{J}_1^{\text{LB}}$, $\tilde{J}_2^{\text{LB}}$, and $\tilde{P}_{\text{out}}^{\text{DAS/SC,LB}}$ denote the asymptotic lower bounds of J_1, J_2, and $P_{\text{out}}^{\text{DAS/SC}}$, respectively.

Corollary 7. From Theorem 4, $\tilde{J}_1^{\text{LB}}$ can be obtained as

$$\tilde{J}_1^{\text{LB}} = \left(1 - \left(1 - e^{-\frac{1}{\mu_2}}\right)^{N_{rt}}\right) \left(\frac{z}{\bar{\gamma}_{SD}}\right)^{N_t} \left(\frac{z}{\bar{\gamma}_{SR}}\right)^{N_{rr}N_t}. \quad (5.31)$$

Proof. This result follows directly from (5.29), by using the MacLaurin series expansion of the exponential function and dropping the terms beyond the second. □

Corollary 8. From Theorem 5, $\tilde{J}_2^{\text{LB}}$ can be obtained as

$$\tilde{J}_2^{\text{LB}} = \left(\frac{z}{\bar{\gamma}_{SD}}\right)^{N_t} \left(\frac{N_{rt}}{\mu_2} \sum_{j=1}^{N_{rt}} \binom{N_{rt}-1}{j-1} (-1)^{j-1} \sum_{i=1}^{N_{rr}} \binom{N_{rr}}{i} (-1)^i \Omega\right), \quad (5.32)$$

where Ω is defined as

$$\Omega = \begin{cases} \frac{\left(\frac{iz}{\bar{\gamma}_{SR}}\right)^{n_1+1}\left(\frac{j}{\mu_2}\right)^{n_1}}{n_1!(n_1+1)!} \left(\ln \frac{jiz}{\bar{\gamma}_{RD}}\right), & \text{if } N_{rr} > N_{rt} \\[2ex] \frac{\left(\frac{iz}{\bar{\gamma}_{SR}}\right)^{n_1+1}\left(\frac{j}{\mu_2}\right)^{n_1}}{(n_1+1)!} \left(\frac{1}{n_1!} \ln \frac{jiz}{\bar{\gamma}_{RD}} - (-1)^{n_1+1} \Gamma\left(-n_1, \frac{j}{\mu_2}\right)\right), & \text{if } N_{rr} < N_{rt} \\[2ex] \frac{\left(\frac{iz}{\bar{\gamma}_{SR}}\right)^{n_1+1}\left(\frac{j}{\mu_2}\right)^{n_1}}{(n_1+1)!} \left(\frac{1}{n_1!} \left(\ln \frac{jiz}{\bar{\gamma}_{RD}} - \psi(n_1+1) - \psi(n_1+2)\right)\right. \\ \left. -(-1)^{n_1+1}\Gamma\left(-n_1, \frac{j}{\mu_2}\right)\right), & \text{if } N_{rr} = N_{rt}, \end{cases} \quad (5.33)$$

with $\mu_2 \triangleq \bar{\gamma}_{RD}/\bar{\gamma}_{SR}$ and $n_1 \triangleq \min(N_{rr}, N_{rt}) - 1$, as already defined for the DAS/MRC scheme.

Proof. This proof[6] is similar to that of Corollary 4. □

Finally, these asymptotic lower bounds for J_1 and J_2 can be added as in (5.24), yielding corresponding bound for the outage probability. This is detailed in the following theorem.

---

[5]Although in the original manuscript this proof has been omitted for the lack of space, it is presented here for completeness, in Appendix E.9.

[6]Although in the original manuscript this proof has been omitted for the lack of space, it is presented here for completeness, in Appendix E.10.

Theorem 6. An asymptotic lower bound for $P_{\text{out}}^{\text{DAS/SC}}$ is obtained as

$$\tilde{P}_{\text{out}}^{\text{DAS/SC,LB}} = \begin{cases} \tilde{J}_1^{\text{LB}} + \tilde{J}_2^{\text{LB}}, & \text{if } N_t = 1 \text{ and } N_{rr} \leq N_{rt} \\[2ex] \tilde{J}_2^{\text{LB}}, & \text{otherwise.} \end{cases} \tag{5.34}$$

Proof. This proof is similar to that of Theorem 3. □

Remarks:

- A discussion equivalent to that in the proof of Theorem 3 applies to Theorem 6. Accordingly, the proposed DAS/SC scheme is also shown to achieve full diversity order, that is, $N_t + \min(N_{rr}, N_{rt})$.

- The proposed DAS/SC scheme is attractive in practice, because it is much simpler to implement than the DAS/MRC scheme, while achieving the same diversity order.

5.4 Numerical Results and Discussions

In this section, we present sample numerical results and Monte Carlo simulations to evaluate the performance of the proposed DAS/MRC and DAS/SC schemes and validate the derived analytical bounds. As a term of comparison, the performance of the corresponding optimal centralized schemes—TAS/MRC and TAS/SC—is also shown in the figures. For illustration purposes, we assume the following scenario: (a) the target spectral efficiency is $\Re_0 = 1$ bit/s/Hz; (b) the path loss exponent is $\beta = 4$; (c) the network has a linear topology, in which $d_{SD} = d_{SR} + d_{RD}$, with d_{SD}, d_{SR}, and d_{RD} being the lengths of the links $S \to D$, $S \to R$, and $R \to D$, respectively; (d) S and R have identical transmit powers, i.e., $P_S = P_R = P$; (e) each channel mean power is proportional to $d^{-\beta}$, with d being the distance between the corresponding transceivers, so that $\bar{\gamma}_{SD} = Pd_{SD}^{-\beta}/N_0$, $\bar{\gamma}_{SR} = Pd_{SR}^{-\beta}/N_0$, and $\bar{\gamma}_{RD} = Pd_{RD}^{-\beta}/N_0$; (f) the distance between S and D is normalized to unity, i.e., $d_{SD} = 1$.

5.4.1 Impact of Relay Location and Number of Antennas

Figs. 5.2 and 5.3 show simulation results for the impact of relay location (d_{SR}) on the outage probability of DAS/MRC and DAS/SC, respectively, for different numbers transmit and receive antennas at the relay ($N_{rr} = 1$ and $N_{rt} = 1$; $N_{rr} = 1$ and $N_{rt} = 2$; $N_{rr} = 2$ and $N_{rt} = 1$; and $N_{rr} = 2$ and $N_{rt} = 2$) and different numbers of transmit antennas at the source ($N_t = 2$ in Figs. 5.2a and 5.3a, and $N_t = 3$ in Figs. 5.2b and 5.3b). As mentioned before, the optimal centralized TAS/MRC and TAS/SC schemes are also plotted. In these figures, we highlight three main aspects:

1. *The outage performances of the distributed and optimal centralized schemes bear similar shapes.* In both cases investigated—DAS/MRC and DAS/SC—the outage probability curves of the distributed scheme and its centralized counterpart evolve similarly as the relay is moved from source ($d_{SR} = 0$) to destination ($d_{SR} = 1$).
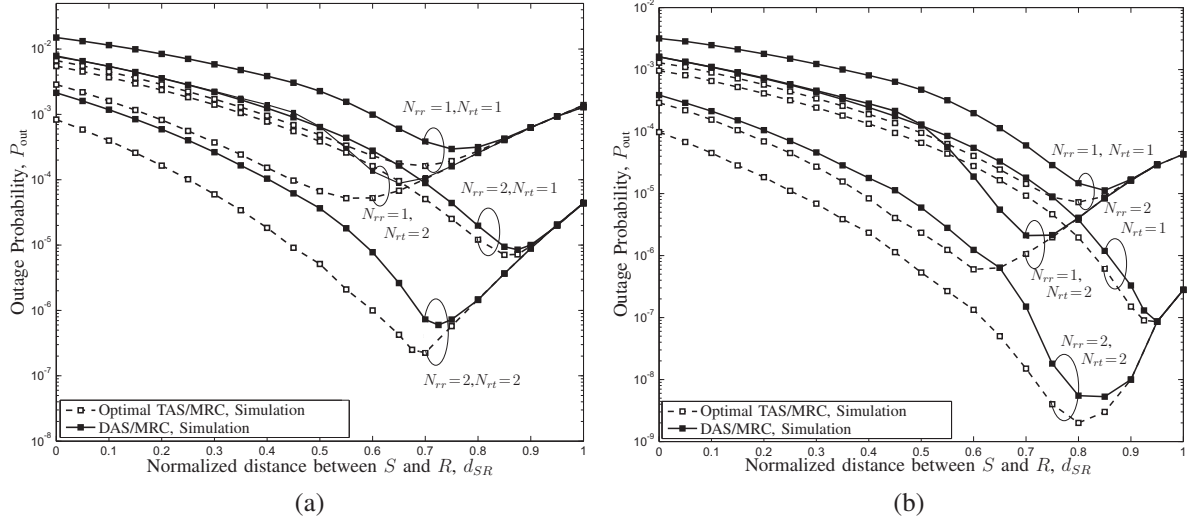
Figure 5.2: Comparison of proposed DAS/MRC and optimal centralized TAS/MRC in terms of outage probability ($P/N_0 = 10$ dB): (a) $N_t = 2$ e (b) $N_t = 3$.
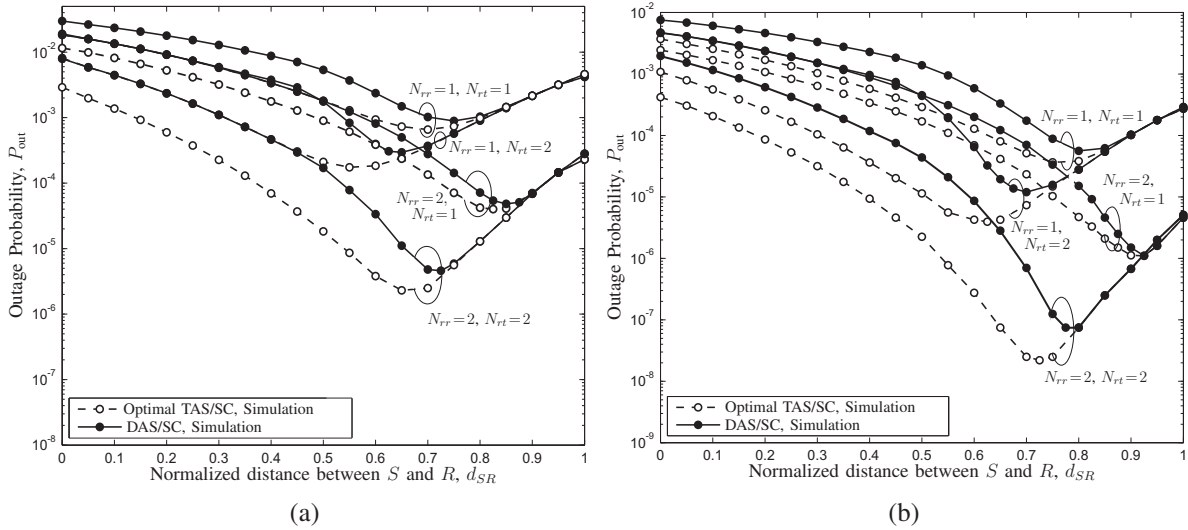

Figure 5.3: Comparison of proposed DAS/SC and optimal centralized TAS/SC in terms of outage probability ($P/N_0 = 10$ dB): (a) $N_t = 2$ e (b) $N_t = 3$.

In particular, the outage probability achieves a minimum when the relay is placed somewhere between the midpoint ($d_{SR} = 1/2$) and the destination, depending on the scheme considered and on the antenna configuration. One may conjecture why the best performance is not achieved with the relay being placed exactly at the midpoint. This is because the end-to-end SNR for fixed-gain relaying is not commutative with respect to the first- and second-hop SNRs, as can be seen in (5.1) and (5.2). For variable-gain relaying, however, that would be the case.

2. *The distributed schemes become optimal as the relay approaches the destination.* As the relay is placed closer to the destination ($d_{SR} \to 1$), the performances of DAS/MRC and DAS/SC approach those of TAS/MRC and TAS/SC, respectively. This is explained as follows. When $d_{SR} \to 1$, the channel quality of the second hop improves, so that the probability of $\gamma_{R_{j^*}D} \geq C$ increases. Consequently, from (5.7) and (5.8), most of the time DAS/MRC applies the selection rule $i^* = \bar{i} = \arg\max_i \{\gamma_{S_iD} + \max_k \{\gamma_{S_iR_k}\}\}$ and DAS/SC applies the selection rule $i^* = \bar{i} = \arg\max_i \max \left[\gamma_{S_iD}, \max_k \{\gamma_{S_iR_k}\}\right]$. In addition, as the probability of $\gamma_{R_{j^*}D} \geq C$ increases, $\frac{\gamma_{S_iR_k}\gamma_{R_jD}}{\gamma_{R_jD}+C} \approx \gamma_{S_iR_k}$ proves more accurate, so that the optimal selection rule in (5.3) reduces to $(i^*, k^*, j^*) \approx \arg\max_{i,k,j} \{\gamma_{S_iD} + \gamma_{S_iR_k}\}$ for TAS/MRC and to $(i^*, k^*, j^*) \approx \arg\max_{i,k,j} \{\max [\gamma_{S_iD}, \gamma_{S_iR_k}]\}$ for TAS/SC. Note that these rules are indeed identical to their distributed $\bar{i}$-case counterparts. Therefore, as $d_{SR} \to 1$, the proposed distributed schemes become optimal.

3. *The imbalance between the number of transmit and receive antennas at the relay sets its best position.* To illustrate this, consider the antenna configuration ($N_{rr} = 1, N_{rt} = 1$) for reference, against which the other configurations ($N_{rr} = 1, N_{rt} = 2$), ($N_{rr} = 2, N_{rt} = 1$), and ($N_{rr} = 2, N_{rt} = 2$) shall be compared in terms of best relay position (minimum outage probability). First, when ($N_{rr} = 2, N_{rt} = 2$), we observe that the best relay position is roughly preserved. We have empirically verified that this always happens when $N_{rr} = N_{rt}$. On the other hand, when ($N_{rr} = 1, N_{rt} = 2$), the best relay position is observed to move toward the source. We have also verified that this always happens when $N_{rr} \leq N_{rt}$. Finally, when ($N_{rr} = 2, N_{rt} = 1$), the best relay position is observed to move toward the destination, which is again a general behavior for $N_{rr} \geq N_{rt}$. Note that a counterbalance mechanism is at play here. The addition of a transmit antenna at the relay improves the quality of the second hop, as well the addition of a receive antenna at the relay improves the quality of the first hop. Accordingly, in each case, the best relay position always moves in a direction so as to weaken the hop improved by the antenna addition.

5.4.2 Impact of Average SNR

In order to validate our bound expressions and assess the outage probability of the proposed DAS/MRC and DAS/SC schemes while varying the average SNR of the source-destination link, we present simulation and analytical results for different numbers transmit and receive antennas at the relay ($N_{rr} = 1$ and $N_{rt} = 1$; $N_{rr} = 1$ and $N_{rt} = 2$;
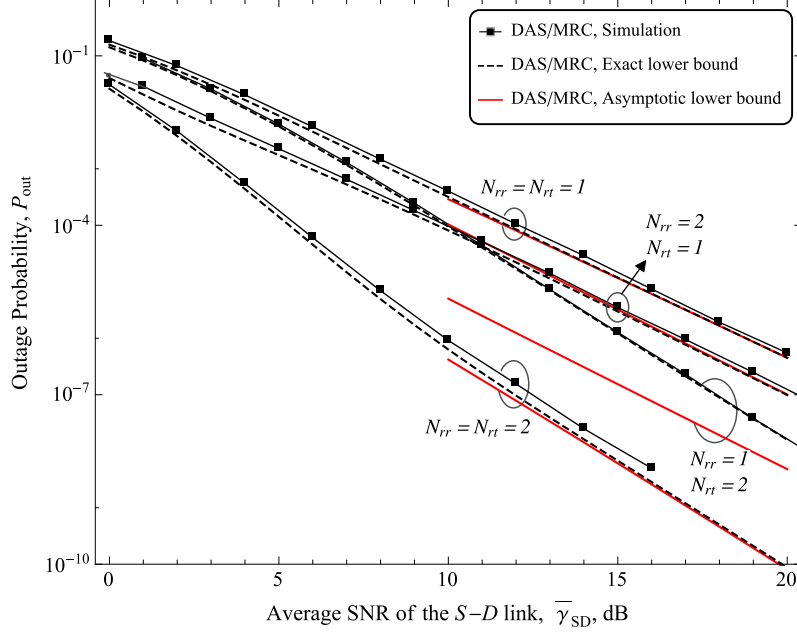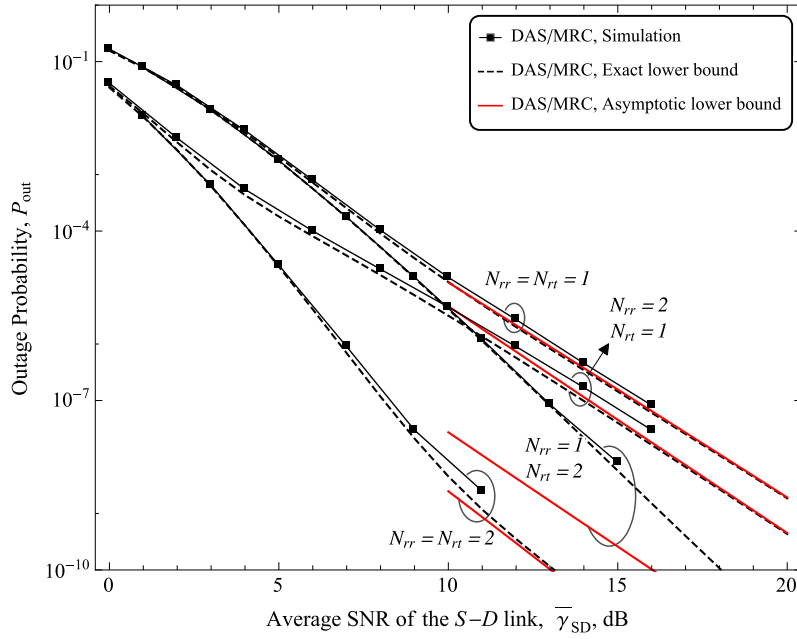
Figure 5.4: Outage probability versus average SNR of the *S-D* link for the proposed DAS/MRC scheme: (a) $d_{SR} = 0.7$ and $N_t = 2$; (b) $d_{SR} = 0.8$ and $N_t = 3$.
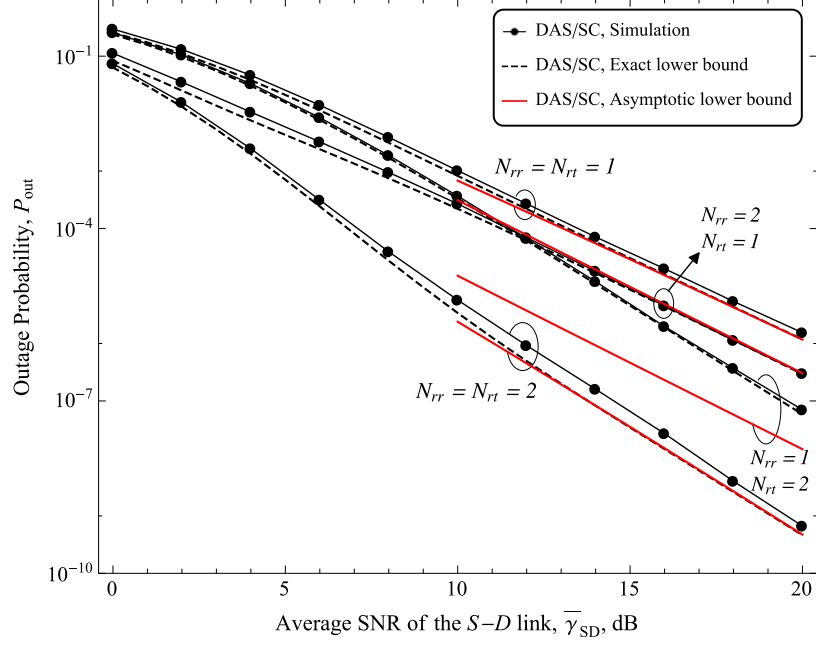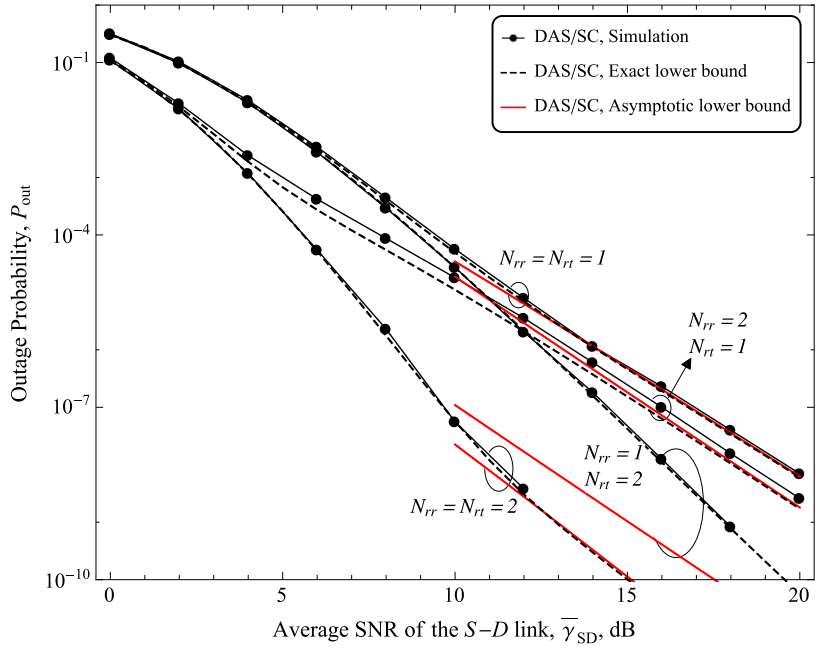
Figure 5.5: Outage probability versus average SNR of the *S-D* link for the proposed DAS/SC scheme: (a) $d_{SR} = 0.7$ and $N_t = 2$; (b) $d_{SR} = 0.8$ and $N_t = 3$.

$N_{rr} = 2$ and $N_{rt} = 1$; and $N_{rr} = 2$ and $N_{rt} = 2$) and different numbers of transmit antennas at the source ($N_t = 2$ in Figs. 5.4a and 5.5a, and $N_t = 3$ in Figs. 5.4b and 5.5b). For a better clarity of the simulated and exact bound results at low to medium SNR, the asymptotic curves have been truncated at 10 dB. In each scenario, the relay has been placed close to the position that provides the best outage performance for the optimal centralized schemes with the antenna configuration ($N_{rr} = 1$, $N_{rt} = 1$), as a term of comparison ($d_{SR} = 0.7$ for $N_t = 2$ and $d_{SR} = 0.8$ for $N_t = 3$).

In Figs. 5.4 and 5.5, it can be observed that, for both DAS/MRC and DAS/SC, our lower bound expressions are extremely close to the simulation curves over the entire SNR range in all the cases. The curves confirm that the proposed schemes achieve full diversity order, which is equal to $N_t + \min(N_{rr}, N_{rt})$. For instance, under the antenna configuration $N_t = N_{rr} = N_{rt} = 2$, the diversity order equals 4, matching the asymptotic slope of the corresponding curves in Figs. 5.4a and 5.5a. Note that for some antenna configurations the lower bound meets its asymptotic expression outside the SNR range presented in the figures.

5.5 Conclusions

In this work, we designed and analyzed two distributed transmit-antenna selection schemes for dual-hop fixed-gain amplify-and-forward relaying networks. Our results generalize previous works to the multi-antenna relay scenario. We derived extremely tight lower bounds for the outage probability of both schemes, as well as closed-form asymptotic expressions for each of these bounds. We also showed that the proposed distributed schemes achieve the same diversity order as their optimal centralized counterparts, and perform increasingly close to these as the relay approaches the destination.

Bibliography

[1] S. Sanayei and A. Nosratinia, "Antenna selection in MIMO systems," *IEEE Commun. Mag.*, vol. 42, no. 10, pp. 68–73, Oct. 2004.

[2] N. T. B. Tam, T. Tran-Thien, T. Do-Hong, and V. N. Q. Bao, "Performance analysis of decode-and-forward relaying for multi-hop Alamouti transmission over Rayleigh fading channels," in *Proc. IEEE Conference International Advanced Technologies for Communications (ATC)*, Ho Chi Minh City, Vietnam, 20–22 Oct. 2010, pp. 195–200.

[3] Z. Chen, J. Yuan, and B. Vucetic, "Analysis of transmit antenna selection/maximal-ratio combining in Rayleigh fading channels," *IEEE Trans. Veh. Technol.*, vol. 54, no. 4, pp. 1312–1321, Jul. 2005.

[4] M. K. Simon and M. Alouini, *Digital ommunication over fading channels: A unified approach to performance analysis.* John Wiley & Sons, 2000.

[5] S. W. Peters and R. W. Heath, "Nonregenerative MIMO relaying with optimal transmit antenna selection," *IEEE Signal Process. Lett*, vol. 15, pp. 421–424, 2008.

[6] L. Cao, X. Zhang, Y. Wang, and D. Yang, "Transmit antenna selection strategy in amplify-and-forward MIMO relaying," in *Proc. IEEE Conference Wireless Communications and Networking (WCN)*, Budapest, Hungary, 5–8 Apr. 2009, pp. 1–4.

[7] A. A. Tarkhan, F. Farzaneh, and B. H. Khalaj, "Efficient suboptimal transmit antenna selection for MIMO relay channels," in *Proc. IEEE International Symposium on Computer Networks and Distributed Systems (CNDS)*, Tehran, Iran, 23–24 Feb. 2011, pp. 45–48.

[8] P. L. Yeoh, M. Elkashlan, Y. Nan, D. B. da Costa, and T. Duong, "Unified analysis of transmit antenna selection in MIMO multirelay networks," *IEEE Trans. Veh. Technol.*, vol. 62, no. 2, pp. 933–939, Feb. 2013.

[9] S. Chen, W. Wang, X. Zhang, and D. Zhao, "Performance of amplify-and-forward MIMO relay channels with transmit antenna selection and maximal-ratio combining," in *Proc. IEEE Conference Wireless Communications and Networking (WCN)*, Budapest, Hungary, 5–8 Apr. 2009, pp. 1–6.

[10] P. L. Yeoh, M. Elkashlan, and I. Collings, "Exact and asymptotic SER of distributed TAS/MRC in MIMO relay networks," *IEEE Trans. Wireless Commun.*, vol. 10, no. 3, pp. 751–756, Mar. 2011.

[11] H. A. Suraweera, P. J. Smith, A. Nallanathan, and J. S. Thompson, "Amplify-and-forward relay transmission with end-to-end antenna selection," *IEEE Trans. Wireless Commun.*, vol. 10, no. 6, pp. 1–6, Jun. 2010.

[12] G. Amarasuriya, C. Tellambura, and M. Ardakani, "Performance analysis framework for transmit antenna selection strategies of cooperative MIMO AF relay networks," *IEEE Trans. Veh. Technol.*, vol. 60, no. 7, pp. 3030–3044, Sep. 2011.

[13] I. L. Karaevli, I. Altunbas, and G. Karabulut, "Performance analysis of cooperative relaying scheme applying TAS/SC," in *Proc. IEEE Symposium on Computers and Communications (ISCC)*, Riccione, Italy, 22–25 Jun. 2010, pp. 127–132.

[14] H. Ding, J. Ge, D. B. da Costa, and T. Tsiftsis, "A novel distributed antenna selection scheme for fixed-gain amplify-and-forward relaying systems," *IEEE Trans. Veh. Technol.*, vol. 61, no. 6, pp. 2836–2842, Jul. 2012.

[15] D. C. Gonzalez, D. B. da Costa, and J. C. S. Santos Filho, "Distributed suboptimal schemes for TAS/SC and TAS/LS in fixed-gain AF relaying systems," *IEEE Trans. Wireless Commun.*, vol. 13, no. 11, pp. 6041–6053, Nov. 2014.

[16] G. Levin and S. Loyka, "From multi-keyholes to measure of correlation and power imbalance in MIMO channels: Outage capacity analysis," *IEEE Trans. Inf. Theory*, vol. 57, no. 6, pp. 3515–3529, Jun. 2011.

[17] G. Akemann, M. Kieburg, and L. Wei, "Singular value correlation functions for products of Wishart random matrices," *J. Phys. A, Math. Theor.*, vol. 46, no. 27, Jun. 2013.

[18] G. Akemann, J. R. Ipsen, and M. Kieburg, "Products of rectangular random matrices: Singular values and progressive scattering," *Phys. Rev. E, Stat. Nonlin. Soft Matter Phys.*, vol. 88, no. 5, Nov. 2013.

[19] G. K. Karagiannidis, "Performance bounds of multihop wireless communications with blind relays over generalized fading channels," *IEEE Trans. Wireless Commun.*, vol. 5, no. 3, pp. 498–503, Mar. 2006.

[20] E. W. Weisstein. (2014) Pinching theorem. [Online]. Available: http://mathworld.wolfram.com/PinchingTheorem.html

[21] I. S. Gradshteyn and I. M. Ryzhik, *Table of Integrals, Series, and Products*, 7th ed. San Diego, CA: Academic Press, 2007.

[22] Milton Abramowitz and Irene A. Stegun. *Handbook of Mathematical Functions.* Dover, New York, 1972.

Chapter 6

Distributed Transmit-Antenna Selection in Variable-Gain Relaying Systems

Diana C. González, Daniel B. da Costa, and José Cândido S. Santos Filho[1]

Abstract

Recently, distributed transmit-antenna selection schemes have attracted great interest, since they capture the essential benefits of multi-antenna systems while reducing their cost, complexity, delay, and feedback overhead. In those distributed schemes, the antenna selection is based on local channel-state information, in contrast to their optimal centralized counterparts, which require knowing the channel state of all links. Herein, we design two such distributed schemes for a dual-hop variable-gain amplify-and-forward relaying system with one multi-antenna source, one single-antenna relay, and one single-antenna destination. The two schemes differ in the diversity method used at the destination, namely, selection combining or maximal-ratio combining, and in the selection rule accordingly. In addition to conceiving these new schemes, we analyze their outage performance. Since an exact analysis proves intractable, we tackle the outage probability in terms of lower-bound expressions and their asymptotes at high signal-to-noise ratio. Importantly, the derived bounds turn out to be almost indistinguishable from the true performance, assessed via simulation. Our results reveal that the proposed distributed schemes achieve the same diversity order of their optimal centralized counterparts and perform closely to these, specially when the relay is near the source or destination.

6.1 Introduction

Multi-antenna cooperative communications are regarded as a key emerging paradigm for enhancing next-generation wireless networks in terms of reliability and spectral efficiency, by leveraging the fundamental benefits of multiple-input–multiple-output (MIMO) technologies, such as spatial diversity and spatial multiplexing [1], [2]. In practice, however, fully exploiting a high number of antennas increases the hardware cost and complexity, since the required multiple radio-frequency chains are expensive and power consuming. Alternatively, an attractive strategy is to lay hold of a transmit-antenna selection (TAS) scheme, as it captures the essential advantages of multi-antenna systems at a reduced cost and complexity [3]. In optimal *centralized* TAS schemes, the destination terminal collects the full channel-state information (CSI) of all available links and use it to choose the best antenna that the source terminal should transmit with. Afterwards, the destination feeds the selected-antenna index back to the source, which then proceeds with the transmission process [3]. Thereby, centralized TAS schemes may incur a considerable delay and feedback overhead associated with the assessment of all links. Indeed, such overhead may rapidly become prohibitive in practice, as the number of antennas increases. To alleviate the need for CSI estimation and feedback, suboptimal *distributed* TAS (a.k.a. DAS) schemes are of great practical interest. In these schemes, the antenna-selection mechanism is based on the partial CSI of a subset of links, usually the *local* ones, i.e., those links directly interfacing with the node that selects the antenna. This partial channel-state information is referred to as the local CSI. On the other hand, the TAS and DAS schemes are usually complemented by means of some diversity-combining method at the receiver side, such as maximal-ratio combining (MRC) and selection combining (SC) [4],[5]. These methods are used to merge the signals received from the direct and relaying links.

Several studies have proposed and analyzed amplify-and-forward (AF) relaying schemes with the joint use of TAS techniques at the transmitter side and diversity combining methods at the receiver side, including those in [6]-[18] and the references therein. In a pioneering work [6], optimal selection criteria for TAS/MRC were derived, and it was analytically demonstrated that the optimal TAS scheme achieves the same diversity order of a communication scheme that fully and simultaneously exploits all transmit antennas. The main drawback of such an optimal TAS scheme is its high complexity when performing an exhaustive search for the best transmit antenna. Aiming to reduce this complexity, some suboptimal TAS strategies have been also explored in the literature. In most cases, however, antenna selection criteria have been considered that ignore the CSI of some links [7]-[10]. In those works, suboptimal schemes were studied for the same basic TAS/MRC network configuration adopted in [6]. In [7], two TAS rules were considered and assessed via simulation, based on the direct-link and first-hop CSIs, respectively. In [8], the schemes in [7] have been assessed on an analytical basis. In [9], an adaptive TAS rule was considered, based either on the direct-link CSI or on the direct-link and first-hop CSIs, depending on the local channel state at the source. Finally, in [10], two TAS rules were considered and assessed analytically in terms of outage performance: the optimal one and a suboptimal one, with the latter being based on the direct-link CSI. In other cases, AF relaying schemes employing TAS techniques have been considered that
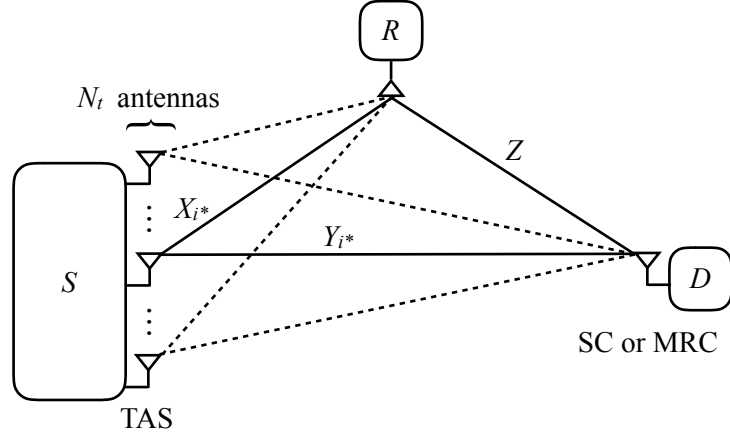
Figure 6.1: System configuration for the distributed TAS/SC and TAS/MRC schemes.

ignore the direct link as a transmission path [11]-[16]. In [11], the error rate and outage probability were derived for a TAS/MRC relaying network with a multi-antenna source, a multi-antenna destination, and a single-antenna variable-gain AF relay. This scheme was generalized in [12] and [13], by assuming a multi-antenna relay. Based on the same network configuration, a suboptimal strategy for TAS/MRC and TAS/SC schemes was proposed in [14] and [15], by considering Nakagami-m channels. In [16], TAS/MRC and TAS/SC were investigated for Weibull channels in a multi-relay scenario.

An efficient distributed approach was introduced in [17] for a DAS/MRC scheme operating over a single-antenna fixed-gain AF relay. This approach avoids the full CSI of optimal centralized schemes while considering all the links in the antenna-selection mechanism. More recently, in [18], the new approach was applied to DAS/SC, by considering again a single-antenna fixed-gain AF relay. In this work, we extend the distributed approach used in [17] and [18] to the *variable-gain* scenario. More specifically, we design and analyze efficient DAS/MRC and DAS/SC schemes operating over a single-antenna variable-gain AF relay. Analytical lower bounds for the outage probability of the proposed schemes are derived, since an exact analysis proves intractable. Importantly, the obtained bounds prove to be extremely tight approximations to the exact outage performance. In addition, we provide simple closed-form asymptotic expressions for the derived bounds, which reveal that the proposed schemes achieve full diversity. Strikingly, the proposed suboptimal schemes turn out to perform very closely to their optimal centralized counterparts, mainly when the relay is located near the source or destination. Monte Carlo simulation is used to validate our analytical results.

In what follows, $f_A(\cdot)$ denotes the probability density function (PDF) of a generic random variable A, $\mathrm{E}[\cdot]$ denotes expectation, $\Pr(\cdot)$ denotes probability, and "$\simeq$" denotes asymptotic equivalence.

6.2 System Model

Consider the dual-hop relaying system depicted in Fig. 6.1, composed by one source S with N_t antennas, one single-antenna destination D, and one single-antenna, half-duplex, variable-gain AF relay R. The system operates on a time-division multiple access basis, and all the channels undergo independent flat Rayleigh fading and additive white Gaussian noise with mean power N_0.

Before each data transmission, an antenna selection is carried out at the source, desirably by choosing the best antenna for transmission, i.e., the one that maximizes the end-to-end signal-to-noise ratio (SNR). The selection procedure shall be presented in the next Section. Subsequently, a conventional cooperative transmission is held in two time slots. In the first time slot, S broadcasts the data stream to R and D. In the second time slot, R amplifies the received signal according to the variable-gain AF protocol and forwards it to D, which then combines the replicas from S and R via SC or MRC. Accordingly, the end-to-end SNR from the ith antenna at S to D can be formulated as

$$\text{SC:} \quad \gamma_i = \max\left[Y_i, \frac{X_i Z}{X_i + Z + 1}\right] \tag{6.1}$$

$$\text{MRC:} \quad \gamma_i = Y_i + \frac{X_i Z}{X_i + Z + 1}, \tag{6.2}$$

where $Y_i \triangleq \frac{P_S}{N_0}|h_{Y,i}|^2$ is the direct-link received SNR from the ith antenna at S to D, $X_i \triangleq \frac{P_S}{N_0}|h_{X,i}|^2$ is the first-hop received SNR from the ith antenna at S to R, and $Z \triangleq \frac{P_R}{N_0}|h_Z|^2$ is the second-hop received SNR from R to D. Moreover, P_S and P_R denote the transmit powers at S and R, respectively, and $|h_{Y_i}|^2$, $|h_{X,i}|^2$, and $|h_Z|^2$ denote the channel power coefficients of the links from the ith antenna at S to D, from the ith antenna at S to R, and from R to D, respectively. Note that, due to the Rayleigh fading condition, X_i, Y_i, and Z are exponential random variables. Herein, we assume an homogeneous network, so that all links from S to D (or to R) undergo identically distributed fading conditions, i.e., $\mathrm{E}[X_i] = \bar{X}$ and $\mathrm{E}[Y_i] = \bar{Y}$, $\forall i \in \{1, \ldots, N_t\}$, and $\mathrm{E}[Z] = \bar{Z}$.

6.3 Antenna Selection Scheme

In the optimal centralized scheme, the i^*th transmit antenna at S is selected that maximizes the end-to-end SNR, i.e.,

$$\text{Optimal TAS/MRC and TAS/SC:} \quad i^* = \arg\max_i\{\gamma_i\}, \tag{6.3}$$

where γ_i is defined in (6.1) and (6.2) for TAS/SC and TAS/MRC, respectively. As mentioned before, the optimal decision requires the full knowledge of the entire system CSI, which involves a large amount of delay and feedback overhead. To reduce such impairments, we propose here efficient suboptimal DAS/SC and DAS/MRC schemes, inspired by the corresponding schemes for fixed-gain AF relaying presented in [17] and [18], respectively. In those works, the antenna-selection mechanism is based on local CSI at S, namely, X_i and Y_i, $i \in \{1, \ldots, N_t\}$, and on a 1-bit partial CSI related to the second hop

Z. The point here is to avoid feeding back to S the full value of Z estimated at R or D—which would demand a certain number of bits—while not ignoring altogether the value of Z in the selection mechanism. Herein, we shall not discuss how X_i and Y_i, $i \in \{1, \ldots, N_t\}$, are made available at S, as this is also required in many suboptimal schemes proposed in the literature, thus not distinguishing those schemes from ours. Instead, we focus on showing how the addition of a minor 1-bit feedback overhead associated with Z can be used to enable a great improvement in performance.

Our DAS/SC and DAS/MRC schemes are motivated by key inequalities involving the respective end-to-end SNRs, which are obtained by replacing the known inequality $X_i Z / (X_i + Z + 1) < \min[X_i, Z]$ into (6.1) and (6.2), leading to

$$\text{SC:} \quad \gamma_i < \max[Y_i, \min[X_i, Z]] \triangleq \widetilde{\gamma}_i \tag{6.4}$$

$$\text{MRC:} \quad \gamma_i < Y_i + \min[X_i, Z] \triangleq \widetilde{\gamma}_i. \tag{6.5}$$

Note in (6.4) and (6.5) that the upper bound $\widetilde{\gamma}_i$ of γ_i depends on $\min[X_i, Z]$. From this, a DAS mechanism can be designed based on the local CSI available at S, X_i and Y_i, $i \in \{1, \ldots, N_t\}$, and on the whether $Z \geq \max_i\{X_i\}$ or $Z < \max_i\{X_i\}$. The latter information can be fed back from R to S by using a 1-bit message. This is the underlying rationale:

- If $Z \geq \max_i\{X_i\}$, then $\min[X_i, Z] = X_i$, $\forall i$. In this case, from (6.4) and (6.5), based on the local CSI X_i and Y_i available as S, a suboptimal selection rule $\max_i\{\widetilde{\gamma}_i\}$ can be applied.

- If $Z < \max_i\{X_i\}$, then $\min[X_i, Z] = Z$ for some value(s) of i. In this case, the application of the selection rule $\max_i\{\widetilde{\gamma}_i\}$ would require the knowledge of Z, which is unavailable at S. Instead, somewhat arbitrarily, we suggest the suboptimal selection rule $\max_i\{Y_i\}$ that maximizes the direct-link received SNR.

All in all, in the proposed DAS schemes, the i^*th transmit antenna at S is selected as follows:

$$\text{DAS/SC:} \quad i^* = \begin{cases} \bar{i} \triangleq \arg\max_i\left\{\max[Y_i, X_i]\right\}, & \text{if } Z \geq \max_i\{X_i\} \\ \underline{i} \triangleq \arg\max_i\{Y_i\}, & \text{if } Z < \max_i\{X_i\} \end{cases} \tag{6.6}$$

$$\text{DAS/MRC:} \quad i^* = \begin{cases} \bar{i} \triangleq \arg\max_i\{Y_i + X_i\}, & \text{if } Z \geq \max_i\{X_i\} \\ \underline{i} \triangleq \arg\max_i\{Y_i\}, & \text{if } Z < \max_i\{X_i\}. \end{cases} \tag{6.7}$$

In comparison with optimal centralized schemes, the main advantage of the proposed DAS schemes is a considerably reduced delay/feedback overhead, while achieving a slightly worse performance, as discussed in [17] and [18]. Moreover, in comparison with other suboptimal TAS schemes that ignore the CSI of the second hop, the main advantage of the proposed DAS schemes is an improved outage performance at the expense of a minor additional 1-bit feedback overhead.

6.4   Outage Analysis

In this section, we examine the outage performance of the proposed DAS/SC and DAS/MRC schemes. By definition, an outage event occurs whenever the end-to-end SNR falls below a predefined threshold τ, usually obtained in terms of a target spectral efficiency $\Re_s$. For half-duplex relaying systems, which is the case here, $\tau = 2^{2\Re_s} - 1$. As in many related studies, an exact mathematical treatment proves intractable, since the outage event is related to the SNRs of the multiple links in a very complicated manner. Because of that, we tackle the outage probability in terms of lower bounds and handy closed-form asymptotic expressions at high SNR. Importantly, the derived bounds turn out to be highly accurate approximations to the exact outage performance. For the sake of clarity and fluidity, our analytical results shall be presented in the form of Lemmas and Propositions, all the proofs of which are postponed to appendices, even the small ones.

6.4.1   DAS/SC

By using (6.6) into (6.1), the outage probability $P_{\text{out}}^{\text{DAS/SC}}$ of the DAS/SC scheme can be formulated as

$$P_{\text{out}}^{\text{DAS/SC}} = \underbrace{\Pr\left(Z \geq \max_i \{X_i\}, \max\left[Y_{\bar{i}}, \frac{X_{\bar{i}}Z}{X_{\bar{i}} + Z + 1}\right] < \tau\right)}_{\triangleq I_1}$$

$$+ \underbrace{\Pr\left(Z < \max_i \{X_i\}, \max\left[Y_{\underline{i}}, \frac{X_{\underline{i}}Z}{X_{\underline{i}} + Z + 1}\right] < \tau\right)}_{\triangleq I_2}. \tag{6.8}$$

Note in (6.8) that we have defined two probability terms, namely, I_1 and I_2, the sum of which gives the referred outage probability. Next we provide lower bounds for each of these terms, as well as corresponding high-SNR asymptotic expressions.

Bound Analysis

The following lower-bound expressions are based on the key inequality presented in (6.4). Hereafter, I_1^{LB}, I_2^{LB}, and $P_{\text{out}}^{\text{DAS/SC,LB}}$ denote the lower bounds of I_1, I_2, and $P_{\text{out}}^{\text{DAS/SC}}$, respectively.

Lema 6.1. *A lower bound for the term I_1 defined in (6.8) can be elaborated as*

$$I_1^{LB} = \Pr\left(Y_i < \tau\right)^{N_t} \Pr\left(Z \geq \max_i \{X_i\}, \max_i \{X_i\} < \tau\right). \tag{6.9}$$

Proof. See Appendix F.1.   □

Lema 6.2. *A lower bound for the term I_2 defined in (6.8) can be elaborated as*

$$I_2^{LB} = \Pr\left(Y_i < \tau\right)^{N_t} \Pr\left(Z < \max_i \{X_i\}, \min\left[X_i, Z\right] < \tau\right). \tag{6.10}$$

Proof. See Appendix F.2.   □

Proposition 3. For independent flat Rayleigh fading, as is the case here, the lower bound I_1^{LB} specializes to the following closed-form expression:

$$I_1^{\text{LB}} = \left(1 - e^{-\frac{\tau}{\overline{Y}}}\right)^{N_t} \left(e^{-\frac{\tau}{\overline{Z}}} \left(1 - e^{-\frac{\tau}{\overline{X}}}\right)^{N_t} + \sum_{k=0}^{N_t} \binom{N_t}{k} \frac{(-1)^k \overline{X}}{\overline{X} + k\overline{Z}} \left(1 - e^{-\tau\left(\frac{k}{\overline{X}} + \frac{1}{\overline{Z}}\right)}\right)\right). \quad (6.11)$$

Proof. See Appendix F.3. $\qquad\qquad\square$

Proposition 4. For independent flat Rayleigh fading, as is the case here, the lower bound I_2^{LB} specializes to the following single-fold integral-form expression:

$$I_2^{\text{LB}} = \left(1 - e^{-\frac{\tau}{\overline{Y}}}\right)^{N_t} \left(\left(1 - e^{-\frac{\tau}{\overline{X}}}\right) + \left(1 - e^{-\frac{\tau}{\overline{Z}}}\right) - \left(1 - e^{-\frac{\tau}{\overline{X}}}\right)\left(1 - e^{-\frac{\tau}{\overline{Z}}}\right)\right.$$

$$\left. - \int_\tau^\infty \frac{1}{\overline{Z}} e^{-\frac{b}{\overline{Z}}} \left(1 - e^{-\frac{b}{\overline{X}}}\right)^{N_t-1} \left(1 - e^{-\frac{\tau}{\overline{X}}}\right) db - \int_0^\tau \frac{1}{\overline{Z}} e^{-\frac{z}{\overline{Z}}} \left(1 - e^{-\frac{z}{\overline{X}}}\right)^{N_t} dz\right). \quad (6.12)$$

Proof. See Appendix F.4. $\qquad\qquad\square$

By using (6.11) and (6.12) into (6.8), a lower-bound expression for the outage probability of the DAS/SC scheme operating over independent flat Rayleigh fading can be obtained as $P_{\text{out}}^{\text{DAS/SC,LB}} = I_1^{\text{LB}} + I_2^{\text{LB}}$.

Asymptotic Bound Analysis

In order to gain insights into the high-SNR trends of the proposed DAS/SC scheme, we now investigate the asymptotic behavior of the derived lower bounds. To this end, $\tilde{I}_1^{\text{LB}}$, $\tilde{I}_2^{\text{LB}}$, and $\tilde{P}_{\text{out}}^{\text{DAS/SC,LB}}$ denote the asymptotic lower bounds of I_1, I_2, and $P_{\text{out}}^{\text{DAS/SC}}$, respectively.

Proposition 5. A high-SNR asymptotic expression for the lower bound in (6.11) can be obtained as

$$\tilde{I}_1^{\text{LB}} = \left(\frac{\tau}{\overline{Y}}\right)^{N_t} \left(\frac{\tau}{\overline{X}}\right)^{N_t}. \quad (6.13)$$

Proof. See Appendix F.5. $\qquad\qquad\square$

Proposition 6. A high-SNR asymptotic expression for the lower bound in (6.12) can be obtained as

$$\tilde{I}_2^{\text{LB}} = \frac{\tau^{N_t+1}}{\overline{Y}^{N_t}\overline{X}} + \frac{\tau^{N_t+1}}{\overline{Y}^{N_t}\overline{Z}} \left(1 - B\left(\frac{\overline{X}}{\overline{Z}}, N_t\right)\right), \quad (6.14)$$

where $B(\cdot, \cdot)$ is the beta function [14, Eq. (3.312.1)].

Proof. See Appendix F.6. $\qquad\qquad\square$

Proposition 7. A high-SNR asymptotic lower bound for the outage probability of the DAS/SC scheme operating over independent flat Rayleigh fading can be obtained as

$$\tilde{P}_{\text{out}}^{\text{DAS/SC,LB}} \simeq \begin{cases} \frac{2\tau^2}{\overline{Y}\overline{X}} + \frac{\tau^2}{\overline{Y}\overline{Z}}\left(1 - B\left(\frac{\overline{X}}{\overline{Z}}, N_t\right)\right) & \text{if } N_t = 1 \\[2ex] \frac{\tau^{N_t+1}}{\overline{Y}^{N_t}\overline{X}} + \frac{\tau^{N_t+1}}{\overline{Y}^{N_t}\overline{Z}}\left(1 - B\left(\frac{\overline{X}}{\overline{Z}}, N_t\right)\right) & \text{if } N_t \geq 2. \end{cases} \quad (6.15)$$

Proof. See Appendix F.7. □

It is noteworthy that a similar procedure can be applied to derive a corresponding *upper* bound for the outage probability of the proposed DAS/SC scheme. The resulting upper bound is somewhat loose, but it bears the same diversity order as the lower bound presented here. Thus, from the Pinching Theorem, it follows that our DAS/SC scheme achieves full diversity order, namely, $N_t + 1$.

6.4.2 DAS/MRC

By using (6.7) into (6.2), the outage probability $P_{\text{out}}^{\text{DAS/MRC}}$ of the DAS/MRC scheme can be formulated as

$$P_{\text{out}}^{\text{DAS/MRC}} = \underbrace{\Pr\left(Z \geq \max_i \{X_i\}, Y_{\bar{i}} + \frac{X_{\bar{i}}Z}{X_{\bar{i}} + Z + 1} < \tau\right)}_{\triangleq L_1}$$

$$+ \underbrace{\Pr\left(Z < \max_i \{X_i\}, Y_{\underline{i}} + \frac{X_{\underline{i}}Z}{X_{\underline{i}} + Z + 1} < \tau\right)}_{\triangleq L_2}. \tag{6.16}$$

Note in (6.16) that we have defined two probability terms, namely, L_1 and L_2, the sum of which gives the referred outage probability. Next we provide lower bounds for each of these terms, as well as corresponding high-SNR asymptotic expressions.

Bound Analysis

The following lower-bound expressions are based on the key inequality presented in (6.5). Hereafter, L_1^{LB}, L_2^{LB}, and $P_{\text{out}}^{\text{DAS/MRC,LB}}$ denote the lower bounds of L_1, L_2, and $P_{\text{out}}^{\text{DAS/MRC}}$, respectively.

Lema 6.3. *A lower bound for the term L_1 defined in* (6.16) *can be elaborated as*

$$L_1^{LB} = \Pr\left(Z \geq \max_i \{X_i\}, \max_i \{Y_i + X_i\} < \tau\right). \tag{6.17}$$

Proof. See Appendix F.8. □

Lema 6.4. *A lower bound for the term L_2 defined in* (6.16) *can be elaborated as*

$$L_2^{LB} = \Pr\left(Z < \max_i \{X_i\}, \max_i \{Y_i\} + \min[X_i, Z] < \tau\right). \tag{6.18}$$

Proof. See Appendix F.9. □

Proposition 8. For independent flat Rayleigh fading, as is the case here, the lower bound L_1^{LB} specializes to the following single-fold integral-form expression:

$$L_1^{\text{LB}} = \int_0^\tau \frac{1}{\bar{Z}} e^{-\frac{z}{\bar{Z}}} \left(1 - e^{-\frac{z}{\bar{X}}} - \frac{\bar{Y}}{\bar{X} - \bar{Y}} e^{-\frac{\tau}{\bar{Y}}} \left(-1 + e^{-z\left(\frac{1}{\bar{X}} - \frac{1}{\bar{Y}}\right)}\right)\right)^{N_t} dz$$

$$+ \int_\tau^\infty \frac{1}{\bar{Z}} e^{-\frac{z}{\bar{Z}}} \left(1 - e^{-\frac{\tau}{\bar{X}}} - \frac{\bar{Y}}{\bar{X} - \bar{Y}} e^{-\frac{\tau}{\bar{Y}}} \left(-1 + e^{-\tau\left(\frac{1}{\bar{X}} - \frac{1}{\bar{Y}}\right)}\right)\right)^{N_t} dz. \tag{6.19}$$

Proof. See Appendix F.10. □

Proposition 9. For independent flat Rayleigh fading, as is the case here, the lower bound L_2^{LB} specializes to the following two-fold integral-form expression:

$$L_2^{\mathrm{LB}} = \int_0^\tau N_t \frac{1}{\overline{Y}} e^{-\frac{y}{\overline{Y}}} \left(1 - e^{-\frac{y}{\overline{Y}}}\right)^{N_t-1} \left(\left(1 - e^{-\frac{\tau-y}{\overline{X}}}\right) + \left(1 - e^{-\frac{\tau-y}{\overline{Z}}}\right) - \left(1 - e^{-\frac{\tau-y}{\overline{X}}}\right)\left(1 - e^{-\frac{\tau-y}{\overline{Z}}}\right) \right.$$
$$\left. - \int_{\tau-y}^\infty \frac{1}{\overline{Z}} e^{-\frac{b}{\overline{Z}}} \left(1 - e^{-\frac{b}{\overline{X}}}\right)^{N_t-1} \left(1 - e^{-\frac{\tau-y}{\overline{X}}}\right) db - \int_0^{\tau-y} \frac{1}{\overline{Z}} e^{-\frac{z}{\overline{Z}}} \left(1 - e^{-\frac{z}{\overline{X}}}\right)^{N_t} dz \right) dy. \tag{6.20}$$

Proof. See Appendix F.11. □

By using (6.19) and (6.20) into (6.16), a lower-bound expression for the outage probability of the DAS/MRC scheme operating over independent flat Rayleigh fading can be obtained as $P_{\mathrm{out}}^{\mathrm{DAS/MRC,LB}} = L_1^{\mathrm{LB}} + L_2^{\mathrm{LB}}$.

Asymptotic Bound Analysis

As for the DAS/SC case, in order to gain insights into the high-SNR trends of the proposed DAS/MRC scheme, we now investigate the asymptotic behavior of the derived lower bounds. To this end, $\tilde{L}_1^{\mathrm{LB}}$, $\tilde{L}_2^{\mathrm{LB}}$, and $\tilde{P}_{\mathrm{out}}^{\mathrm{DAS/MRC,LB}}$ denote the asymptotic lower bounds of L_1, L_2, and $P_{\mathrm{out}}^{\mathrm{DAS/MRC}}$, respectively.

Proposition 10. A high-SNR asymptotic expression for the lower bound in (6.19) can be obtained as

$$\tilde{L}_1^{\mathrm{LB}} = \left(\frac{1}{2} \frac{\tau^2}{\overline{X}\,\overline{Y}}\right)^{N_t}. \tag{6.21}$$

Proof. See Appendix F.12. □

Proposition 11. A high-SNR asymptotic expression for the lower bound in (6.20) can be obtained as

$$\tilde{L}_2^{\mathrm{LB}} = \left(\frac{1}{\overline{Y}}\right)^{N_t} \frac{1}{\overline{X}} \left(\frac{\tau^{N_t+1}}{N_t+1}\right) + \left(\frac{1}{\overline{Y}}\right)^{N_t} \frac{1}{\overline{Z}} \left(\frac{\tau^{N_t+1}}{N_t+1}\right) \left(1 - B\left(\frac{\overline{X}}{\overline{Z}}, N_t\right)\right). \tag{6.22}$$

Proof. See Appendix F.13. □

Proposition 12. A high-SNR asymptotic lower bound for the outage probability of the DAS/MRC scheme operating over independent flat Rayleigh fading can be obtained as

$$\tilde{P}_{\mathrm{out}}^{\mathrm{DAS/MRC,LB}} \simeq \begin{cases} \left(\frac{1}{2} \frac{\tau^2}{\overline{X}\,\overline{Z}}\right)^{N_t} e^{-\frac{\tau}{\overline{Y}}} + \frac{1}{\overline{Z}^{N_t}\overline{X}} \frac{\tau^{N_t+1}}{(N_t+1)} + \frac{1}{\overline{Z}^{N_t}\overline{Y}} \frac{\tau^{N_t+1}}{(N_t+1)} \left(1 - B\left(\frac{\overline{X}}{\overline{Y}}, N_t\right)\right) & \text{if } N_t = 1 \\[3mm] \frac{1}{\overline{Z}^{N_t}\overline{X}} \frac{\tau^{N_t+1}}{(N_t+1)} + \frac{1}{\overline{Z}^{N_t}\overline{Y}} \frac{\tau^{N_t+1}}{(N_t+1)} \left(1 - B\left(\frac{\overline{X}}{\overline{Y}}, N_t\right)\right) & \text{if } N_t \geq 2. \end{cases} \tag{6.23}$$

Proof. This proof is similar to that of Proposition 7. □

As for the DAS/SC case, it is noteworthy that a similar procedure can be applied to derive a corresponding *upper* bound for the outage probability of the proposed DAS/MRC scheme. The resulting upper bound is somewhat loose, but it bears the same diversity order as the lower bound presented here. Thus, from the Pinching Theorem, it follows that our DAS/MRC scheme achieves full diversity order, namely, $N_t + 1$.

6.5   Numerical Results and Discussions

In this section, we provide some application scenarios to verify our analytical results for the proposed DAS/MRC and DAS/SC schemes, as well as to exemplify the outage performance of these schemes in comparison with their optimal centralized counterparts TAS/MRC and TAS/SC. To this end, Monte Carlo simulation results are also included. For illustration purposes, we consider the following system configuration: the target spectral efficiency is $\Re_s = 1$ bit/s/Hz; the path loss exponent is $\beta = 4$; the network follows a linear topology, in which $d_{SD} = d_{SR} + d_{RD}$, with d_{SD}, d_{SR}, and d_{RD} being the lengths of the source-destination, source-relay, and relay-destination links, respectively; S and R have identical transmit powers, i.e., $P_S = P_R = P$; each channel mean power is $d^{-\beta}$, with d being the distance between the corresponding transceivers, so that $\bar{Y} = Pd_{SD}^{-\beta}/N_0$, $\bar{X} = Pd_{SR}^{-\beta}/N_0$, and $\bar{Z} = Pd_{RD}^{-\beta}/N_0$; and the distance between S and D is normalized to unity, i.e., $d_{SD} = 1$.

Fig. 6.2 presents simulation results that show the impact of relay location on the outage performance of the proposed distributed schemes and their optimal centralized counterparts. Two scenarios are presented for each scheme, by considering two and three antennas at the source. The following can be observed from the curves:

- As expected, DAS/MRC outperforms DAS/SC in all the cases. Interestingly, the outage curves of all distributed and optimal schemes bear very similar shapes over the entire range of relay location.

- The outage performances of all investigated schemes are asymmetric functions of the relay location: for no scheme the best performance is achieved when the relay is placed at the midpoint between the source and destination. Instead, this is achieved at $d_{SR} \approx 0.72$ and $d_{SR} \approx 0.82$ with $N_t = 2$ and $N_t = 3$, respectively, for both DAS/SC and DAS/MRC. The best relay location is biased toward the destination because the number of transmit antennas in the first hop (N_t) is higher than in the second hop (one). Therefore, an optimal balance is achieved by strengthening somewhat the weakest hop, i.e., by positioning the relay a bit closer to the destination.

- As expected, the optimal centralized schemes outperform the distributed ones. However, their performances become increasingly close to each other as the relay approaches either the source ($d_{SR} \to 0$) or the destination ($d_{SR} \to 1$). This is explained as follows. On the one hand, as $d_{SR} \to 0$, $Z < \max_i\{X_i\}$ with high probability, causing the DAS/SC and DAS/MRC rules in (6.6) and (6.7) to be both very likely $i^* = \arg\max_i\{Y_i\}$. Also, if $Z < \max_i\{X_i\}$, then, from (6.1) and (6.2),
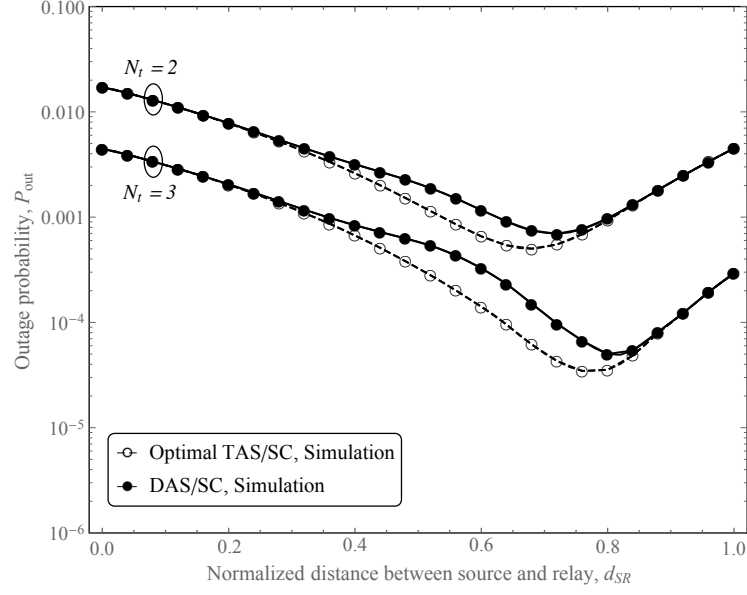
(a)
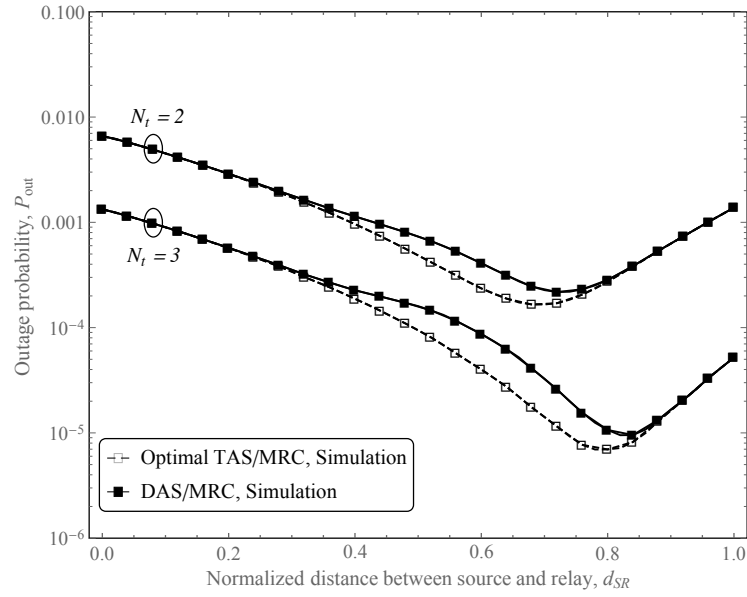
(b)

Figure 6.2: Outage probability versus normalized distance between source and relay for the proposed distributed schemes and their optimal centralized counterparts ($P/N_0 = 10$ dB): (a) DAS/SC; (b) DAS/MRC.

$\gamma_i \approx \max[Y_i, Z]$ for DAS/SC and $\gamma_i \approx Y_i + Z$ for DAS/MRC. As a result, the DAS rules tend to coincide with the optimal ones, since $\arg\max_i\{Y_i\} = \arg\max_i\{Y_i + Z\} = \arg\max_i\{\max[Y_i, Z]\}$, with the last equality being true iff $Z < \max_i\{Y_i\}$, which is much probably the case. On the other hand, as $d_{SR} \to 1$, $Z \geq \max_i\{X_i\}$ with high probability, causing the DAS/SC and DAS/MRC rules in (6.6) and (6.7) to be very likely $i^* = \arg\max_i\{\max[Y_i, X_i]\}$ and $i^* = \arg\max_i\{Y_i + X_i\}$, respectively. Also, if $Z \geq \max_i\{X_i\}$, then, from (6.1) and (6.2), $\gamma_i \approx \max[Y_i, X_i]$ for DAS/SC and $\gamma_i \approx Y_i + X_i$ for DAS/MRC. Therefore, once again the DAS rules tend to coincide with the optimal ones.

Fig. 6.3 presents simulation and analytical results for the outage probability of the proposed distributed schemes and their optimal centralized counterparts while varying the average received SNR of the source-destination link. Here again, two scenarios are presented for each scheme, by considering two and three antennas at the source and the corresponding best relay locations, estimated from Fig. 6.2. The following can be observed from the curves:

- Our lower bound expressions are extremely close to the exact (simulated) outage performance of the proposed distributed schemes over the entire range of SNR.

- The proposed distributed schemes achieve full diversity order, namely, $N_t + 1$, which is the same of the optimal centralized schemes.

- When the relay is positioned at the best location, the performance of proposed distributed schemes is very close to that of their centralized counterparts.

6.6   Conclusions

This work proposed and analyzed a low-complexity, low-cost, distributed transmit-antenna selection approach for dual-hop variable-gain amplify-and-forward relaying systems. Two different diversity-combining methods were considered at the destination, namely, selection combining and maximal-ratio combining. Each method led to a distinct design of the antenna selection rule. We derived extremely tight lower bounds for the outage probability of each proposed scheme, as well as useful closed-form asymptotic expressions for each of the obtained bounds. In comparison with optimal centralized schemes, our distributed schemes achieve the same diversity order and a slightly worse performance, while reducing the cost, complexity, delay, and feedback overhead.
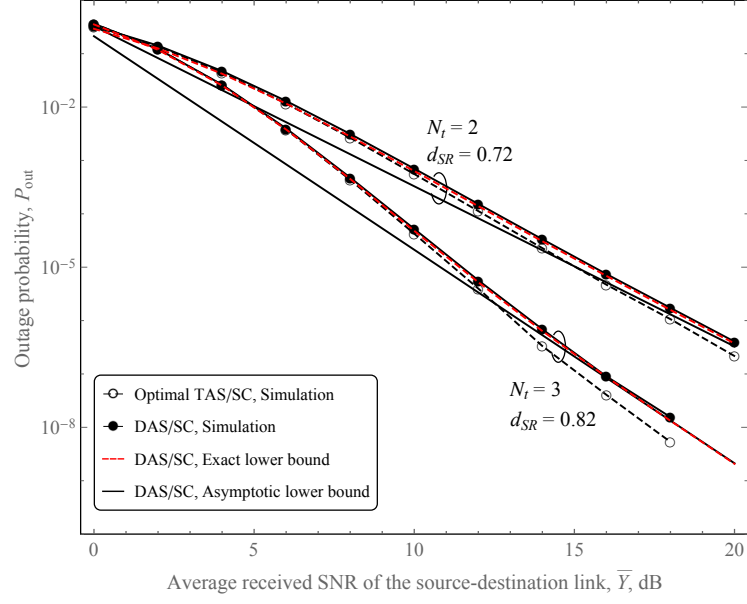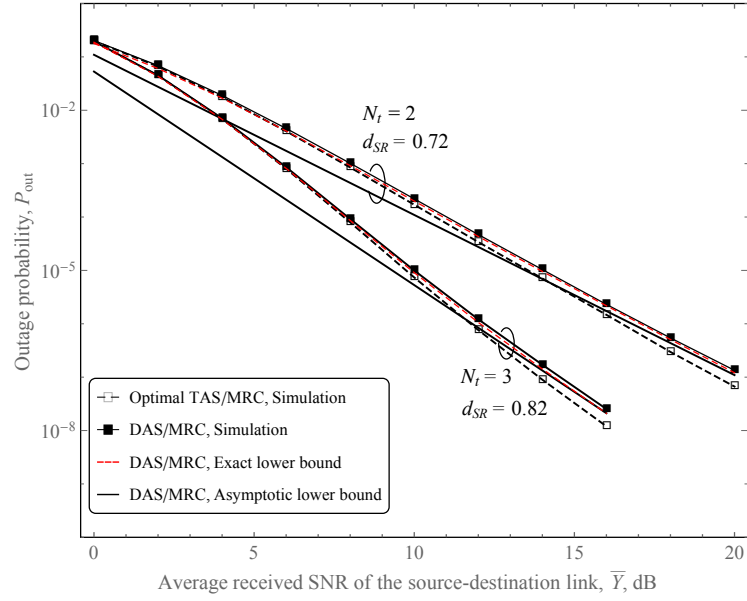
Figure 6.3: Outage probability versus average received SNR of the source-destination link for the proposed schemes and their centralized counterparts: (a) DAS/SC; (b) DAS/MRC.

Bibliography

[1] D. Tse and P. Viswanath, *Fundamentals of Wireless Communication*, 1st ed. New York, NY: Cambridge University Press, 2005.

[2] L. Zheng, and D. N. C. Tse, "Diversity and freedom: A fundamental tradeoff in multiple antenna channels," in *Proc. IEEE Int. Symp. Information Theory (ISIT)*, Lausanne, Switzerland, 2002, p. 476.

[3] S. Sanayei and A. Nosratinia, "Antenna selection in MIMO systems," *IEEE Commun. Mag.*, vol. 42, no. 10, pp. 68–73, Oct. 2004.

[4] K. J. R. Liu, W. Su, and A. K. Wasinki, *Cooperative Communications and Networking*, 1st ed. Cambridge, UK: Cambridge University Press, 2009.

[5] M. Dohler and Y. Li, *Cooperative Communications: Hardware, Channel and PHY*, 1st ed. Chichester, UK: John Wiley and Sons Ltd, 2010.

[6] S. W. Peters and R. W. Heath, "Nonregenerative MIMO relaying with optimal transmit antenna selection," *IEEE Signal Process. Lett*, vol. 15, pp. 421–424, 2008.

[7] L. Cao, X. Zhang, Y. Wang, and D. Yang, "Transmit antenna selection strategy in amplify-and-forward MIMO relaying," in *Proc. IEEE Conference Wireless Communications and Networking (WCN)*, Budapest, Hungary, 5–8 Apr. 2009, pp. 1–4.

[8] G. Amarasuriya, C. Tellambura, and M. Ardakani, "Performance analysis framework for transmit antenna selection strategies of cooperative MIMO AF relay networks," *IEEE Trans. Veh. Technol.*, vol. 60, no. 7, pp. 3030–3044, Sep. 2011.

[9] A. A. Tarkhan, F. Farzaneh, and B. H. Khalaj, "Efficient suboptimal transmit antenna selection for MIMO relay channels," in *Proc. IEEE International Symposium on Computer Networks and Distributed Systems (CNDS)*, Tehran, Iran, 23–24 Feb. 2011, pp. 45–48.

[10] H. A. Suraweera, P. J. Smith, A. Nallanathan, and J. S. Thompson, "Amplify-and-forward relaying with optimal and suboptimal transmit antenna selection," *IEEE Trans. Wireless Commun.*, vol. 10, no. 6, pp. 1874–1885, Jun. 2011.

[11] S. Chen, W. Wang, X. Zhang, and D. Zhao, "Performance of amplify-and-forward MIMO relay channels with transmit antenna selection and maximal-ratio combining," in *Proc. IEEE Conference Wireless Communications and Networking (WCN)*, Budapest, Hungary, 5–8 Apr. 2009, pp. 1–6.

[12] H. A. Suraweera, P. J. Smith, A. Nallanathan, and J. S. Thompson, "Amplify-and-forward relay transmission with end-to-end antenna selection," *IEEE Trans. Wireless Commun.*, vol. 10, no. 6, pp. 1–6, Jun. 2010.

[13] J. B. Kim and D. Kim, "BER analysis of dual-hop amplify-and-forward MIMO relaying with best antenna selection in Rayleigh fading channels," *IEICE Trans. Commun*, vol. E91-B, no. 8, pp. 2772–2775, Aug. 2008.

[14] P. L. Yeoh, M. Elkashlan, and I. Collings, "Exact and asymptotic SER of distributed TAS/MRC in MIMO relay networks," *IEEE Trans. Wireless Commun.*, vol. 10, no. 3, pp. 751–756, Mar. 2011.

[15] M. Elkashlan, P. L. Yeoh, N. Yang, T. Duong, and C. Leung, "A comparison of two MIMO relaying protocols in Nakagami-*m* fading," *IEEE Trans. Veh. Technol.*, vol. 61, no. 3, pp. 1416–1442, Mar. 2012.

[16] P. Yeoh, M. Elkashlan, N. Yang, D. Benevides da Costa, and T. Duong, "MIMO multi-relay networks with TAS/MRC and TAS/SC in Weibull fading channels," in *Proc. IEEE 23rd International Symposium on Personal Indoor and Mobile Radio Communications (PIMRC)*, Sydney, NSW, 9–12 Sep. 2012, pp. 2314–2318.

[17] H. Ding, J. Ge, D. B. da Costa, and T. Tsiftsis, "A novel distributed antenna selection scheme for fixed-gain amplify-and-forward relaying systems," *IEEE Trans. Veh. Technol.*, vol. 61, no. 6, pp. 2836–2842, Jul. 2012.

[18] D. C. Gonzalez, D. B. da Costa, and J. C. S. Santos Filho, "Distributed suboptimal schemes for TAS/SC and TAS/LS in fixed-gain AF relaying systems," *IEEE Trans. Wireless Commun.*, vol. 13, no. 11, pp. 6041–6053, Nov. 2014.

[19] I. S. Gradshteyn and I. M. Ryzhik, *Table of Integrals, series, and Products*, 7th ed. San Diego, CA: Academic Press, 2007.

Chapter 7

Decode-and-Forward Multirelay Systems with Lossy Intra-Links and Distributed Source Coding: Outage Probability and Power Allocation

Diana C. González, Albrecht Wolf, José Cândido S. Santos Filho and Gerhard Fettweis[1]

Abstract

The so-called Chief Executive Officer problem has inspired some relay transmission schemes. It suggests that the source message can be recovered at the destination by combining a set of corrupted replicas sent by multiple relays, as long as the replicas are sufficiently correlated with the original message. In this work, we build on the Slepian-Wolf theorem to assess the outage performance of a distributed source coding scheme for a decode-and-forward multirelay system in which the direct link is unavailable to convey information. As in the CEO problem, the replicas forwarded by the relays are allowed to contain intra-link errors due to previous unreliable hops, and the destination is expected to reconstruct the original message by jointly decoding all the received replicas. In addition to analyzing the outage probability of such scheme, we derive a simple yet efficient power allocation strategy for the multiple relays, which is asymptotically optimal at high signal-to-noise ratio.

7.1   Introduction

In some abnormal scenarios, wireless networks may be faced with challenging requirements in terms of energy efficiency and reliable information transfer under a constantly changing network topology. For example, in case of severe environmental disasters, the communication infrastructure of mobile cellular networks may be seriously damaged, which in turn may lead to a collapse of the entire communication system. In such a scenario, intact mobile devices can be used to establish a mesh network without the need for central coordination and backbone infrastructure. However, the transmit power of mobile devices is inherently restricted by their limited power supply, so that low signal-to-noise ratios (SNRs) are likely to occur, resulting in an unreliable information transfer across the mesh network.

Cooperative communication techniques have emerged as a promising approach to support these restrictive transmissions, by exploiting the spatial diversity through a collection of intermediate relay nodes between source and destination [1]. Normally, before forwarding information, a relay node checks the received message and discard it if any uncorrectable error is detected, in order to ensure a reliable communication. However, in such mesh networks, intra-link errors between the source and each relay are common and inevitable, so that a huge amount of retransmissions would be needed to enable a reliable multi-hop connectivity.

In order to prevent energy inefficiency and improve the robustness of the referred network, an innovative distributed source coding (DSC) scheme was proposed in [2]. The DSC scheme exploits the fact that an erroneous message at the relay can be still highly correlated with the original source message and thus can assist in the decoding process at the destination—instead of being merely discarded. The performance gain of this approach can be reasoned with use of the Slepian-Wolf correlated source coding theorem [3]. In [2] and related studies, the link between the source and relay was considered to be lossy, being described as a binary symmetric channel (BSC) with a certain bit flipping probability [4]. This assumption is indeed a plausible amalgamated model for multiple unreliable hops that connect the source and relay. At the relay, a possibly erroneous message is detected, re-encoded, interleaved, and forwarded to the destination. Finally, at the destination, a joint decoding (JD) technique is applied to exploit the correlation between the original direct-link message and the unreliable relay message, by means of a likelihood ratio update function [2]. A significant improvement of the decoding performance is observed when compared with the relay message being discarded. In [5], a comprehensive outage analysis of the coding scheme proposed in [2] was carried out, by using the theorems for lossy source-channel separation and source coding with side information. In [6], the authors capitalized on the Slepian-Wolf theorem to analyze the outage probability of a correlated-source transmission scheme, assuming a decode-and-forward (DF) relay system with a BSC source-relay (SR) link and a relay-destination (RD) link under block Rayleigh fading. More recently, the same authors proposed in [7] a corresponding power allocation strategy to minimize the outage probability derived in [6].

In this work, based on the results in [6] and [7], we analyze the outage performance of a DSC scheme for a DF relay network with lossy intra-links, as well as we design a power
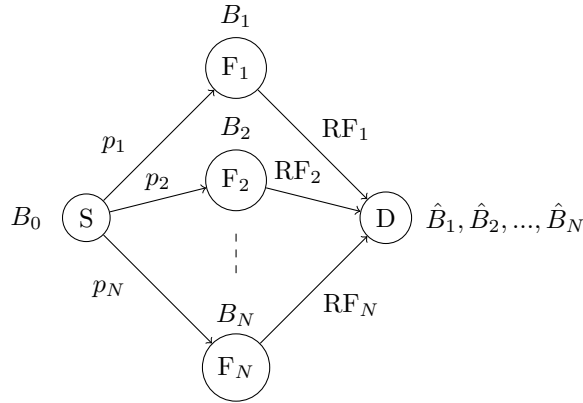
Figure 7.1: System model for the multirelay scheme based on the CEO problem.

allocation strategy for the investigated scheme. However, differently from [6] and [7], we consider a more realistic scenario, in which no direct link exists between the source and destination. In addition, more generally than those works, we consider that each message is simultaneously transmitted along an arbitrary number of relay routes—instead of a single relay. It was shown in [8] that the joint decoder at the destination can exploit the correlation among the replicas received from multiple relays, and that a significant performance gain can be attained compared to conventional coding schemes. However, error-free retrieval of the original message cannot be achieved [9]. This is known as the chief executive officer (CEO) problem in network information theory [10]. Similarly to [6], we capitalize on the Slepian-Wolf correlated source coding theorem to assess the outage performance of the investigated transmission scheme. This is a reasonable framework, since the various relays can be regarded as mutually correlated sources of information. We illustrate the derivation process by providing exact outage expressions for the particular cases of two and three relays, obtained in integral form. More interestingly, we derive a closed-form asymptotic outage expression for the general case with an arbitrary number of relays. Finally, based on this general result, we derive a remarkably simple power allocation strategy that is asymptotically optimal at high SNR. To the best of our knowledge, Slepian-Wolf-based outage analysis and power allocation design for DSC relay networks with lossy intra-links have not been addressed yet in the context of multiple relays or unavailable direct transmission.

In what follows, $\Pr[\cdot]$ denotes probability, $f_X(\cdot)$ is the probability density function (PDF) of a continuous random variable X, $p_Y(\cdot)$ is the probability mass function (PMF) of a discrete random variable Y, $H(Y)$ is the entropy of Y, z is a sample realization of a generic random variable Z, $h_b(x) \triangleq -x \log_2(x) - (1-x) \log_2(1-x)$ is the binary entropy function, $|\mathcal{S}|$ is the cardinality of a set $\mathcal{S}$, $\mathcal{B} = \{0,1\}$ is the binary set, and $\{A_i | i \in \mathcal{S}\}$ is an indexed series (e.g., $\{A_i | i \in \{1,5,7\}\} = \{A_1, A_5, A_7\}$).

7.2 System Model

We consider a half-duplex dual-hop[2] relay system as shown in Fig. 7.1. It consists of one source (S), one destination (D) and N DF relays $(F_1, F_2, \ldots, F_N)$. The system operation is based on the CEO problem. An i.i.d. binary information sequence[3] B_0 is originated by S with uniform probabilities $\Pr[B_0 = 0] = \Pr[B_0 = 1] = 1/2$. The source sequence is transmitted via N mutually independent BSCs with associated memoryless binary error sequences E_i, $i \in \{1, \ldots, N\}$—a representation of the accumulated error caused by the multiple wireless hops up to the last one. The PMF of E_i can be written as

$$p_{E_i}(e) = p_i \delta(e - 1) + (1 - p_i)\delta(e), \tag{7.1}$$

$e \in \{0, 1\}$, in which $0 < p_i \leq 0.5$ is the bit-flipping probability and $\delta(\cdot)$ is the discrete delta function. Therefore, the ith relay F_i observes an information sequence $B_i = B_0 \oplus E_i$, $i \in \{1, \ldots, N\}$, with "$\oplus$" denoting the binary exclusive OR operation. Note that, like the source sequence, all relay sequences are also uniformly distributed, so that $H(B_i) = 1$, $i \in \{0, 1, \ldots, N\}$. In addition, note that the relay sequences $B_1, \ldots, B_N$ are mutually correlated. Those sequences are transmitted to D over independent channels undergoing flat Rayleigh fading (RF) and additive white Gaussian noise with mean power N_0. At the destination, the relay sequences are estimated as $\hat{B}_1, \ldots, \hat{B}_N$ and, based on these, the source sequence is finally estimated as $\hat{B}_0$. The PDF of the received instantaneous SNR Γ_i at the ith second hop is exponentially distributed, thus given by

$$f_{\Gamma_i}(\gamma_i) = \frac{1}{\bar{\Gamma}_i} \exp(-\frac{\gamma_i}{\bar{\Gamma}_i}), \tag{7.2}$$

where $\bar{\Gamma}_i$ is the average SNR, obtained as

$$\bar{\Gamma}_i = \frac{P_i}{N_0} \cdot d_i^{-\eta}, \tag{7.3}$$

with P_i being the transmit power at F_i, d_i is the distance between F_i and D, and η is the pathloss exponent.

7.3 Preliminaries

In any effective JD scheme, the best recovery of the source message B_0 at the destination is obviously expected to be achieved when all recovered relay messages $\hat{B}_1, \ldots, \hat{B}_N$ are error-free. However, even in such a favorable scenario at the second hops, the source error probability $\Pr[\hat{B}_0 \neq B_0]$ cannot be zero, since the formulation of the CEO problem excludes error-free BSCs at the first hops $(p_i > 0, \forall i)$. So far, only a few JD schemes for the referred problem have been proposed that exchange decoding information among the

---

[2]As mentioned before, in our model the first hop is an amalgamated representation of possibly multiple hops between the source and relay.

[3]In order to alleviate the notation, we shall drop the time index when denoting information and error sequences.

relays as a means to reduce the source error probability. In particular, the joint decoder proposed in [11] shows a significant performance gain when compared to other coding schemes. The exact calculation of the source error probability for the joint decoder in [11] is provided in [9].

In this work, we neither address any specific DSC/JD scheme nor perform any error probability calculations. Instead, following the approach in [6], we assess the outage performance limits of a generic DSC/JD scheme from an information-theoretical perspective. To this end, the joint decoder performance gain can be reasoned by means of the Slepian-Wolf correlated source coding theorem [3], because the multiple relay messages can be seen as correlated information sources, each of which resembles to some extent the original source message.

7.3.1 Slepian-Wolf Theorem: the original scope

The Slepian-Wolf theorem states that if the transmission rates R_i at the relays, $i \in \{1, \ldots, N\}$, measured in bits per channel use, satisfy the inequality constraints [3]

$$
\begin{aligned}
\sum_{i \in \mathcal{S}} R_i &\geq H\left(\{B_i | i \in \mathcal{S}\} | \{B_j | j \in \mathcal{S}^c\}\right) \\
&= H\left(B_1, \ldots, B_N\right) - H\left(\{B_j | j \in \mathcal{S}^c\}\right)
\end{aligned}
\tag{7.4}
$$

for all subsets $\mathcal{S} \subseteq \{1, \ldots, N\}$, then all relay sequences $B_1, \ldots, B_N$ can be recovered error-free, with $\mathcal{S}^c$ denoting the complement of $\mathcal{S}$. The set of N-tuples $R_1, \ldots, R_N$ that satisfy all the constraints in (7.4) is referred to as the Slepian-Wolf admissible rate region. We now find this region in terms of the bit-flipping probabilities of the first hops. Note in (7.4) that each constraint is written in terms of (i) the joint entropy of all relay sequences and (ii) the joint entropy of a certain subset $\{B_j | j \in \mathcal{S}^c\}$ of relay sequences. Any of these entropies can be evaluated as special cases of the following general formula:

$$
H(\{B_i | i \in S\}) = - \sum_{\{b_i\} \in \mathcal{B}^{|\mathcal{S}|}} \Pr\left[\{B_i | i \in S\} = \{b_i\}\right] \log_2 \left(\Pr\left[\{B_i | i \in S\} = \{b_i\}\right]\right).
\tag{7.5}
$$

The required probabilities $\Pr\left[\{B_i | i \in S\} = \{b_i\}\right]$ can be obtained by knowing that the source bits are equally likely and by recognizing that both $B_0 = 0$ and $B_0 = 1$ may lead to each possible sample realization of $\{B_i | i \in S\}$, which gives

$$
\Pr\left[\{B_i | i \in S\} = \{b_i\}\right] = \frac{1}{2}\left[\prod_{i \in \mathcal{S}} p_{E_i}(b_i) + \prod_{i \in \mathcal{S}} \bar{p}_{E_i}(b_i)\right],
\tag{7.6}
$$

where we have used (i) the independence among the error sequences and (ii) the auxiliary PMF

$$
\bar{p}_{E_i}(e) \triangleq (1 - p_i)\delta(e - 1) + p_i \delta(e)
\tag{7.7}
$$

defined by swapping the probabilities of E_i. Note that (7.6) is ultimately given in terms of the bit-flipping probabilities p_i associated with the first hops. Accordingly, using this into (7.5) and then into (7.4), we obtain each rate constraint of the Slepian-Wolf theorem also in terms of the individual bit-flipping probabilities.

7.3.2 Slepian-Wolf Theorem: a modified scope

In its original scope, the Slepian-Wolf theorem provides the rate conditions for recovering all relay messages at the destination. However, from an engineering perspective, this is not the primary aim. In the investigated system, the destination is ultimately not interested in recovering all relay messages—which are possibly erroneous replicas, indeed—, but in merging them somehow to recover the original source message. Note that each relay sequence contains a different amount of information about the source sequence, according to the channel quality of the first hop. To gain insight, let us consider two extreme sample cases. First, when the first hop is fully unreliable, i.e., if the bit-flipping probability equals 1/2, then the relay sequence does not contain any useful information about the source sequence and thus should be discarded altogether. In such case, no rate constraint should be imposed at all. Second, when the first hop is fully reliable, i.e., if the bit-flipping probability is zero, then the relay sequence is identical to the source sequence. In such case, it would be desirable to fully recover the relay sequence and thus the rate constraint should be maximal. These two examples suggest that, in the general case, an appropriate rate requirement for a given relay should not depend on the absolute information content of the relay message (entropy), but on how much of this content concerns at most the source message (mutual information). This can be accomplished by adapting the Slepian-Wolf Theorem accordingly, as done in [6] and [7] under a different context. All in all, we propose modifying the original scope of the Slepian-Wolf Theorem by replacing each entropy term with a corresponding mutual information term involving the source message. Specifically, the transmission rates R_i at the relays, $i \in \{1, \ldots, N\}$, must satisfy the inequality constraints

$$\sum_{i \in \mathcal{S}} R_i \geq I\left(\{B_i | i \in \mathcal{S}\}; B_0 | \{B_j | j \in \mathcal{S}^c\}\right)$$
$$= I\left(B_1, \ldots, B_N; B_0\right) - I\left(\{B_j | j \in \mathcal{S}^c\}; B_0\right). \tag{7.8}$$

Hereafter, the set of N-tuples $R_1, \ldots, R_N$ that satisfy all the constraints in (7.8) is referred to as the modified Slepian-Wolf admissible rate region. We now find this region in terms of the bit-flipping probabilities of the first hops. This is paramount for many derivations that follow. Note in (7.8) that each constraint is written in terms of (i) the mutual information between all relay sequences and the source sequence and (ii) the mutual information between a certain subset $\{B_j | j \in \mathcal{S}^c\}$ of relay sequences and the source sequence. Any of these mutual informations can be evaluated as special cases of the following general formula:

$$I(\{B_i | i \in S\}; B_0) = H(\{B_i | i \in S\}) - H(B_0, \{B_i | i \in S\}) + 1, \tag{7.9}$$

where $H(\{B_i | i \in S\})$ is defined as in (7.5) and

$$H(B_0, \{B_i | i \in S\}) = - \sum_{\{b_0, \{b_i\}\} \in \mathcal{B}^{|S|+1}} \Pr\left[\{B_0, \{B_i | i \in S\}\} = \{b_0, \{b_i\}\}\right]$$
$$\times \log_2\left(\Pr\left[\{B_0, \{B_i | i \in S\}\} = \{b_0, \{b_i\}\}\right]\right). \tag{7.10}$$
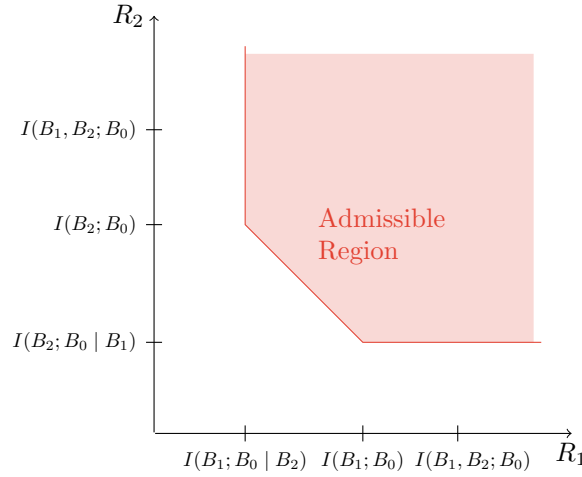
Figure 7.2: Modified Slepian-Wolf admissible rate region for two relays.

By knowing that the source bits are equally likely, the required probabilities $\Pr\left[\{B_0, \{B_i | i \in S\}\} = \{b_0, \{b_i\}\}\right]$ can be obtained as

$$\Pr\left[\{B_0, \{B_i | i \in S\}\} = \{b_0, \{b_i\}\}\right] = \frac{1}{2}\left[\delta(b_0)\prod_{i \in S} p_{E_i}(b_i) + \delta(b_0 - 1)\prod_{i \in S}\bar{p}_{E_i}(b_i)\right]. \quad (7.11)$$

Note that (7.11) is ultimately given in terms of the bit-flipping probabilities p_i associated with the first hops. Accordingly, using this into (7.10) and then into (7.9) and (7.8), we obtain each rate constraint of the modified Slepian-Wolf theorem also in terms of the individual bit-flipping probabilities. Next we illustrate this process for the particular cases of two and three relays.

7.3.3 Two Relays

In Fig. 7.2, the modified admissible rate region is shown for two relays. In this case, R_1 and R_2 must satisfy three inequality constraints:

$$\begin{aligned}
R_1 &\geq I\left(B_1; B_0 | B_2\right), \\
R_2 &\geq I\left(B_2; B_0 | B_1\right), \\
R_1 + R_2 &\geq I\left(B_1, B_2; B_0\right).
\end{aligned} \quad (7.12)$$

In other words, the transmission rate at each relay has to be greater than or equal to the mutual information between its sequence and the source sequence conditioned on the other relay sequence, and the rate sum has to be greater than or equal to the mutual information between the two relay sequences and the source sequence. By using (7.9), (7.10), and (7.11), after some algebraic manipulations, those mutual informations are obtained in terms of the bit-flipping probabilities p_1 and p_2 as

$$\begin{aligned}
I(B_1; B_0 | B_2) &= h_2(p_1, p_2) - h_{02}(p_1, p_2) - h_b(p_2), \\
I(B_2; B_0 | B_1) &= h_2(p_1, p_2) - h_{02}(p_1, p_2) - h_b(p_1), \\
I(B_1, B_2; B_0) &= h_2(p_1, p_2) - h_{02}(p_1, p_2) + 1,
\end{aligned} \quad (7.13)$$
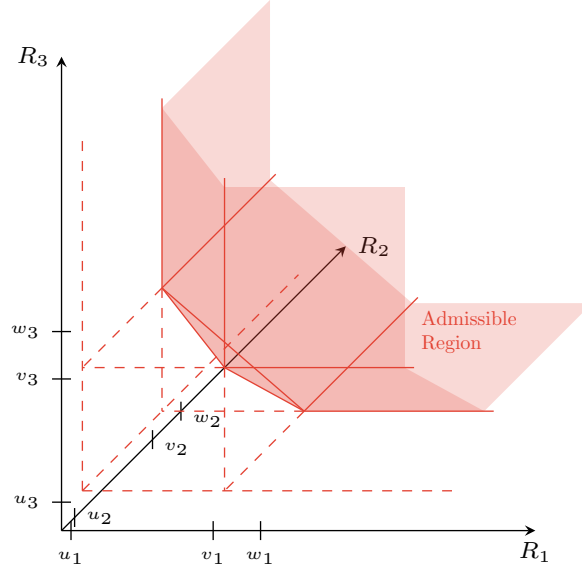
Figure 7.3: Modified Slepian-Wolf admissible rate region for three relays, where $u_1 = I(B_1; B_0|B_2, B_3)$, $u_2 = I(B_2; B_0|B_1, B_3)$, $u_3 = I(B_3; B_0|B_1, B_2)$, $v_1 = I(B_1; B_0)$, $v_2 = I(B_2; B_0)$, $v_3 = I(B_3; B_0)$, $w_1 = I(B_1, B_3, B_2; B_0)$, $w_2 = I(B_1, B_2, B_3; B_0)$, and $w_3 = I(B_2, B_3, B_1; B_0)$.

where

$$h_2(p_1, p_2) \triangleq -2 \sum_{i=1}^{2} a_2(i) \log_2(a_2(i)), \tag{7.14}$$

with

$$a_2(1) = 0.5[p_1 p_2 + (1 - p_1)(1 - p_2)],$$
$$a_2(2) = 0.5[p_1(1 - p_2) + (1 - p_1)p_2], \tag{7.15}$$

and

$$h_{02}(p_1, p_2) \triangleq -2 \sum_{i=1}^{4} a_{02}(i) \log_2(a_{02}(i)), \tag{7.16}$$

with

$$a_{02}(1) = 0.5[p_1 p_2],$$
$$a_{02}(2) = 0.5[p_1(1 - p_2)],$$
$$a_{02}(3) = 0.5[(1 - p_1)p_2], \tag{7.17}$$
$$a_{02}(4) = 0.5[p_1(1 - p_2)].$$

7.3.4 Three Relays

The modified admissible rate region for three relays is shown in Fig. 7.3. This is less easy to visualize than the previous one. In this case, the rates R_1, R_2, and R_3 must satisfy

seven inequality constraints:

$$R_1 \geq I(B_1; B_0|B_2, B_3),$$
$$R_2 \geq I(B_2; B_0|B_1, B_3),$$
$$R_3 \geq I(B_3; B_0|B_1, B_2),$$
$$R_1 + R_2 \geq I(B_1, B_2; B_0|B_3),$$
$$R_1 + R_3 \geq I(B_1, B_3; B_0|B_2),$$
$$R_2 + R_3 \geq I(B_2, B_3; B_0|B_1),$$
$$R_1 + R_2 + R_3 \geq I(B_1, B_2, B_3; B_0).$$

$$(7.18)$$

In other words, the transmission rate at each relay has to be greater than or equal to the mutual information between its sequence and the original source sequence conditioned on the other two relay sequences; each sum of two relay rates has to be greater than or equal to the mutual information between the two relay sequences and the source sequence conditioned on the remaining relay sequence; and the sum of all relay rates has to be greater than or equal to the mutual information between all relay sequences and the source sequence. By using (7.9), (7.10), and (7.11), after some algebraic manipulations, those entropies are obtained in terms of the bit-flipping probabilities p_1, p_2, and p_3 as

$$I(B_1; B_0|B_2, B_3) = h_3(p_1, p_2, p_3) - h_{03}(p_1, p_2, p_3) - h_2(p_2, p_3) + h_{02}(p_2, p_3),$$
$$I(B_2; B_0|B_1, B_3) = h_3(p_1, p_2, p_3) - h_{03}(p_1, p_2, p_3) - h_2(p_1, p_3) + h_{02}(p_1, p_3),$$
$$I(B_3; B_0|B_1, B_2) = h_3(p_1, p_2, p_3) - h_{03}(p_1, p_2, p_3) - h_2(p_1, p_2) + h_{02}(p_1, p_2),$$
$$I(B_1, B_2; B_0|B_3) = h_3(p_1, p_2, p_3) - h_{03}(p_1, p_2, p_3) - h_b(p_3),$$
$$I(B_1, B_3; B_0|B_2) = h_3(p_1, p_2, p_3) - h_{03}(p_1, p_2, p_3) - h_b(p_2),$$
$$I(B_2, B_3; B_0|B_1) = h_3(p_1, p_2, p_3) - h_{03}(p_1, p_2, p_3) - h_b(p_1),$$
$$I(B_1, B_2, B_3; B_0) = h_3(p_1, p_2, p_3) - h_{03}(p_1, p_2, p_3) + 1,$$

$$(7.19)$$

where

$$h_3(p_1, p_2, p_3) \triangleq -2 \sum_{i=1}^{4} a_3(i) \log_2(a_3(i)), \qquad (7.20)$$

with

$$a_3(1) = 0.5[p_1 p_2 p_3 + (1 - p_1)(1 - p_2)(1 - p_3)],$$
$$a_3(2) = 0.5[p_1 p_2 (1 - p_3) + (1 - p_1)(1 - p_2) p_3],$$
$$a_3(3) = 0.5[p_1 (1 - p_2) p_3 + (1 - p_1) p_2 (1 - p_3)],$$
$$a_3(4) = 0.5[(1 - p_1) p_2 p_3 + p_1 (1 - p_2)(1 - p_3)],$$

$$(7.21)$$

and

$$h_{03}(p_1, p_2, p_3) \triangleq -2 \sum_{i=1}^{8} a_{03}(i) \log_2(a_{03}(i)), \qquad (7.22)$$

with

$$
\begin{aligned}
a_{03}(1) &= 0.5[p_1 p_2 p_3], \\
a_{03}(2) &= 0.5[p_1 p_2 (1 - p_3)], \\
a_{03}(3) &= 0.5[p_1 (1 - p_2) p_3], \\
a_{03}(4) &= 0.5[p_1 (1 - p_2)(1 - p_3)], \\
a_{03}(5) &= 0.5[(1 - p_1) p_2 p_3], \\
a_{03}(6) &= 0.5[(1 - p_1) p_2 (1 - p_3)], \\
a_{03}(7) &= 0.5[(1 - p_1)(1 - p_2) p_3], \\
a_{03}(8) &= 0.5[(1 - p_1)(1 - p_2)(1 - p_3)].
\end{aligned}
\tag{7.23}
$$

Capitalizing on the general formulations (7.9), (7.10), and (7.11), the same rationale illustrated here for two and three relays can be applied to an arbitrary number of relays.

7.4 Outage Probability

In the proposed system, an outage event occurs whenever the transmission rates $R_1, \ldots, R_N$ fall outside the modified Slepian-Wolf admissible rate region. Such condition means that, at least for one of the relays, the information content regarding the source message cannot be entirely recovered at the destination. The maximum achievable value of R_i is related to the received SNR Γ_i by means of [5]

$$
R_i = \frac{1}{R_{ci}} \log_2 (1 + \Gamma_i),
\tag{7.24}
$$

where R_{ci} represents the spectrum efficiency associated with the modulation and channel coding schemes [7]. In many parts of this work, for simplicity, we shall assume $R_{ci} = R_c, \forall i$. Using (7.24), each rate constraint in (7.8) that defines an outage event can be mapped into an equivalent SNR constraint. In this Section, we follow this approach to derive exact integral-form expressions for the outage probability of the particular cases with two and three relays, as well as a simple and insightful closed-form asymptotic outage expression for the general case with an arbitrary number of relays.

7.4.1 Two Relays

Fig. 7.4 shows the modified inadmissible rate region for two relays. It is divided into two areas, with associated probabilities $J_{2,1}$ and $J_{2,2}$. Thus, the outage probability P_{out} for two relays can be formulated as

$$
P_{\text{out}} = J_{2,1} + J_{2,2}.
\tag{7.25}
$$

Substituting (7.24) into the rate inequalities in (7.12), $J_{2,1}$ and $J_{2,2}$ can be expressed in
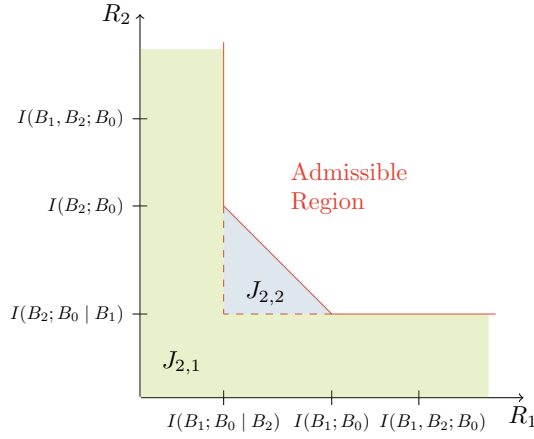
Figure 7.4: Modified Slepian-Wolf inadmissible rate region for two relays, divided into two areas.

terms of SNR constraints as

$$
\begin{aligned}
J_{2,1} =&\, 1 - \Pr\left[R_1 > I\left(B_1; B_0 | B_2\right), R_2 > I\left(B_2; B_0 | B_1\right)\right] \\
=&\, 1 - \Pr\left[2^{R_{c1} I(B_1; B_0 | B_2)} - 1 < \Gamma_1 < \infty, 2^{R_{c2} I(B_2; B_0 | B_1)} - 1 < \Gamma_2 < \infty\right], \quad (7.26)
\end{aligned}
$$

$$
\begin{aligned}
J_{2,2} =&\, \Pr\left[I\left(B_1; B_0 | B_2\right) < R_1 < I\left(B_1; B_0\right), I\left(B_2; B_0 | B_1\right) < R_2 < I\left(B_1, B_2; B_0\right) - R_1\right] \\
=&\, \Pr\left[2^{R_{c1} I(B_1; B_0 | B_2)} - 1 < \Gamma_1 < 2^{R_{c1} I(B_1; B_0)} - 1,\right. \\
&\, \left. 2^{R_{c2} I(B_2; B_0 | B_1)} - 1 < \Gamma_2 < 2^{R_{c2} I(B_1, B_2; B_0) - \frac{R_{c2}}{R_{c1}} \log_2 (\Gamma_1 + 1)} - 1\right]. \quad (7.27)
\end{aligned}
$$

These expressions can be evaluated by integrating the joint PDF $f_{\Gamma_1, \Gamma_2}(\gamma_1, \gamma_2) = f_{\Gamma_1}(\gamma_1) f_{\Gamma_2}(\gamma_2)$ over the corresponding ranges defined in (7.26) and (7.27). This is done in Appendices G.1 and G.2. By combining the results therein, P_{out} can be finally written in exact single-fold integral form as

$$
\begin{aligned}
P_{\text{out}} =&\, 1 - e^{-\frac{2^{R_{c1} I(B_1; B_0 | B_2)} - 1}{\bar{\Gamma}_1} - \frac{2^{R_{c2} I(B_2; B_0 | B_1)} - 1}{\bar{\Gamma}_2}} + \frac{1}{\bar{\Gamma}_1} e^{-\frac{2^{R_{c2} I(B_2; B_0 | B_1)} - 1}{\bar{\Gamma}_2}} \\
&\, \times \int_{2^{R_{c1} I(B_1; B_0 | B_2)} - 1}^{2^{R_{c1} I(B_1; B_0)} - 1} e^{-\frac{\gamma_1}{\bar{\Gamma}_1}} \left(1 - e^{\frac{2^{R_{c2} I(B_1, B_2; B_0) - \frac{R_{c2}}{R_{c1}} \log_2 (1 + \gamma_1)} + 2^{R_{c2} I(B_2; B_0 | B_1)}}{\bar{\Gamma}_2}}\right) d\gamma_1.
\end{aligned}
$$
$$(7.28)$$

Although the outage expression in (7.28) cannot be solved in exact closed form, a simple asymptotic solution can be derived at high SNR. This is also done in Appendices G.1 and G.2, for $J_{2,1}$ and $J_{2,2}$ separately, by assuming $R_{c1} = R_{c2} = R_c$. From the results therein, it turns out that the diversity order of $J_{2,2}$ is greater than that of $J_{2,1}$, so that the latter dominates the high-SNR outage behavior. Accordingly, an asymptotic expression of P_{out} for two relays can be written in compact form as

$$
P_{\text{out}} \simeq \frac{C_1}{\bar{\Gamma}_1} + \frac{C_2}{\bar{\Gamma}_2}, \quad (7.29)
$$

where the constants C_1 and C_2 are defined as

$$
C_1 \triangleq 2^{R_c I(B_1; B_0 | B_2)} - 1, \quad (7.30)
$$

$$
C_2 \triangleq 2^{R_c I(B_2; B_0 | B_1)} - 1, \quad (7.31)
$$
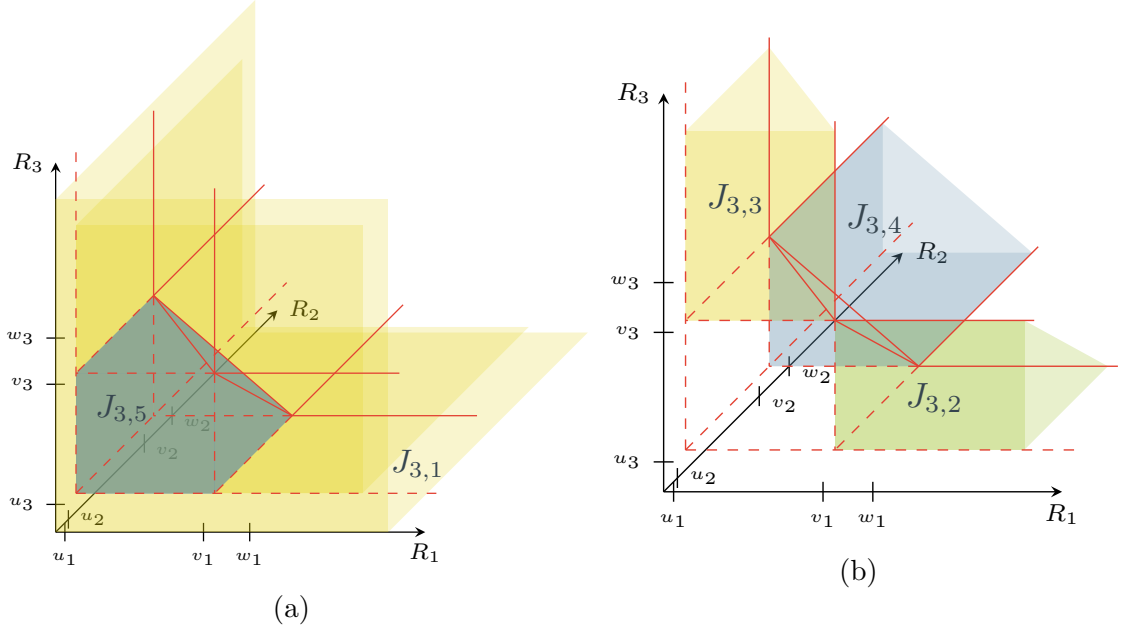
Figure 7.5: Modified Slepian-Wolf inadmissible rate region for three relays, divided into five volumes.

with the mutual informations $I(B_1; B_0|B_2)$ and $I(B_2; B_0|B_1)$ being given as in (7.13) in terms of the bit-flipping probabilities.

7.4.2 Three Relays

Following a similar procedure, we now derive the outage probability for three relays. Fig. 7.5 shows the modified inadmissible rate region, which is divided into five regions or volumes, with associated probabilities $J_{3,1}$ to $J_{3,5}$. Thus, the outage probability can be formulated as

$$P_{\text{out}} = J_{3,1} + J_{3,2} + J_{3,3} + J_{3,4} + J_{3,5}. \tag{7.32}$$

Substituting (7.24) into the rate inequalities in (7.18), $J_{3,1}$, $J_{3,2}$, $J_{3,3}$, and $J_{3,4}$ can be expressed in terms of SNR constraints as

$$
\begin{aligned}
J_{3,1} =& 1 - \Pr\left[R_1 I(B_1; B_0|B_2, B_3), R_2 > I(B_2; B_0|B_1, B_3), R_3 > I(B_3; B_0|B_1, B_2)\right] \\
=& 1 - \Pr\left[\, 0 < \Gamma_1 < 2^{R_{c1} I(B_1; B_0|B_2, B_3)} - 1, 0 < \Gamma_2 < 2^{R_{c2} I(B_2; B_0|B_1, B_3)} - 1, \right. \\
& \left. 0 < \Gamma_3 < 2^{R_{c3} I(B_3; B_0|B_1, B_2)} - 1 \,\right],
\end{aligned}
\tag{7.33}
$$

$$
\begin{aligned}
J_{3,2} =& \Pr\left[R_1 > I(B_1; B0), I(B_2; B_0|B_1, B_3) < R_2 < I(B_2; B_0|B_1), \right. \\
& \left. I(B_3; B_0|B_1, B_2) < R_3 < I(B_2, B_3; B_0|B_1) - R_2 \,\right] \\
=& \Pr\left[2^{R_{c1} I(B_1; B_0)} - 1 < \Gamma_1 < \infty, 2^{R_{c2} I(B_2; B_0|B_1, B_3)} - 1 < \Gamma_2 < 2^{R_{c2} I(B_2; B_0|B_1)} - 1, \right. \\
& \left. 2^{R_{c3} I(B_3; B_0|B_1, B_2)} - 1 < \Gamma_3 < 2^{R_{c3} I(B_2, B_3; B_0|B_1) - \frac{R_{c3}}{R_{c2}} \log(1 + \Gamma_2)} - 1 \,\right],
\end{aligned}
\tag{7.34}
$$

$$
\begin{aligned}
J_{3,3} =& \Pr\left[I(B_1;B_0|B_2,B_3) < R_1 < I(B_1;B_0|B_3), I(B_2;B_0|B_1,B_3) < R_2 < I(B_1,B_2;B_0|B_3) - R_1, \right.\\
& \left. R_3 > I(B_3;B_0)\right]\\
=& \Pr\left[2^{R_{c1}I(B_1;B_0|B_2,B_3)} - 1 < \Gamma_1 < 2^{R_{c1}I(B_1;B_0|B_3)} - 1, \right.\\
& \left. 2^{R_{c2}I(B_2;B_0|B_1,B_3)} - 1 < \Gamma_2 < 2^{R_{c2}I(B_1,B_2;B_0|B_3) - \frac{R_{c2}}{R_{c1}}\log(1+\Gamma_1)} - 1, 2^{R_{c3}I(B_3;B_0)} - 1 < \Gamma_3 < \infty\right],
\end{aligned}
$$
$$(7.35)$$

$$
\begin{aligned}
J_{3,4} =& \Pr\left[I(B_1;B_0|B_2,B_3) < R_1 < I(B_1,B_3;B_0|B_2) - R_3, R_2 > I(B_2;B_0), \right.\\
& \left. I(B_3;B_0|B_1,B_2) < R_3 < H(B_3;B_0|B_2)\right]\\
=& \Pr\left[2^{R_{c1}I(B_1;B_0|B_2,B_3)} - 1 < \Gamma_1 < 2^{R_{c1}I(B_1,B_3;B_0|B_2) - \frac{R_{c1}}{R_{c3}}\log(1+\Gamma_3)} - 1, \right.\\
& \left. 2^{R_{c2}I(B_2;B_0)} - 1 < \Gamma_2 < \infty, 2^{R_{c3}I(B_3;B_0|B_1,B_2)} - 1 < \Gamma_3 < 2^{R_{c3}I(B_3;B_0|B_2)} - 1\right].
\end{aligned}
$$
$$(7.36)$$

In addition, $J_{3,5}$ can be decomposed into three terms as

$$
J_{3,5} = J_{3,5a} - J_{3,5b} - J_{3,5c}, \tag{7.37}
$$

where $J_{3,5a}$, $J_{3,5b}$, and $J_{3,5c}$ are given by

$$
\begin{aligned}
J_{3,5a} =& \Pr\left[I(B_1;B_0|B_2,B_3) < R_1 < I(B_1;B_0), \right.\\
& I(B_2;B_0|B_1,B_3) < R_2 < I(B_1,B_2,B_3;B_0) - R_1 - R_3,\\
& \left. I(B_3;B_0|B_1,B_2) < R_3 < I(B_1,B_3;B_0) - R_1\right]\\
=& \Pr\left[2^{R_{c2}I(B_1;B_0|B_2,B_3)} - 1 < \Gamma_1 < 2^{R_{c1}I(B_1;B_0)} - 1, \right.\\
& 2^{R_{c2}I(B_2;B_0|B_1,B_3)} < \Gamma_2 < 2^{R_{c2}I(B_1,B_2,B_3;B_0) - \frac{R_{c2}}{R_{c3}}\log(1+\Gamma_3) - \frac{R_{c2}}{R_{c1}}\log(1+\Gamma_1)},\\
& \left. 2^{R_{c3}I(B_3;B_0|B_1,B_2)} - 1 < \Gamma_3 < 2^{R_{c3}(I(B_1,B_3;B_0)) - \frac{R_{c3}}{R_{c1}}\log(1+\Gamma_1)} - 1\right],
\end{aligned}
$$
$$(7.38)$$

$$
\begin{aligned}
J_{3,5b} =& \Pr\left[I(B_1;B_0|B_2,B_3) < R_1 < I(B_1;B_0|B_2), \right.\\
& I(B_2;B_0) < R_2 < I(B_1,B_2,B_3;B_0) - R_1 - R_3,\\
& \left. I(B_3;B_0|B_1,B_2) < R_3 < I(B_1,B_3;B_0|B_2) - R_1\right]\\
=& \Pr\left[2^{R_{c2}I(B_1;B_0|B_2,B_3)} - 1 < \Gamma_1 < 2^{R_{c1}I(B_1;B_0|B_2)} - 1, \right.\\
& 2^{R_{c2}I(B_2;B_0)} - 1 < \Gamma_2 < 2^{R_{c2}I(B_1,B_2,B_3;B_0) - \frac{R_{c2}}{R_{c3}}\log(1+\Gamma_3) - \frac{R_{c2}}{R_{c1}}\log(1+\Gamma_1)} - 1,\\
& \left. 2^{R_{c3}I(B_3;B_0|B_1,B_2)} - 1 < \Gamma_3 < 2^{R_{c3}I(B_1,B_2;B_0|B_3) - \frac{R_{c3}}{R_{c1}}\log(1+\Gamma_1)} - 1\right],
\end{aligned}
$$
$$(7.39)$$

$$
\begin{aligned}
J_{3,5c} =& \Pr\left[I(B_1;B_0|B_2,B_3) < R_1 < I(B_1;B_0|B_3), \right.\\
& I(B_2;B_0|B_1,B_3) < R_2 < I(B_1,B_2,B_3;B_0) - R_1 - R_3,\\
& \left. I(B_3;B_0) < R_3 < I(B_1,B_3;B_0) - R_1\right]\\
=& \Pr\left[2^{R_{c2}I(B_1;B_0|B_2,B_3)} - 1 < \Gamma_1 < 2^{R_{c1}I(B_1;B_0|B_3)} - 1, \right.\\
& 2^{R_{c2}I(B_2;B_0|B_1,B_3)} - 1 < \Gamma_2 < 2^{R_{c2}I(B_1,B_2,B_3;B_0) - \frac{R_{c2}}{R_{c3}}\log(1+\Gamma_3) - \frac{R_{c2}}{R_{c1}}\log(1+\Gamma_1)} - 1,\\
& \left. 2^{R_{c3}I(B_3;B_0)} - 1 < \Gamma_3 < 2^{R_{c3}(I(B_1,B_3;B_0)) - \frac{R_{c3}}{R_{c1}}\log(1+\Gamma_1)} - 1\right].
\end{aligned}
$$
$$(7.40)$$

As before, all of these expressions can be evaluated by integrating the joint PDF $f_{\Gamma_1,\Gamma_2,\Gamma_3}(\gamma_1,\gamma_2,\gamma_3) = f_{\Gamma_1}(\gamma_1)f_{\Gamma_2}(\gamma_2)f_{\Gamma_3}(\gamma_3)$ over the corresponding ranges defined in (7.33) to (7.40). This is done in Appendices G.3, G.4, and G.5. The obtained results are

$$J_{3,1} = \left(1 - e^{-\frac{2^{R_{c1}I(B_1;B_0|B_2,B_3)}-1}{\bar{\Gamma}_1} - \frac{2^{R_{c2}I(B_2;B_0|B_1,B_3)}-1}{\bar{\Gamma}_2} - \frac{2^{R_{c3}I(B_3;B_0|B_1,B_2)}-1}{\bar{\Gamma}_3}}\right), \qquad (7.41)$$

$$J_{3,2} = \frac{1}{\bar{\Gamma}_2} e^{-\frac{2^{R_{c1}I(B1;B_0)}-1}{\bar{\Gamma}_1}}$$
$$\times \int_{2^{R_{c2}I(B_2;B_0|B_1,B_3)}-1}^{2^{R_{c2}I(B_2;B_0|B_1)}-1} e^{-\frac{\gamma_2}{\bar{\Gamma}_2}} \left(e^{-\frac{2^{R_{c3}I(B_3;B_0|B_1,B_2)}-1}{\bar{\Gamma}_3}} - e^{-\frac{2^{R_{c3}I(B_2,B_3;B_0|B_1)}-\frac{R_{c3}}{R_{c2}}\log_2(\gamma_2+1)}{\bar{\Gamma}_3}} \right) d\gamma_2,$$
$$(7.42)$$

$$J_{3,3} = \frac{1}{\bar{\Gamma}_1} e^{-\frac{2^{R_{c3}I(B_3;B_0)}-1}{\bar{\Gamma}_3}}$$
$$\times \int_{2^{R_{c1}I(B_1;B_0|B_2,B_3)}-1}^{2^{R_{c1}I(B_1;B_0|B_3)}-1} e^{-\frac{\gamma_1}{\bar{\Gamma}_1}} \left(e^{-\frac{2^{R_{c2}I(B_2;B_0|B_1,B_3)}-1}{\bar{\Gamma}_2}} - e^{-\frac{2^{R_c I(B_1,B_2;B_0|B_3)}-\frac{R_{c2}}{R_{c1}}\log_2(\gamma_1+1)}{\bar{\Gamma}_2}} \right) d\gamma_1,$$
$$(7.43)$$

$$J_{3,4} = \frac{1}{\bar{\Gamma}_3} e^{-\frac{2^{R_{c2}I(B_2;B_0)}-1}{\bar{\Gamma}_2}}$$
$$\times \int_{2^{R_{c3}I(B_3;B_0|B_1,B_2)}-1}^{2^{R_{c3}I(B_3;B_0|B_2)}-1} e^{-\frac{\gamma_3}{\bar{\Gamma}_3}} \left(e^{-\frac{2^{R_{c1}I(B_1;B_0|B_2,B_3)}-1}{\bar{\Gamma}_1}} - e^{-\frac{2^{R_{c1}I(B_3,B_1;B_0|B_2)}-\frac{R_{c1}}{R_{c3}}\log_2(\gamma_3+1)}{\bar{\Gamma}_1}} \right) d\gamma_3,$$
$$(7.44)$$

$$J_{3,5a} = \frac{1}{\bar{\Gamma}_1\bar{\Gamma}_3} \int_{2^{R_{c1}I(B_1;B_0|B_2,B_3)}-1}^{2^{R_{c1}I(B_1;B_0)}-1} \int_{2^{R_{c3}I(B_3;B_0|B_1,B_2)}-1}^{2^{R_{c3}(I(B_3;B_0|B_1))-\frac{R_{c3}}{R_{c1}}\log_2(\gamma_1+1)}-1} e^{-\frac{\gamma_1}{\bar{\Gamma}_1}} e^{-\frac{\gamma_3}{\bar{\Gamma}_3}}$$
$$\times \left(e^{-\frac{2^{R_{c2}I(B_2;B_0|B_1,B_3)}-1}{\bar{\Gamma}_2}} - e^{-\frac{2^{R_{c2}I(B_1,B_2,B_3;B_0)}-\frac{R_{c2}}{R_{c1}}\log_2(\gamma_1+1)-\frac{R_{c2}}{R_{c3}}\log_2(\gamma_3+1)}{\bar{\Gamma}_2}} \right) d\gamma_3 d\gamma_1,$$
$$(7.45)$$

$$J_{3,5b} = \frac{1}{\bar{\Gamma}_1\bar{\Gamma}_3} \int_{2^{R_{c1}I(B_1;B_0|B_2,B_3)}-1}^{2^{R_{c1}I(B_1;B_0|B_2)}-1} \int_{2^{R_{c3}I(B_3;B_0|B_2,B_1)}-1}^{2^{R_{c3}I(B_1,B_3;B_0|B_2)}-\frac{R_{c3}}{R_{c1}}\log(1+\Gamma_1)-1} e^{-\frac{\gamma_1}{\bar{\Gamma}_1}} e^{-\frac{\gamma_3}{\bar{\Gamma}_3}}$$
$$\times \left(e^{-\frac{2^{R_{c2}I(B2;B_0)}-1}{\bar{\Gamma}_2}} - e^{-\frac{2^{R_{c2}I(B_1,B_2,B_3;B_0)}-\frac{R_{c2}}{R_{c1}}\log_2(\gamma_1+1)-\frac{R_{c2}}{R_{c3}}\log_2(\gamma_3+1)}{\bar{\Gamma}_2}} \right) d\gamma_3 d\gamma_1, \quad (7.46)$$

$$J_{3,5c} = \frac{1}{\bar{\Gamma}_1\bar{\Gamma}_3} \int_{2^{R_{c1}I(B_1;B_0|B_2,B_3)}-1}^{2^{R_{c1}I(B_1;B_0|B_3)}-1} \int_{2^{R_{c3}I(B_3;B_0)}-1}^{2^{R_{c3}I(B_1,B_3;B_0)}-\frac{R_{c3}}{R_{c1}}\log(1+\Gamma_1)-1} e^{-\frac{\gamma_1}{\bar{\Gamma}_1}} e^{-\frac{\gamma_3}{\bar{\Gamma}_3}}$$
$$\times \left(e^{-\frac{2^{R_{c2}I(B_2;B_0|B_1,B_3)}-1}{\bar{\Gamma}_2}} - e^{-\frac{2^{R_{c2}I(B_1,B_2,B_3;B_0)}-\frac{R_{c2}}{R_{c1}}\log_2(\gamma_1+1)-\frac{R_{c2}}{R_{c3}}\log_2(\gamma_3+1)}{\bar{\Gamma}_2}} \right) d\gamma_3 d\gamma_1,$$
$$(7.47)$$

where all of the required mutual informations involving B_1, B_2, and B_3 are provided in (7.19) in terms of the bit-flipping probabilities. Using (7.41)–(7.47) into (7.32) and (7.37), the outage probability is finally obtained as $P_{\text{out}} = J_{3,1} + J_{3,2} + J_{3,3} + J_{3,4} + J_{3,5a} - J_{3,5b} - J_{3,5c}$.

Note that the exact outage probability is obtained in terms of single- and two-fold integral-form expressions. On the other hand, as in the previous case, a simple closed-form asymptotic solution can be derived at high SNR. This is done in Appendices G.3, G.4, and G.5 for each probability component separately, by assuming $R_{c1} = R_{c2} = R_c$. From the results therein, it can be shown that the high-SNR outage behavior is again dominated by a single component, namely $J_{3,1}$. Accordingly, an asymptotic expression of P_{out} for three relays can be written in compact form as

$$P_{\text{out}} \simeq \frac{C_1}{\overline{\Gamma}_1} + \frac{C_2}{\overline{\Gamma}_2} + \frac{C_3}{\overline{\Gamma}_3}, \tag{7.48}$$

where the constants C_1, C_2, and C_3 are defined as

$$C_1 = 2^{R_c I(B_1; B_0 | B_2, B_3)} - 1, \tag{7.49}$$
$$C_2 = 2^{R_c I(B_2; B_0 | B_1, B_3)} - 1, \tag{7.50}$$
$$C_3 = 2^{R_c I(B_3; B_0 | B_1, B_2)} - 1, \tag{7.51}$$

with the mutual informations $I(B_1; B_0 | B_2, B_3)$, $I(B_2; B_0 | B_1, B_3)$, and $I(B_3; B_0 | B_1, B_2)$ being given as in (7.19) in terms of the bit-flipping probabilities.

7.4.3   N Relays

The same approach can be applied to any given number N of relays, by splitting the modified inadmissible rate region into several parts. The contribution of each part is then evaluated by integrating the joint PDF of the individual SNRs over the corresponding range. However, as in the cases of two and three relays, the resulting outage expression is written in $(N-1)$-fold integral form. On the other hand, a simple closed-form asymptotic solution at high SNR can be also obtained for the general case with an arbitrary number of relays. This is based on the following key result of a pioneering work in [12]: the asymptotic outage behavior at high SNR is exclusively determined by the PDF behavior of the SNR in the vicinity of the origin. Therefore, in our case, it suffices to consider those parts of the modified inadmissible rate region that directly interface with at least one of the coordinate axes. From the Slepian-Wolf constraints given in (7.8), the probability mass $J_{N,1}$ of the referred parts can be expressed as

$$\begin{aligned} J_{N,1} =& 1 - \Pr\left[\, R_1 > I(B_1; B_0 | B_2, \ldots, B_N), R_2 > I(B_2; B_0 | B_1, \ldots, B_N), \ldots, \right. \\ & \left. R_N > I(B_N; B_0 | B_1, \ldots, B_{N-1}) \,\right], \\ =& 1 - \Pr\left[2^{R_{c1} I(B_1; B_0 | B_2, \ldots, B_N)} - 1 < \Gamma_1 < \infty, \right. \\ & \left. 2^{R_{c2} I(B_2; B_0 | B_1, \ldots, B_N)} - 1 < \Gamma_2 < \infty, \ldots, 2^{R_{cN} I(B_N; B_0 | B_1, \ldots, B_{N-1})} - 1 < \Gamma_N < \infty \right]. \end{aligned} \tag{7.52}$$

Now, by following the same procedure presented in Appendices G.1 to G.5 for two and three relays, after some algebraic manipulations, an asymptotic high-SNR expression for

the outage probability P_{out} of the general case with an arbitrary number of relays can be finally obtained as

$$P_{\text{out}} \simeq \sum_{i=1}^{N} \frac{C_i}{\bar{\Gamma}_i}, \tag{7.53}$$

where each constant C_i is defined as

$$C_i \triangleq 2^{R_c I(B_i; B_0 | \{B_j, j \neq i\})} - 1, \tag{7.54}$$

with the mutual informations $I(B_i; B_0 | \{B_j, j \neq i\})$, $i \in \{1, \ldots, N\}$, being computed from (7.8)–(7.11) in terms of the bit-flipping probabilities.

7.4.4 Throughput

Although the outage probability is effective in measuring the likelihood that each transmission succeeds, it does not capture how much useful information the destination receives on average per transmission. To capture this, following the standard approach in the literature, we define the system throughput T as the mutual information between the set of relay sequences $B_1, \ldots, B_N$ and the source sequence B_0 times the non-outage probability, which gives

$$T = I(B_1, \ldots, B_N; B_0) \cdot (1 - P_{\text{out}}), \tag{7.55}$$

where $I(B_1, \ldots, B_N; B_0)$ and P_{out} can be computed by using the mathematical framework developed heretofore.

7.5 Asymptotically Optimal Power Allocation

In this section, we design a simple power allocation strategy for the multiple relays in order to improve the outage performance of the investigated system. Despite its simplicity, the proposed allocation proves highly effective, being asymptotically optimal at high SNR. For that reason, we call it Asymptotically Optimal Power Allocation (AOPA).

Given a total amount of transmit power P_T for all relays, the transmit power at the ith relay is assigned as $P_i = \alpha_i P_T$, where $0 \leq \alpha_i \leq 1$ is the power allocation coefficient, $i \in \{1, \ldots, N\}$. Of course, $\sum_{i=1}^{N} \alpha_i = 1$. Then, from (7.3), the average received SNR at the ith second hop can be written as

$$\bar{\Gamma}_i = \frac{\alpha_i \, P_T \, d_i^{-\eta}}{N_0}. \tag{7.56}$$

Our primary aim is to find the set of power allocation coefficients $\alpha_1, \ldots, \alpha_N$ that minimize P_{out}, that is,

$$\begin{aligned} \underset{\alpha_1, \ldots, \alpha_N}{\text{minimize}} \quad & P_{\text{out}}(\alpha_1, \ldots, \alpha_N) \\ \text{subject to} \quad & 0 \leq \alpha_i \leq 1, \forall i, \text{ and } \sum_{i=1}^{N} \alpha_i = 1. \end{aligned} \tag{7.57}$$

Unfortunately, as seen in the previous Section, there exists no general exact closed-form expression for P_{out}. Alternatively, we propose minimizing the simple asymptotic outage expression in (7.53). By using (7.3), this can be formulated as

$$\underset{\alpha_1,\ldots,\alpha_N}{\text{minimize}} \quad \sum_{i=1}^{N} \frac{N_0 C_i d_i^\eta}{P_{\text{T}}} \cdot \frac{1}{\alpha_i} \tag{7.58}$$
$$\text{subject to} \quad 0 \le \alpha_i \le 1, \forall i, \text{ and } \sum_{i=1}^{N} \alpha_i = 1,$$

where each constant C_i is defined as in (7.54). This is a convex optimization problem, as follows. Note that the cost function is a summation, each component of which is a function of a single power allocation coefficient. It turns out that the ith component $N_0 C_i d_i^\eta/(P_{\text{T}}\alpha_i)$ is a convex function of the ith coefficient α_i, because $N_0 C_i d_i^\eta/P_{\text{T}} \ge 0$ and $1/\alpha_i$ is a convex function of α_i. The proof of convexity is completed by recognizing that a sum of convex functions is also a convex function [13]. To find the global minimum, we eliminate the Nth power allocation coefficient α_N by incorporating the constraint $\sum_{i=1}^{N} \alpha_i = 1$ into the cost function, which gives

$$\sum_{i=1}^{N-1} \frac{N_0 C_i d_i^\eta}{P_{\text{T}}} \cdot \frac{1}{\alpha_i} + \frac{N_0 C_N d_N^\eta}{P_{\text{T}}} \cdot \frac{1}{1 - \sum_{i=1}^{N-1} \alpha_i}. \tag{7.59}$$

Then, by differentiating (7.59) with respect to the remaining set of power allocation coefficients $\alpha_1, \ldots, \alpha_{N-1}$, by equating all these partial derivatives to zero, and by solving the resulting system of equations, after some algebraic manipulations omitted here for simplicity, we finally arrive at the AOPA scheme:

$$\alpha_i = \frac{\sqrt{C_i \cdot d_i^\eta}}{\sum_{j=1}^{N} \sqrt{C_j \cdot d_j^\eta}}, \ i \in \{1, \ldots, N\}. \tag{7.60}$$

Note that the proposed power allocation depends ultimately on the distances d_i between each relay and the destination, and on the conditional mutual informations $I(B_i; B_0|\{B_j, j \neq i\})$ between each relay sequence and the source sequence, which, in turn, have been derived here in terms of the bit-flipping probabilities of the first hops. Also note that the solution in (7.60) inherently complies with the constraint $0 \le \alpha_i \le 1$.

7.6 Numerical Results

In this Section, we evaluate the impact of the our AOPA policy on the performance of the investigated DSC scheme, by considering some representative sample scenarios. The equal power allocation (EPA) policy, i.e., $\alpha_i = 1/N, \forall i$, is included for comparison. In each scenario, the outage probability is assessed asymptotically, by means of (7.53), as well as via Monte Carlo simulation, whereas the throughput is assessed via simulation only. For illustration purposes, we assume a binary phase-shift keying modulation and a channel code rate of $1/2$, so that $R_c = 2$. Moreover, we assume $\eta = 4$ and a normalized

(a)   (b)
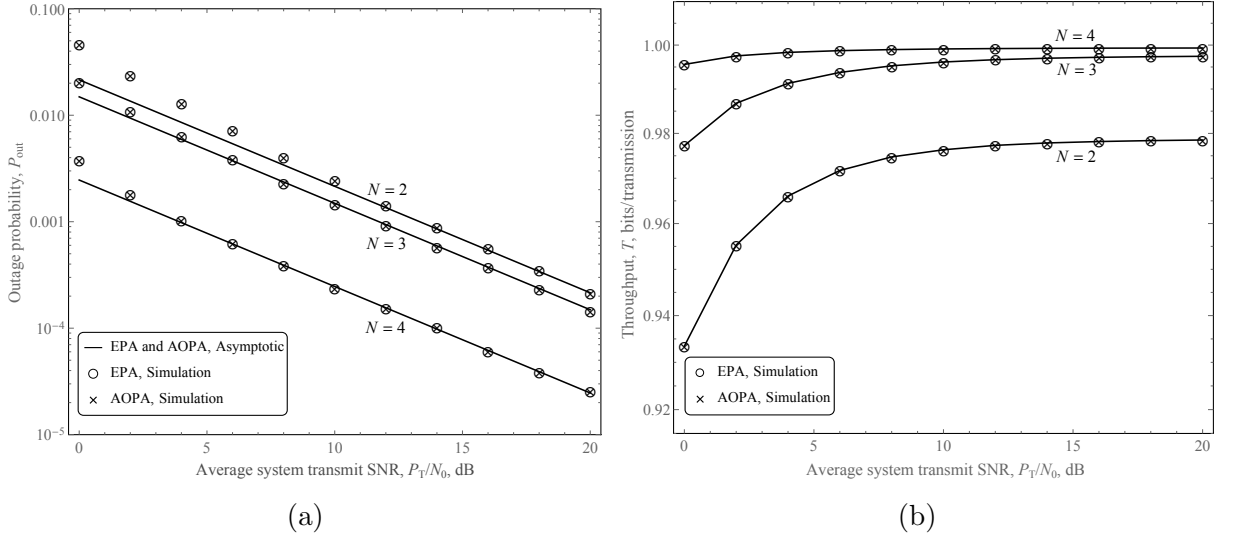
Figure 7.6: Performance comparison between EPA and AOPA for two, three, and four relays under identical bit-flipping probabilities: $p_i = 0.01, \forall i$; (a) outage probability; (b) throughput.

distance $0 \leq d_i \leq 1$ between the relays and destination. We investigate the system performance for two, three, and four relays, by exploiting multiple configurations in terms of bit-flipping probabilities, relay location, and average SNR.

Fig. 7.6 presents the first investigated scenario, which illustrates the outage probability and throughput versus the average system transmit SNR (P_T/N_0) for two, three, and four relays under *identical* bit-flipping probabilities of 0.01. We consider $d_i = 0.5$ for all relays. The following can be observed from the curves: (i) our asymptotic outage expression in (7.53) has an excellent match at medium to high SNR; (ii) under identical bit-flipping probabilities and identical relay-to-destination distances, AOPA coincides with EPA, which is expected intuitively and from (7.60); and (iii) the performance improves as the number of relays increases. Although the last observation may sound obvious at first glance, it subtly involves two conflicting aspects, as follows. On the one hand, as the number of relays increases, the mutual information between the set of relay messages and the source message also increases, rendering the sum-rate inequality $R_1 + \cdots + R_N \geq I(B_1, \ldots, B_N; B_0)$ less likely for a given second-hop scenario. On the other, the mutual information between each relay message and the source message conditioned on the remaining relay messages diminishes, rendering each individual rate inequality $R_i \geq I(B_i; B_0 | \{B_j, j \neq i\})$ more likely. We know from (7.53) that the latter aspect dominates the performance, at least asymptotically, for high SNR. From Fig. 7.6, it becomes apparent that such domination holds true for low to medium SNR.

Fig. 7.7 shows the outage probability versus the average system transmit SNR for two, three, and four relays under *non-identical* bit-flipping probabilities. As before, we consider $d_i = 0.5$ for all relays. The investigated scenarios are listed in Tab. 7.1 along with the power allocation coefficients provided by AOPA and the corresponding SNR gains with respect to EPA. The following can be observed from the curves: (i) once again, our asymptotic expression in (7.53) gives an excellent match at medium to high SNR; (ii) in all the cases, AOPA outperforms EPA at medium to high SNR; and (iii) the more dissimilar

(a)

(b)

(c)
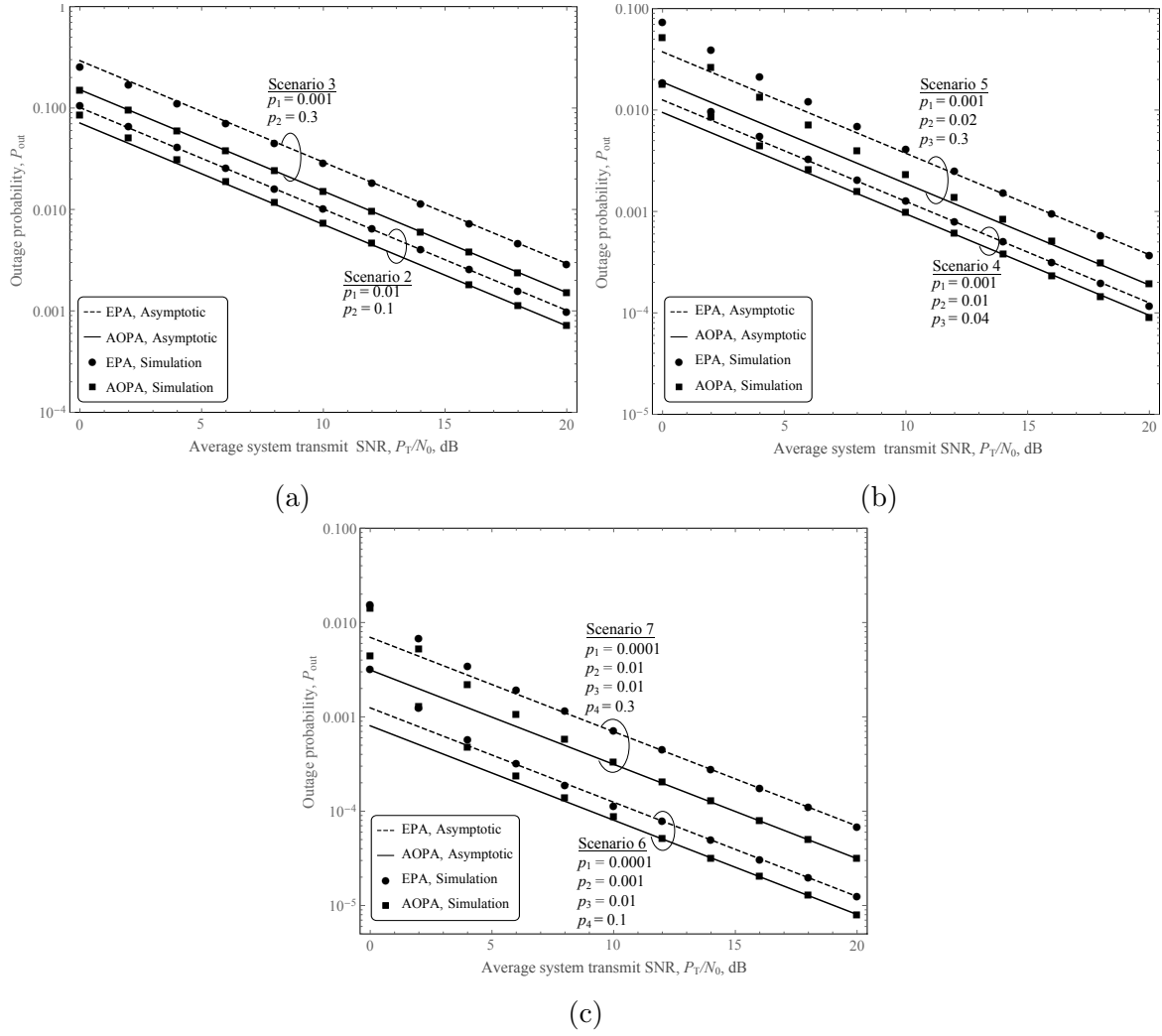
Figure 7.7: Outage comparison between EPA and AOPA under non-identical bit-flipping probabilities: (a) two relays; (b) three relays; (c) four relays. (See Table 7.1 for further details.)

Table 7.1: Bit-flipping probabilities, AOPA coefficients, and AOPA-over-EPA SNR gain for investigated scenarios.

| Scenario	p_1	p_2	p_3	p_4	α_1	α_2	α_3	α_4	AOPA-over-EPA Gain (dB)
2	0.01	0.1			0.8244	0.1756			1.54
3	0.001	0.3			0.9833	0.0167			2.88
4	0.001	0.01	0.04		0.6011	0.2251	0.1738		1.29
5	0.001	0.02	0.3		0.7969	0.1569	0.0462		3.12
6	0.0001	0.001	0.01	0.1	0.5491	0.2409	0.1588	0.0512	2
7	0.0001	0.01	0.01	0.3	0.7225	0.1257	0.1257	0.0261	3.56
8	0.001	0.1			0.94095	0.05905			2.54

(a)   (b)
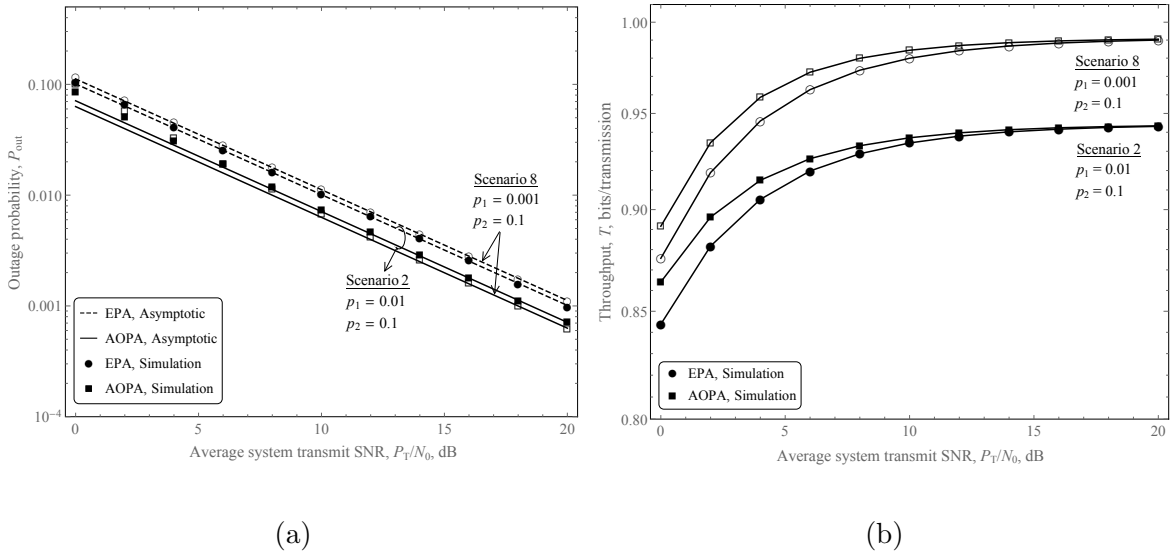
Figure 7.8: Performance comparison between EPA and AOPA for two relays and varying bit-flipping probability at the first relay: (a) outage probability; (b) throughput.

are bit-flipping probabilities of the first hops, the greater is the SNR gain achieved by AOPA when compared with EPA. The last observation is indeed expected, by considering that, for identically distributed first hops and identical relay-to-destination distances, the AOPA coincides with EPA, then providing no gain at all.

Fig. 7.8 depicts the outage probability and throughput versus the average system transmit SNR for two relays, a constant bit-flipping probability of 0.1 at the second relay, and a varying bit-flipping probability at the first relay. The aim is to find out how differently the quality of the first-hop channel impacts each performance metric for EPA and AOPA. From the curves, we notice that the impact is indeed quite different in each case. For EPA, a better quality of the first-hop (lower bit-flipping probability) associated with the first relay deteriorates the outage probability, although it improves the system throughput. This is explained as follows. As the first hop improves, the mutual information between the two relay messages and the source message increases, rendering the sum-rate inequality $R_1 + R_2 \geq I(B_1, B_2; B_0)$ less likely, which deteriorates the outage probability. In contrast, for the same scenario, the referred increases in the mutual information $I(B_1, B_2; B_0)$ and in the outage probability P_{out} have opposite effects on the system throughput, as evidenced by (7.55). From Fig. 7.8, it becomes apparent that the increase in the mutual information dominates the impact, thus increasing the throughput. On the other hand, for AOPA, both metrics—outage probability and throughout—improve as the first hop associated with the first relay improves. In other words, the proposed power allocation redesigns the second-hop resources (by redistributing the transmit power between the two relays) in such an effective manner that the sum-rate inequality $R_1 + R_2 \geq I(B_1, B_2; B_0)$ becomes more likely, even though the required mutual information $I(B_1, B_2; B_0)$ is higher.

Finally, Fig. 7.9 displays the impact of the relay position on the outage probability and throughput for two relays with an average system transmit SNR of $P_T/N_0 = 20$ dB. The first relay is fixed at $d_1 = 0.5$, and the second one is located at varying distances d_2 from the destination, ranging from 0 to 1. Three scenarios are investigated: (a) identical

(a)   (b)
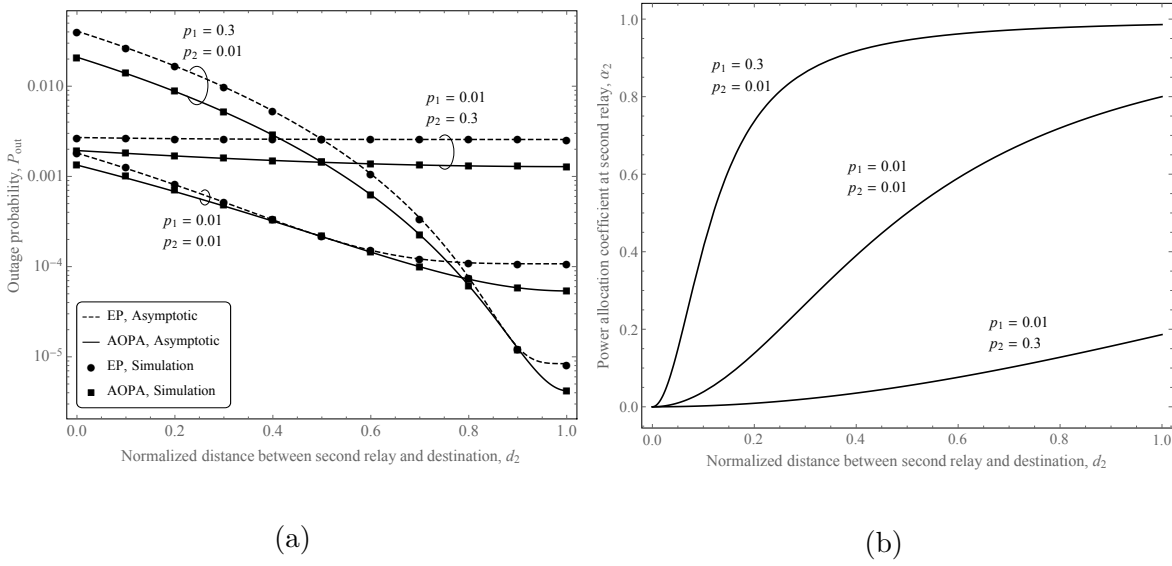
Figure 7.9: Outage comparison between EPA and AOPA for two relays and $P_T/N_0 = 20$ dB in terms of the distance between the second relay and destination: (a) outage probability; (b) AOPA coefficient for the second relay.

bit-flipping probabilities ($p_1 = p_2 = 0.01$), (b) smallest bit-flipping probability assigned to the relay with a variable location ($p_1 = 0.3$ and $p_2 = 0.01$), and (c) highest bit-flipping probability assigned to the relay with a variable location ($p_1 = 0.01$ and $p_2 = 0.3$). The outage probability is shown in Fig. 7.9a and the corresponding AOPA coefficient for the second relay is shown in Fig. 7.9b. The following can be observed from the curves: (i) in all the cases, our asymptotic outage expression in (7.53) has an excellent match; (ii) AOPA outperforms EPA, possibly except for a singular relay location, for which AOPA and EPA have identical performances; (iii) the closer is the relay to the destination, the smaller is the transmit power allocated to it by AOPA. Regarding the observation (ii), the balancing distance d_2 for which EPA and AOPA perform identically is, as expected, $d_2 = d_1 = 0.5$ when the bit-flipping probabilities associated with the two relays are identical. On the other hand, when the bit-flipping probability for the second relay is smaller/higher than that for the first (fixed) relay, the balancing distance d_2 moves toward/outward the destination. There is compensation mechanism at play: if a given relay is moved toward the destination, its second hop tends to improve, but the AOPA criterion counteracts this by reducing the relay's transmit power, which keeps the optimal balance between all the second hops. In particular, for scenario (b), note that the outage performance of both EPA and AOPA are barely affected by the location of the second relay. This is because in this case the fixed (first) relay has a much better first hop (much smaller bit-flipping probability), dominating the performance.

7.7 Conclusions

In this work, we analyzed the outage performance of a distributed source coding scheme for a decode-and-forward multirelay system with intra-link errors and no direct path available from source to destination. In addition, we designed a simple and highly effective

power allocation scheme for the investigated system. To this end, we revisited the Slepian-Wolf Theorem and modified its scope to comply with the engineering requirements of the problem at hand. Our results and discussions find important application in emerging links-on-the-fly technologies for robust and efficient communications in unpredictable environments.

Bibliography

[1] M. Dohler and Y. Li, *Cooperative Communications: Hardware, Channel and PHY*, 1st ed. Chichester, UK: John Wiley and Sons Ltd, 2010.

[2] K. Anwar and T. Matsumoto, "Accumulator-assisted distributed turbo codes for relay systems exploiting source-relay correlation," *IEEE Commun. Lett.*, vol. 16, no. 7, pp. 1114–1117, Jul. 2012.

[3] D. Slepian and J. Wolf, "Noiseless coding of correlated information sources," *IEEE Trans. Inf. Theory*, vol. 19, no. 4, pp. 471–480, Jul 1973.

[4] J. Garcia-Frias and Y. Zhao, "Near-Shannon/Slepian-Wolf performance for unknown correlated sources over AWGN channels," *IEEE Trans. Commun.*, vol. 53, no. 4, pp. 555–559, April 2005.

[5] X. Zhou, M. Cheng, S. Member, X. He, and T. Matsumoto, "Exact and approximated outage probability analyses for decode-and-forward relaying system allowing intra-link errors," *IEEE Trans. Wireless Commun.*, vol. 13, no. 12, pp. 7062–7071, Dec. 2014.

[6] M. Cheng, K. Anwar, and T. Matsumoto, "Outage analysis of correlated source transmission in block Rayleigh fading channels," in *Proc. IEEE Vehicular Technology Conference (VTC Fall)*, Quebec City, QC, 3–6 Sep. 2012, pp. 1–5.

[7] ——, "Outage based power allocation: Slepian-Wolf relaying viewpoint," pp. 807–811, Dec. 2013.

[8] X. Zhou, X. He, K. Anwar, and T. Matsumoto, "Great-CEO : large scale distributed decision making techniques for wireless chief executive officer problems," *IEICE Trans. Commun.*, vol. E95–B, no. 12, pp. 3654–3662, Dec. 2012.

[9] A. Wolf, M. Matthe, and G. Fettweis, "Improved source correlation estimation in wireless sensor networks," in *Proc. IEEE International Conference on Communications Workshop (ICCW)*, London, UK, 8–12 Jun. 2015, pp. 2121–2126.

[10] T. Berger, Z. Zhang, and V. Harish, "The CEO-problem," *IEEE Trans. Inf. Theory*, vol. 42, no. 3, pp. 887–902, 1996.

[11] X. He, X. Zhou, K. Anwar, and T. Matsumoto, "Estimation of observation error probability in wireless sensor networks," *IEEE Commun. Lett.*, vol. 17, no. 6, pp. 1073–1076, 2013.

[12] Z. Wang and G. B. Giannakis, "A simple and general parameterization quantifying performance in fading channels," *IEEE Trans. Commun*, vol. 51, no. 8, pp. 1389–1398, Aug 2003.

[13] S. Boyd and L. Vandenberghe, *Convex Optimization*, 1st ed. Cambridge, UK: Cambridge Univ. Pr., 2004.

Chapter 8

Conclusions

This chapter highlights the main contributions of this dissertation and suggests possible directions of future related work.

8.1 Concluding Remarks

In this dissertation, we proposed and analyzed a myriad of distributed, suboptimal transmit-antenna selection schemes for AF relaying systems, inspired by a recently introduced distributed approach for a DAS/MRC scheme operating over a single-antenna fixed-gain AF relay. This approach circumvents the need for full system CSI, required in optimal centralized schemes, while considering all the links in the antenna-selection mechanism, unlike most suboptimal schemes, in which some links are ignored. In order to bring insight into the potentials of the investigated DAS strategy, five different network scenarios were considered. In the first scenario, the original policy in the DAS/MRC scheme was adapted to operate with SC at the destination, i.e., a DAS/SC scheme with a single-antenna, fixed-gain AF relay was considered. In the second scenario, the selection mechanism between the direct link and the relaying link was moved from the destination to the source, i.e., a DAS/LS scheme with a single-antenna, fixed-gain AF relay was considered. In the third scenario, the original policy in the DAS/MRC scheme was generalized to allow for multiple antennas at the relay, i.e., a DAS/MRC scheme with a multi-antenna, fixed-gain AF relay was considered. In the fourth scenario, such generalization was extended to the DAS/SC case. Finally, in the fifth scenario, both DAS/MRC and DAS/SC schemes with a single-antenna relay were again considered, but now for variable-gain AF. Next, we summarize important aspects of our main contributions, challenges, and conclusions.

Outage probability and spectral efficiency. Due to the inherent intricacy of an exact mathematical treatment, analytical bounds were derived in integral-form for the outage probability of the proposed DAS/SC and DAS/MRC schemes. On the other hand, exact closed-form expressions were derived for the outage probability and mean spectral efficiency of the proposed DAS/LS scheme.

Asymptotic analysis and diversity order. In order to provide further insight into

the achievable diversity order of the investigated scenarios, a closed-form asymptotic analysis at high SNR was performed for the each of the derived bounds and exact expressions. The analysis reveals that all the proposed schemes achieve full diversity order, except the DAS/LS, which achieves full diversity order minus one, as a penalty for its improved spectral efficiency.

Simulation and validation. All of our analytical results were validated by means of Monte Carlo simulations.

Centralized vs. distributed schemes. The proposed distributed schemes were shown to perform closely to their costly, optimal centralized counterparts, mainly when the relay is located near the destination, for the fixed-gain schemes, and near the source or destination, for the variable-gain schemes.

System generalization and analytical complexity. The main challenge we faced in this work was the high mathematical intricacy inherent to the investigated systems. In some cases, an apparently minor generalization of the system setup caused a major increase in the level of difficulty of the analytical treatment. When going from the single-antenna to the multi-antenna relay scenario, for instance, completely different, sophisticated, non-usual mathematical procedures were required to solve the new problem. This is partly the reason we decided to investigate a sequence of small progressive generalizations of the distributed antenna-selection approach.

8.2 Future Directions

According to the results obtained from the analysis of the proposed scenarios, the distributed suboptimal transmit-antenna selection strategy proved to be an interesting approach, especially for practical purposes. On the other hand, there are others aspects and scenarios that could be investigated to bring further insights into the potentials of this promising strategy. Some possible directions for the future related work are summarized as follows.

Variable-gain relay and multi-antenna destination. In this work, we investigated DAS schemes with either a multi-antenna fixed-gain AF relay or a single-antenna variable-gain AF relay. It remains to investigate those schemes for a multi-antenna variable-gain AF relaying, as well as the generalizations of all those schemes to multi-antenna destinations.

Imperfect CSI. In this work, we assumed perfect CSI, because the focus was to provide a benchmark analysis for the best achievable performance of the proposed DAS schemes. In practice, however, the CSI is imperfectly known. Therefore, considering this in the analysis would be very important (and challenging).

Generalized channel models. In this work, we considered that all the channels undergo independent flat Rayleigh fading. It would be important to extend the analysis to more general and realistic fading models, such as Rice, Hoyt, Nakagami-m, Weibull, α-μ, κ-μ, and η-μ.

Single multi-antenna relay vs. multiple single-antenna relays. It would be interesting to compare the performance of the proposed schemes when operating over either a single multi-antenna relay or multiple single-antenna relays. Equivalently, in the battlefield, what is the best reinforcement for a soldier: another equally armed soldier or a twice as powerful weapon?

Appendices

Appendix A

Permission to Reproduce Copyrighted Material

Title: A distributed transmit antenna selection scheme for fixed-gain multi-antenna AF relaying systems

Conference Proceedings: Cognitive Radio Oriented Wireless Networks and Communications (CROWNCOM), 2014 9th International Conference on

Author: Gonzalez, D.C.; Santos Filho, J.C.S.; da Costa, D.B.

Publisher: IEEE

Date: 2-4 June 2014

Copyright © 2014, IEEE

Thesis / Dissertation Reuse

The IEEE does not require individuals working on a thesis to obtain a formal reuse license, however, you may print out this statement to be used as a permission grant:

Requirements to be followed when using any portion (e.g., figure, graph, table, or textual material) of an IEEE copyrighted paper in a thesis:

1) In the case of textual material (e.g., using short quotes or referring to the work within these papers) users must give full credit to the original source (author, paper, publication) followed by the IEEE copyright line © 2011 IEEE.
2) In the case of illustrations or tabular material, we require that the copyright line © [Year of original publication] IEEE appear prominently with each reprinted figure and/or table.
3) If a substantial portion of the original paper is to be used, and if you are not the senior author, also obtain the senior author's approval.

Requirements to be followed when using an entire IEEE copyrighted paper in a thesis:

1) The following IEEE copyright/ credit notice should be placed prominently in the references: © [year of original publication] IEEE. Reprinted, with permission, from [author names, paper title, IEEE publication title, and month/year of publication]
2) Only the accepted version of an IEEE copyrighted paper can be used when posting the paper or your thesis on-line.
3) In placing the thesis on the author's university website, please display the following message in a prominent place on the website: In reference to IEEE copyrighted material which is used with permission in this thesis, the IEEE does not endorse any of [university/educational entity's name goes here]'s products or services. Internal or personal use of this material is permitted. If interested in reprinting/republishing IEEE copyrighted material for advertising or promotional purposes or for creating new collective works for resale or redistribution, please go to http://www.ieee.org/publications_standards/publications/rights/rights_link.html to learn how to obtain a License from RightsLink.

If applicable, University Microfilms and/or ProQuest Library, or the Archives of Canada may supply single copies of the dissertation.

BACK   CLOSE WINDOW

Title: Distributed Suboptimal Schemes for TAS/SC and TAS/LS in Fixed-Gain AF Relaying Systems

Author: Gonzalez, D.C.; da Costa, D.B.; Candido Silveira Santos Filho, J.

Publication: Wireless Communications, IEEE Transactions on

Publisher: IEEE

Date: Nov. 2014

Copyright © 2014, IEEE

Thesis / Dissertation Reuse

The IEEE does not require individuals working on a thesis to obtain a formal reuse license, however, you may print out this statement to be used as a permission grant:

Requirements to be followed when using any portion (e.g., figure, graph, table, or textual material) of an IEEE copyrighted paper in a thesis:

1) In the case of textual material (e.g., using short quotes or referring to the work within these papers) users must give full credit to the original source (author, paper, publication) followed by the IEEE copyright line © 2011 IEEE.
2) In the case of illustrations or tabular material, we require that the copyright line © [Year of original publication] IEEE appear prominently with each reprinted figure and/or table.
3) If a substantial portion of the original paper is to be used, and if you are not the senior author, also obtain the senior author's approval.

Requirements to be followed when using an entire IEEE copyrighted paper in a thesis:

1) The following IEEE copyright/ credit notice should be placed prominently in the references: © [year of original publication] IEEE. Reprinted, with permission, from [author names, paper title, IEEE publication title, and month/year of publication]
2) Only the accepted version of an IEEE copyrighted paper can be used when posting the paper or your thesis on-line.
3) In placing the thesis on the author's university website, please display the following message in a prominent place on the website: In reference to IEEE copyrighted material which is used with permission in this thesis, the IEEE does not endorse any of [university/educational entity's name goes here]'s products or services. Internal or personal use of this material is permitted. If interested in reprinting/republishing IEEE copyrighted material for advertising or promotional purposes or for creating new collective works for resale or redistribution, please go to http://www.ieee.org/publications_standards/publications/rights/rights_link.html to learn how to obtain a License from RightsLink.

If applicable, University Microfilms and/or ProQuest Library, or the Archives of Canada may supply single copies of the dissertation.

BACK | CLOSE WINDOW

Appendix B

Supporting Material to Chapter 2

The references cited in this appendix are listed at the end of Chapter 2.

B.1 High-SNR expression for φ in (2.11)

Here we derive the high-SNR behavior of φ. From its definition, we have

$$
\begin{aligned}
\varphi &= \int_0^1 \frac{C}{\bar{\gamma}_{RD}} e^{-\frac{Cy}{\bar{\gamma}_{RD}}} \, dy - \frac{C}{\bar{\gamma}_{RD}} \int_0^1 e^{-\frac{Cy}{\bar{\gamma}_{RD}} - \frac{z}{y\bar{\gamma}_{SR}}} \, dy \\
&= \left(1 - e^{-\frac{C}{\bar{\gamma}_{RD}}}\right) - \frac{C}{\bar{\gamma}_{RD}} \underbrace{\int_0^1 e^{-\frac{Cy}{\bar{\gamma}_{RD}} - \frac{z}{y\bar{\gamma}_{SR}}} \, dy}_{\rho},
\end{aligned}
\tag{B.1}
$$

where ρ can be expressed as

$$
\begin{aligned}
\rho &\overset{(a)}{=} 2\sqrt{\frac{z\bar{\gamma}_{RD}}{C\bar{\gamma}_{SR}}} K_1\left(2\sqrt{\frac{Cz}{\bar{\gamma}_{SR}\bar{\gamma}_{RD}}}\right) - \int_1^\infty e^{-\frac{Cy}{\bar{\gamma}_{RD}}} \sum_{l=0}^\infty \frac{\left(-\frac{z}{y\bar{\gamma}_{SR}}\right)^l}{l!} \, dy \\
&\overset{(b)}{=} \left(2\sqrt{\frac{z\bar{\gamma}_{RD}}{C\bar{\gamma}_{SR}}}\right)\left(\frac{1}{2}\sqrt{\frac{\bar{\gamma}_{SR}\bar{\gamma}_{RD}}{Cz}}\right) + \left(2\sqrt{\frac{z\bar{\gamma}_{RD}}{C\bar{\gamma}_{SR}}}\right) \\
&\quad \times \sum_{k=0}^\infty \frac{\sqrt{\frac{Cz}{\bar{\gamma}_{SR}\bar{\gamma}_{RD}}}}{k!(k+1)} \left(\ln\sqrt{\frac{Cz}{\bar{\gamma}_{SR}\bar{\gamma}_{RD}}} - \psi(k+1) - \psi(k+2)\right) \\
&\quad - \sum_{l=0}^\infty \frac{\left(-\frac{z}{\bar{\gamma}_{SR}}\right)^l}{l!} \int_1^\infty y^{-l} e^{-\frac{Cy}{\bar{\gamma}_{RD}}} \, dy.
\end{aligned}
\tag{B.2}
$$

Steps (a) and (b) follow from [14, Eq (3.471.9)] and [14, Eq (8.4)], respectively, where $K_1(\cdot)$ is the first-order modified Bessel function of second kind. Hence, by keeping only to the lowest-order terms in $\bar{\gamma}_{SR}$ and $\bar{\gamma}_{RD}$, ρ can be asymptotically written as

$$
\rho \simeq \frac{\bar{\gamma}_{RD}}{C} + \frac{1}{2}\frac{z}{\bar{\gamma}_{SR}} \left(\ln z - \ln\bar{\gamma}_{RD} - \psi(1) - \psi(2)\right) - \frac{\bar{\gamma}_{RD}}{C} e^{-\frac{C}{\bar{\gamma}_{RD}}}.
\tag{B.3}
$$

Finally, replacing (B.3) into (B.1), we obtain, after some algebraic manipulations, the high-SNR asymptote of φ as

$$
\varphi \simeq \frac{z}{\bar{\gamma}_{SR}\mu_2} \left(\ln z - \ln\bar{\gamma}_{RD} - \psi(1) - \psi(2)\right).
\tag{B.4}
$$

Appendix C

Supporting Material to Chapter 3

The references cited in this appendix are listed at the end of Chapter 3.

C.1   High-SNR Asymptote for the Term φ in (3.14)

In this section, we derive an asymptotic high-SNR expression for the term φ defined in (3.14). From its definition, we have

$$
\begin{aligned}
\varphi &= \int_0^1 \frac{C}{\overline{Z}} e^{-\frac{Cv}{\overline{Z}}} \, dy - \frac{C}{\overline{Z}} \int_0^1 e^{-\frac{Cv}{\overline{Z}} - \frac{\tau}{v\overline{X}}} \, dv \\
&= \left(1 - e^{-\frac{C}{\overline{Z}}} \right) - \frac{C}{\overline{Z}} \underbrace{\int_0^1 e^{-\frac{Cv}{\overline{Z}} - \frac{\tau}{v\overline{X}}} \, dv}_{\rho} .
\end{aligned}
\tag{C.1}
$$

where ρ can be expressed as

$$
\begin{aligned}
\rho &\overset{(a)}{=} 2\sqrt{\frac{\tau\overline{Z}}{C\overline{X}}} K_1\left(2\sqrt{\frac{C\tau}{\overline{X}\overline{Z}}} \right) - \int_1^\infty e^{-\frac{Cv}{\overline{Z}}} \sum_{l=0}^\infty \frac{\left(-\frac{\tau}{v\overline{X}}\right)^l}{l!} \, dv \\
&\overset{(b)}{=} \left(2\sqrt{\frac{\tau\overline{Z}}{C\overline{X}}} \right)\left(\frac{1}{2}\sqrt{\frac{\overline{X}\overline{Z}}{C\tau}} \right) + \left(2\sqrt{\frac{\tau\overline{Z}}{C\overline{X}}} \right) \\
&\quad \times \sum_{k=0}^\infty \frac{\sqrt{\frac{C\tau}{\overline{X}\overline{Z}}}}{k!(k+1)} \left(\ln\sqrt{\frac{C\tau}{\overline{X}\overline{Z}}} - \psi(k+1) - \psi(k+2) \right) \\
&\quad - \sum_{l=0}^\infty \frac{\left(-\frac{\tau}{\overline{X}}\right)^l}{l!} \int_1^\infty v^{-l} e^{-\frac{Cv}{\overline{Z}}} \, dv.
\end{aligned}
\tag{C.2}
$$

Steps (a) and (b) follow from [18, Eq. (3.471.9)] and [18, Eq. (8.446)], respectively, where $K_1(\cdot)$ is the first-order modified Bessel function of the second kind. Hence, by keeping only to the lowest-order terms in $\overline{X}$ and $\overline{Z}$, ρ can be asymptotically written as

$$
\rho \simeq \frac{\overline{Z}}{C} - \frac{\tau}{\overline{X}} \left(\ln\tau - \ln\overline{Z} - \psi(1) - \psi(2) + \Gamma\left(0, \frac{C}{\overline{Z}} \right) \right) - \frac{\overline{Z}}{C} e^{-\frac{C}{\overline{Z}}}.
\tag{C.3}
$$

Finally, replacing (C.3) into (C.1), we obtain, after some algebraic manipulations, the high-SNR asymptote of φ as

$$\varphi \simeq \frac{\tau}{\overline{X}\mu_2}\left(\ln\overline{Z} - \ln\tau + \psi(1) + \psi(2) - \Gamma\left(0, \frac{C}{\overline{Z}}\right)\right). \tag{C.4}$$

C.2 Infinite-Series Representation for the term Φ in (3.26)

In this section, we derive an infinite-series representation for the term Φ defined in (3.26). Using the binomial theorem [18, Eq. (3.1.1)], Φ can be rewritten as

$$\Phi = \int_C^\infty \frac{1}{\overline{Z}} e^{-\frac{z}{\overline{Z}}}\left(1 + \sum_{m=1}^{N_t}\binom{N_t}{m}(-1)^m e^{-m\left(\frac{\tau}{\overline{Y}} + \frac{\tau C}{z\overline{Y}}\right)}\right)\left(1 + \sum_{j=1}^{N_t}\binom{N_t}{j}(-1)^j e^{-j\left(\frac{\tau}{\overline{X}} + \frac{\tau C}{z\overline{X}}\right)}\right)dz$$

$$= \int_C^\infty \left[\frac{1}{\overline{Z}}e^{-\frac{z}{\overline{Z}}} + \frac{1}{\overline{Z}}\sum_{j=1}^{N_t}\binom{N_t}{j}(-1)^j\left(e^{-j\frac{\tau}{\overline{X}}}e^{-j\frac{\tau C}{\overline{X}z}}e^{-\frac{z}{\overline{Z}}} + e^{-j\frac{\tau}{\overline{Y}}}e^{-j\frac{\tau C}{\overline{Y}z}}e^{-\frac{z}{\overline{Z}}}\right)\right.$$

$$\left. + \frac{1}{\overline{Z}}\sum_{j=1}^{N_t}\sum_{m=1}^{N_t}\binom{N_t}{j}(-1)^j\binom{N_t}{m}(-1)^m e^{-\tau\left(\frac{m}{\overline{Y}} + \frac{j}{\overline{X}}\right)}e^{-\frac{\tau C}{z}\left(\frac{m}{\overline{Y}} + \frac{j}{\overline{X}}\right)}e^{-\frac{z}{\overline{Z}}}\right]dz. \tag{C.5}$$

Then, using the Maclaurin series for the exponential function in step (a), [18, Eq. (3.381.9)] in step (b), and after some albegraic manipulations, an infinite-series representation for Φ is obtained as

$$\Phi \overset{(a)}{=} e^{-\frac{C}{\overline{Z}}}$$

$$+ \sum_{j=1}^{N_t}\binom{N_t}{j}\frac{(-1)^j}{\overline{Z}}\left(e^{-j\frac{\tau}{\overline{X}}}\sum_{k=0}^\infty\frac{\left(-\frac{j\tau C}{\overline{X}}\right)^k}{k!}\int_C^\infty z^{-k}e^{-\frac{z}{\overline{Z}}}dz + e^{-j\frac{\tau}{\overline{Y}}}\sum_{k=0}^\infty\frac{\left(-\frac{j\tau C}{\overline{Y}}\right)^k}{k!}\int_C^\infty z^{-k}e^{-\frac{z}{\overline{Z}}}dz\right)$$

$$+ \frac{1}{\overline{Z}}\sum_{j=1}^{N_t}\sum_{m=1}^{N_t}\binom{N_t}{j}(-1)^j\binom{N_t}{m}(-1)^m e^{-\tau\left(\frac{m}{\overline{Y}} + \frac{j}{\overline{X}}\right)}\sum_{k=0}^\infty\frac{\left(-\tau C\left(\frac{m}{\overline{Y}} + \frac{j}{\overline{X}}\right)\right)^k}{k!}\int_C^\infty z^{-k}e^{-\frac{z}{\overline{Z}}}dz$$

$$\overset{(b)}{=} e^{-\frac{C}{\overline{Z}}} + \sum_{j=1}^{N_t}\binom{N_t}{j}(-1)^j\left(e^{-j\frac{\tau}{\overline{X}}}\sum_{k=0}^\infty\frac{\left(-\frac{j\tau C}{\overline{X}}\right)^k}{k!}\frac{\Gamma\left(1-k, \frac{c}{z}\right)}{\overline{Z}^k} + e^{-j\frac{\tau}{\overline{Y}}}\sum_{k=0}^\infty\frac{\left(-\frac{j\tau C}{\overline{Y}}\right)^k}{k!}\frac{\Gamma\left(1-k, \frac{c}{z}\right)}{\overline{Z}^k}\right)$$

$$+ \sum_{j=1}^{N_t}\sum_{m=1}^{N_t}\binom{N_t}{j}(-1)^j\binom{N_t}{m}(-1)^m e^{-\tau\left(\frac{m}{\overline{Y}} + \frac{j}{\overline{X}}\right)}\sum_{k=0}^\infty\frac{\left(-\tau C\left(\frac{m}{\overline{Y}} + \frac{j}{\overline{X}}\right)\right)^k}{k!}\frac{\Gamma\left(1-k, \frac{c}{z}\right)}{\overline{Z}^k}$$

$$= e^{-\frac{C}{\overline{Z}}} + \sum_{k=0}^\infty\sum_{j=1}^{N_t}\binom{N_t}{j}(-1)^j\frac{(-\tau C)^k}{k!}\frac{\Gamma\left(1-k, \frac{c}{z}\right)}{\overline{Z}^k}$$

$$\times\left(e^{-j\tau}j^k\left(\frac{e^{-\frac{1}{\overline{X}}}}{(\overline{X})^k} + \frac{e^{\frac{-1}{\overline{Y}}}}{(\overline{Y})^k}\right) + \sum_{m=1}^{N_t}\binom{N_t}{m}(-1)^m e^{-\tau\left(\frac{m}{\overline{Y}} + \frac{j}{\overline{X}}\right)}\left(\frac{m}{\overline{Y}} + \frac{j}{\overline{X}}\right)^k\right). \tag{C.6}$$

C.3 Infinite-Series Representation for the term Ψ in (3.26)

In this section, we derive an infinite-series representation for the term Ψ defined in (3.26). From its definition,

$$\Psi = \int_C^\infty \frac{1}{\overline{Z}} e^{-\frac{z}{\overline{Z}}} \underbrace{\int_0^{\tau+\frac{C\tau}{z}} N_t \left(1 - e^{-\frac{y}{\overline{Y}}}\right)^{N_t-1} \frac{1}{\overline{Y}} e^{-\frac{y}{\overline{Y}}} \left(1 - e^{-\frac{y}{\overline{X}}}\right)^{N_t} dy}_{\xi}\, dz, \qquad \text{(C.7)}$$

where the term ξ can be solved using the binomial theorem [18, Eq. (3.1.1)] as

$$\xi = \int_0^{\tau+\frac{C\tau}{z}} N_t \sum_{j=0}^{N_t} \binom{N_t}{j} (-1)^j e^{-\frac{jy}{\overline{Y}}} \frac{1}{\overline{Y}} e^{-\frac{y}{\overline{Y}}} \sum_{m=0}^{N_t} \binom{N_t}{m} (-1)^m e^{-\frac{my}{\overline{X}}} dy$$

$$= \sum_{j=0}^{N_t} \sum_{m=0}^{N_t} \binom{N_t}{j} (-1)^j \binom{N_t}{m} (-1)^m \frac{\left(1 - e^{-\tau\left(\frac{(1+j)}{\overline{Y}}+\frac{m}{\overline{X}}\right)} e^{-\frac{\tau C}{z}\left(\frac{(1+j)}{\overline{Y}}+\frac{m}{\overline{X}}\right)}\right) \overline{X}}{m\overline{Y} + (1+j)\overline{X}}. \qquad \text{(C.8)}$$

Substituting (C.8) into (C.7), Ψ is then rewritten as

$$\Psi = \int_C^\infty \frac{1}{\overline{Z}} e^{-\frac{z}{\overline{Z}}} \sum_{j=0}^{N_t} \sum_{m=0}^{N_t} \binom{N_t}{j} (-1)^j \binom{N_t}{m} (-1)^m \frac{\left(1 - e^{-\tau\left(\frac{(1+j)}{\overline{Y}}+\frac{m}{\overline{X}}\right)} e^{-\frac{\tau C}{z}\left(\frac{(1+j)}{\overline{Y}}+\frac{m}{\overline{X}}\right)}\right) \overline{X}}{m\overline{Y} + (1+j)\overline{X}} dz$$

$$= \sum_{j=0}^{N_t} \sum_{m=0}^{N_t} \frac{\binom{N_t}{j}(-1)^j \binom{N_t}{m}(-1)^m \overline{X}}{m\overline{Y} + (1+j)\overline{X}} \int_C^\infty \frac{1}{\overline{Z}} e^{-\frac{z}{\overline{Z}}} - \frac{1}{\overline{Z}} e^{-\tau\left(\frac{(1+j)}{\overline{Y}}+\frac{m}{\overline{X}}\right)} e^{-\frac{z}{\overline{Z}}} e^{-\frac{\tau C}{z}\left(\frac{(1+j)}{\overline{Y}}+\frac{m}{\overline{X}}\right)} dz.$$

$$\text{(C.9)}$$

Finally, using the Maclaurin series for the exponential function in step (a) and [18, Eq. (3.381.9)] in step (b), an infinite-series representation for Ψ is obtained as

$$\Psi \overset{(a)}{=} \sum_{j=0}^{N_t} \sum_{m=0}^{N_t} \frac{\binom{N_t}{j}(-1)^j \binom{N_t}{m}(-1)^m \overline{X}}{m\overline{Y} + (1+j)\overline{X}}$$

$$\times \left(e^{-\frac{C}{\overline{Z}}} - \frac{1}{\overline{Z}} e^{-\tau\left(\frac{(1+j)}{\overline{Y}}+\frac{m}{\overline{X}}\right)} \sum_{k=0}^\infty \frac{\left(-\tau C \left(\frac{(1+j)}{\overline{Y}}+\frac{m}{\overline{X}}\right)\right)^k}{k!} \int_C^\infty e^{-\frac{z}{\overline{Z}}} \frac{1}{z^k} dz\right)$$

$$\overset{(b)}{=} \sum_{j=0}^{N_t} \sum_{m=0}^{N_t} \frac{\binom{N_t}{j}(-1)^j \binom{N_t}{m}(-1)^m \overline{X}}{m\overline{Y} + (1+j)\overline{X}}$$

$$\times \left(e^{-\frac{C}{\overline{Z}}} - e^{-\tau\left(\frac{(1+j)}{\overline{Y}}+\frac{m}{\overline{X}}\right)} \sum_{k=0}^\infty \frac{\left(-\tau C \left(\frac{(1+j)}{\overline{Y}}+\frac{m}{\overline{X}}\right)\right)^k}{k!} \frac{\Gamma\left(1-k, \frac{c}{z}\right)}{\overline{Z}^k}\right). \qquad \text{(C.10)}$$

C.4 Exact Closed-Form Expression for $\Pr\left(X_{\overline{i}} > Y_{\overline{i}}\right)$

In this section, we derive a closed-form expression for $\Pr\left(X_{\overline{i}} > Y_{\overline{i}}\right)$, with the transmit-antenna index $\overline{i}$ being defined by the DAS rule in (3.4). Because this index is chosen so

as to provide $\max_i \left[\max \left[Y_i, X_i \right] \right]$, then the probability of $X_{\bar{i}} > Y_{\bar{i}}$ equals the probability of $\max_i X_i > \max_i Y_i$, that is,

$$\Pr \left(X_{\bar{i}} > Y_{\bar{i}} \right) = \Pr \left(\max_i \left[X_i \right] \triangleq X > \max_i \left[Y_i \right] \triangleq Y \right). \tag{C.11}$$

Knowing that X and Y are independent variates, it follows that

$$\begin{aligned}
\Pr \left(X_{\bar{i}} > Y_{\bar{i}} \right) &= \int_0^\infty \int_y^\infty f_{XY}(x, y) dx dy \\
&= \int_0^\infty \int_y^\infty f_X(x) f_Y(y) dx dy \\
&= \int_0^\infty f_Y(y) \int_y^\infty f_X(x) dx dy \\
&= \int_0^\infty f_Y(y) \left(1 - \int_0^y f_X(x) dx \right) dy \\
&= \int_0^\infty f_Y(y) \left(1 - F_X(y) \right) dy \\
&\overset{(a)}{=} \int_0^\infty N_t \left(1 - e^{-\frac{y}{\overline{Y}}} \right)^{N_t - 1} \frac{1}{\overline{Y}} e^{-\frac{y}{\overline{Y}}} \left(1 - \left(1 - e^{-\frac{y}{\overline{X}}} \right)^{N_t} \right) dy \\
&\overset{(b)}{=} \int_0^\infty N_t \sum_{j=1}^{N_t} \binom{N_t - 1}{j - 1} (-1)^j e^{-\frac{jy}{\overline{Y}}} \frac{1}{\overline{Y}} \sum_{m=1}^{N_t} \binom{N_t}{m} (-1)^m e^{-\frac{my}{\overline{X}}} dy \\
&= N_t \sum_{j=1}^{N_t} \sum_{m=1}^{N_t} \binom{N_t - 1}{j - 1} (-1)^j \binom{N_t}{m} (-1)^m \frac{\overline{X}}{m \overline{Y} + j \overline{X}}, \tag{C.12}
\end{aligned}$$

where in step (a) we used the fact that X and Y are the maximum of N_t i.i.d. exponentially distributed variates, and in step (b) we used the binomial theorem [18, Eq. (3.1.1)].

Appendix D

Supporting Material to Chapter 4

The references cited in this appendix are listed at the end of Chapter 4.

D.1 High-SNR Expression for the Term Φ_0 in (4.23)

Here we consider Φ_n for $n = 0$, which is defined in (4.23) as

$$\Phi_0 = \frac{z^{N_t+1}}{(N_t+1)} \frac{C}{\bar{\gamma}_{RD}} \underbrace{\int_0^1 u^{-1} e^{-\frac{iz}{u\bar{\gamma}_{SR}}} e^{-\frac{jCu}{\bar{\gamma}_{RD}}} du}_{\rho_0} . \tag{D.1}$$

The term ρ_0 can be rewritten through the help of [6, Eq. (3.471.9)], [6, Eq. (1.211.1)], and [6, Eq. (8.446)] as

$$\begin{aligned}
\rho_0 =& 2K_0\left(2\sqrt{\frac{jCiz}{\bar{\gamma}_{SR}\bar{\gamma}_{RD}}}\right) - \int_1^\infty u^{-1} e^{-\frac{jCu}{\bar{\gamma}_{RD}}} \sum_{l=0}^\infty \frac{\left(-\frac{iz}{u\bar{\gamma}_{SR}}\right)^l}{l!} du \\
=& -\ln\frac{jCiz}{\bar{\gamma}_{SR}\bar{\gamma}_{RD}} \sum_{k_1=0}^\infty \frac{\left(\sqrt{\frac{jCiz}{\bar{\gamma}_{SR}\bar{\gamma}_{RD}}}\right)^{2k_1}}{k_1!^2} + \sum_{k_2=0}^\infty \frac{\left(\sqrt{\frac{jCiz}{\bar{\gamma}_{SR}\bar{\gamma}_{RD}}}\right)^{2k_2}}{k_2!^2} \\
& \times 2\psi(k_2+1) - \sum_{l=0}^\infty \frac{\left(-\frac{iz}{\bar{\gamma}_{SR}}\right)^l}{l!} \left(\frac{jC}{\bar{\gamma}_{RD}}\right)^l \Gamma\left(-l, \frac{jC}{\bar{\gamma}_{RD}}\right),
\end{aligned} \tag{D.2}$$

in which $K_n(\cdot)$ denotes the nth-order modified Bessel function of the second kind [6, Eq.(8.446)], $\psi(\cdot)$ represents the Euler psi function [6, Eq.(8.360)] and $\Gamma(\cdot)$ is the gamma function [6, Eq.(8.310.1)]. It is important to mention that in order to conduct the high-SNR analysis of the inner expression that defines Φ_0 in (4.23), the outer summations in i and j must be considered. To this end, we define the variable λ_0 as

$$\lambda_0 = \sum_{i=1}^{N_{rr}} \binom{N_{rr}-1}{i-1} (-1)^{i-1} \sum_{j=1}^{N_{rt}} \binom{N_{rt}-1}{j-1} \times (-1)^{j-1} \Phi_0. \tag{D.3}$$

Plugging (D.2) into (D.1) and this into (D.3), λ_0 can be rewritten as

$$
\begin{aligned}
\lambda_0 =& \frac{z^{N_t+1}}{(N_t+1)} \frac{C}{\bar{\gamma}_{RD}} \left(-\sum_{k_1=0}^{\infty} \frac{\left(\frac{Cz}{\bar{\gamma}_{SR}\bar{\gamma}_{RD}}\right)^{k_1}}{k_1!^2} \sum_{i=1}^{N_{rr}} \binom{N_{rr}-1}{i-1} i^{k_1} \right. \\
&\times (-1)^{i-1} \sum_{j=1}^{N_{rt}} \binom{N_{rt}-1}{j-1} (-1)^{j-1} j^{k_1} \left(\ln\left(\frac{j}{\bar{\gamma}_{RD}}\right) + \ln(iz) \right) \\
&+ \sum_{k_2=0}^{\infty} \frac{\left(\frac{Cz}{\bar{\gamma}_{SR}\bar{\gamma}_{RD}}\right)^{k_2}}{k_2!^2} \psi(k_2+1) \sum_{i=1}^{N_{rr}} \binom{N_{rr}-1}{i-1} (-1)^{i-1} i^{k_2} \\
&\times \sum_{j=1}^{N_{rt}} \binom{N_{rt}-1}{j-1} (-1)^{j-1} j^{k_2} - \sum_{l=0}^{\infty} \frac{\left(\frac{-Cz}{\bar{\gamma}_{SR}\bar{\gamma}_{RD}}\right)^{l}}{l!^2} \sum_{i=1}^{N_{rr}} \binom{N_{rr}-1}{i-1} \\
&\times \left. (-1)^{i-1} i^l \sum_{j=1}^{N_{rt}} \binom{N_{rt}-1}{j-1} (-1)^{j-1} j^l \Gamma\left(-l, \frac{jC}{\bar{\gamma}_{RD}}\right) \right).
\end{aligned}
\tag{D.4}
$$

Observe that λ_0 is composed by the sum of three terms, corresponding to the summations in k_1, k_2, and l. Using the fact that $\sum_{a=1}^{b} \binom{b-1}{a-1} (-1)^{a-1} a^c$ is null for $c = 0, 1, 2, \ldots, b-2$, after a careful inspection it was attested that each term presents a different behavior at high-SNR regime, and this will be described next. The first term is non-null for values of k_1 greater than $\min(N_{rr}, N_{rt}) - 1$, the second term is non-null for values of k_2 greater than $\max(N_{rr}, N_{rt}) - 1$, and the third term is non-null for values of l greater than $N_{rr} - 1$. Using this and preserving only the lowest-order terms so as to derive a high-SNR expression, we arrive at three cases: (i) if $N_{rr} = N_{rt}$, the three terms must be considered; (ii) if $N_{rr} < N_{rt}$, the first and third terms must be considered; and (iii) if $N_{rr} > N_{rt}$, only the first term must be considered. In all the cases, the diversity order of λ_0 is observed to be given by $n_1 \triangleq \min(N_{rr}, N_{rt}) - 1$. By incorporating these results into the definition of Φ_0 given by (D.1) and (D.2), we finally arrive at the high-SNR expression for Φ_0 as given in (4.24).

D.2 High-SNR Expression for the Term Φ_n in (4.23), $n > 0$

We now consider Φ_n for $n > 0$, which is defined in (4.23) as

$$
\Phi_n = \frac{z^{N_t+n+1}}{n! \, (N_t+n+1)} \underbrace{\bar{\gamma}_{SR}^{-n} i^n \int_0^1 \frac{C}{\bar{\gamma}_{RD}} u^{-n-1} e^{-\frac{iz}{u\bar{\gamma}_{SR}}} e^{-\frac{jCu}{\bar{\gamma}_{RD}}} du}_{\rho_n}.
\tag{D.5}
$$

The term ρ_n can be rewritten as

$$
\rho_n \overset{(a)}{=} 2\bar{\gamma}_{SR}^{-\frac{n}{2}} \left(\frac{iz\bar{\gamma}_{RD}}{jC}\right)^{-\frac{n}{2}} K_n\left(2\sqrt{\frac{jCiz}{\bar{\gamma}_{SR}\bar{\gamma}_{RD}}}\right) - \sum_{l=0}^{\infty} \frac{\bar{\gamma}_{SR}^{-n}\left(-\frac{iz}{\bar{\gamma}_{SR}}\right)^l}{l!} \int_1^{\infty} u^{-n-l-1} e^{-\frac{jCu}{\bar{\gamma}_{RD}}}\, du
$$

$$
\overset{(b)}{=} 2\bar{\gamma}_{SR}^{-\frac{n}{2}} \left(\frac{iz\bar{\gamma}_{RD}}{jC}\right)^{\frac{-n}{2}} \sum_{m_1=0}^{n-1} \frac{(-1)^{m_1}(n-m_1-1)}{m_1!} \left(\frac{jCiz}{\bar{\gamma}_{SR}\bar{\gamma}_{RD}}\right)^{m_1-\frac{n}{2}} + 2\bar{\gamma}_{SR}^{-n}\left(\frac{iz\bar{\gamma}_{RD}}{jC}\right)^{-\frac{n}{2}}
$$

$$
\times (-1)^{n+1} \sum_{m_2=0}^{\infty} \frac{\sqrt{\frac{jCiz}{\bar{\gamma}_{SR}\bar{\gamma}_{RD}}}^{\,n+2m_2}}{m!(n+m_2)!} \left(\ln\sqrt{\frac{jCiz}{\bar{\gamma}_{SR}\bar{\gamma}_{RD}}} - \frac{1}{2}\psi(m_2+1) - \frac{1}{2}\psi(n+m_2+1)\right)
$$

$$
- \sum_{l=0}^{\infty} \frac{\bar{\gamma}_{SR}^{-l-n}(iz)^l}{l!} \left(\frac{jC}{\bar{\gamma}_{RD}}\right)^l \Gamma\left(-n-l, \frac{jC}{\bar{\gamma}_{RD}}\right)
$$

$$
= \sum_{m_1=0}^{n-1} (-1)^{m_1} \frac{(n-m_1-1)}{m_1!} z^{m_1-n} \bar{\gamma}_{SR}^{-m_1} i^{m_1} \left(\frac{jC}{\bar{\gamma}_{RD}}\right)^{m_1} + 2\sum_{m_2=0}^{\infty} \frac{z^{m_2}}{m_2!(n+m_2)!} \left(\frac{jC}{\bar{\gamma}_{RD}}\right)^{m_2+n}
$$

$$
\times \left(\frac{i}{\bar{\gamma}_{SR}}\right)^{n+m_2} \left(\ln\sqrt{\frac{jCiz}{\bar{\gamma}_{SR}\bar{\gamma}_{RD}}} - \frac{1}{2}\psi(m_2+1) - \frac{1}{2}\psi(n+m_2+1)\right)
$$

$$
- \sum_{l=0}^{\infty} \frac{\bar{\gamma}_{SR}^{-l-n} i^{n+l} z^l}{l!} \left(\frac{jC}{\bar{\gamma}_{RD}}\right)^{l+n} \Gamma\left(-n-l, \frac{jC}{\bar{\gamma}_{RD}}\right), \tag{D.6}
$$

in which we have used [6, Eq. (3.471.9)] and [6, Eqs. (8.446) and (3.381.3)] in steps (a) and (b), respectively. The analysis that follows is similar to that in App. D.1. To this end, we define the variable λ_n as

$$
\lambda_n = \sum_{i=1}^{N_{rr}} \binom{N_{rr}-1}{i-1} (-1)^{i-1} \sum_{j=1}^{N_{rt}} \binom{N_{rt}-1}{j-1} (-1)^{j-1} \Phi_n. \tag{D.7}
$$

Plugging (D.6) into (D.5) and this into (D.7), λ_n can be rewritten as

$$
\lambda_n = \frac{z^{N_t+n+1}}{n!\,(N_t+n+1)} \frac{C}{\bar{\gamma}_{RD}} \left(\sum_{m_1=0}^{n-1} (-1)^{m_1} \frac{(n-m_1-1)}{m_1!} \frac{z^{m_1}}{\bar{\gamma}_{SR}^{m_1}} \left(\frac{C}{\bar{\gamma}_{RD}}\right)^{m_1}\right.
$$

$$
\times \sum_{j=1}^{N_{rt}} \binom{N_{rt}-1}{j-1} (-1)^{j-1} j^{m_1} \sum_{i=1}^{N_{rr}} \binom{N_{rr}-1}{i-1} (-1)^{i-1} i^{m_1}
$$

$$
+ 2\sum_{m_2=0}^{\infty} \frac{\left(\frac{C}{\bar{\gamma}_{RD}}\right)^{n+m_2}\left(\frac{i}{\bar{\gamma}_{SR}}\right)^{n+m_2}}{m_2!(n+m_2)!} \sum_{j=1}^{N_{rt}} \binom{N_{rt}-1}{j-1} (-1)^{j-1} j^{n+m}
$$

$$
\times \sum_{i=1}^{N_{rr}} \binom{N_{rr}-1}{i-1} (-1)^{i-1} i^{n+m_2} \left(\ln\sqrt{\frac{jCiz}{\bar{\gamma}_{SR}\bar{\gamma}_{RD}}} - \frac{1}{2}\psi(m_2+1) - \frac{1}{2}\psi(n+m_2+1)\right)
$$

$$
- \sum_{l=0}^{\infty} \frac{\bar{\gamma}_{SR}^{-l-n}(-z)^l}{l!} \left(\frac{C}{\bar{\gamma}_{RD}}\right)^l \sum_{j=1}^{N_{rt}} \binom{N_{rt}-1}{j-1} (-1)^{j-1} j^{n+l}
$$

$$
\left.\times \sum_{i=1}^{N_{rr}} \binom{N_{rr}-1}{i-1} (-1)^{i-1} i^{n+l} \Gamma\left(-n-l, \frac{jC}{\bar{\gamma}_{RD}}\right)\right). \tag{D.8}
$$

Observe that, similarly to λ_0, λ_n is composed by the sum of three terms, corresponding to the summations in m_1, m_2, and l. The first term is non-null for values of m_1 greater than $\max(N_{rr}, N_{rt}) - 1$; the second term is non-null for values of m_2 greater than $\min(N_{rr}, N_{rt}) - 1$; and the third term is non-null for values of l greater than $N_{rr} - 1$. Using this and preserving only the lowest-order terms so as to derive a high-SNR expression, we arrive at three cases: (a) if $N_{rr} = N_{rt}$, the three terms must be considered; (b) if $N_{rr} < N_{rt}$, the second and third terms must be considered; and (c) if $N_{rr} > N_{rt}$, only the second term must be considered. In all the cases, the diversity order of λ_n is observed to be given by $n_1 \triangleq \min(N_{rr}, N_{rt}) - 1$. By incorporating these results into the definition of Φ_n given by (D.5) and (D.6), we finally arrive at the high-SNR expression for Φ_n as given in (4.25) and (4.26).

Appendix E

Supporting Material to Chapter 5

The references cited in this appendix are listed at the end of Chapter 5.

E.1 Proof of Corollary 1

By replacing the right-hand side inequality of (5.13) into (5.11), the lower bound I_1^{LB} for I_1 can be derived as

$$
\begin{aligned}
I_1 &> \Pr\left(\gamma_{R_{j*}D} \geq C, \gamma_{S_{\bar{i}}D} + \gamma_{S_{\bar{i}}R_{k*}} \min\left[\frac{\gamma_{R_{j*}D}}{C}, 1\right] < z\right) \\
&\overset{(a)}{=} \Pr\left(\gamma_{R_{j*}D} \geq C, \max_i\{\gamma_{S_iD} + \max_k\{\gamma_{S_iR_k}\}\} < z\right) \triangleq I_1^{\mathrm{LB}} \\
&= \Pr\left(\gamma_{R_{j*}D} \geq C\right) \Pr\left(\gamma_{S_iD} + \max_k\{\gamma_{S_iR_k}\} < z\right)^{N_t},
\end{aligned}
\tag{E.1}
$$

where in step (a) we have used (5.9) and the DAS rule given in (5.7) for $\gamma_{R_{j*}D} \geq C$. Then, using (5.6) into (E.1), (5.14) is obtained.

E.2 Proof of Corollary 2

By replacing the right-hand side inequality of (5.13) into (5.12), the lower bound I_2^{LB} for I_2 can be derived as

$$
\begin{aligned}
I_2 &> \Pr\left(\gamma_{R_{j*}D} < C, \gamma_{S_{\bar{i}}D} + \gamma_{S_{\bar{i}}R_{k*}} \min\left[\frac{\gamma_{R_{j*}D}}{C}, 1\right] < z\right) \\
&= \Pr\left(\gamma_{R_{j*}D} < C, \gamma_{S_{\bar{i}}D} + \frac{\gamma_{S_{\bar{i}}R_{k*}}\gamma_{R_{j*}D}}{C} < z\right) \triangleq I_2^{\mathrm{LB}} \\
&= \Pr\left(\gamma_{R_{j*}D} < C, \max_m\{\gamma_{S_mD}\} + \max_k\{\gamma_{S_iR_k}\}\frac{\gamma_{R_{j*}D}}{C} < z\right),
\end{aligned}
\tag{E.2}
$$

where we have used the DAS rule given in (5.7) for $\gamma_{R_{j*}D} < C$. Then, using (5.6) into (E.2), (5.15) is obtained.

E.3 Proof of Theorem 1

The general expression for I_1^{LB} in (5.14) can be specialized to the Rayleigh-fading scenario by using the corresponding PDFs and CDFs, as well as some principles of probability

theory, as follows:

$$
\begin{aligned}
I_1^{\mathrm{LB}} &= \Pr\left(\max_j\{\gamma_{R_jD}\} \geq C\right) \Pr\left(\gamma_{S_iD} + \max_k\{\gamma_{S_iR_k}\} < z\right)^{N_t} \\
&= \Pr\left(\max_j\{\gamma_{R_jD}\} \geq C\right) \left(\int_0^z f_{\gamma_{SD}}(x) \Pr\left(x + \max_k\{\gamma_{S_iR_k}\} < z\right) dx\right)^{N_t} \\
&= \Pr\left(\max_j\{\gamma_{R_jD}\} \geq C\right) \left(\underbrace{\int_0^z \frac{1}{\bar{\gamma}_{SD}} e^{-\frac{x}{\bar{\gamma}_{SD}}} \left(1 - e^{-\frac{z-x}{\bar{\gamma}_{SR}}}\right)^{N_{rr}} dx}_{\alpha}\right)^{N_t}.
\end{aligned} \tag{E.3}
$$

The term α can be rewritten using the binomial theorem [21, Eq. (1.111)] as

$$
\begin{aligned}
\alpha &= \int_0^z \frac{1}{\bar{\gamma}_{SD}} e^{-\frac{x}{\bar{\gamma}_{SD}}} \sum_{j=0}^{N_{rr}} \binom{N_{rr}}{j} (-1)^j e^{-j\frac{z-x}{\bar{\gamma}_{SR}}} dx \\
&= \sum_{j=0}^{N_{rr}} \binom{N_{rr}}{j} (-1)^j e^{-j\frac{z}{\bar{\gamma}_{SR}}} \frac{1}{\bar{\gamma}_{SD}} \int_0^z e^{j\frac{x}{\bar{\gamma}_{SR}} - \frac{x}{\bar{\gamma}_{SD}}} dx \\
&= \sum_{j=0}^{N_{rr}} \binom{N_{rr}}{j} (-1)^j e^{-j\frac{z}{\bar{\gamma}_{SR}}} \left(\frac{\left(1 - e^{-\frac{z}{\bar{\gamma}_{SD}} + \frac{jz}{\bar{\gamma}_{SR}}}\right) \bar{\gamma}_{SR}}{j\bar{\gamma}_{SD} - \bar{\gamma}_{SR}}\right).
\end{aligned} \tag{E.4}
$$

Finally, using (E.4) into (E.3), a lower bound for I_1 can be derived in closed form as in (5.16).

E.4 Proof of Theorem 2

The general expression for I_2^{LB} in (5.15) can be specialized to the Rayleigh-fading scenario by using the corresponding PDFs and CDFs, as well as some principles of probability theory, as follows:

$$
\begin{aligned}
I_2^{\mathrm{LB}} &= \int_0^C f_{\gamma_{RD}}(x) \Pr\left(\max_m\{\gamma_{S_mD}\} + \max_k\{\gamma_{S_iR_k}\}\frac{x}{C} < z\right) dx \\
&= \int_0^1 C f_{\gamma_{RD}}(Cu) \Pr\left(\max_m\{\gamma_{S_mD}\} + \max_k\{\gamma_{S_iR_k}\}u < z\right) du \\
&= \int_0^1 C f_{\gamma_{RD}}(Cu) \int_0^z f_{\gamma_{SR}}(y) \Pr\left(\max_m\{\gamma_{S_mD}\} + yu < z\right) dy\, du \\
&= \int_0^1 C f_{\gamma_{RD}}(Cu) \int_0^z \frac{1}{u} f_{\gamma_{SR}}\left(\frac{v}{u}\right) \Pr\left(\max_m\{\gamma_{S_mD}\} < z - v\right) dv\, du \\
&= \int_0^1 \frac{C N_{rt}}{\bar{\gamma}_{RD}} e^{-\frac{Cu}{\bar{\gamma}_{RD}}} \left(1 - e^{-\frac{Cu}{\bar{\gamma}_{RD}}}\right)^{N_{rt}-1} \frac{N_{rr}}{u\bar{\gamma}_{SR}} \\
&\quad \times \underbrace{\int_0^z e^{-\frac{v}{u\bar{\gamma}_{SR}}} \left(1 - e^{-\frac{v}{u\bar{\gamma}_{SR}}}\right)^{N_{rr}-1} \left(1 - e^{-\frac{z-v}{\bar{\gamma}_{SD}}}\right)^{N_t} dv}_{\varphi}\, du,
\end{aligned} \tag{E.5}
$$

where the term φ can be calculated using the binomial theorem [21, Eq. (1.111)] as

$$\varphi = \sum_{m=0}^{N_t} \sum_{j=0}^{N_{rr}} \binom{N_t}{m} \binom{N_{rr}-1}{j} (-1)^m (-1)^j \frac{\left(e^{-\frac{(1+j)z}{u\bar{\gamma}_{SR}}} - e^{-\frac{mz}{\bar{\gamma}_{SD}}}\right) u\bar{\gamma}_{SR}\bar{\gamma}_{SD}}{mu\bar{\gamma}_{SR} - (1+j)\bar{\gamma}_{SD}}. \tag{E.6}$$

Finally, by substituting (E.6) into (E.5), a lower bound for I_2 can be derived in single-fold integral form as in (5.17).

E.5 Proof of Corollary 3

In order to obtain an asymptotic lower bound $\tilde{I}_1^{\text{LB}}$ for I_1, a high-SNR expression for the term α in (E.3) can be derived from its definition as

$$\alpha = \int_0^z \frac{1}{\bar{\gamma}_{SD}} e^{-\frac{z-y}{\bar{\gamma}_{SD}}} \left(1 - e^{-\frac{y}{\bar{\gamma}_{SR}}}\right)^{N_{rr}} dy \simeq \left(\frac{1}{\bar{\gamma}_{SR}}\right)^{N_{rr}} \frac{1}{\bar{\gamma}_{SD}} \frac{z^{N_{rr}+1}}{(N_{rr}+1)}, \tag{E.7}$$

where the MacLaurin series of exponential functions [21, Eq. (1.211.1)] has been used. By using (E.7) into (E.3), $\tilde{I}_1^{\text{LB}}$ is then obtained as in (5.18).

E.6 Proof of Corollary 4

In order to obtain an asymptotic lower bound $\tilde{I}_2^{\text{LB}}$ for I_2, we rewrite the term φ defined in (E.5) by using the binomial theorem [21, Eq. (1.111)] and the MacLaurin series of exponential functions, obtaining

$$\begin{aligned} \varphi &= \sum_{i=1}^{N_{rr}} \binom{N_{rr}-1}{i-1} (-1)^{i-1} \int_0^z e^{-\frac{iv}{u\bar{\gamma}_{SR}}} \left(\frac{z-v}{\bar{\gamma}_{SD}}\right)^{N_t} dv \\ &= \sum_{i=1}^{N_{rr}} \binom{N_{rr}-1}{i-1} (-1)^{i-1} e^{-\frac{iz}{u\bar{\gamma}_{SR}}} \left(\frac{1}{\bar{\gamma}_{SD}}\right)^{N_t} \sum_{n=0}^{\infty} \left(\frac{i}{u\bar{\gamma}_{SR}}\right)^n \frac{z^{N_t+n+1}}{n!\,(N_t+n+1)}. \end{aligned} \tag{E.8}$$

By substituting (E.8) into (E.5) and using again the binomial theorem, I_2^{LB} can be also rewritten as

$$\begin{aligned} I_2^{\text{LB}} = {} & N_{rt} \frac{N_{rr}}{\bar{\gamma}_{SR}} \left(\frac{1}{\bar{\gamma}_{SD}}\right)^{N_t} \sum_{i=1}^{N_{rr}} \binom{N_{rr}-1}{i-1} (-1)^{i-1} \\ & \times \sum_{j=0}^{N_{rt}} \binom{N_{rt}-1}{j-1} (-1)^{j-1} \sum_{n=0}^{\infty} \frac{z^{N_t+n+1} i^n \bar{\gamma}_{SR}^{-n}}{n!\,(N_t+n+1)} \underbrace{\int_0^1 \frac{C}{\bar{\gamma}_{RD}} u^{-n-1} e^{-\frac{iz}{u\bar{\gamma}_{SR}}} e^{-\frac{jCu}{\bar{\gamma}_{RD}}} du}_{\Phi_n}. \end{aligned} \tag{E.9}$$

Next, with the purpose of characterizing the behavior of Φ_n in the high-SNR regime, we address the cases $n=0$ and $n>0$ in Appendices E.6.1 and E.6.2, separately.

E.6.1 High-SNR Expression for the Term Φ_0 in (E.9)

Here we consider Φ_n for $n = 0$, which is defined in (E.9) as

$$\Phi_0 = \frac{z^{N_t+1}}{(N_t+1)}\frac{C}{\bar{\gamma}_{RD}}\underbrace{\int_0^1 u^{-1}e^{-\frac{iz}{u\bar{\gamma}_{SR}}}e^{-\frac{jCu}{\bar{\gamma}_{RD}}}du}_{\rho_0}.$$
(E.10)

The term ρ_0 can be rewritten with use of [21, Eqs. (3.471.9), (1.211.1), and (8.446)] as

$$\rho_0 = 2K_0\left(2\sqrt{\frac{jCiz}{\bar{\gamma}_{SR}\bar{\gamma}_{RD}}}\right) - \int_1^\infty u^{-1}e^{-\frac{jCu}{\bar{\gamma}_{RD}}}\sum_{l=0}^\infty \frac{\left(-\frac{iz}{u\bar{\gamma}_{SR}}\right)^l}{l!}du$$

$$= -\ln\frac{jCiz}{\bar{\gamma}_{SR}\bar{\gamma}_{RD}}\sum_{k_1=0}^\infty \frac{\left(\sqrt{\frac{jCiz}{\bar{\gamma}_{SR}\bar{\gamma}_{RD}}}\right)^{2k_1}}{k_1!^2} + \sum_{k_2=0}^\infty \frac{\left(\sqrt{\frac{jCiz}{\bar{\gamma}_{SR}\bar{\gamma}_{RD}}}\right)^{2k_2}}{k_2!^2}$$

$$\times 2\psi(k_2+1) - \sum_{l=0}^\infty \frac{\left(-\frac{iz}{\bar{\gamma}_{SR}}\right)^l}{l!}\left(\frac{jC}{\bar{\gamma}_{RD}}\right)^l \Gamma\left(-l, \frac{jC}{\bar{\gamma}_{RD}}\right),$$
(E.11)

in which $K_n(\cdot)$ denotes the nth-order modified Bessel function of the second kind [21, Eq.(8.446)] and $\Gamma(\cdot)$ is the gamma function [21, Eq. 8.310.1]. It is noteworthy that the high-SNR analysis of Φ_0 cannot be performed from its definition alone in (E.10). Instead, the term must considered in the whole context of the outer summations over i and j that appear in (E.9). To this end, we define an auxiliary variable λ_0 as

$$\lambda_0 \triangleq \sum_{i=1}^{N_{rr}}\binom{N_{rr}-1}{i-1}(-1)^{i-1}\sum_{j=1}^{N_{rt}}\binom{N_{rt}-1}{j-1}\times(-1)^{j-1}\Phi_0.$$
(E.12)

Plugging (E.11) into (E.10) and this into (E.12), λ_0 can be rewritten as

$$\lambda_0 = \frac{z^{N_t+1}}{(N_t+1)}\frac{C}{\bar{\gamma}_{RD}}$$

$$\times\left(-\sum_{k_1=0}^\infty \frac{\left(\frac{Cz}{\bar{\gamma}_{SR}\bar{\gamma}_{RD}}\right)^{k_1}}{k_1!^2}\sum_{i=1}^{N_{rr}}\binom{N_{rr}-1}{i-1}i^{k_1}(-1)^{i-1}\sum_{j=1}^{N_{rt}}\binom{N_{rt}-1}{j-1}(-1)^{j-1}j^{k_1}\ln\left(\frac{jiz}{\bar{\gamma}_{RD}}\right)\right.$$

$$+\sum_{k_2=0}^\infty \frac{\left(\frac{Cz}{\bar{\gamma}_{SR}\bar{\gamma}_{RD}}\right)^{k_2}}{k_2!^2}\psi(k_2+1)\sum_{i=1}^{N_{rr}}\binom{N_{rr}-1}{i-1}(-1)^{i-1}i^{k_2}\sum_{j=1}^{N_{rt}}\binom{N_{rt}-1}{j-1}(-1)^{j-1}j^{k_2}$$

$$\left.-\sum_{l=0}^\infty \frac{\left(\frac{-Cz}{\bar{\gamma}_{SR}\bar{\gamma}_{RD}}\right)^l}{l!^2}\sum_{i=1}^{N_{rr}}\binom{N_{rr}-1}{i-1}(-1)^{i-1}i^l\sum_{j=1}^{N_{rt}}\binom{N_{rt}-1}{j-1}(-1)^{j-1}j^l\Gamma\left(-l,\frac{jC}{\bar{\gamma}_{RD}}\right)\right).$$
(E.13)

Observe that λ_0 is composed by three outer summations, over k_1, k_2, and l. Each of these summations contains two inner summations, over i and j, some of which are of the

form $\sum_{a=1}^{b} \binom{b-1}{a-1} (-1)^{a-1} a^c$, $c \in \{k_1, k_2, l\}$. Such a sum has a very interesting property: it is null for $c = 0, 1, 2, \ldots, b-2$. Indeed, this is a reformulated version of a known property of Stirling numbers of the second kind [22, pp. 824–825]. For brevity, we shall omit further details here. Now, applying this property, one can verify that the first nonzero term of the summation over k_1 occurs for $k_1 = \min(N_{rr}, N_{rt}) - 1$, the first nonzero term of the summation over k_2 occurs for $k_2 = \max(N_{rr}, N_{rt}) - 1$, and the first nonzero term of the summation over l occurs for $l = N_{rr} - 1$.

Using this and preserving only the lowest-order terms so as to derive a high-SNR expression, we arrive at three cases: (i) if $N_{rr} = N_{rt}$, all three summations must be considered; (ii) if $N_{rr} < N_{rt}$, only the summations over k_1 and l must be considered; and (iii) if $N_{rr} > N_{rt}$, only the first term the summation over k_1 must be considered. In all the cases, the diversity order of λ_0 is observed to be given by $\min(N_{rr}, N_{rt}) - 1$. By incorporating these results into the definition of Φ_0 given by (E.10) and (E.11), we finally arrive at the high-SNR expression $\tilde{\Phi}_0$ for Φ_0 as given in (5.20).

E.6.2 High-SNR Expression for the Term Φ_n in (E.9), $n > 0$

We now consider Φ_n for $n > 0$, which is defined in (E.9) as

$$\Phi_n = \frac{z^{N_t + n + 1}}{n! \, (N_t + n + 1)} \underbrace{\bar{\gamma}_{SR}^{-n} i^n \int_0^1 \frac{C}{\bar{\gamma}_{RD}} u^{-n-1} e^{-\frac{iz}{u\bar{\gamma}_{SR}}} e^{-\frac{jCu}{\bar{\gamma}_{RD}}} du}_{\rho_n} \, . \tag{E.14}$$

The term ρ_n can be rewritten as

$$\rho_n \overset{(a)}{=} 2\bar{\gamma}_{SR}^{-\frac{n}{2}} \left(\frac{iz\bar{\gamma}_{RD}}{jC}\right)^{-\frac{n}{2}} K_n \left(2\sqrt{\frac{jCiz}{\bar{\gamma}_{SR}\bar{\gamma}_{RD}}}\right) - \sum_{l=0}^{\infty} \frac{\bar{\gamma}_{SR}^{-n} \left(-\frac{iz}{\bar{\gamma}_{SR}}\right)^l}{l!} \int_1^{\infty} u^{-n-l-1} e^{-\frac{jCu}{\bar{\gamma}_{RD}}} du$$

$$\overset{(b)}{=} 2\bar{\gamma}_{SR}^{-n} \left(\frac{iz\bar{\gamma}_{RD}}{jC}\right)^{-\frac{n}{2}} (-1)^{n+1} \sum_{k_1=0}^{\infty} \frac{\sqrt{\frac{jCiz}{\bar{\gamma}_{SR}\bar{\gamma}_{RD}}}^{n+2k_1}}{k_1!(n+k_1)!} \left(\ln\sqrt{\frac{jCiz}{\bar{\gamma}_{SR}\bar{\gamma}_{RD}}} - \frac{1}{2}\psi(k_1+1) \right.$$

$$\left. - \frac{1}{2}\psi(n+k_1+1) \right) + 2\bar{\gamma}_{SR}^{-\frac{n}{2}} \left(\frac{iz\bar{\gamma}_{RD}}{jC}\right)^{\frac{-n}{2}} \sum_{k_2=0}^{n-1} \frac{(-1)^{k_2}(n-k_2-1)}{k_2!} \left(\frac{jCiz}{\bar{\gamma}_{SR}\bar{\gamma}_{RD}}\right)^{k_2-\frac{n}{2}}$$

$$- \sum_{l=0}^{\infty} \frac{\bar{\gamma}_{SR}^{-l-n}(iz)^l}{l!} \left(\frac{jC}{\bar{\gamma}_{RD}}\right)^l \Gamma\left(-n-l, \frac{jC}{\bar{\gamma}_{RD}}\right)$$

$$= 2\sum_{k_1=0}^{\infty} \frac{z^{k_1}}{k_1!(n+k_1)!} \left(\frac{jCi}{\bar{\gamma}_{RD}\bar{\gamma}_{SR}}\right)^{k_1+n} \left(\ln\sqrt{\frac{jCiz}{\bar{\gamma}_{SR}\bar{\gamma}_{RD}}} - \frac{1}{2}\psi(k_1+1) - \frac{1}{2}\psi(n+k_1+1) \right)$$

$$+ \sum_{k_2=0}^{n-1} (-1)^{k_2} \frac{(n-k_2-1)}{k_2! z^n} \left(\frac{jCiz}{\bar{\gamma}_{RD}\bar{\gamma}_{SR}}\right)^{k_2} - \sum_{l=0}^{\infty} \frac{z^l}{l!} \left(\frac{jCi}{\bar{\gamma}_{RD}\bar{\gamma}_{SR}}\right)^{l+n} \Gamma\left(-n-l, \frac{jC}{\bar{\gamma}_{RD}}\right), \tag{E.15}$$

in which we have used [21, Eq. (3.471.9)] and [21, Eqs. (8.446) and (3.381.3)] in steps (a) and (b), respectively. The analysis that follows is similar to that in Appendix E.6.1. To

this end, we define the auxiliary variable λ_n as

$$\lambda_n \triangleq \sum_{i=1}^{N_{rr}} \binom{N_{rr}-1}{i-1} (-1)^{i-1} \sum_{j=1}^{N_{rt}} \binom{N_{rt}-1}{j-1} (-1)^{j-1} \Phi_n. \tag{E.16}$$

Plugging (E.15) into (E.14) and this into (E.16), λ_n can be rewritten as

$$
\begin{aligned}
\lambda_n = {} & \frac{Cz^{N_t+n+1}}{n!\,(N_t+n+1)\,\bar{\gamma}_{RD}} \Bigg(2 \sum_{k_1=0}^{\infty} \frac{\left(\frac{C}{\bar{\gamma}_{RD}\bar{\gamma}_{SR}}\right)^{n+k_1}}{k_1!(n+k_1)!} \sum_{j=1}^{N_{rt}} \binom{N_{rt}-1}{j-1} (-1)^{j-1} j^{n+k_1} \\
& \times \sum_{i=1}^{N_{rr}} \binom{N_{rr}-1}{i-1} (-1)^{i-1} i^{n+k_1} \left(\ln\sqrt{\frac{jCiz}{\bar{\gamma}_{SR}\bar{\gamma}_{RD}}} - \frac{1}{2}\psi(k_1+1) - \frac{1}{2}\psi(n+k_1+1) \right) \\
& - \sum_{k_2=0}^{n-1} (-1)^{k_2} \frac{(n-k_2-1)}{k_2!} \left(\frac{Cz}{\bar{\gamma}_{RD}\bar{\gamma}_{SR}}\right)^{k_2} \sum_{j=1}^{N_{rt}} \binom{N_{rt}-1}{j-1} (-1)^{j-1} j^{k_2} \sum_{i=1}^{N_{rr}} \binom{N_{rr}-1}{i-1} (-1)^{i-1} i^{k_2} \\
& - \sum_{l=0}^{\infty} \frac{\bar{\gamma}_{SR}^{-l-n}}{l!} \left(-\frac{Cz}{\bar{\gamma}_{RD}}\right)^l \sum_{j=1}^{N_{rt}} \binom{N_{rt}-1}{j-1} (-1)^{j-1} j^{n+l} \sum_{i=1}^{N_{rr}} \binom{N_{rr}-1}{i-1} (-1)^{i-1} i^{n+l} \Gamma\left(-n-l, \frac{jC}{\bar{\gamma}_{RD}}\right).
\end{aligned}
\tag{E.17}
$$

Observe that, similarly to λ_0, λ_n is composed by three outer summations, over k_1, k_2, and l. Following the same rationale presented for λ_0, one can verify that the first nonzero term of the summation over k_1 occurs for $k_1 = \min(N_{rr}, N_{rt}) - 1$, the first nonzero term of the summation over k_2 occurs for $k_2 = \max(N_{rr}, N_{rt}) - 1$, and the first nonzero term of the summation over l occurs for $l = N_{rr} - 1$. Using this and preserving only the lowest-order terms so as to derive a high-SNR expression, we arrive at three cases: (a) if $N_{rr} = N_{rt}$, all three summations must be considered; (b) if $N_{rr} < N_{rt}$, only the summations over k_1 and l must be considered; and (c) if $N_{rr} > N_{rt}$, only the summation over k_1 must be considered. In all the cases, the diversity order of λ_n is observed to be given by $\min(N_{rr}, N_{rt}) - 1$. By incorporating these results into the definition of Φ_n given by (E.14) and (E.15), we finally arrive at the high-SNR expressions $\tilde{\Phi}_n$ for Φ_n as given in (5.21) and (5.22).

E.7 Proof of Corollary 5

By replacing the right-hand side inequality of (5.13) into (5.25), the lower bound J_1^{LB} for J_1 can be derived as

$$
\begin{aligned}
J_1 & > \mathrm{Pr}\left(\gamma_{R_{j^*}D} \geq C, \max\left[\gamma_{S_{\bar{i}}D}, \gamma_{S_{\bar{i}}R_{k^*}} \min\left[\frac{\gamma_{R_{j^*}D}}{C}, 1\right]\right] < z \right) \triangleq J_1^{\mathrm{LB}} \\
& = \mathrm{Pr}\left(\gamma_{R_{j^*}D} \geq C, \max\left[\gamma_{S_{\bar{i}}D}, \gamma_{S_{\bar{i}}R_{k^*}}\right] < z \right) \\
& \overset{(a)}{=} \mathrm{Pr}\left(\gamma_{R_{j^*}D} \geq C, \max_i\left\{ \max\left[\gamma_{S_iD}, \max_k\{\gamma_{S_iR_k}\}\right] \right\} < z \right),
\end{aligned}
\tag{E.18}
$$

where in step (a) we have used (5.9) and the DAS rule given in (5.8) for $\gamma_{R_{j^*}D} \geq C$. Then, using (5.6) into (E.18), (5.27) is obtained.

E.8   Proof of Corollary 6

By replacing the right-hand side inequality of (5.13) into (5.26), the lower bound J_2^{LB} for J_2 can be derived as

$$
\begin{aligned}
J_2 &> \Pr\left(\gamma_{R_{j^*}D} < C, \max\left[\gamma_{S_i D}, \gamma_{S_i R_{k^*}} \min\left[\frac{\gamma_{R_{j^*}D}}{C}, 1\right]\right] < z\right) \\
&= \Pr\left(\gamma_{R_{j^*}D} < C, \max\left[\gamma_{S_i D}, \frac{\gamma_{S_i R_{k^*}} \gamma_{R_{j^*}D}}{C}\right] < z\right) \triangleq J_2^{\text{LB}} \\
&\overset{(a)}{=} \Pr\left(\gamma_{R_{j^*}D} < C, \max\left[\max_m\{\gamma_{S_m D}\}, \max_k\{\gamma_{S_i R_k}\}\frac{\gamma_{R_{j^*}D}}{C}\right] < z\right),
\end{aligned}
\tag{E.19}
$$

where in step (a) we have used the DAS rule given in (5.8) for $\gamma_{R_{j^*}D} < C$. Then, using (5.6) into (E.19), (5.28) is obtained.

E.9   Proof of Theorem 5

The general expression for J_2^{LB} in (5.28) can be specialized to the Rayleigh-fading scenario by using the corresponding PDFs and CDFs, as well as some principles of probability theory, as follows:

$$
\begin{aligned}
J_2^{\text{LB}} &= \int_0^C f_{\gamma_{RD}}(x) \Pr\left(\max\left[\max_m\{\gamma_{S_m D}\}, \max_k\{\gamma_{S_i R_k}\}\frac{x}{C}\right] < z\right) dx \\
&= \int_0^1 C f_{\gamma_{RD}}(Cu) \Pr\left(\max\left[\max_m\{\gamma_{S_m D}\}, \max_k\{\gamma_{S_i R_k}\}u\right] < z\right) du \\
&= \int_0^1 C f_{\gamma_{RD}}(Cu) \Pr\left(\max\left[\max_m\{\gamma_{S_m D}\} < z\right) \Pr\left(\max_k\{\gamma_{S_i R_k}\}u\right] < z\right) du \\
&= \int_0^1 C f_{\gamma_{RD}}(Cu) \int_0^z \frac{1}{u} f_{\gamma_{SR}}\left(\frac{v}{u}\right) \Pr\left(\max_m\{\gamma_{S_m D}\} < z - v\right) dv\, du \\
&= \int_0^1 \frac{C N_{rt}}{\bar{\gamma}_{RD}} e^{-\frac{Cu}{\bar{\gamma}_{RD}}} \left(1 - e^{-\frac{Cu}{\bar{\gamma}_{RD}}}\right)^{N_{rt}-1} \left(1 - e^{-\frac{z}{u\bar{\gamma}_{SR}}}\right)^{N_{rr}} \left(1 - e^{-\frac{z}{\bar{\gamma}_{SD}}}\right)^{N_t} du,
\end{aligned}
\tag{E.20}
$$

which is identical to the expression for J_2^{LB} presented in (5.30).

E.10   Proof of Corollary 8

In order to obtain an asymptotic lower bound $\tilde{J}_2^{\text{LB}}$ for J_2, we rewrite (5.30) by using the binomial theorem as

$$
J_2^{\text{LB}} = \sum_{j=1}^{N_{rt}} \binom{N_{rt}-1}{j-1} (-1)^{j-1} \left(1 - e^{-\frac{z}{\bar{\gamma}_{SD}}}\right)^{N_t} \frac{C N_{rt}}{\bar{\gamma}_{RD}} \underbrace{\int_0^1 e^{-\frac{jCu}{\bar{\gamma}_{RD}}} \left(1 - e^{-\frac{z}{u\bar{\gamma}_{SR}}}\right)^{N_{rr}} du}_{\eta}.
\tag{E.21}
$$

By using again the binomial theorem, η can be also rewritten as

$$\eta = \int_0^1 e^{-\frac{jCu}{\bar\gamma_{RD}}} \left(1 + \sum_{i=1}^{N_{rr}} \binom{N_{rr}}{i} (-1)^i e^{-\frac{iz}{u\bar\gamma_{SR}}}\right) du$$

$$= \frac{\bar\gamma_{RD}}{jC} \left(1 - e^{-\frac{jC}{\bar\gamma_{RD}}}\right) + \sum_{i=1}^{N_{rr}} \binom{N_{rr}}{i} (-1)^i \underbrace{\int_0^1 e^{-\frac{jCu}{\bar\gamma_{RD}}} e^{-\frac{iz}{u\bar\gamma_{SR}}} du}_{\delta}, \qquad \text{(E.22)}$$

which, replaced back into (E.21), gives

$$J_2^{\text{LB}} = \left(1 - e^{-\frac{z}{\bar\gamma_{SD}}}\right)^{N_t} \frac{CN_{rt}}{\bar\gamma_{RD}} \left(\sum_{j=1}^{N_{rt}} \binom{N_{rt}-1}{j-1} (-1)^{j-1} \frac{\bar\gamma_{RD}}{jCu} \left(1 - e^{-\frac{jCu}{\bar\gamma_{RD}}}\right)\right.$$

$$\left. + \sum_{j=1}^{N_{rt}} \binom{N_{rt}-1}{j-1} (-1)^{j-1} \sum_{i=1}^{N_{rr}} \binom{N_{rr}}{i} (-1)^i \delta \right). \qquad \text{(E.23)}$$

The term δ can be elaborated as

$$\delta = \int_0^1 e^{-\frac{jCu}{\bar\gamma_{RD}}} e^{-\frac{iz}{u\bar\gamma_{SR}}} du$$

$$= \int_0^\infty e^{-\frac{jCu}{\bar\gamma_{RD}}} e^{-\frac{iz}{u\bar\gamma_{SR}}} du - \int_1^\infty e^{-\frac{jCu}{\bar\gamma_{RD}}} e^{-\frac{iz}{u\bar\gamma_{SR}}} du$$

$$\stackrel{(a)}{=} 2\sqrt{\frac{iz\bar\gamma_{RD}}{jC\bar\gamma_{SR}}} K_1\left(2\sqrt{\frac{jCiz}{\bar\gamma_{SR}\bar\gamma_{RD}}}\right) - \int_1^\infty e^{-\frac{jCu}{\bar\gamma_{RD}}} \sum_{l=0}^\infty \frac{\left(-\frac{iz}{u\bar\gamma_{SR}}\right)^l}{l!} du$$

$$\stackrel{(b)}{=} \left(2\sqrt{\frac{iz\bar\gamma_{RD}}{jC\bar\gamma_{SR}}}\right) \left(\frac{1}{2}\sqrt{\frac{\bar\gamma_{SR}\bar\gamma_{RD}}{jCiz}}\right) + \left(2\sqrt{\frac{iz\bar\gamma_{RD}}{jC\bar\gamma_{SR}}}\right)$$

$$\times \sum_{k=0}^\infty \frac{\left(\sqrt{\frac{jCiz}{\bar\gamma_{SR}\bar\gamma_{RD}}}\right)^{1+2k}}{k!(k+1)} \left(\ln\sqrt{\frac{jCiz}{\bar\gamma_{SR}\bar\gamma_{RD}}} - \frac{1}{2}\psi(k+1) - \frac{1}{2}\psi(k+2)\right)$$

$$- \sum_{l=0}^\infty \frac{\left(-\frac{iz}{\bar\gamma_{SR}}\right)^l}{l!} \left(\frac{jC}{\bar\gamma_{RD}}\right)^l \Gamma\left(1-l, \frac{jC}{\bar\gamma_{RD}}\right).$$

$$= \frac{\bar\gamma_{RD}}{jC} + \sqrt{\frac{iz\bar\gamma_{RD}}{jC\bar\gamma_{SR}}} \sum_{k=0}^\infty \frac{\left(\sqrt{\frac{jCiz}{\bar\gamma_{SR}\bar\gamma_{RD}}}\right)^{1+2k}}{k!(k+1)} \left(\ln\frac{jCiz}{\bar\gamma_{SR}\bar\gamma_{RD}} - \psi(k+1) - \psi(k+2)\right)$$

$$- \sum_{l=0}^\infty \frac{\left(-\frac{iz}{\bar\gamma_{SR}}\right)^l}{l!} \left(\frac{jC}{\bar\gamma_{RD}}\right)^l \Gamma\left(1-l, \frac{jC}{\bar\gamma_{RD}}\right). \qquad \text{(E.24)}$$

Steps (a) and (b) follow from [21, Eq. (3.471.9)] and [21, Eqs. (8.446)], respectively. Now, the high-SNR analysis of δ is similar to that of Φ_0 in Appendix E.6.1. To this end, we

define an auxiliary variable λ as

$$\lambda \triangleq \frac{CN_{rt}}{\bar{\gamma}_{RD}} \sum_{j=1}^{N_{rt}} \binom{N_{rt}-1}{j-1} (-1)^{j-1} \sum_{i=1}^{N_{rr}} \binom{N_{rr}}{i} (-1)^i \delta$$

$$= -1 + \frac{CN_{rt}}{\bar{\gamma}_{RD}} \Bigg(\sum_{k_1=0}^{\infty} \frac{\left(\frac{z}{\bar{\gamma}_{SR}}\right)^{k_1+1} \left(\frac{C}{\bar{\gamma}_{RD}}\right)^{k_1}}{k_1!(k_1+1)!} \sum_{j=1}^{N_{rt}} \binom{N_{rt}-1}{j-1} (-1)^{j-1} j^{k_1}$$

$$\times \sum_{i=1}^{N_{rr}} \binom{N_{rr}}{i} (-1)^i i^{k_1+1} \ln \frac{jiz}{\bar{\gamma}_{RD}} - \sum_{k_2=0}^{\infty} \frac{\left(\frac{z}{\bar{\gamma}_{SR}}\right)^{k_2+1} \left(\frac{C}{\bar{\gamma}_{RD}}\right)^{k_2}}{k_2!(k_2+1)!} (\psi(k_2+1) + \psi(k_2+2))$$

$$\times \sum_{j=1}^{N_{rt}} \binom{N_{rt}-1}{j-1} (-1)^{j-1} j^{k_2} \sum_{i=1}^{N_{rr}} \binom{N_{rr}}{i} (-1)^i i^{k_2+1}$$

$$- \sum_{l=0}^{\infty} \frac{\left(-\frac{z}{\bar{\gamma}_{SR}}\right)^l \left(\frac{C}{\bar{\gamma}_{RD}}\right)^{l-1}}{l!} \sum_{j=1}^{N_{rt}} \binom{N_{rt}-1}{j-1} (-1)^{j-1} j^{l-1} \Gamma\left(1-l, \frac{jC}{\bar{\gamma}_{RD}}\right) \sum_{i=1}^{N_{rr}} \binom{N_{rr}}{i} (-1)^i i^l \Bigg).$$

$$\text{(E.25)}$$

Observe that, similarly to λ_0 in (E.13), λ is composed by three outer summations, over k_1, k_2, and l. Following the same rationale presented for λ_0, one can verify that the first nonzero term of the summation over k_1 occurs for $k_1 = \min(N_{rr}, N_{rt}) - 1$, the first nonzero term of the summation over k_2 occurs for $k_2 = \max(N_{rr}, N_{rt}) - 1$, and the first and second nonzero terms of the summation over l occurs for $l = 0$ and $l = N_{rr} + 1$.

Using this and preserving only the lowest-order terms so as to derive a high-SNR expression, we arrive at two cases: (a) if $N_{rr} = N_{rt}$, all three summations must be considered; and (b) if $N_{rr} \neq N_{rt}$, only the summations over k_1 and l must be considered. In all the cases, the diversity order of λ is observed to be given by $\min(N_{rr}, N_{rt}) - 1$. By incorporating these results into (E.23), after some algebraic manipulations, we finally arrive at the high-SNR expression for Ω as given in (5.33).

Appendix F

Supporting Material to Chapter 6

The references cited in this appendix are listed at the end of Chapter 6.

F.1 Proof of Lemma 6.1

By using (6.4) into the definition of I_1 in (6.8), a lower bound I_1^{LB} can be derived as

$$
\begin{aligned}
I_1 &\geq \Pr\left(Z \geq \max_i \{X_i\}, \max\left[Y_{\bar{i}}, \min\left[X_{\bar{i}}, Z\right]\right] < \tau\right) \triangleq I_1^{\mathrm{LB}} \\
&= \Pr\left(Z \geq \max_i \{X_i\}, \max\left[Y_{\bar{i}}, X_{\bar{i}}\right] < \tau\right) \\
&\overset{(a)}{=} \Pr\left(Z \geq \max_i \{X_i\}, \max_i\left\{\max\left[Y_i, X_i\right]\right\} < \tau\right) \\
&= \underbrace{\Pr\left(Z \geq \max_i \{X_i\}, \max_i \{X_i\} < \tau\right)}_{\triangleq \rho} \Pr\left(Y_i < \tau\right)^{N_t},
\end{aligned}
\tag{F.1}
$$

which coincides with the result in (6.9). In step (a) we have used the DAS/SC rule for $Z \geq \max_i \{X_i\}$, given in (6.6).

F.2 Proof of Lemma 6.2

By using (6.4) into the definition of I_2 in (6.8), a lower bound I_2^{LB} can be derived as

$$
\begin{aligned}
I_2 &\geq \Pr\left(Z < \max_i \{X_i\}, \max\left[Y_{\underline{i}}, \min\left[X_{\underline{i}}, Z\right]\right] < \tau\right) \triangleq I_2^{\mathrm{LB}} \\
&\overset{(a)}{=} \Pr\left(Z < \max_i \{X_i\}, \max_i \{Y_i\} < \tau, \min\left[X_i, Z\right] < \tau\right) \\
&= \underbrace{\Pr\left(Z < \max_i \{X_i\}, \min\left[X_i, Z\right] < \tau\right)}_{\triangleq J} \Pr\left(Y_i < \tau\right)^{N_t},
\end{aligned}
\tag{F.2}
$$

which coincides with the result in (6.10). In step (a) we have used the DAS/SC rule for $Z < \max_i \{X_i\}$, given in (6.6).

F.3 Proof of Proposition 3

Relying on basic principles of the probability theory, the term ρ defined in (F.1) can be elaborated as

$$
\begin{aligned}
\rho &= \Pr\left(Z \geq \max_i\{X_i\}, \max_i\{X_i\} < \tau\right) \\
&= \Pr\left(Z \geq \tau, \max_i\{X_i\} < \tau\right) + \Pr\left(Z < \tau, \max_i\{X_i\} < Z\right) \\
&= \Pr\left(Z \geq \tau\right)\Pr\left(X_i < \tau\right)^{N_t} + \int_0^\tau f_Z(z)\Pr\left(X_i < z\right)^{N_t} dz.
\end{aligned}
\tag{F.3}
$$

By using this into (F.1), as well as the exponential PDFs and cumulative distribution functions (CDFs) of X_i, Y_i, and Z, I_1^{LB} can be rewritten as

$$
I_1^{\text{LB}} = \left(1 - e^{-\frac{\tau}{\bar{Y}}}\right)^{N_t}\left(e^{-\frac{\tau}{\bar{Z}}}\left(1 - e^{-\frac{\tau}{\bar{X}}}\right)^{N_t} + \underbrace{\int_0^\tau \frac{1}{\bar{Z}} e^{-\frac{z}{\bar{Z}}}\left(1 - e^{-\frac{z}{\bar{X}}}\right)^{N_t} dz}_{\triangleq \sigma}\right).
\tag{F.4}
$$

Finally, by using the binomial theorem [19, Eq. (1.111)] to solve the integral term σ defined in (F.4), a closed-form expression for I_1^{LB} is then obtained as in (6.11).

F.4 Proof of Proposition 4

Relying on basic principles of the probability theory, the term J defined in (F.2) can be elaborated as

$$
J = \underbrace{\Pr\left(Z < \max_i\{X_i\}, X_i < \tau\right)}_{\triangleq J_1} + \underbrace{\Pr\left(Z < \max_i\{X_i\}, Z < \tau\right)}_{\triangleq J_2}
$$
$$
- \underbrace{\Pr\left(Z < \max_i\{X_i\}, X_i < \tau, Z < \tau\right)}_{\triangleq J_3}.
\tag{F.5}
$$

Below, the component terms J_1, J_2, and J_2 are analyzed. The term J_1 can be solved as

$$
\begin{aligned}
J_1 &= \Pr\left(X_i < \tau\right) - \Pr\left(\max_i\{X_i\} < Z, X_i < \tau\right) \\
&= \Pr\left(X_i < \tau\right) - \Pr\left(X_1 < Z, X_2 < Z, \ldots, X_i < Z, \ldots, X_{N_t} < Z, X_i < \tau\right) \\
&= \Pr\left(X_i < \tau\right) - \Pr\left(X_1 < Z, X_2 < Z, \ldots, X_i < \min\left[\tau, Z\right], \ldots, X_{N_t} < Z\right) \\
&= \Pr\left(X_i < \tau\right) - \Pr\left(Z < \tau, X_1 < Z, X_2 < Z, \ldots, X_i < Z, \ldots, X_{N_t} < Z\right) \\
&\quad - \Pr\left(Z > \tau, X_1 < Z, X_2 < Z, \ldots, X_i < \tau, \ldots, X_{N_t} < Z\right) \\
&= \Pr\left(X_i < \tau\right) - \Pr\left(Z < \tau, \max_i\{X_i\} < Z\right) - \Pr\left(Z > \tau, \max_i\{X_i\} < Z, X_i < \tau\right) \\
&\overset{(a)}{=} \left(1 - e^{-\frac{\tau}{\bar{X}}}\right) - \int_0^\tau \frac{1}{\bar{Z}} e^{-\frac{a}{\bar{Z}}}\left(1 - e^{-\frac{a}{\bar{X}}}\right)^{N_t} da - \underbrace{\int_\tau^\infty \frac{1}{\bar{Z}} e^{-\frac{b}{\bar{Z}}}\left(1 - e^{-\frac{b}{\bar{X}}}\right)^{N_t - 1}\left(1 - e^{-\frac{\tau}{\bar{X}}}\right) db}_{\triangleq \delta},
\end{aligned}
$$
$$
\tag{F.6}
$$

the term J_2 as

$$
\begin{aligned}
J_2 &= \Pr\left(Z < \max_i\{X_i\}, Z < \tau\right) \\
&= \int_0^\tau f_Z(z)\Pr\left(z < \max_i\{X_i\}\right) dz \\
&\overset{(a)}{=} \int_0^\tau \frac{1}{\bar{Z}} e^{-\frac{z}{\bar{Z}}} \left(1 - \left(1 - e^{-\frac{z}{\bar{X}}}\right)^{N_t}\right) dz,
\end{aligned}
\tag{F.7}
$$

and the term J_3 as

$$
\begin{aligned}
J_3 &= \Pr\left(Z < \max_i\{X_i\}, X_i < \tau, Z < \tau\right) \\
&= \Pr\left(X_i < \tau, Z < \tau\right) - \Pr\left(Z > \max_i\{X_i\}, X_i < \tau, Z < \tau\right) \\
&= \Pr\left(X_i < \tau, Z < \tau\right) - \int_0^\tau f_Z(z)\Pr\left(z > \max_i\{X_i\}, X_i < \tau\right) dz \\
&\overset{(a)}{=} \left(1 - e^{-\frac{\tau}{\bar{X}}}\right)\left(1 - e^{-\frac{\tau}{\bar{Z}}}\right) - \int_0^\tau \frac{1}{\bar{Z}} e^{-\frac{z}{\bar{Z}}} \left(1 - e^{-\frac{z}{\bar{X}}}\right)^{N_t} dz,
\end{aligned}
\tag{F.8}
$$

where in step (a) of the above expressions we have used the exponential PDFs and CDFs of X_i and Z. Finally, by substituting (F.6)–(F.8) into (F.5) and then into (F.2), with use of the exponential CDF of Y_i, a single-fold integral form expression for I_2^{LB} is then obtained as in (6.12).

F.5 Proof of Proposition 5

By using the MacLaurin series of the exponential function [19, Eq. (1.211.1)] into the term σ defined in (F.4), we obtain

$$
\begin{aligned}
\sigma &\simeq \int_0^\tau \frac{1}{\bar{Z}} e^{-\frac{z}{\bar{Z}}} \left(\frac{z}{\bar{X}}\right)^{N_t} dz \\
&= \frac{1}{\bar{Z}} \left(\frac{1}{\bar{X}}\right)^{N_t} \sum_{n=0}^\infty \left(\frac{1}{\bar{Z}}\right)^n \frac{1}{n!} \frac{\tau^{N_t+n+1}}{N_t+n+1}.
\end{aligned}
\tag{F.9}
$$

Then, by substituting (F.9) into (F.4), and by using again the MacLaurin series of the exponential function, I_1^{LB} can be asymptotically expressed as

$$
I_1^{\mathrm{LB}} \simeq \left(\frac{\tau}{\bar{Y}}\right)^{N_t} \left(\left(1 - \frac{\tau}{\bar{Z}}\right)\left(\frac{\tau}{\bar{X}}\right)^{N_t} + \frac{1}{\bar{Z}}\left(\frac{1}{\bar{X}}\right)^{N_t} \frac{\tau^{N_t+1}}{N_t+1}\right).
\tag{F.10}
$$

Finally, by preserving only the lowest-order terms in (F.10), it reduces to $\tilde{I}_1^{\mathrm{LB}}$ as in (6.13).

F.6 Proof of Proposition 6

By using the MacLaurin series of the exponential function into the term δ defined in (F.6), we obtain

$$
\begin{aligned}
\delta &= \left(1 - e^{-\frac{\tau}{X}}\right) \int_{\tau}^{\infty} \frac{1}{\bar{Z}} e^{-\frac{b}{\bar{Z}}} \left(1 - e^{-\frac{b}{\bar{X}}}\right)^{N_t - 1} db \\
&= \left(1 - e^{-\frac{\tau}{X}}\right) \left(\int_{0}^{\infty} \frac{1}{\bar{Z}} e^{-\frac{b}{\bar{Z}}} \left(1 - e^{-\frac{b}{\bar{X}}}\right)^{N_t - 1} db - \int_{0}^{\tau} \frac{1}{\bar{Z}} e^{-\frac{b}{\bar{Z}}} \left(1 - e^{-\frac{b}{\bar{X}}}\right)^{N_t - 1} db \right) \\
&\simeq \frac{\tau}{\bar{Z}} B\left(\frac{\bar{X}}{\bar{Z}}, N_t\right) - \frac{\tau}{\bar{Z}} \left(\frac{1}{\bar{X}}\right)^{N_t + 1} \sum_{n=0}^{\infty} \left(\frac{1}{\bar{Z}}\right)^{n} \frac{1}{n!} \frac{\tau^{N_t + n}}{N_t + n}.
\end{aligned}
\tag{F.11}
$$

Then, by substituting (F.9) and (F.11) into (6.12), and by using again the MacLaurin series of the exponential function, I_2^{LB} can be asymptotically expressed as

$$
I_2^{\mathrm{LB}} \simeq \left(\frac{\tau}{\bar{Y}}\right)^{N_t} \left(\frac{\tau}{\bar{X}} - \frac{\tau}{\bar{Z}} B\left(\frac{\bar{X}}{\bar{Z}}, N_t\right) - \frac{1}{\bar{Z}} \left(\frac{1}{\bar{X}}\right)^{N_t + 1} \frac{\tau^{N_t + 1}}{N_t} + \frac{\tau}{\bar{Z}} - \frac{1}{\bar{Z}} \left(\frac{1}{\bar{X}}\right)^{N_t} \frac{\tau^{N_t + 1}}{N_t + 1} - \frac{\tau^2}{\bar{X}\bar{Z}} \right).
\tag{F.12}
$$

Finally, by preserving only the lowest-order terms in (F.12), it reduces to $\tilde{I}_2^{\mathrm{LB}}$ as in (6.14).

F.7 Proof of Proposition 7

An asymptotic expression for the outage probability is obtained by preserving only the lowest-order terms in the sum $\tilde{I}_1^{\mathrm{LB}} + \tilde{I}_2^{\mathrm{LB}}$. From (6.13) and (6.14), it becomes apparent that the individual diversity orders of $\tilde{I}_1^{\mathrm{LB}}$ and $\tilde{I}_2^{\mathrm{LB}}$ are $2N_t$ and $N_t + 1$, respectively. Therefore, only for the particular case of $N_t = 1$ these two diversity orders coincide, so that the both terms must be preserved in the asymptotic outage bound. Otherwise, when $N_t \geq 2$, the diversity order of $\tilde{I}_1^{\mathrm{LB}}$ is higher than that of $\tilde{I}_2^{\mathrm{LB}}$, and thus $\tilde{I}_1^{\mathrm{LB}}$ can be ignored. Taking all this into account, we arrive at (6.15).

F.8 Proof of Lemma 6.3

By using (6.5) into the definition of L_1 in (6.16), a lower bound L_1^{LB} can be derived as

$$
\begin{aligned}
L_1 &\geq \Pr\left(Z \geq \max_i \{X_i\}, Y_{\bar{i}} + \min[X_{\bar{i}}, Z] < \tau \right) \triangleq I_1^{\mathrm{LB}} \\
&= \Pr\left(Z \geq \max_i \{X_i\}, Y_{\bar{i}} + X_{\bar{i}} < \tau \right) \\
&\overset{(a)}{=} \Pr\left(Z \geq \max_i \{X_i\}, \max_i \{Y_i + X_i\} < \tau \right),
\end{aligned}
\tag{F.13}
$$

which coincides with the result in (6.17). In step (a) we have used the DAS/MRC rule for $Z \geq \max_i \{X_i\}$, given in (6.7).

F.9 Proof of Lemma 6.4

By using (6.5) into the definition of L_2 in (6.16), a lower bound L_2^{LB} can be derived as

$$L_2 \geq \Pr\left(Z < \max_i\{X_i\}, Y_{\underline{i}} + \min[X_{\underline{i}}, Z] < \tau\right) \triangleq L_2^{\text{LB}}$$

$$\overset{(a)}{=} \Pr\left(Z < \max_i\{X_i\}, \max_i\{Y_i\} + \min[X_i, Z] < \tau\right), \tag{F.14}$$

which coincides with the result in (6.18). In step (a) we have used the DAS/MRC rule for $Z < \max_i\{X_i\}$, given in (6.7).

F.10 Proof of Proposition 8

Relying on basic principles of the probability theory, the lower bound L_1^{LB} in (F.13) can be elaborated as

$$L_1^{\text{LB}} = \Pr\left(Z \geq \max_i\{X_i\}, \max_i\{Y_i + X_i\} < \tau\right)$$

$$= \int_0^\infty f_Z(z)\Pr\left(\max_i\{X_i\} \leq z, \max_i\{Y_i + X_i\} < \tau\right)dz$$

$$= \int_0^\infty f_Z(z)\Pr\left(\max_i\{X_i\} \leq \min[z, \tau], \max_i\{Y_i + X_i\} < \tau\right)dz$$

$$= \int_0^\tau f_Z(z)\Pr\left(\max_i\{X_i\} \leq z, \max_i\{Y_i + X_i\} < \tau\right)dz$$

$$+ \int_\tau^\infty f_Z(z)\Pr\left(\max_i\{X_i\} \leq \tau, \max_i\{Y_i + X_i\} < \tau\right)dz$$

$$= \int_0^\tau f_Z(z)\left(\int_0^z f_{X_i}(x)\Pr(Y_i + x < \tau)dx\right)^{N_t}dz$$

$$+ \int_\tau^\infty f_Z(z)\left(\int_0^\tau f_{X_i}(x)\Pr(Y_i + x < \tau)dx\right)^{N_t}dz$$

$$\overset{(a)}{=} \int_0^\tau f_Z(z)\left(\int_0^z \frac{1}{\overline{X}}e^{-\frac{x}{\overline{X}}}\left(1 - e^{-\frac{\tau-x}{\overline{Y}}}\right)dx\right)^{N_t}dz$$

$$+ \int_\tau^\infty f_Z(z)\left(\int_0^\tau \frac{1}{\overline{X}}e^{-\frac{x}{\overline{X}}}\left(1 - e^{-\frac{\tau-x}{\overline{Y}}}\right)dx\right)^{N_t}dz$$

$$= \int_0^\tau f_Z(z)\underbrace{\left(1 - e^{-\frac{z}{\overline{X}}} - \frac{1}{\overline{X}}e^{-\frac{\tau}{\overline{Y}}}\int_0^z e^{-x\left(\frac{1}{\overline{X}} - \frac{1}{\overline{Y}}\right)}dx\right)^{N_t}}_{\triangleq \alpha_1}dz$$

$$+ \int_\tau^\infty f_Z(z)\underbrace{\left(1 - e^{-\frac{\tau}{\overline{X}}} - \frac{1}{\overline{X}}e^{-\frac{\tau}{\overline{Y}}}\int_0^\tau e^{-x\left(\frac{1}{\overline{X}} - \frac{1}{\overline{Y}}\right)}dx\right)^{N_t}}_{\triangleq \alpha_2}dz, \tag{F.15}$$

where in step (a) we have used the exponential PDFs and CDFs of X_i and Y_i. Finally, by using the exponential PDF of Z into (F.15), a single-fold integral-form expression for L_1^{LB} is then obtained as in (6.19).

F.11 Proof of Proposition 9

Relying on basic principles of the probability theory, the lower bound L_2^{LB} in (F.14) can be elaborated as

$$
\begin{aligned}
L_2^{\mathrm{LB}} &= \Pr\left(Z < \max_i\{X_i\}, \max_i\{Y_i\} + \min[X_i, Z] < \tau\right) \\
&= \int_0^\tau f_{Y_i}(y) \underbrace{\Pr\left(Z < \max_i\{X_i\}, \min[X_i, Z] < \tau - y\right)}_{\triangleq K} dy,
\end{aligned}
\tag{F.16}
$$

where the term K defined above can be split into three components as

$$
\begin{aligned}
K &= \underbrace{\Pr\left(Z < \max_i\{X_i\}, X_i < \tau - y\right)}_{\triangleq K_1} + \underbrace{\Pr\left(Z < \max_i\{X_i\}, Z < \tau - y\right)}_{\triangleq K_2} \\
&\quad - \underbrace{\Pr\left(Z < \max_i\{X_i\}, X_i < \tau - y, Z < \tau - y\right)}_{\triangleq K_3}.
\end{aligned}
\tag{F.17}
$$

By comparing (F.17) and (F.5), it becomes apparent that the definitions of K_1, K_2, and K_3 coincide with those of J_1, J_2, and J_3, respectively, except that τ (in the latter) is replaced by $\tau - y$ (in the former). Therefore, expressions for K_1, K_2, and K_3 can be respectively obtained as in (F.6), (F.7), and (F.8), by substituting $\tau - y$ for τ. Finally, by applying those expressions into (F.17) and then into (F.16), with use of the exponential PDF of Y_i, a two-fold integral form expression for L_2^{LB} is then obtained as in (6.20).

F.12 Proof of Proposition 10

By using the MacLaurin series of the exponential function into the term α_1 defined in (F.15), we obtain

$$
\begin{aligned}
\alpha_1 &= 1 - e^{-\frac{z}{\overline{X}}} - \frac{1}{\overline{X}} e^{-\frac{\tau}{\overline{Y}}} \int_0^z e^{-x\left(\frac{1}{\overline{X}} - \frac{1}{\overline{Y}}\right)} dx \\
&\simeq 1 - \left(1 - \frac{z}{\overline{X}} + \frac{z^2}{2\overline{X}^2}\right) - \frac{1}{\overline{X}} e^{-\frac{\tau}{\overline{Y}}} \int_0^z \left(1 - x\left(\frac{1}{\overline{X}} - \frac{1}{\overline{Y}}\right)\right) dx \\
&\simeq \frac{1}{2} \frac{z^2}{\overline{X}\,\overline{Y}}.
\end{aligned}
\tag{F.18}
$$

The term α_2, also defined in (F.15), can be obtained in the same way, by substituting τ for z. Then, by using (F.18) into (F.15), L_1^{LB} can be asymptotically expressed as

$$
L_1^{\mathrm{LB}} \simeq \int_0^\tau \frac{1}{\overline{Z}} e^{-\frac{z}{\overline{Z}}} \left(\frac{1}{2} \frac{z^2}{\overline{X}\,\overline{Y}}\right)^{N_t} dz + \int_\tau^\infty \frac{1}{\overline{Z}} e^{-\frac{z}{\overline{Z}}} \left(\frac{1}{2} \frac{\tau^2}{\overline{X}\,\overline{Y}}\right)^{N_t} dz.
\tag{F.19}
$$

Finally, by solving the integrals in (F.19) with use of the MacLaurin series of the exponential function, and preserving only the lowest-order terms, it reduces to $\tilde{L}_1^{\mathrm{LB}}$ as in (6.21).

F.13   Proof of Proposition 11

To begin with, let us rewrite the lower bound L_2^{LB} in (6.20) as

$$
L_2^{\text{LB}} = \underbrace{\int_0^\tau N_t \frac{1}{\bar{Y}} e^{-\frac{y}{\bar{Y}}} \left(1 - e^{-\frac{y}{\bar{Y}}}\right)^{N_t - 1} \left(1 - e^{-\frac{\tau - y}{\bar{X}}}\right) dy}_{\triangleq \epsilon_1}
$$

$$
+ \underbrace{\int_0^\tau N_t \frac{1}{\bar{Y}} e^{-\frac{y}{\bar{Y}}} \left(1 - e^{-\frac{y}{\bar{Y}}}\right)^{N_t - 1} \left(1 - e^{-\frac{\tau - y}{\bar{Z}}}\right) dy}_{\triangleq \epsilon_2}
$$

$$
- \underbrace{\int_0^\tau N_t \frac{1}{\bar{Y}} e^{-\frac{y}{\bar{Y}}} \left(1 - e^{-\frac{y}{\bar{Y}}}\right)^{N_t - 1} \int_{\tau - y}^\infty \frac{1}{\bar{Z}} e^{-\frac{b}{\bar{Z}}} \left(1 - e^{-\frac{b}{\bar{X}}}\right)^{N_t - 1} \left(1 - e^{-\frac{\tau - y}{\bar{X}}}\right) db\, dy}_{\triangleq \epsilon_3}
$$

$$
- \underbrace{\int_0^\tau N_t \frac{1}{\bar{Y}} e^{-\frac{y}{\bar{Y}}} \left(1 - e^{-\frac{y}{\bar{Y}}}\right)^{N_t - 1} \int_0^{\tau - y} \frac{1}{\bar{Z}} e^{-\frac{z}{\bar{Z}}} \left(1 - e^{-\frac{z}{\bar{X}}}\right)^{N_t} dz\, dy}_{\triangleq \epsilon_4}
$$

$$
- \underbrace{\int_0^\tau N_t \frac{1}{\bar{Y}} e^{-\frac{y}{\bar{Y}}} \left(1 - e^{-\frac{y}{\bar{Y}}}\right)^{N_t - 1} \left(1 - e^{-\frac{\tau - y}{\bar{X}}}\right) \left(1 - e^{-\frac{\tau - y}{\bar{Z}}}\right) dy}_{\triangleq \epsilon_5}. \tag{F.20}
$$

Now, high-SNR asymptotic expressions for the terms ϵ_1, ϵ_2, ϵ_3, ϵ_4, and ϵ_5 defined above can be obtained by appropriately using the MacLaurin series of the exponential function into each definition. For ϵ_1, we obtain

$$
\begin{aligned}
\epsilon_1 &\simeq \int_0^\tau N_t \frac{1}{\bar{Y}} e^{-\frac{y}{\bar{Y}}} \left(\frac{y}{\bar{Y}}\right)^{N_t - 1} \left(1 - e^{-\frac{\tau - y}{\bar{X}}}\right) dy \\
&= N_t \left(\frac{1}{\bar{Y}}\right)^{N_t} \int_0^\tau \left(e^{-\frac{y}{\bar{Y}}} (y)^{N_t - 1} - e^{-\frac{y}{\bar{Y}}} (y)^{N_t - 1} e^{-\frac{\tau}{\bar{X}}} e^{\frac{y}{\bar{X}}}\right) dy \\
&= N_t \left(\frac{1}{\bar{Y}}\right)^{N_t} \int_0^\tau e^{-\frac{y}{\bar{Y}}} (y)^{N_t - 1} dy - N_t \left(\frac{1}{\bar{Y}}\right)^{N_t} e^{-\frac{\tau}{\bar{X}}} \int_0^\tau e^{-\frac{y}{\bar{Y}}} (y)^{N_t - 1} e^{\frac{y}{\bar{X}}} dy \\
&= N_t \left(\frac{1}{\bar{Y}}\right)^{N_t} \sum_{n=0}^\infty \left(-\frac{1}{\bar{Y}}\right)^n \frac{1}{n!} \frac{\tau^{N_t + n}}{N_t + n} - N_t \left(\frac{1}{\bar{Y}}\right)^{N_t} \sum_{n=0}^\infty \left(-\frac{1}{\bar{Y}} + \frac{1}{\bar{X}}\right)^n \frac{1}{n!} \frac{\tau^{N_t + n}}{N_t + n} \\
&\quad + N_t \left(\frac{1}{\bar{Y}}\right)^{N_t} \frac{\tau}{\bar{X}} \sum_{n=0}^\infty \left(-\frac{1}{\bar{Y}} + \frac{1}{\bar{X}}\right)^n \frac{1}{n!} \frac{\tau^{N_t + n}}{N_t + n} \\
&\simeq \left(\frac{1}{\bar{Y}}\right)^{N_t} \frac{1}{\bar{X}} \left(\frac{\tau^{N_t + 1}}{N_t + 1}\right). \tag{F.21}
\end{aligned}
$$

From (F.20), note that an expression for ϵ_2 can be obtained by replacing $\bar{X}$ with $\bar{Z}$ into the expression for ϵ_1, which gives

$$
\epsilon_2 \simeq \left(\frac{1}{\bar{Y}}\right)^{N_t} \frac{1}{\bar{Z}} \left(\frac{\tau^{N_t + 1}}{N_t + 1}\right). \tag{F.22}
$$

In addition, expressions for ϵ_3, ϵ_4, and ϵ_5 are obtained as follows:

$$\epsilon_3 \simeq \int_0^\tau N_t \frac{1}{\bar{Y}} e^{-\frac{y}{\bar{Y}}} \left(1 - e^{-\frac{y}{\bar{Y}}}\right)^{N_t-1} \int_{\tau-y}^\infty \frac{1}{\bar{\bar{Z}}} e^{-\frac{b}{\bar{Z}}} \left(1 - e^{-\frac{b}{\bar{X}}}\right)^{N_t-1} \left(1 - e^{-\frac{\tau-y}{\bar{X}}}\right) db\, dy$$

$$\simeq \int_0^\tau N_t \frac{1}{\bar{Y}} e^{-\frac{y}{\bar{Y}}} \left(\frac{y}{\bar{Y}}\right)^{N_t-1} \frac{(\tau-y)}{\bar{Z}} B\left(\frac{\bar{X}}{\bar{Z}}, N_t\right) dy$$

$$\simeq \frac{1}{\bar{Z}} \left(\frac{1}{\bar{Y}}\right)^{N_t} \left(\frac{\tau^{N_t+1}}{N_t+1}\right) B\left(\frac{\bar{X}}{\bar{Z}}, N_t\right) \tag{F.23}$$

$$\epsilon_4 \simeq \int_0^\tau N_t \frac{1}{\bar{Y}} e^{-\frac{y}{\bar{Y}}} \left(\frac{y}{\bar{Y}}\right)^{N_t-1} \int_0^{\tau-y} \frac{1}{\bar{Z}} e^{-\frac{z}{\bar{Z}}} \left(\frac{z}{\bar{X}}\right)^{N_t} dz\, dy$$

$$= \left(\frac{1}{\bar{Y}}\right)^{N_t} N_t \int_0^\tau e^{-\frac{y}{\bar{Y}}} (y)^{N_t-1} \frac{1}{\bar{Z}} \left(\frac{1}{\bar{X}}\right)^{N_t} \sum_{n=0}^\infty \left(\frac{1}{\bar{Z}}\right)^n \frac{1}{n!} \frac{(\tau-y)^{N_t+n+1}}{N_t+n+1} dy$$

$$\simeq \left(\frac{1}{\bar{Y}\bar{X}}\right)^{N_t} \frac{1}{\bar{Z}} \frac{N_t}{(N_t+1)} \int_0^\tau e^{-\frac{y}{\bar{Y}}} (y)^{N_t-1} (\tau-y)^{N_t+1} dy$$

$$= \left(\frac{1}{\bar{Y}\bar{X}}\right)^{N_t} \frac{1}{\bar{Z}} \frac{N_t}{(N_t+1)} \sum_{k=0}^\infty \binom{N_t+1}{k} (-1)^k \tau^{N_t+1-k} \int_0^\tau e^{-\frac{y}{\bar{Y}}} y^{N_t-1+k} dy$$

$$\simeq \left(\frac{1}{\bar{Y}\bar{X}}\right)^{N_t} \frac{1}{\bar{Z}} \frac{\tau^{N_t+1}}{(N_t+1)} \sum_{k=0}^\infty \binom{N_t+1}{k} (-1)^k \frac{N_t}{Nt+k}$$

$$= \left(\frac{1}{\bar{Y}\bar{X}}\right)^{N_t} \frac{1}{\bar{Z}} \frac{\tau^{N_t+1}}{(N_t+1)} \frac{\Gamma(Nt+1)\Gamma(N_t+2)}{\Gamma(2Nt+2)} \tag{F.24}$$

$$\epsilon_5 \simeq \int_0^\tau N_t \frac{1}{\bar{Y}} e^{-\frac{y}{\bar{Y}}} \left(\frac{y}{\bar{Y}}\right)^{N_t-1} \left(\frac{\tau-y}{\bar{X}}\right) \left(\frac{\tau-y}{\bar{Z}}\right) dy$$

$$= N_t \left(\frac{1}{\bar{Y}}\right)^{N_t} \frac{1}{\bar{X}} \frac{1}{\bar{Z}} \int_0^\tau e^{-\frac{y}{\bar{Y}}} \left(\tau^2 y N_t - 1 - 2\tau y N_t + y N_t + 1\right) dy$$

$$\simeq \left(\frac{1}{\bar{Y}}\right)^{N_t} \frac{1}{\bar{X}\bar{Z}} \frac{2\tau^{N_t+2}}{(N_t+1)(N_t+2)}. \tag{F.25}$$

Finally, by using (F.21)–(F.25) into (F.20), and preserving only the lowest-order terms, it reduces to $\tilde{L}_2^{\mathrm{LB}}$ as in (6.22).

Appendix G

Supporting Material to Chapter 7

G.1 Exact and High-SNR Expressions for $J_{2,1}$

The SNRs Γ_1 and Γ_2 are mutually independent, with marginal PDFs given in (7.2). Using this into (7.26), and exact closed-form expression for $J_{2,1}$ is obtained as

$$
\begin{aligned}
J_{2,1} &= 1 - \int_{2^{R_{c1}I(B_1;B_0|B_2)}-1}^{\infty} \int_{2^{R_{c2}I(B_2;B_0|B_1)}-1}^{\infty} \frac{1}{\bar{\Gamma}_1} e^{-\frac{\gamma_1}{\bar{\Gamma}_1}} \frac{1}{\bar{\Gamma}_2} e^{-\frac{\gamma_2}{\bar{\Gamma}_2}} d\gamma_2 d\gamma_1, \\
&= 1 - e^{-\frac{2^{R_{c1}I(B_1;B_0|B_2)}-1}{\bar{\Gamma}_1} - \frac{2^{R_{c2}I(B_2;B_0|B_1)}-1}{\bar{\Gamma}_2}}.
\end{aligned}
\tag{G.1}
$$

Assuming $R_{c1} = R_{c2} = R_c$, a corresponding high-SNR expression can be obtained by invoking the approximation $\exp(x) \approx 1 - x$, $x \ll 1$, which gives

$$
J_{2,1} \simeq \frac{2^{R_c I(B_1;B_0|B_2)}-1}{\bar{\Gamma}_1} + \frac{2^{R_c I(B_2;B_0|B_2)}-1}{\bar{\Gamma}_2}.
\tag{G.2}
$$

G.2 Exact and High-SNR Expressions for $J_{2,2}$

The SNRs Γ_1 and Γ_2 are mutually independent, with marginal PDFs given in (7.2). Using this into (7.27), and exact closed-form expression for $J_{2,1}$ is obtained as

$$
\begin{aligned}
J_{2,2} &= \int_{2^{R_{c1}I(B_1;B_0|B_2)}-1}^{2^{R_{c1}I(B_1;B_0)}-1} \int_{2^{R_{c2}I(B_2;B_0|B_1)}-1}^{2^{R_{c2}I(B_1,B_2;B_0)-\frac{R_{c2}}{R_{c1}}\log_2(1+\gamma_1)}-1} \frac{1}{\bar{\Gamma}_1} e^{-\frac{\gamma_1}{\bar{\Gamma}_1}} \frac{1}{\bar{\Gamma}_2} e^{-\frac{\gamma_2}{\bar{\Gamma}_2}} d\gamma_2 d\gamma_1, \\
&= \frac{1}{\bar{\Gamma}_1} e^{-\frac{2^{R_{c2}I(B_2;B_0|B_1)}-1}{\bar{\Gamma}_2}} \\
&\quad \times \int_{2^{R_{c1}I(B_1;B_0|B_2)}-1}^{2^{R_{c1}I(B_1;B_0)}-1} e^{-\frac{\gamma_1}{\bar{\Gamma}_1}} \left(1 - e^{\frac{2^{R_{c2}I(B_1,B_2;B_0)-\frac{R_{c2}}{R_{c1}}\log_2(1+\gamma_1)}}{\bar{\Gamma}_2} + \frac{2^{R_{c2}I(B_2;B_0|B_1)}}{\bar{\Gamma}_2}} \right) d\gamma_1.
\end{aligned}
\tag{G.3}
$$

Assuming $R_{c1} = R_{c2} = R_c$, a corresponding high-SNR expression can be obtained by invoking the approximation $\exp(x) \approx 1 - x$, $x \ll 1$, which gives

$$
\begin{aligned}
J_{2,2} \simeq \frac{1}{\bar{\Gamma}_1\bar{\Gamma}_2} \Big\{ &2^{R_c I(B_1;B_0|B_2)+R_c I(B_2;B_0|B_1)} - 2^{R_c I(B_1;B_0)+R_c I(B_2;B_0|B_1)} \\
&+ 2^{R_c I(B_1,B_2;B_0)} \left[\mathrm{Ei}\left(-\frac{2^{R_c I(B_1;B_0)}}{\bar{\Gamma}_1} \right) - \mathrm{Ei}\left(-\frac{2^{R_c I(B_1;B_0|B_2)}}{\bar{\Gamma}_1} \right) \right] \Big\},
\end{aligned}
\tag{G.4}
$$

where $\mathrm{Ei}(\cdot)$ is the exponential integral function.

G.3 Exact and High-SNR Expressions for $J_{3,1}$

The SNRs Γ_1, Γ_2, and Γ_3 are mutually independent, with marginal PDFs given in (7.2). Using this into (7.33), and exact closed-form expression for $J_{3,1}$ is obtained as

$$J_{3,1} = 1 -$$
$$\int_{2^{R_{c1}I(B_1;B_0|B_2,B_3)}-1}^{\infty} \int_{2^{R_{c2}I(B_2;B_0|B_1,B_3)}-1}^{\infty} \int_{2^{R_{c3}I(B_3;B_0|B_1,B_2)}-1}^{\infty} \frac{1}{\bar{\Gamma}_1}e^{-\frac{\gamma_1}{\bar{\Gamma}_1}} \frac{1}{\bar{\Gamma}_2}e^{-\frac{\gamma_2}{\bar{\Gamma}_2}} \frac{1}{\bar{\Gamma}_3}e^{-\frac{\gamma_3}{\bar{\Gamma}_3}} d\gamma_3 d\gamma_2 d\gamma_1$$
$$= 1 - e^{-\frac{2^{R_{c1}I(B_1;B_0|B_2,B_3)}-1}{\bar{\Gamma}_1} - \frac{2^{R_{c2}I(B_2;B_0|B_1,B_3)}-1}{\bar{\Gamma}_2} - \frac{2^{R_{c3}I(B_3;B_0|B_1,B_2)}-1}{\bar{\Gamma}_3}}. \tag{G.5}$$

Assuming $R_{c1} = R_{c2} = R_{c3} = R_c$, a corresponding high-SNR expression can be obtained by invoking the approximation $\exp(x) \approx 1 - x$, $x \ll 1$, which gives

$$J_{3,1} \simeq \frac{2^{R_cI(B_1;B_0|B_2,B_3)}-1}{\bar{\Gamma}_1} + \frac{2^{R_cI(B_2;B_0|B_1,B_3)}-1}{\bar{\Gamma}_2} + \frac{2^{R_cI(B_3;B_0|B_1,B_2)}-1}{\bar{\Gamma}_3}. \tag{G.6}$$

G.4 Exact and High-SNR Expressions for $J_{3,2}$, $J_{3,3}$, and $J_{3,4}$

The SNRs Γ_1, Γ_2, and Γ_3 are mutually independent, with marginal PDFs given in (7.2). Using this into (7.34), (7.35), and (7.36), and exploiting the symmetry among the volumes associated to $J_{3,2}$, $J_{3,3}$, and $J_{3,4}$, these probabilities can be obtained in an unified manner as

$$J_{3,l} = \int_{2^{R_{ci}I(B_i;B_0)}-1}^{\infty} \int_{2^{R_{cj}I(B_j;B_0|B_i,B_k)}-1}^{2^{R_{cj}I(B_i;B_0|B_j)}-1}$$
$$\int_{2^{R_{ck}I(B_k;B_0|B_i,B_j)}-1}^{2^{R_{ck}I(B_j,B_k;B_0|B_i)-\frac{R_{ck}}{R_{cj}}\log_2(\gamma_j+1)}-1} \frac{1}{\bar{\Gamma}_i}e^{-\frac{\gamma_i}{\bar{\Gamma}_i}} \frac{1}{\bar{\Gamma}_j}e^{-\frac{\gamma_j}{\bar{\Gamma}_j}} \frac{1}{\bar{\Gamma}_k}e^{-\frac{\gamma_k}{\bar{\Gamma}_k}} d\gamma_i d\gamma_j d\gamma_k$$
$$= \frac{1}{\bar{\Gamma}_j}e^{-\frac{2^{R_{ci}I(B_i;B_0)}-1}{\bar{\Gamma}_i}}e^{-\frac{2^{R_{ck}I(B_k;B_0|B_i,B_j)}-1}{\bar{\Gamma}_k}}$$
$$\times \int_{2^{R_{cj}I(B_j;B_0|B_j,B_k)}-1}^{2^{R_{cj}I(B_i;B_0|B_j)}-1} e^{-\frac{\gamma_j}{\bar{\Gamma}_j}} \left(1 - e^{\frac{2^{R_{ck}I(B_k;B_0|B_i,B_j)}}{\bar{\Gamma}_k} + \frac{2^{R_{ck}I(B_j,B_k;B_0|B_i)-\frac{R_{ck}}{R_{cj}}\log_2(\gamma_j+1)}}{\bar{\Gamma}_k}}\right) d\gamma_j, \tag{G.7}$$

where $(l,i,j,k) \in \{(2,1,2,3),(3,3,1,2),(4,2,3,1)\}$. Assuming $R_{c1} = R_{c2} = R_{c3} = R_c$, a corresponding high-SNR expression can be obtained by invoking the approximation $\exp(x) \approx 1 - x$, $x \ll 1$, which gives

$$J_{3,l} \simeq \frac{1}{\bar{\Gamma}_j\bar{\Gamma}_k} \left(2^{R_c(I(B_j;B_0|B_k,B_i)+I(B_k;B_0|B_iB_j))} - 2^{R_c(I(B_j;B_0|B_i)+I(B_k;B_0|B_i,B_j)} + 2^{R_cI(B_j,B_k;B_0|B_i)}\right.$$
$$\left.\times \left(\mathrm{Ei}\left[-2^{R_cI(B_j;B_0|B_i)}\frac{1}{\bar{\Gamma}_j}\right] - \mathrm{Ei}\left[-2^{R_cI(B_j;B_0|B_i,B_k)}\frac{1}{\bar{\Gamma}_j}\right]\right)\right). \tag{G.8}$$

G.5 Exact and High-SNR Expressions for $J_{3,5}$

Following (7.37), $J_{3,5}$ is composed of three terms. Initially, we analyze the term $J_{3,5a}$. The SNRs Γ_1, Γ_2, and Γ_3 are mutually independent, with marginal PDFs given in (7.2). Using this into (7.38), and exact closed-form expression for $J_{3,5a}$ is obtained as

$$
\begin{aligned}
J_{3,5a} &= \int_{2^{R_{c1}I(B_1;B_0|B_2,B_3)}-1}^{2^{R_{c1}I(B_1;B_0)}-1} \int_{2^{R_{c3}I(B_3;B_0|B_1,B_2)}-1}^{2^{R_{c3}(I(B_3;B_0|B_1))-\frac{R_{c3}}{R_{c1}}\log_2(\gamma_1+1)}-1} \\
&\quad \int_{2^{R_{c2}I(B_2;B_0|B_1,B_3)}-1}^{2^{R_{c2}I(B_1,B_2,B_3;B_0)-\frac{R_{c2}}{R_{c1}}\log_2(\gamma_1+1)-\frac{R_{c2}}{R_{c3}}\log_2(\gamma_3+1)}-1} \frac{1}{\bar{\Gamma}_1}e^{-\frac{\gamma_1}{\bar{\Gamma}_1}}\frac{1}{\bar{\Gamma}_2}e^{-\frac{\gamma_2}{\bar{\Gamma}_2}}\frac{1}{\bar{\Gamma}_3}e^{-\frac{\gamma_3}{\bar{\Gamma}_3}}d\gamma_2 d\gamma_3 d\gamma_1, \\
&= \frac{1}{\bar{\Gamma}_1\bar{\Gamma}_3}e^{-\frac{2^{R_{c2}I(B_2;B_0|B_1,B_3)}-1}{\bar{\Gamma}_2}} \int_{2^{R_{c1}I(B_1;B_0|B_2,B_3)}-1}^{2^{R_{c1}I(B_1;B_0)}-1} \int_{2^{R_{c3}I(B_3;B_0|B_1,B_2)}-1}^{2^{R_{c3}(I(B_3;B_0|B_1))-\frac{R_{c3}}{R_{c1}}\log_2(\gamma_1+1)}-1} e^{-\frac{\gamma_1}{\bar{\Gamma}_1}}e^{-\frac{\gamma_3}{\bar{\Gamma}_3}} \\
&\quad \times \left(1 - e^{\frac{2^{R_{c2}I(B_2;B_0|B_1,B_3)}}{\bar{\Gamma}_2} - \frac{2^{R_{c2}I(B_1,B_2,B_3;B_0)-\frac{R_{c2}}{R_{c1}}\log_2(\gamma_1+1)-\frac{R_{c2}}{R_{c3}}\log_2(\gamma_3+1)}}{\bar{\Gamma}_2}}\right) d\gamma_3 d\gamma_1. \quad \text{(G.9)}
\end{aligned}
$$

Assuming $R_{c1} = R_{c2} = R_{c3} = R_c$, a corresponding high-SNR expression can be obtained by invoking the approximation $\exp(x) \approx 1 - x$, $x \ll 1$, which gives

$$
\begin{aligned}
J_{3,5a} &\simeq \frac{1}{\bar{\Gamma}_1\bar{\Gamma}_2\bar{\Gamma}_3}\left(1 - \frac{2^{R_cI(B_2;B_0|B_1,B_3)}-1}{\bar{\Gamma}_2}\right)\int_{2^{R_cI(B_1;B_0|B_2,B_3)}-1}^{2^{R_cI(B_1;B_0)}-1}\left(1 - \frac{\gamma_1}{\bar{\Gamma}_1}\right) \\
&\quad \int_{2^{R_cI(B_3;B_0|B_1,B_2)}-1}^{2^{\frac{R_cI(B_1,B_3;B_0)}{(\gamma_1+1)}}-1}\left(1 - \frac{\gamma_3}{\bar{\Gamma}_3}\right)\left(2^{\frac{R_cI(B_1,B_2,B_3;B_0)}{(\gamma_1+1)(\gamma_3+1)}} - 2^{R_cI(B_2;B_0|B_1,B_3)}\right) d\gamma_3 d\gamma_1, \\
&= \frac{1}{\bar{\Gamma}_1\bar{\Gamma}_2\bar{\Gamma}_3} \\
&\quad \Bigg(2^{R_c(I(B_1;B_0)+I(B_2;B_0|B_1,B_3)+I(B_3;B_0|B_1,B_2))} - 2^{R_c(I(B_1;B_0|B_2,B_3)+B(B_2;B_0|B_1,B_3)+I(B_3;B_0|B_1,B_2))} \\
&\quad - 2^{R_cI(B_1,B_2,B_3;B_0)}\log\left[2^{R_cI(B_1;B_0)}\right]\left(1 - \log\left[2^{\frac{R_cI(B_1;B_0)}{2}}2^{R_c(-I(B_3;B_0|B_1,B_2)+I(B_3;B_0|B_1))}\right] + 1\right) \\
&\quad + 2^{R_cI(B_1,B_2,B_3;B_0)}\log\left[2^{R_cI(B_1;B_0|B_2,B_3)}\right] \\
&\quad \left(1 - \log\left[2^{\frac{R_cI(B_1;B_0|B_2,B_3)}{2}}2^{R_c(I(B_2,B_3;B_0)-I(B_2;B_0|B_1,B_2)-I(B_3;B_0|B_1,B_2))}\right]\right)\Bigg)\Bigg). \quad \text{(G.10)}
\end{aligned}
$$

Exact and asymptotic expressions for $J_{3,5b}$ and $J_{3,5c}$ can be obtained on a similar basis. For brevity, we present here only the final asymptotic results, which are

$$
J_{3,5b} \simeq \frac{2^{R_c I(B_1,B_2,B_3;B_0)}}{\bar{\Gamma}_1 \bar{\Gamma}_2 \bar{\Gamma}_3}
$$
$$
\times \left(1 - 2^{R_c(I(B_3;B_0|B_1,B_2) - I(B_3;B_0|B_2))} - \log\left[2^{R_c I(B_1;B_0|B_2)} \right] \left(1 + \log\left[2^{\frac{R_c I(B_1;B_0|B_2)}{2}} \right] \right) \right.
$$
$$
+ \log\left[2^{R_c I(B_1;B_0|B_2,B_3)} \right]
$$
$$
\left. \times \left(1 - \log\left[2^{-\frac{R_c I(B_1|B_2,B_3)}{2}} \right] + \log\left[2^{R_c(I(B_1,B_2;B_0) - 2H(B_2,B_3;B_0) + I(B_2;B_0))} \right] \right) \right), \quad \text{(G.11)}
$$
$$
J_{3,5c} \simeq \frac{2^{R_c I(B_1,B_2,B_3;B_0)}}{\bar{\Gamma}_1 \bar{\Gamma}_2 \bar{\Gamma}_3}
$$
$$
\times \left(- 2^{R_c(I(B_1;B_0|B_2,B_3) - I(B_1;B_0|B_3))} + 1 + \log\left[2^{R_c I(B_1;B_0|B_3)} \right] \left(\log\left[2^{\frac{R_c I(B_1;B_0|B_3)}{2}} \right] - 1 \right) \right.
$$
$$
+ \log\left[2^{R_c I(B_1;B_0|B_2,B_3)} \right]
$$
$$
\left. \times \left(1 - \log\left[2^{-\frac{R_c I(B_1;B_0|B_2,B_3)}{2}} \right] - \log\left[2^{R_c(I(B_1;B_0|B_3) - I(B_1;B0|B_2,B_3))} \right] \right) \right). \quad \text{(G.12)}
$$